UNIVERSITY OF CALIFORNIA, SAN DIEGO

A New Way To Look At Sleep:
Separation & Convergence

A Dissertation submitted in partial satisfaction of the
Requirements for the degree Doctor of Philosophy

in

Biology / Specialization in Computational Neurobiology

by

Philip Steven Low

Committee in charge:

Professor Charles F. Stevens, Chair
Professor Sean P. Drummond
Professor Fred H. Gage
Professor Terrence J. Sejnowski
Professor Larry R. Squire

2007

The Dissertation of Philip Steven Low is approved, and it is acceptable in quality and form for publication on microfilm:

Chair

University of California, San Diego

2007

DEDICATION

In recognition that passion is not as much a way to work as it is a way to live, a way to question and to consider, a way to treat others and perhaps a way to leave as well, this dissertation is dedicated to the passion of J. Christian Gillin and Francis H. Crick.

To my family, who showed me that dreams can

be found even in the wake of many oscillations.

EPIGRAPH

We shall not cease from exploration,
and the end of all our exploring will be to
arrive where we started
and know the place for the first time.

T. S. Eliot

TABLE OF CONTENTS

LIST OF ABBREVIATIONS

2NS	Doubly Normalized Spectrogram
AIC	Art Institute of Chicago, Chicago, IL, USA
ANOVA	Analysis of Variance
ART	Artifact
AUT	Automated scoring
C-M	Crick-Mitchison theory of REM sleep
D	Epoch scored as Disconnected
DOWN	non-fragmented REM
DSS	Dynamic Spectral Scoring
EEG	Electroencephalogram
EMG	Electromyogram
EOG	Electrooculogram
ICA	Independent Component Analysis
IS	Intermediate Sleep
INTER	Intermediate Sleep
K	K-complex
KS	Kolmogorov-Smirnov test

M	Epoch scored as Movement
MAN	Manual Scoring
MPI	Max-Planck-Institut für Psychiatrie, Munich, Germany
NS	Normalized Spectrogram
PCA	Principal Component Analysis
PFS	Preferred Frequency Space
REM sleep	Rapid Eye Movement sleep
R-K	Rechtschaffen-Kales classification
SPEARS	Sleep Parametric EEG Automated Recognition System
SWS	Slow Wave Sleep
TOP	fragmented REM
VA	Veterans' Affairs Hospital, University of California, San Diego, CA, USA
W	Waking state

LIST OF FIGURES

LIST OF SCHEMES

LIST OF TABLES

PREFACE

In mammals, a typical night of sleep is composed by successive episodes of Slow Wave Sleep (SWS), Intermediate Sleep (IS) and Rapid Eye Movement (REM) sleep. In humans, IS and SWS are further subdivided into stages I and II and into stages III and IV, respectively. REM sleep is also strongly associated with dreaming in humans. IS tends to act as a transition state between SWS and REM. Throughout the night, there is a progression towards less SWS and more REM sleep. Electroencephalograms (EEGs) associated with these sleep stages follow a 1/f distribution, i.e. higher frequencies EEGs have smaller raw amplitudes and thus less spectral power. SWS are characterized by high amplitude and low frequency EEGs while REM sleep corresponds to a more “awake-like” raw signal with low amplitudes and high frequencies. Brief EEG landmarks known as spindles and K-complexes are often seen in IS.

While diverse neurotransmitters are known to be selectively activated in REM and Non-REM (NREM) sleep, the underlying mechanisms leading to these patterns are not known. In the cortex, a

higher degree of synchrony has been observed across neurons in SWS than in REM. Moreover K-complexes as well as the interdigitation of high and low frequencies as observed in EEGs have been recorded in the cortex. This suite of observations, which has never been observed outside of mammals, has led many to believe that the cortex was necessary for their generation.

Recent studies in zebra finches have however shown a sleep dependent replay of activity similar to that observed in mammals, suggesting that birds and mammals alike might be using similar features of sleep to consolidate information. A detailed study of avian sleep was thus needed in order to gain a better understanding of the roles of the cortex in sleep oscillations as well as the role of sleep in learning.

The systematic study of sleep in a new species is hampered by the same assumptions one makes when assessing sleep in pathological cases or genetically modified animals as there is no guarantee one can *a priori* use the same set of rules than in healthy human controls and wild type rodents. Moreover the guidelines used to assess sleep in the latter groups rely on the Rechtschaffen-Kales (RK) method. This method is based on a set of rules which make two important assumptions about sleep and

EEGs: 1) that scoring rules should minimize the degree of fragmentation of each sleep state, 2) a simple threshold can suffice to delineate certain sleep stages, i.e. that EEGs are linearly separable. Based on the implementation of these rules, the same 30 second segment of EEG data can be assigned a different designation depending on which 3 minute window the 30 sec epoch resides in -therefore suggesting that brain activity could be entirely different when the patterns produced are the same. These rules have been difficult to adhere to in humans their applicability has been increasingly called into question. This is mainly due to the individual variability in both sleep scorers and subjects (both longitudinally and across subjects). Given the somewhat poor reliability across human scorers, neural networks developed to emulate human scoring have been lacking in performance and further fail to make their clustering variables known. Thus, almost 40 years after the formulation of RK, sleep researchers and clinicians are bound to rely on human scoring of multiple electrophysiological channels in addition to behavioral monitoring in order to make more accurate classifications of sleep. There is thus an urgent need in the sleep field to formulate a new system to

classify sleep, one that makes the fewest assumptions about the data and which can be broadly applied across individuals and across laboratories.

My work in birds shows that finches produce patterns strikingly similar to the ones produced by mammals, even though they lack a neocortex. These observations were validated by both manual and automated scoring. The approach I developed for human sleep reveals human sleep to have a fine structure, observable in multiple subjects across multiple laboratories. This structure is apparent using a single channel of data, usually EEG, and can be used to develop powerful sleep scoring algorithms. Consequently, human REM sleep should no longer be perceived as being “awake-like” or “paradoxical.”

Besides their ease of application, these analyses demonstrate a yet unreported convergence of sleep patterns across phylogeny as well as clearer taxonomy of sleep within clades: a new way to look at sleep.

ACKNOWLEDGEMENTS

I am indebted to Dr. Terrence J. Sejnowski, the Francis Crick Professor and Director of the Computational Neurobiology Laboratory at the Salk Institute and the Institute for Neural Computation at UCSD, for his wonderful scientific generosity, curiosity and enthusiastic and unwavering support. Terry put aside early reservations about projects which were initially outside the focus of his laboratory's research and, in the Computational Neurobiology Laboratory at the Salk Institute, provided me with an exceptional working environment in which I learned much about the fields of thalamocortical oscillations, computation and EEGs, from world class experts in each field… an ideal place to freely engage in the pursuit of science, and in retrospect, to devise a new computational analysis of sleep EEGs from the ground up and perhaps a new way to look at sleep altogether. I have also very much benefitted from Terry's many elegant revisions of the countless number of manuscripts I have placed in front of his door at all hours of the day and night as well as from the many epic presentations I gave to the laboratory. I also thank Terry for helping me launch NeuroVigil, Inc. and for taking

an active role in it. Terry consistently sees and brings out the best in people. I do not believe that, in light of my background, I could have had a better place to work in than in his laboratory, or for that matter, a better mentor than Terry, at both professional and personal levels. I am most grateful to Francis Crick for referring me to Terry when I became increasingly more curious about Neuroscience in College.

I have benefitted immeasurably from many conversations with my committee members, Drs. Charles Stevens, Larry Squire, Sean Drummond, Terry Sejnowski and Fred Gage. I thank them for having taken the time to review the progression of my work over the years. I thank my thesis co-advisor, Dr. Fred Gage, for developing a growing interest in sleep, monitoring the progression of my work and especially for making it quite clear to me that I could not *a priori* use a mammalian classification on avian sleep. An unsupervised technique was indeed needed. In fact, the same was true for human sleep as well, which Terry persuaded me to take a serious look at. I have also much benefitted from my many technical conversations with D. Spencer, G. Seurat, L. Finelli and T. Bell.

I thank Dr. Sean P.A. Drummond from the UCSD Veterans' Affairs Hospital in San Diego and Drs. Florian Holsboer, Thomas Wetter and Elizabeth Friess from the Max-Planck Institute für Psychiatrie in Munich, who have made their data available for me to analyze and explore. In particular, I would like to thank Arlene Schlosser, Ryan Wong and Renate Wehrle, U. Ambrosius, S. Litzenmaier, H. Mien, I. Spokoyny for assistance with human EEGs and S. Shank at the University of Chicago for assistance with avian EEGs.

I thank Dr. Deborah Nelson for her wonderful support as well as for loaning me equipment to build a sleep rig at the University of Chicago, where I developed an avian epidural EEG method.

I thank Drs. Romana Nowak and Dan Margoliash for opening their laboratories to me, at Harvard Medical School and The University of Chicago, respectively, and Drs. J. Cowan and P. Ulinski for being my first teachers in Computational Neuroscience at The University of Chicago.

I thank Drs. Jean-Paul Spire from the University of Chicago, Chris Gillin from the UCSD VA hospital and Francis Crick from the Salk

Institute for never being too busy, too famous, and in some cases too ill, to share their fascination about sleep, and science in general, with me. I have learned a lot from these gentlemen and miss Chris and Francis dearly.

Special thanks also to the entire Computational Neurobiology Laboratory's technical support and administrative staff.

I thank the original Computational Neurobiology Steering committee at UCSD, which has unknowingly provided me with great scientific freedom. Saru Mo Ki Kara Ochiru.

This work would not have been possible without graduate support from the Sloan-Swartz center for Theoretical Neurobiology at the Salk Institute and the Swartz Foundation. I am grateful to Jerry Swartz for taking a personal interest in my research from a very early stage.

I thank my father, Steven Low, Terry Sejnowski, Don Spencer, Fred Gage, Sydney Brenner, Roger Guillemin, Andrew Viterbi, Jean-Paul

Spire, Sonia Ancoli-Israel, Jerry Siegel, Stephen Wolfram, Ron Graham and my lawyers at Mayer Brown for helping me launch NeuroVigil, Inc. and for playing an active part in this most daring enterprise.

Chapter A1 is, in full, being prepared for publication. Co-authors are S. Shank, T. Sejnowski and D. Margoliash. The dissertation author was responsible for the techniques described and main observations therein and was the primary investigator and author of this paper.

Chapter A2 is, in part, being prepared for publication. The co-author is T. Sejnowski. The dissertation author was responsible for the techniques described and main observations therein and was the primary investigator and author of this paper.

The patents in the Appendix are awaiting prosecution from the United States Patent Office. The dissertation author was responsible for the techniques described therein and was the primary investigator and author of these patents.

VITA

Crick-Jacobs Center for Computational

& Theoretical Neurobiology - CNL

Salk Institute for Biological Studies.

10010 North Torrey Pines Road. La Jolla, CA 92037, USA.

Tel: +1 (858) 453-4100 x 1489, Email: philip@salk.edu,

http://www.cnl.salk.edu/~philip

Country of Birth: Austria. Country of Citizenship: Canada.

- PhD in Computational Neurobiology, Division of Biological Sciences, University of California, San Diego, 2007.
- Committee in charge: Charles F. Stevens (Chair), Terrence J. Sejnowski (advisor), Fred H. Gage (advisor), Sean P. A. Drummond, Larry R. Squire.
- The University of Chicago, Chicago, IL, USA, 1996-2000: Bachelor’s degree of Science in Pure Mathematics.
- Institut Le Rosey, Rolle & Gstaad, Switzerland, 1991-1996: French Scientific Baccalaureate, specialization in Mathematics.
- Cours Hattemer, Paris, France, 1984-1991.

PROFFESSIONAL EXPERIENCE

- NeuroVigil, Inc. La Jolla, CA, USA. Founder, CEO and CSO. 02/07 – current.
- Board of Advisors: Sonia Ancoli-Israel, Sydney Brenner, Fred Gage, Ron Graham, Terry Sejnowski, Jerome Siegel, Donald Spencer, Andrew Viterbi and Stephen Wolfram.
- The University of Chicago, Chicago, IL, USA, Margoliash Laboratory, Research Assistant, 06/00 - 08/01, 06/02-08/02.
- Developed EEG experimental technique and equipment for the Zebra Finch, *Taeniopygia guttata*, in order to relate nocturnal Robustus Archistriatalis (RA) song rehearsal to sleep states.
- Harvard Medical School / Brigham and Women's Hospital & Children's Hospital Boston, Boston, MA, USA, Nowak Lab, Intern, 06-09/99
- Verified the potential of Compound H, a collagen type I inhibitor, against fibroid tumor cell proliferation, using immunostaining, Tritium assays and mathematical modeling.

PUBLICATIONS

"The Organization of Sleep States in Zebra Finches"

P Low, S Shank & D Margoliash. Computational Neuroscience 2003 Proceedings.

"A Pattern of Mammalian-like Features in Zebra Finch Sleep"

P Low, S Shank & D Margoliash. Society for Neuroscience 2003 Abstracts.

"An unbiased automated approach to single channel sleep scoring"

P Low, FH Gage & TJ Sejnowski. Society for Neuroscience 2004 Abstracts.

"The anti-fibrotic drug halofuginone inhibits proliferation and collagen production by leiomyoma smooth muscle cells."

RA Nowak, P Low, JE Wubben, RJ Belton, Jr. 2nd NIH Int. Congress on Advances in Uterine Leiomyoma Research. 2005.

"Dynamic Spectral Scoring: A New Way to Look at Sleep", P Low, FH Gage, & TJ Sejnowski. WiR Workshop on Data-driven Modelling and Computation in Neuroscience, Hohenwart Forum, Germany, May 2005.

"A New Way To Look At Sleep" PS Low, FH Gage & TJ Sejnowski. Society for Neuroscience 2005 Abstracts.

"Fine Structure of Human Sleep" PS Low & TJ Sejnowski. Society for Neuroscience 2006 Abstracts.

"REM revisited" PS Low & TJ Sejnowski. Society for Neuroscience 2007 Abstracts.

"The Antifibrotic Drug Halofuginone Inhibits Proliferation and Collagen Production by Human Leiomyoma and Myometrial Smooth Muscle Cells." MM Grudzien, P Low, PC Manning, M Arredondo, RJ Belton, Jr & RA Nowak. In Review.

"Mammalian-like Features of Sleep Structure in a Songbird" PS Low, S Shank, TJ Sejnowski & D Margoliash. In Preparation.

"Fine Structure of Human Sleep" PS Low & TJ Sejnowski. In Preparation.

PATENTS

U.S. Provisional Patent Application Serial No. 60/679,951 filed May 10, 2005, entitled "Dynamic Signal Processing"

Inventors: Philip Low and Terrence Sejnowski

PCT Patent Application Serial No. US2005/027562 filed August 2, 2005, entitled "Dynamic Signal Processing"

Inventors: Philip Low and Terrence Sejnowski

U.S. Patent Application Serial No. 11/431,425 filed May 9, 2006, entitled "Automated Detection of Sleep and Waking States"

Inventors: Philip Low and Terrence Sejnowski

PCT Patent Application Serial No. US2006/018120 filed May 9, 2006, entitled "Automated Detection of Sleep and Waking States"

Inventors: Philip Low and Terrence Sejnowski

AWARDS

NSF-IGERT Fellowship (2001), Merck Fellowship (2001), Sloan-Swartz Fellowship (2002-present). Ray Thomas Edwards Award (2006). Kavli Brain and Mind Award for Innovative Research (2007). Top Executive Summary Selection and Business Plan Competition Finalist,

UC San Diego 50K Triton Innovation Award Jury (2007).

PRESS

"The dream of the zebra finch" Biomednet, Elsevier Press.

October 9th 2003.

"To sleep, perchance to dream" Biomednet, Elsevier Press.

October 12th 2003.

"Sleeping with the Finches" The Economist. London.

October 22nd 2003, Science & Technology, p. 79

Who'sWho in America, 2007-8. Who'sWho in The World, 2008.

"The Secrets of Sleep". MIT Technology Review. December 2006.

Researcher's hub. E-newsletter. CONNECT. March 2007.

"Memories Are Made Like This". Howard Hughes Medical Institute Bulletin. May 2007.

TEACHING

BGGN 246 B: Designed and taught graduate Advanced Biology of Sleep Oscillations with Dr. Sejnowski. Spring 2006.

MENTORING / TRAINING

Experiments: S. Shank (avian EEG preparation, University of Chicago),

Analysis: H. Mien, I. Spokoyny, D. Schuetz, H. Schuetz and S. Barton (EEG analysis, Salk Institute).

TALKS

Sloan-Swartz informal talk, Salk Institute, San Diego, CA, USA.

February 2002.

Institute for Neural Computation, UCSD, San Diego, CA, USA.

February 2003.

Sleep & Chronobiology**,** UCSD, San Diego, CA, USA. February 2003.

Neurophysics Laboratory, UCSD, San Diego, CA, USA. February 2003.

Society for Neuroscience, New Orleans, LA, USA. October 2003.

Institute for Nonlinear Dynamics, UCSD, San Diego, CA, USA.

May 2004.

Merck Symposium, UCSD, San Diego, CA, USA. June 2004.

Society of Research Fellows, Salk Institute, San Diego, CA, USA.

October 2004.

Invited Talk, Data Driven Modelling and Simulation in Computational Neuroscience, Hohenwart Forum, Germany. May 2005.

Invited Talk, Max-Planck Institute for Psychiatry, Munich, Germany. May 2005.

Sloan-Swartz Annual Symposium, Caltech, Pasadena, CA, USA. July 2005.

Swartz Center for Computational Neuroscience, UCSD, San Diego, CA, USA. November 2005.

Sleep & Chronobiology**,** UCSD, San Diego, CA, USA. April 2006.

UCSD Rady School of Management, Salk Institute, San Diego, CA, USA. April 2006.

Invited Talk, Redwood Center for Theoretical Neuroscience, UC Berkeley, Berkeley, CA, USA. June 2006.

Invited Talk, Sleep Grand Rounds, Stanford University, Palo Alto, CA, USA. June 2006.

Invited Talk, Keck Center for Integrative Neuroscience, UCSF, San Francisco, CA, USA. June 2006.

Sloan-Swartz Annual Symposium, Columbia University, New York, NY, USA. July 2006.

Society for Neuroscience, Atlanta, GA, USA. October 2006.

Waking Up To Sleep, The Science Network, The Salk Institute, San Diego, CA, USA. February 2007.

UCSD50K Triton Innovation Award Finalist presentation, San Diego, CA, USA. June 2007.

Aspen Consciousness Research Retreat, Aspen, CO, USA. August 2007.

Almaden Research Center, IBM, San Jose, CA, USA. September 2007.

Invited Talk, Scripps Clinic Sleep Center, La Jolla, CA, USA, October 2007.

Thesis Defense: "A New Way To Look At Sleep: *Separation & Convergence*". Salk Institute, La Jolla, CA, USA. October 2007.

Society for Neuroscience, San Diego, CA, USA. November 2007.

ACTIVITIES

American Association for the Advancement of Science (AAAS): Member, 2004-current.

Computational Neuroscience (CNS): Board of Directors, Travel Grant & Future Meeting Sites committees. 2003-2005.

Institut Le Rosey: Chess Club founder and president 1991-96; Debate Club co-founder and co-president 1994-1996; Cultural Academy Vice-President, 1995-6; Students' UN member, 1993-1996; Ski and Tennis teams member, 1991-1996. Mathematical Association of America (MAA): Member, 1997-current. Society for Neuroscience (SfN): Member, 2001-current. The Science Network (TSN): Special Projects Advisor, 2003-current. The University of Chicago: Chess Club co-president, 1999-2001; French Club President, 2000-2001.UCSD / SALK: Neuroscience Journal Club organizer, 2001; Computational Neurobiology Journal Club member, 2001-current; Synaptic Physiology Journal Club member; Computational Neurobiology Lounge founder, 2001; Sloan-Swartz ChalkTalks organizer, 2002. Society of Research Fellows, 2002-present.

MISCELLANEOUS

Fluent in French, English and German. Working knowledge of Italian. Exposure to Russian. Proficiency with Microsoft and Linux OS, MS PowerPoint, Final Cut Pro, Media Cleaner Pro, Nodus, Matlab.

ABSTRACT OF THE DISSERTATION

A New Way To Look At Sleep:
Separation & Convergence

by

Philip Steven Low

Doctor of Philosophy in Biology / Specialization in Computational Neurobiology

University of California, San Diego, 2007

Professor Charles F. Stevens, Chair

Despite over 70 years of active research in mammalian EEGs, most of the neural structures responsible for sleep and waking rhythms have yet

to be identified. At time of writing, three major beliefs pervade the field of sleep:

1) The neocortex is largely necessary for the production of “mammalian” sleep rhythms;

2) Human REM sleep is “paradoxical” insofar as the oscillations produced during REM sleep are “awake-like”;

3) Human sleep can only be objectively analyzed by human scorers.

This way of looking at sleep is in need of major revision, as:

1) Birds, devoid of a neocortex, can produce oscillations which bare great similarity with those observed in mammals, in terms of both their raw signals and ultradian properties;

2) A temporal map of brain activity produced using a single channel of EEG is sufficient to clearly show that REM sleep and Waking have different and separable EEG profiles. Human REM sleep is therefore not paradoxical.

3) Sleep and Waking Stages can in fact be easily identified computationally using a single channel of EEG, obviating the need for human based sleep scoring.

Moreover, it appears that low-passing from the skull reflected in EEGs can be easily circumvented, thus providing researchers and clinicians with a non-invasive window into brain activity, with high resolution in both the time and frequency domains. Furthermore, the possibility of there being yet another human sleep state should be fully explored. The use of these and similar techniques will hopefully

minimize the significant strain placed on both humans and animals in at least the contexts of medicine as well as basic and clinical research.

CHAPTER 1

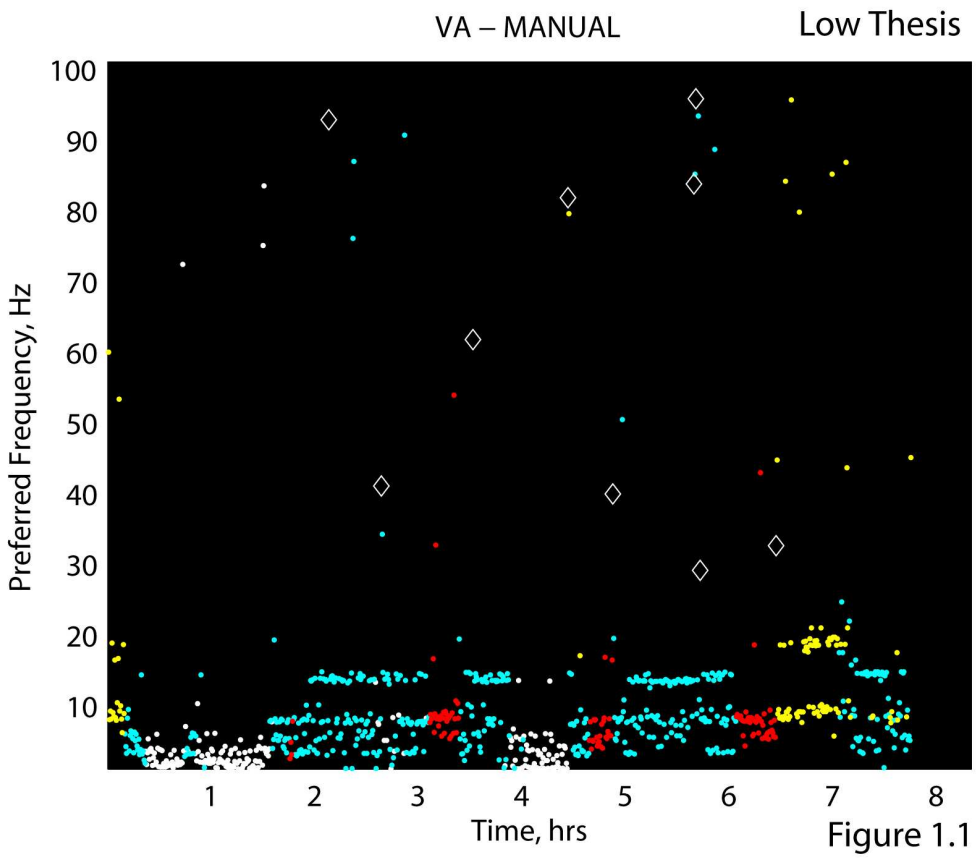

Figure 1.1. Preferred Frequency Space. Every dot corresponds to the frequency with the highest normalized power value throughout the entire night at a given 30 second window extracted from a single channel of EEG. Colours and symbols are drawn from manual labeling (SWS = white, IS = cyan, REM = red, W = yellow, M = white diamonds). Raw data courtesy VA.

Most of my doctoral work can be immediately traced back to the concept outlined in this figure or treated as an elaborate variation, corollary or motivation thereof. Further refinements, explanations, implications and applications are put forth in the Preface, Abstract and, in significant detail, in the following Appendix.

APPENDIX

CHAPTER A1

Mammalian-like Features of Sleep Structure in a Songbird

A suite of complex electroencephalographic patterns of sleep occurs in mammals. In sleeping zebra finches, we observed slow wave sleep (SWS), rapid eye movement (REM) sleep, an intermediate sleep (IS) stage commonly occurring in, but not limited to, transitions between other stages, and high amplitude transients reminiscent of K-complexes. SWS density decreased while REM density increased throughout the night, with late-night characterized by substantially more REM than SWS, and relatively long bouts of REM. Birds share many features of sleep in common with mammals, but this collective suite of characteristics had not been known in any one species outside of mammals. Our results falsify the hypothesis that the patterns of sleep common in mammals require a neocortex. We hypothesize that shared, ancestral characteristics of sleep in amniotes evolved under selective pressures common to songbirds and mammals, resulting in convergent characteristics of sleep.

In mammals, a typical night of sleep is composed by successive episodes of Slow Wave Sleep (SWS), Intermediate Sleep (IS) and Rapid Eye Movement (REM) sleep. In humans, IS and SWS are further subdivided into stages I and II and into stages III and IV, respectively. REM sleep is also strongly associated with vivid dreaming in humans. IS tends to act as a transition state between SWS and REM. Throughout the night, there is typically a progression towards less SWS and more REM sleep. Electroencephalograms (EEGs) associated with these sleep stages follow a 1/f distribution, i.e. higher frequencies in the EEG have smaller raw amplitudes and thus less spectral power. SWS is characterized by a high amplitude and low frequency EEG signal while REM sleep corresponds to a more “awake-like” raw signal with lower amplitudes and higher frequencies (1-2). Brief EEG landmarks known as spindles and K-complexes are often seen in Non-REM sleep (NREM) (1, 3-4). Since this suite of characteristics has never been observed outside of mammals, it has been proposed that the cortex was necessary for its generation (5-6).

It is now well established that avian and mammalian forebrain organization share far more commonalities than has traditionally been

recognized (7). These similarities are observed at molecular, cellular, and systems levels (8). A new terminology has been created to correct misconceptions especially regarding the avian forebrain, and which recognizes forebrain homologies comparing birds and mammals (8-9). Of relevance to this report, direct reciprocal thalamocortical projections have been implicated in generation of sleep rhythms in mammals (6). These are not known in birds, but recent studies have identified descending recurrent projections of sensory pathways in birds that might serve similar functional roles, for example in the auditory system (10-11).

Both REM and NREM are known for birds, with sleep in most species being dominated by NREM with brief REM episodes (12), although passerine birds exhibit greater amounts of REM (13-14). Circadian patterns in REM and NREM are commonly known in birds (15), and there is also fragmentary evidence regarding other characteristics (16). From these bases, and given our interest in sleep-dependent mechanisms of birdsong learning, we explored the organization of sleep states in zebra finches.

We chronically implanted five birds with EEG electrodes, three with bilateral electrode pairs. From the recordings made after birds acclimated to the recording environment (including a cable leading to an overhead commutator), one full-night record was selected for each bird. These records were characterized by good quality EEG signals with relatively few movement-related or other artifacts and video monitoring of eye movements throughout the night (see Experimental Procedures). Sleep is associated with species-specific postures. Zebra finches commonly adopt a head-forward position and occasionally a head-backward position during sleep. Our birds adopted both positions. Although we did not assess the relative frequency of these two behaviors compared to controls, this suggests that the birds experienced relatively undisturbed sleep in our experimental conditions.

The EEG data from these recordings were scored both manually and automatically. Manual scoring relied on visual inspection of EEGs in parallel with scoring of overt behaviors such as eye, head and body movements. Sleep stages were scored in 3 s epochs to achieve sufficient temporal resolution for the rapid stage transitions commonly observed.

Manual scoring classified each epoch as either REM, NREM or awake. REM occurred reliably in conjunction with eye and low amplitude head movements, as seen in other species (3, 17). The eye movements were on the order of one saccade per second. The head movements were not as reliable, but tended to follow the directional movement of the eyes when present. As well as visible differences in EEG waveforms, during NREM birds breathed slowly and regularly; eye and head movements were slow and infrequent, did not follow a stereotypical pattern and were quite distinct from those in REM.

Automated scoring relied on 3 s EEG power spectra computed over 2 orthogonal tapers following a standard multitaper estimation technique (18), over 1 s increments. Automated scoring was restricted to the data collected from sleeping birds as defined by manual scoring (i.e. excluding awake and artifacts). The automated scoring initially subdivided the sleep data into REM, NREM, SWS and non-SWS (NSWS). Epochs that were scored neither as REM nor as SWS were labeled as IS. While IS was observed by visual inspection, it was not systematically distinguished from SWS. Epochs that were automatically labeled as both REM and

SWS were relabeled as outliers. There were very few outliers in the data (Table A1.1). The agreement rate between manual and automated scoring was calculated by assessing each epoch scored as REM by only the manual or the automated scoring as an error, resulting in an average agreement rate of 84.30 ± 3.81 % (mean ± S.E.M.) (Table A1.1, Figs. A1.5).

Full night spectrograms of the EEG signals identified temporal variations in power in the 1-4 Hz (Delta) and 30-55 Hz (Gamma) frequency bands, which were selected for automated classification of sleep stages. The interdigitation of power in Delta and Gamma observed in the birds (Fig. A1.1A) was similar to interdigitation of low and high frequencies reported for cat cortical local field potentials (LFP) (Fig. A1.1B) (19). The power in Delta was used to separate SWS from NSWS. Since REM was not linearly separable from NREM in Gamma, the power ratio Gamma/Delta was used as a more robust parameter to extract REM. This separation of epochs into different stages was accomplished using a k-means clustering algorithm. Three additional variables were included for both separations: the standard deviation of the 3 s waveform and the

absolute values of the differences in Delta power and Gamma/Delta between successive and preceding epochs. REM epochs formed segments which punctured the sleep data in the latter variable at a 1 sec temporal resolution (Fig. A1.5).

In each bird, a multivariate ANOVA on the 5-dimensional clustering space separated REM, SWS and IS ($P < 0.001$). When plotting Delta, Gamma/Delta and the differences in Gamma/Delta, SWS would form a spear along Delta and the differences in Gamma/Delta because during SWS epochs the Gamma/Delta ratio was not only low but stable across successive epochs as well (Fig. A1.1C). Conversely, when the differences in Gamma/Delta were replaced by the differences in Delta, REM sleep would now collapse into a spear (Fig. A1.1D) as variations in Delta tended to be small in REM sleep. Thus the intermediate state is distinct from SWS and REM, and can be thought of as the only sleep state which does not collapse into either spear in the two aforementioned parameter spaces. IS has previously only been reported in mammals (3-4, 20-21).

The REM, SWS and IS epochs could also be visualized in a 3-dimensional space defined by a Principal Component Analysis (PCA) of the 5-dimensional space spanned by Delta, Gamma, the standard deviation of each waveform and the differences in Delta and Delta/Gamma. The three sleep stages occupied separate regions in the 3-dimensional space (Fig. A1.1E). SWS and REM formed orthogonal planes in this space, with IS corresponding to a distinct, warped transitional region linking the two planes (Fig. A1.1F). A similar 3-dimensional structure was observed when PCA was applied to data from each of the five birds (Fig. A1.6).

Each sleep stage was associated with specific EEG characteristics. SWS had a high amplitude EEG signal with significant power in the Delta range (Figs. A1.1A, A1.2A), as has been observed in mammals (Fig. A1.1B). REM was characterized by a very low amplitude “awake-like” EEG signal (Figs. A1.2B, A1.2D), typically about ±30 μV with higher power in Gamma (Fig. A1.1A) than NREM, also consistent with REM in mammals (1-2, 22). Birds with relatively little power increase in the 30-55 Hz range for REM had a greater power increase in the 70-100 Hz range.

IS had highly variable amplitude, centered around ±50 μV and did not have significant power in either the Delta or Gamma ranges (Figs. A1.1A, A1.2C). Large, brief amplitude transients observed in NREM sleep, with biphasic waveforms were observed in two birds (Fig. A1.2D, Table A1.2). These transients are reminiscent of mammalian K-complexes (1). As in mammals, all birds exhibited a 1/f type pattern, i.e. higher frequencies had lower power (Fig. A1.3).

We also observed instances when one eye was open and the other was closed. The hemisphere contralateral to the open eye displayed a low amplitude and high frequency EEG while the hemisphere contralateral to the closed eye displayed SWS oscillations (Fig. A1.2F). These instances of unihemispheric sleep were almost exclusively restricted to the light phase, and were especially frequent towards the end of the subjective day when birds had a greater tendency to nap (Table A1.1). Unihemispheric sleep is broadly observed in birds, cetaceans and other marine mammals (20, 23-24).

SWS and REM sleep were associated with specific circadian patterns, whose structure was not constrained by our classification

procedure for the epochs. There was an overall decrease in SWS density throughout the night (Figs. A1.4A, A1.7A, Table A1.1). REM episodes were typically brief early in the night and became longer throughout the night (Fig. A1.4C, A1.7C, Table A1.1) as the REM density increased (Figs. A1.4B, A1.7B, Table A1.1) and the inter-REM intervals decreased (Figs. A1.4D, A1.7D, Table A1.1). These features are similar to patterns of sleep staging in mammals (25-26). The total amount of REM sleep averaged 22.99 ± 3.83 % (mean ± S.E.M.) (Table A1.1) of the dark period, greater than reported in most avian sleep studies, including the few studies of oscines (13-14). The intermediate epochs were brief and numerous (Figs. A1.7 F,H, Table A1.1) and were usually more stable throughout the night than REM and SWS in terms of density, average episode duration and average number of episodes per hour. As is the case in mammals (3-4), the intermediate stage consistently acted as, but was not limited to, a transition phase between SWS and REM (Fig. A1.7G, Table A1.1).

Sleep patterning is thought to differ between birds and mammals. NREM and REM are known broadly among birds. The observation of REM sleep is by itself an insufficient basis to equate avian and mammalian sleep patterns, except to distinguish them from reptilian sleep (27), where REM is poorly established (28), but other similarities of sleep architecture in birds and mammals have not been well established. Avian REM periods are reported to be extremely brief and infrequent in most species hence “rudimentary” (12) with the exception that oscine passerines have more REM (13-14, 23, 29). Mammalian sleep has a circadian distribution, is triphasic and is associated with precise electroencephalograhic and spectral patterns. While birds exhibit a pattern of sleep closer to mammals than reptiles insofar as they both have SWS and REM, and circadian rhythms of SWS and REM, mammalian sleep also entails other features such as intermediate sleep, Gamma oscillations during REM sleep, K-complexes and Up and Down states which have set them apart from birds.

In contrast, the present study helps to bridge the gap between birds and mammals by highlighting a broad suite of characteristics of sleep

which mammals were not known to share with birds. These include the existence of similar spectral signatures, Delta (30) and Gamma interdigitations, overnight increases in REM associated with an elongation of REM episodes, IS (a transition state between SWS and REM, distinct from the drowsy state taking place during transitions from Waking to NREM (14), K-complexes, and other similarities. Moreover, the interdigitation between Delta and Gamma power activation described here (Fig. A1.1A) and K-complexes (Fig. A1.2D, Table A1.2) during sleep have been observed in – and sometimes specifically attributed to – the mammalian cortex (5-6, 19, 31) (Fig. A1.1B). In mammals these patterns have been associated with Up and Down states (19, 32), raising the question as to whether these patterns are also generated in the avian brain. Birds have a well-developed thalamus but are devoid of a neocortex. Therefore, a neocortex is not necessary for the development of complex sleep stages as defined by the systematic variation in EEG signals which we have observed. Our observation of K-complexes leaves open the possibility that these signals are not of cortical origin in mammals as has been suggested (5). Our results are therefore consistent with previous studies of K-complexes in reptiles (33) and non-laminar networks from

multiple species displaying increased power in a given frequency range due to network synchronization (34-40).

Recent observations of REM-like sleep in basal mammals (17) are consistent with the hypothesis that the characteristics of sleep in the amniotes leading to birds and mammals may have been more complex than has been generally assumed. One hypothesis is that REM is associated with greater connectivity in avian and mammalian forebrain as compared to reptiles that apparently lack REM (28). However, the complex sleep architecture we have observed in zebra finches has not been reported in the numerous non-oscine (non-songbird) species that have been examined (23) but is likely to be broadly shared across songbirds (13-14). Thus, this remarkable similarity of characteristics may have resulted from a convergent evolution in mammals and songbirds. It has been hypothesized that birds possess a mammalian cortex homolog (8-9). A specific form of this hypothesis homologizes regions of the avian forebrain with cortical layers (41). If so, then the patterns of cortical activation, interactions between thalamus and cortex, and the change in those patterns in response to changes in behavioral state, may be similarly

expressed in the avian forebrain. The developmental molecular basis conserving forebrain homologies, and potential homologies of sleep rhythms, between birds and mammals is not yet known.

The selective pressures that resulted in these features of sleep developing so prominently in songbirds but apparently not generally among birds remains unresolved. Juvenile song learning and adult territorial and mating behaviors involving song are complex sensorimotor skills and social behaviors proving strong selective pressures on songbirds. A causal link between song learning and associated behaviors and the complex sleep architecture we have described here remains speculative, and a viable alternate hypothesis is that there exists greater complexity to sleep structure broadly expressed across bird species than has commonly been recognized. The independent development of vocal learning in parrots and some hummingbirds (42) and application broadly across birds of the analysis procedures described herein, provides good material to test this hypothesis.

Materials and Methods

Experimental procedures were approved by the Institutional Animal Care and Use Committee at the University of Chicago. In preliminary acute experiments in urethane anesthetized animals, we determined coordinates for recording and ground platinum electrodes relative to the midsagittal sinus (in mm): (1.5R, 3L), (3R, 2L) and (0.5C, 0L). The electrode impedance was 90 kΩ measured in saline.

For chronic recordings, birds were briefly anesthetized (Equithesin) and L-shaped platinum electrodes were epidurally implanted, secured and attached to a head connector. In subsequent days, during recordings, a cable was attached linking the bird's head to an overhead mercury commutator (Drangonfly Inc, WV), allowing for free movement in the cage during data acquisition. Video recording was accomplished by an infrared (IR) light and an IR camera (Ikegama, Japan). Strategically placed mirrors facilitated detection of eye, head, and body movements. In one case the animal’s eyes were obscured from view for approximately 1 hr, but nevertheless the EEG signal was easy to score manually. EEGs

were amplified by 1K, sampled at 1 kHz and filtered at 1-100 Hz (with 60Hz notch filter, except for B133). In two birds (B133 and E1), which exhibited low frequency artifacts, the data was filtered at 2-100 Hz. For these birds, Delta was set at 2-4 Hz for the automated analysis.

As part of the automated analysis, EEGs were downsampled to 200 Hz and DC filtered. Spectral power was computed in μV^2 /Hz using 0.33Hz bins. For each epoch, the power differences in Delta power and in Gamma/Delta were computed over the preceding and successive epochs, using the Matlab "gradient" function. All clustering variables were normalized by z-scoring prior to the sleep stage classification. Following initial REM/NREM and SWS/NSWS classification, the score of each epoch was smoothed using a 5 second window in order to minimize the score contamination by brief artifacts which might not have been isolated by manual scoring. When artifacts occurring during sleep were manually labeled, the algorithm would score such an artifact according to the state of the following epoch unless the latter was awake, in which case the algorithm would assign the sleep artifact the score of the preceding epoch.

For bilateral recordings during the dark phase, the automated scoring algorithm filtered out epochs inconsistent with unihemispheric sleep. The small number of remaining epochs, in conjunction with simultaneous video recordings were subsequently examined manually to assess whether they constituted instances of unihemispheric sleep.

The data analysis technique we developed enabled us to resolve changes in power over a broad spectral range and a high temporal resolution, which were a key differentiating factor for automated REM sleep detection. This analysis was further corroborated by extensive manual scoring (Figs. A1.5, A1.8), which was restricted to identification of REM, NREM, awake and artifacts, distinctions and signals observable by inspection of the EEG and video. Moreover, the automated EEG scoring relied on whole night statistics (21) rather than on arbitrarily defined thresholds, maximum likelihood methods or supervised nonlinear classifiers all of which tend to reflect and impose a human bias on the data analysis.

The double separation used in the automated separation allows for a minimum of two categories (REM and SWS) and a maximum of four categories (REM, SWS, IS and the outliers which are unclustered). Therefore, the algorithm does not assume a fixed number of states. In that respect, running the algorithm on data without REM (and wakefulness) or SWS greatly shortened the length of the respective REM and SWS spears while removing IS from the data caused the algorithm to detect insignificant levels of IS.

Acknowledgements

The authors thank J. Aldana, D. Baleckaitis, M. Castelle, D. Nelson and J.-P. Spire for valuable technical assistance, J.-M. Fellous, L. Finelli, R. Kerr, D. Spencer and D. Vucinic for comments regarding the data analysis and C. W. Ragsdale and N. H. Shubin for comments on the manuscript. This work was supported by the Sloan-Swartz Center for Theoretical Neurobiology and the Swartz Foundation (P. Low), the Howard Hughes Medical Institute (T. Sejnowski), and the NIH and the Palmer Family Foundation (D. Margoliash). Experimental technique: P. Low (Salk); Implants for recordings presented in this chapter: S. Shank (U. Chicago), P. Low (Salk); Recordings presented in this chapter: S. Shank (U. Chicago); manual scoring of states and artifacts at 3 sec. resolution: S. Shank (U. Chicago); manual scoring of K-complexes: P. Low (Salk), I. Spokoyny (Salk); analysis: P. Low (Salk); Text: P. Low (Salk), S. Shank (U. Chicago), T. Sejnowski (Salk), D. Margoliash (U. Chicago). Figures and Tables: Sleep Parametric EEG Automated Recognition System (SPEARS) algorithm (except for Figure A1.8, courtesy S. Shank). SPEARS was conceived and created by P. Low at the

Salk Institute. The Salk Institute has filed patents covering this algorithm and is in licensing negotiations with NeuroVigil, Inc. a company founded by P. Low and T. Sejnowski.

References

1. A. Rechstchaffen, A. Kales, R. J. Berger, W. C. Dement, A. Jacobson, L. C. Johnson, M. Jouvet, L. J. Monroe, I. Oswald, H.P. Roffwarg, B. R. Roth, R. D. Walter, in *A Manual of Standardized Terminology, Techniques, and Scoring System for Sleep Stages of Human Subjects,* A. Rechstchaffen, A. Kales, Eds. (U.S. Government Printing Office, Washington D.C., 1968).

2. K. J. Maloney, E. G. Cape, J. Gotman, B. E. Jones, *Neuroscience* **76**, 541 (1997).

3. L. Glin, C. Arnaud, D. Berracochea, D. Galey, R. Jaffard, C. Gottesmann. *Physiol. Behav*. **50**, 951 (1991).

4. C. Gottesmann, *Neurosci. Biobehav. Rev*. **20**, 367 (1996).

5. F. Amzica, M. Steriade, *Neurosci.* **82**, 671 (1998).

6. A. Destexhe, T. J. Sejnowski, in *Thalamocortical Assemblies,* A. Destexhe, T. J. Sejnowski, Eds. (Oxford Univ. Press, Oxford, 2001) pp. 347-391.

7. W. H. J Nauta, H. J. Karten. In *The Neurosciences: Second Study Program,* F. O. Schmitt, Ed. (The Rockefeller Univ. Press, New York, 1970) pp. 7–26.

8. A. Reiner, D. J. Perkel, L. L. Bruce, A. B. Butler, A. Csillag, W. Kuenzel, L. Medina, G. Paxinos, T. Shimizu, G. Striedter, M. Wild, G. F. Ball, S. Durand, O. Güntürkün, D. W. Lee, C. V. Mello, A. Powers, S. A. White, G. Hough, L. Kubikova, T. V. Smulders, K. Wada, J. Dugas-Ford, S. Husband, K. Yamamoto, J. Yu, C. Siang, E. D. Jarvis, *J. Comp. Neurol.* **473**, 377 (2004).

9. E. D. Jarvis, O. Güntürkün, L. Bruce, A. Csillag, H. Karten, W. Kuenzel, L. Medina, G. Paxinos, D. J. Perkel, T. Shimizu, G. Striedter, J. M. Wild, G. F. Ball, J. Dugas-Ford, S. E. Durand, G. E. Hough, S. Husband, L. Kubikova, D. W. Lee, C. V. Mello, A. Powers, C. Siang, T. V. Smulders, K. Wada, S. A. White, K. Yamamoto, J. Yu, A. Reiner, A. B. Butler, *Nature Reviews* **6**, 151 (2005).

10. J. M. Wild, *J. Comp. Neurol.* **338**, 225 (1993).

11. C.V. Mello, G. E. Vates, S. Okuhata , F. Nottebohm, *J. Comp. Neurol.* **395**, 137 (1998).

12. C. Amlaner, N. J. Ball, in *Principles and Practice of Sleep Medicine*, M. Kryger, T. Roth, W. Dement, Eds. (Saunders, Philadelphia, ed. 2, 1994), pp. 81–94.

13. J. T. Szymczak, H. W. Helb, W. Kaiser, *Physiol. Behav.* **53**, 1201 (1993).

14. N. C. Rattenborg, B. H. Mandt, W. H. Obermeyer, P. J. Winsauer, R. Huber, M. Wikelski, R. M. Benca, *PLoS Biol.* **2**, E212 (2004).

15. I. Tobler, A. Borbély, *J. Comp. Physiol. [A]* **163**, 729 (1988).

16. T. Fuchs, J. J. Siegel, J. Burgdorf, V. P. Bingman, *Physiol. Behav.* **87**, 575 (2006).

17. J. M. Siegel, P. R. Manger, R. Nienhuis, H. M. Fahringer, T. Shalita, J. D. Pettigrew, *Neuroscience* **91**, 391 (1999).

18. D. J. Thomson, *Proc. IEEE* **70**, 1055 (1982).

19. A. Destexhe, D. Contreras, M. Steriade, *J. Neurosci*. **19**, 4595 (1999).

20. R. Kirov, S. Moyanova, *Neurosci. Lett.* **322**, 134 (2002).

21. D. Gervasoni, S. C. Lin, S. Ribeiro, E. S. Soares, J. Pantoja, M. A. Nicolelis, *J. Neurosci.* **24**, 11137 (2004).

22. R. R. Llinás, U. Ribary, *Proc. Natl. Acad. Sci. USA* **90**, 2078 (1993).

23. N. C. Rattenborg, C. J. Amlaner, in *Sleep Medicine,* T. L. Lee-Chiong Jr, M. J. Sateia, M. A. Carskadon, Eds. (Hanley & Belfus, Philadelphia, 2002), pp. 7-22.

24. O. I. Lyamin, L. M. Mukhametov, J. M. Siegel, *Arch. Ital. Biol.* **142**, 557 (2004).

25. L. Trachsel, I. Tobler, A. A. Borbély, *Am. J. Physiol. Regulatory Integrative Comp. Physiol.* **251**, 1037 (1986).

26. I. I. Tobler, P. Franken, L. Trachsel, A. A. Borbely, *J. Sleep Res.* **1**, 125 (1992).

27. J. A. Lesku, N. C. Rattenborg, C. J. Amlaner, in *Sleep: A Comprehensive Handbook,* T. J. Lee-Chiong, Ed. (Wiley, New Jersey, 2006), pp. 49-61.

28. J. M. Siegel, (1999) *in Handbook of Behavioral State Control*, R. Lydic, H. A. Baghdoyan, Eds. (CRC Press, Boca Raton, 1999), pp. 87-100.

29. N. C. Rattenborg, *Brain Res. Bull.* **69**, 20 (2006).

30. H. V. Twyver, T. Allison, *Exp. Neurol.* **35**, 138 (1972).

31. I. Timofeev, F. Grenier, M. Bazhenov, T. J. Sejnowski, M. Steriade, *Cereb. Cortex* **10**, 1185 (2000).

32. M. Steriade, F. Amzica, *Sleep Res. Online* **1**, 1 (1998).

33. L. De Vera, J. González, R. V. Rial, *Electroencephalogr. Clin. Neurophysiol.* **90**, 298 (1994).

34. G. Laurent, *Nat. Rev. Neurosci.* **3**, 884 (2002).

35. G. Laurent, H. Dawidowitz, H. *Science* **265**, 1872 (1994).

36. M. Stopfer, S. Bhagavan, B. H. Smith, G. Laurent, *Nature* **390**, 70 (1997).

37. K. MacLeod, G. Laurent, *Science* **274**, 976 (1996).

38. A. Gelperin, D. W. Tank, *Nature* **345**, 437 (1990).

39. G. Laurent, M. Naraghi, *J. Neurosci.* **14**, 2993 (1994).

40. K. MacLeod, A. Backer, G. Laurent, *Nature* **395**, 693 (1998).

41. H. J. Karten, *Proc. Natl. Acad. Sci. USA* **94**, 2800 (1997).

42. F. Nottebohm, *Amer. Nat*. **106**, 116 (1972).

Figure A1.1. Stage Separation in Zebra Finch Sleep. A) Delta power (top trace) and Gamma power (bottom trace) for 2 hours, represented in units of standard deviations from the mean which has been set to 0 (i.e., the whole Delta power time series and Gamma power time series have been normalized). The dots correspond to 3 second epochs, separated over 1 second increments. Z[variable] indicates that the variable has been z-scored. Delta and Gamma power activation interdigitate with SWS (blue) occurring in the Up states of Delta and Down states of Gamma whereas REM (red) occurs during the Down states of Delta and Up states of Gamma. The intermediate and awake states are in cyan and yellow respectively. The awake state had amplitudes in the Gamma range which were not always comparable to those of REM. Artifacts are not shown. B) Delta (0.1-4 Hz) and Gamma (16-75 Hz) power components from eight local field potentials (LFP) recording from cat cortex during 20 seconds of sleep. The interdigitation of low and high frequencies is seen here as in A. Adapted from (19).
C) One night of sleep is represented in a 3-D space spanned by Delta, Gamma/Delta and the power differences in Gamma/Delta. In this space, SWS (blue) forms a spear. IS and REM are shown in cyan and red, respectively. D) When the differences in Gamma/Delta in C) are replaced with the differences in Delta, REM sleep collapses into a spear. E-F. Separation of states in a reduced parameter space. A 5-dimensional space is reduced to three dimensions with PCA. REM (red), IS (cyan), SWS (blue) are spatially localized (E). REM and SWS form orthogonal planes and IS (cyan) corresponds to the warped region linking the two planes (F).

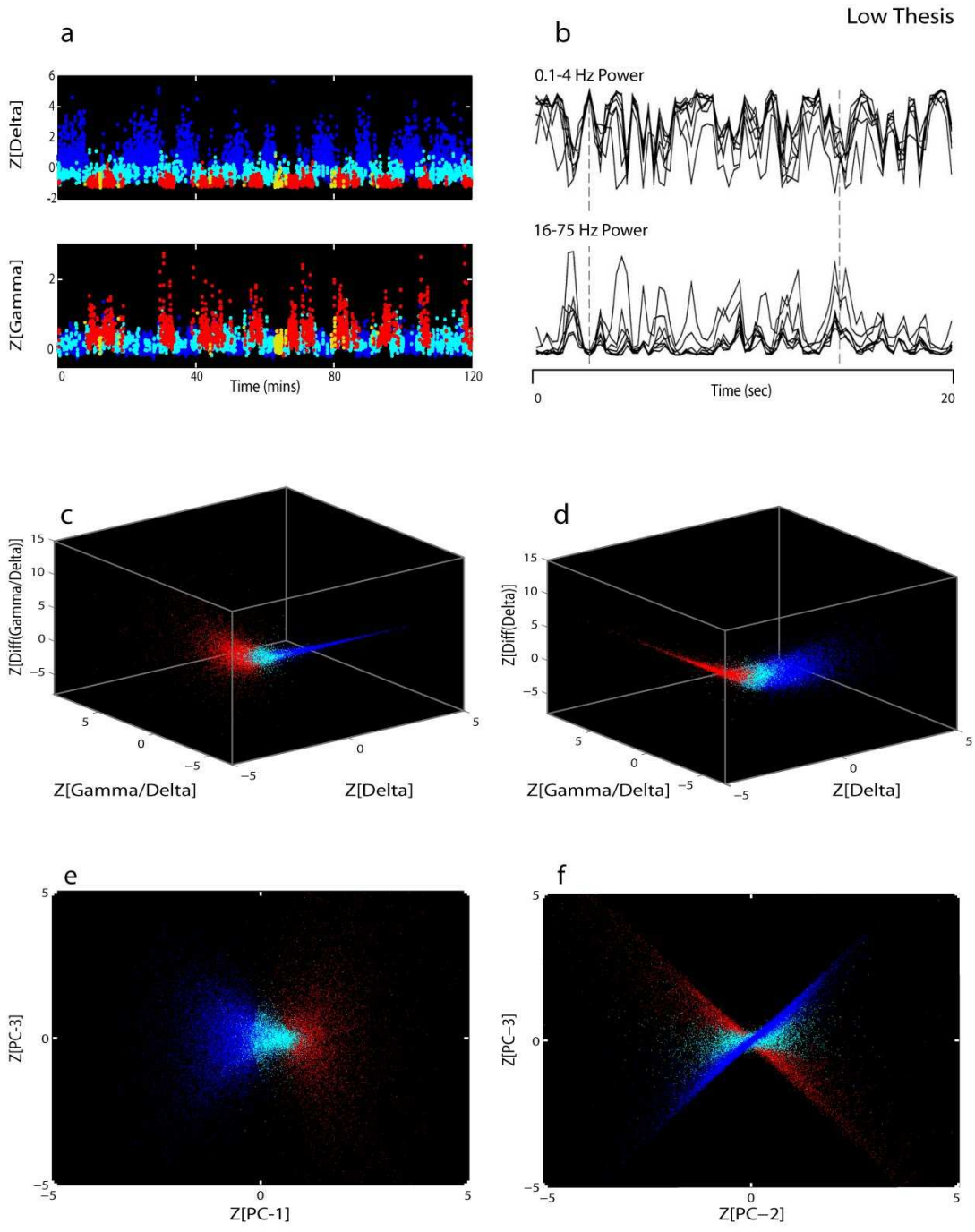
Low Thesis
a
b
Z[Delta]
Z[Gamma]
Time (mins)
0.1-4 Hz Power
16-75 Hz Power
Time (sec)
c
d
Z[Diff(Gamma/Delta)]
Z[Diff(Delta)]
Z[Gamma/Delta]
Z[Delta]
e
f
Z[PC-3]
Z[PC-1]
Z[PC−2]

Figure A1.1

Figure A1.2. Representative samples of Zebra Finch EEG Patterns. Representative EEG samples for SWS (A), REM (B), IS (C), a K-complex like transient (D), the awake state (E) and unihemispheric sleep (F). A-C and E were automatically generated using the MATLAB “silhouette” function on the scatter plot in Figures A1.1 E-F. A-E were chosen from W 147; F was chosen from B 133 which exhibited the most unihemispheric epochs (Table A1.1).

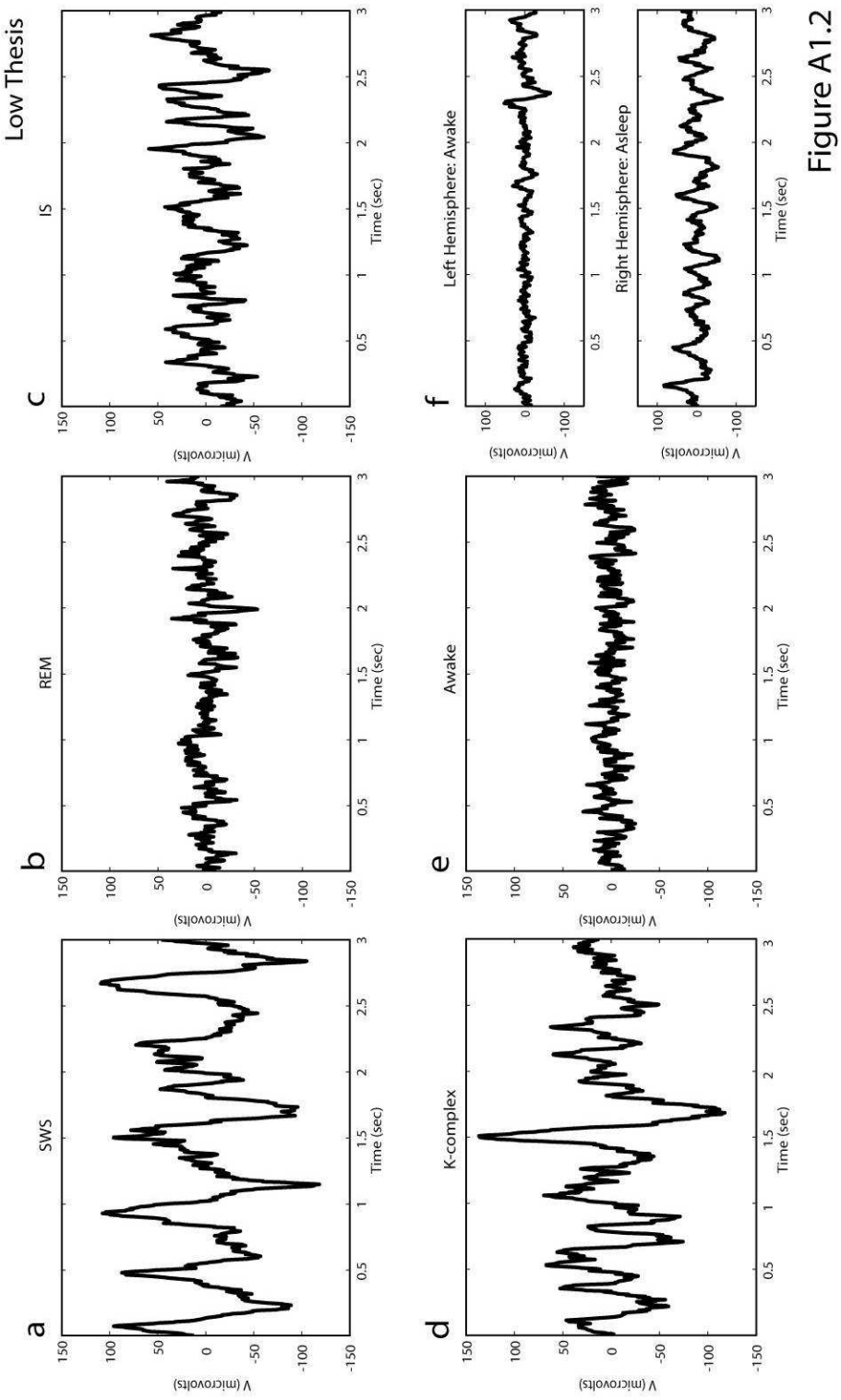
Low Thesis
a
SWS
b
REM
c
IS
d
K-complex
e
Awake
f
Left Hemisphere: Awake
Right Hemisphere: Asleep
V (microvolts)
Time (sec)

Figure A1.2

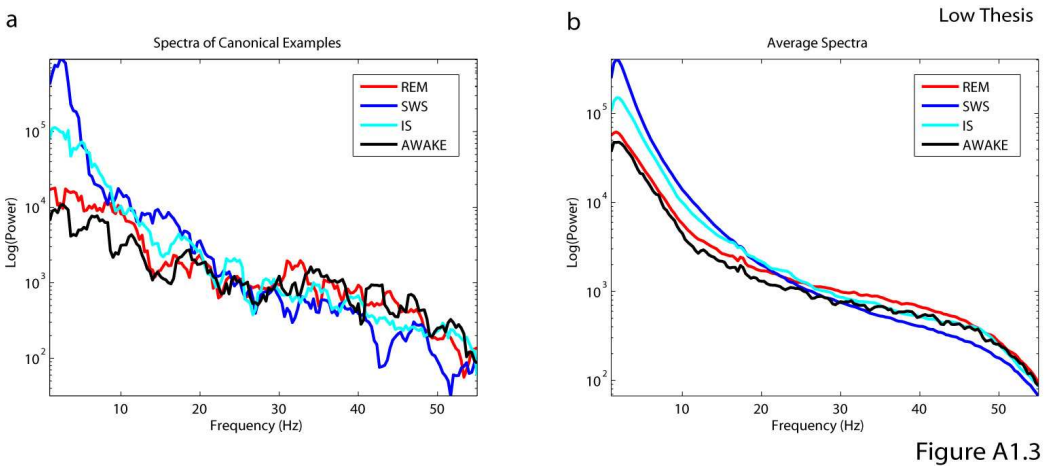

Figure A1.3. Representative Spectra of Zebra Finch EEG Patterns. Power Spectra. A) The log of the power (μV^2) vs frequency (0.33 Hz bins) for samples shown in Figure A1.2 A-C and E. B) The log of the average of the power in all 3 second windows scored as REM, SWS, IS and awake is shown across frequency.

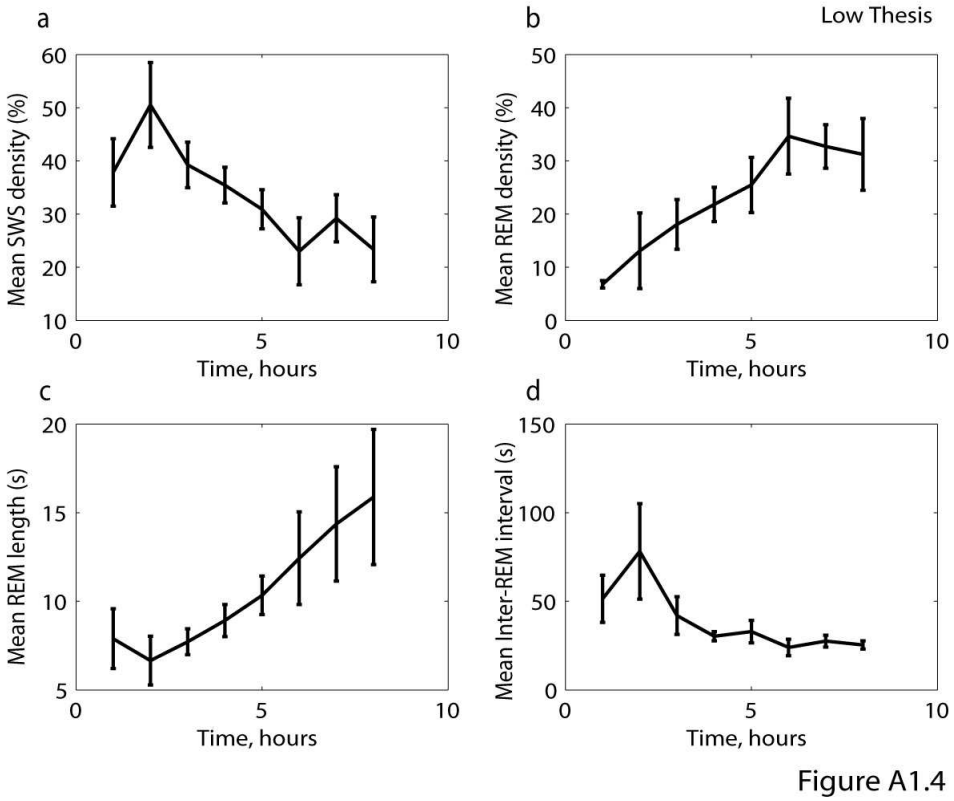

Figure A1.4. A Mammalian-like Distribution. A-D: Average stage statistics are plotted for each hour of the dark period for all birds. Birds exhibited a significant decrease in SWS density (A), a significant increase in REM sleep density (B) and average REM episode length (C) and a significant decrease in inter-REM intervals throughout the night. Bars correspond to the standard error of the mean. Individual data for each bird is plotted in Fig. A1.7.

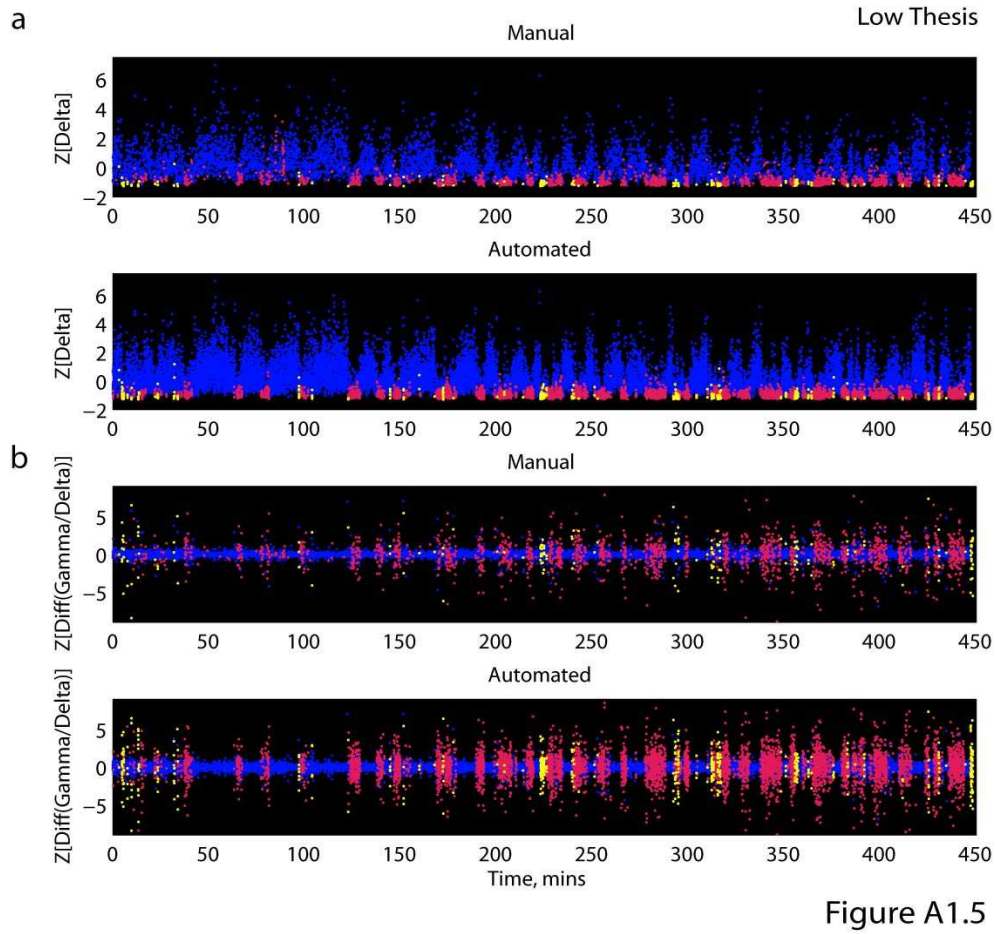

Figure A1.5. Manual and Automated Scoring of Zebra Finch Sleep. Manual (top traces) and automated (bottom traces) scoring of the same night. Delta and the difference in Gamma/Delta are shown in A and B, respectively. The traces corresponding to the automated scoring have 3 times as many points as those displaying the manual scoring. NREM, REM and awake periods are shown in blue, red and yellow, respectively.

Figure A1.6. Reduced Parameter Space. A-E: Reduced parameter space for W 147, F1, R 244, B 133 and E1, respectively. SWS, IS and REM are displayed in black, cyan and red, respectively.

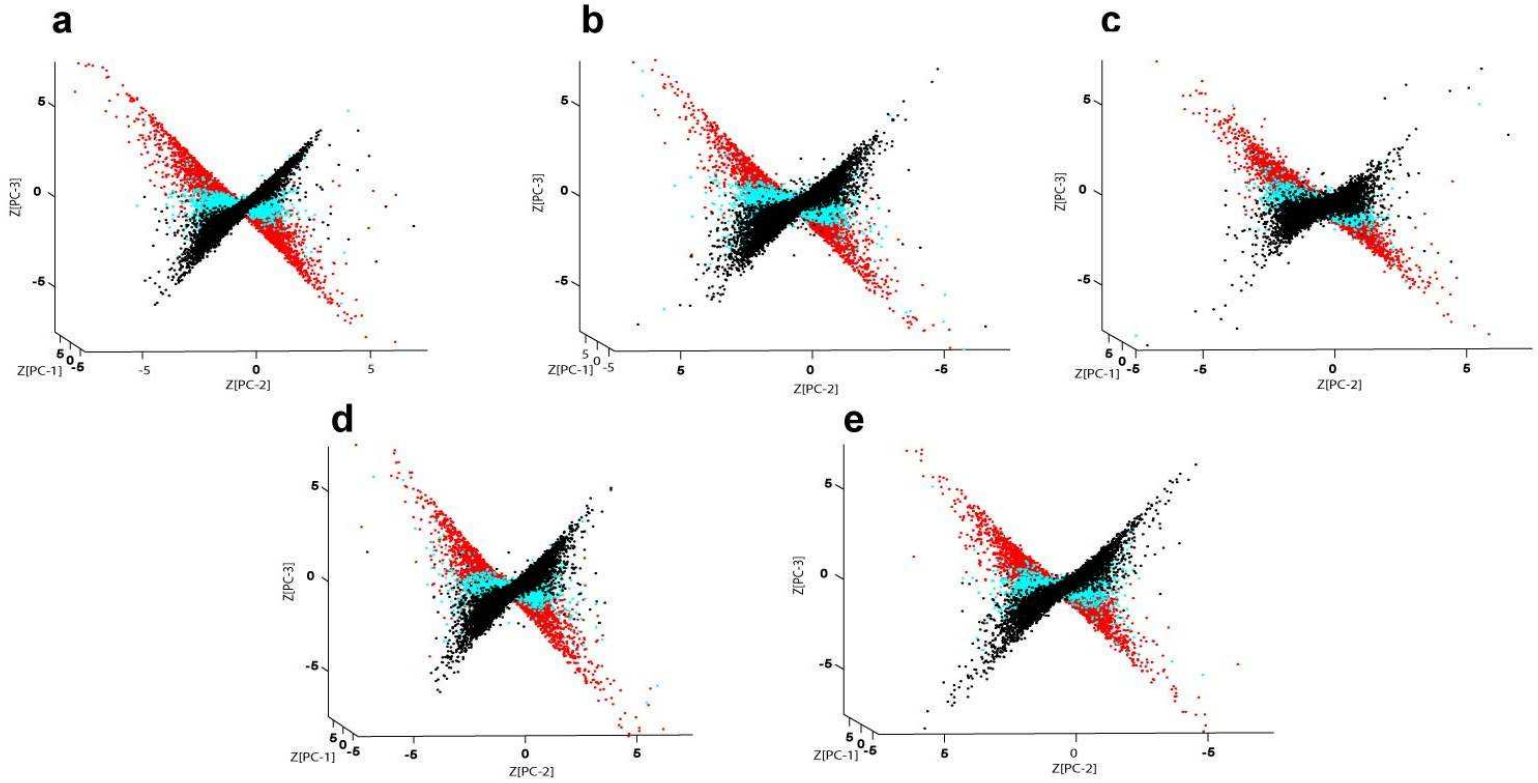

Figure A1.6

Figure A1.7. Detailed Mammalian-like Distribution Statistics.A Mammalian-like Distribution. A-D: Stage statistics are plotted for each hour of the dark period for all birds. 3 birds (W 147, E 1, F 1) exhibited a significant decrease in SWS density (A) throughout at least 7 consecutive hours. 4 birds (R 244 being the exception) exhibited a significant increase in REM sleep density (B) and average REM episode length (C) throughout at least 7 consecutive hours. Of these 4 birds, all except E1, exhibited a significant decrease in inter-REM intervals throughout the night. E-F: Comparing SWS, IS and REM for all birds. E. IS was shorter than SWS and REM (E) in all birds. Error bars correspond to the standard error of the mean. F. From left to right: percentage of SWS epochs followed by IS; percentage of IS epochs followed by SWS; percentage of REM epochs followed by IS; percentage of IS epochs followed by REM. In all birds, SWS and REM tended to be exclusively followed by IS which in turn would lead to SWS or REM. G. There were more IS episodes than there were SWS or REM episodes in all birds.

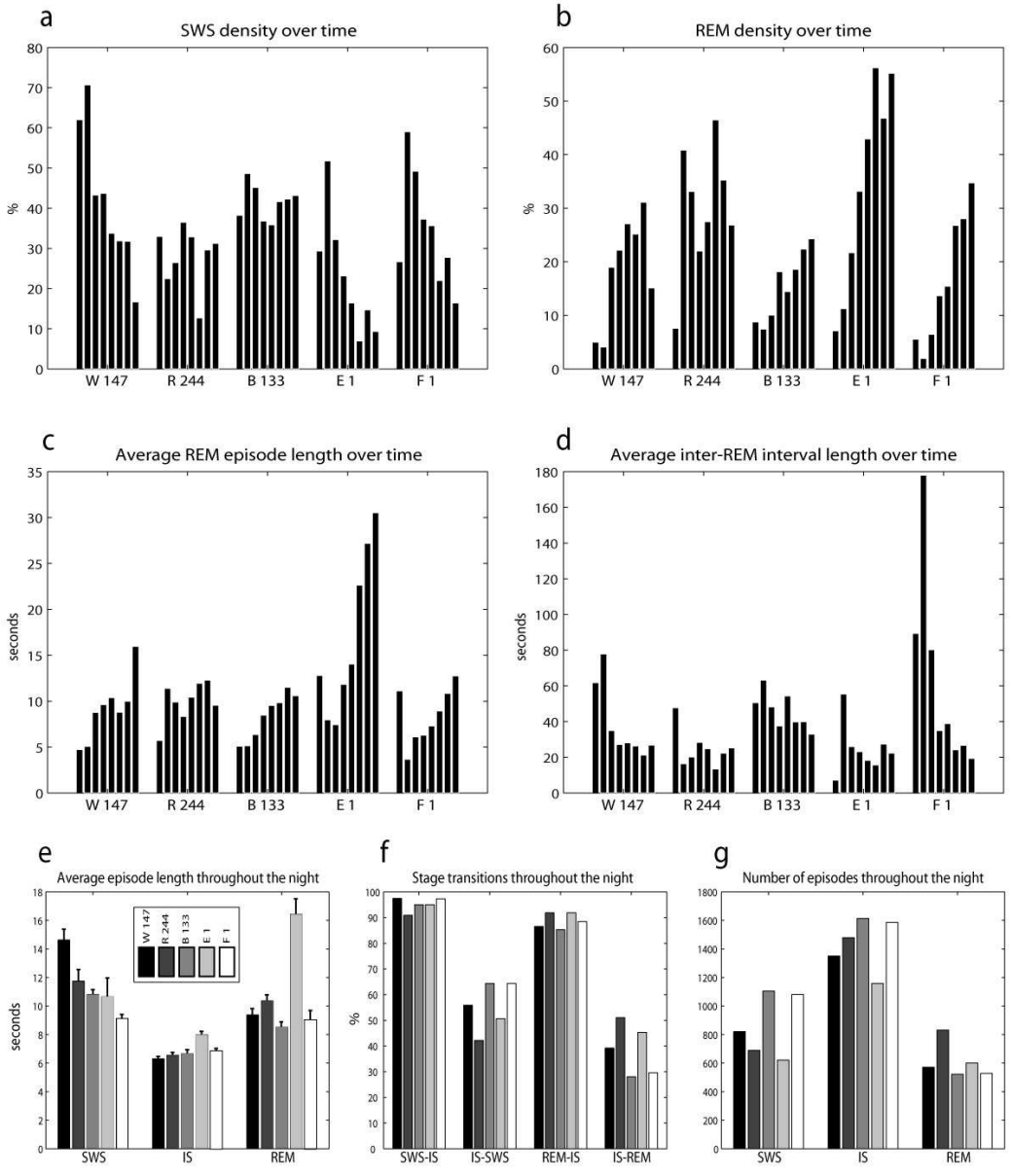
a
SWS density over time
%
W 147
R 244
B 133
E 1
F 1
b
REM density over time
%
W 147
R 244
B 133
E 1
F 1
c
Average REM episode length over time
seconds
W 147
R 244
B 133
E 1
F 1
d
Average inter-REM interval length over time
seconds
W 147
R 244
B 133
E 1
F 1
e
Average episode length throughout the night
seconds
W 147
R 244
B 133
E 1
F 1
SWS
IS
REM
f
Stage transitions throughout the night
%
SWS-IS
IS-SWS
REM-IS
IS-REM
g
Number of episodes throughout the night
SWS
IS
REM

Figure A1.7

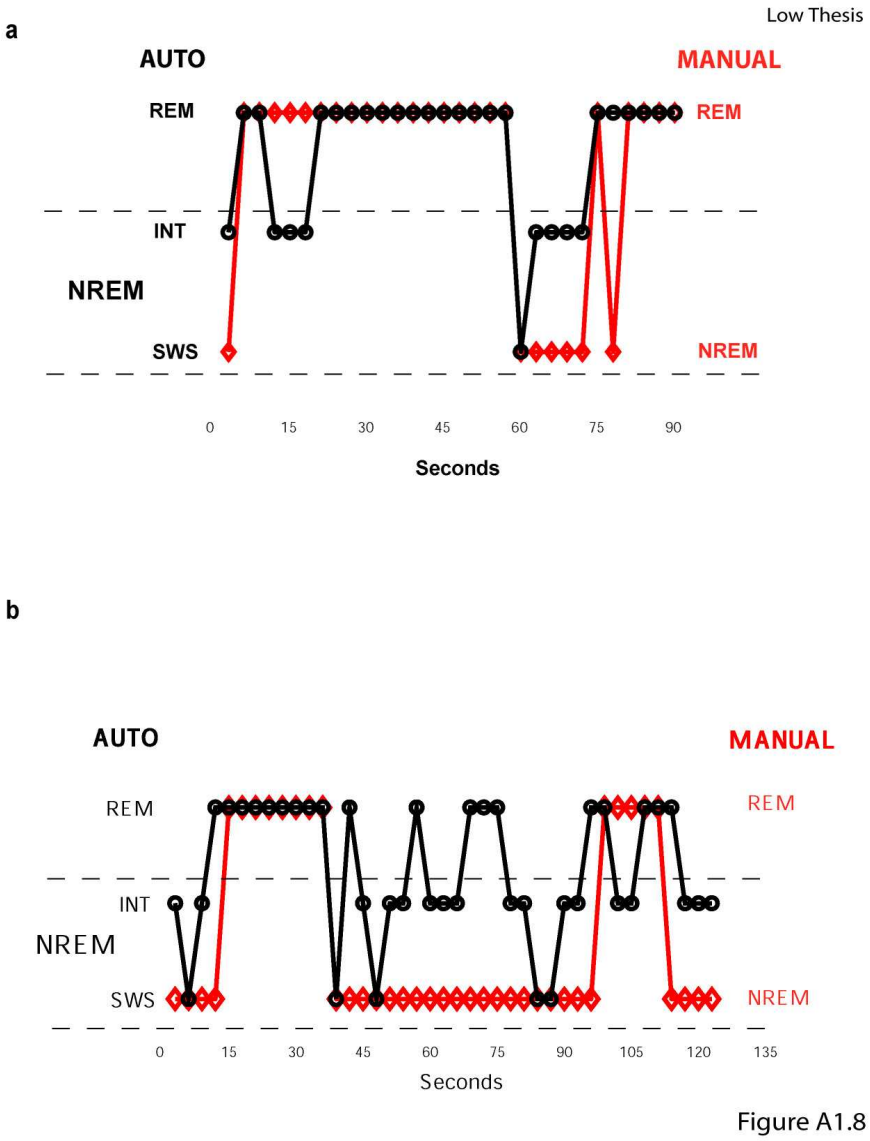

Figure A1.8

Figure A1.8. Two hypnograms showing automated (black) and manual (RED) scoring. The algorithm distinguishes between REM, IS (INT), outliers and SWS using a channel of EEG while the human scorer recognizes REM, NREM, wakefulness and artifacts using EEG and video. Human and automated classifications are performed at a 3 and 1 sec temporal resolution, respectively. Every third score is displayed for the hypnogram produced by the automated scoring. The agreements between automated and manual scoring are 86.7% (top) and 75% (bottom). Figures A and B correspond to supplementary videos 1 and 2, respectively. Drawings courtesy of Sylvan Shank, University of Chicago.

Table A1.1. Stage statistics for 5 nights of sleep in 5 birds. Stage density, average episode duration and number and stage transitions were determined. The percentage of transitions out of each stage towards the intermediate stage and the percentage of transitions out of the intermediate stage towards the other stages are shown. For the bihemispherically implanted birds (W147, R244 and B133), unihemispheric sleep is reported and the other statistics were computed over the hemisphere with the most reliable data as determined by visual inspection of the EEG and video and the absence of outliers. The coefficient of regression was computed over the stage densities and inter-REM intervals for each hour and reflect the circadian distribution of SWS and REM (* = [$r^2 > 0.5$ and $p < 0.05$], § = [$r^2 > 0.5$ and $p = 0.05$], £ for values calculated for hours 2-8, € for values calculated for hours 1-7). The agreement rate between automated and manual scoring was determined with and without artifact rejection.

Table A1.1 Stage Statistics	W 147	R 244	B 133	E 1	F 1
Stage Density (%)					
SWS	41.72	28.10	41.47	22.98	34.25
IS	29.51	33.72	37.29	32.12	37.74
REM	18.59	29.96	15.51	34.30	16.56
AWAKE	10.18	8.18	5.73	10.56	11.45
UNIHEM	0.09	0.59	0.65	N/A	N/A
OUTLIER	0.00	0.03	0.00	0.00	0.00
Average Episode Duration (sec)					
SWS	14.63	11.75	10.81	10.65	9.12
IS	6.30	6.56	6.66	7.98	6.85
REM	9.38	10.37	8.53	16.43	9.03
AWAKE	11.37	12.10	9.30	16.11	12.02
UNIHEM	3.38	3.89	3.13	N/A	N/A
OUTLIER	N/A	2.25	N/A	N/A	N/A
Number of Episodes					
SWS	821	689	1105	621	1081
IS	1350	1479	1613	1159	1586
REM	571	832	523	601	528
AWAKE	85	113	158	65	100
UNIHEM	8	44	60	N/A	N/A
OUTLIER	0	4	0	0	0
Transitions					
SWS → IS (% SWS)	97.44	90.86	95.02	95.00	97.32
REM → IS (% REM)	86.51	91.83	85.25	91.85	88.45
AWAKE → IS (% AWAKE)	65.48	76.99	74.68	27.69	67.68
IS → SWS (% IS)	55.93	42.15	64.35	50.65	64.38
IS → REM (% IS)	39.19	51.01	28.02	45.30	29.63
IS → AWAKE (% IS)	4.89	6.83	7.63	4.06	5.99
Regression Coefficients					
SWS Density (%/hour)	-6.62*****	-0.25	-0.11	-4.86*****	-6.64***£**
REM Density (%/hour)	4.59***€**	1.81	2.44*	7.47*****	4.73*****
REM avg. Episode Duration (sec/hour)	1.24**§**	0.47	0.98*****	3.19*****	1.4***£**
Inter-REM-interval (sec/hour)	-6.57*****	-1.81	-2.96*****	-0.84	-16.80*****
Agreement Rate (%)	90.86	77.41	90.87	72.88	89.49
Agreement Rate - No artifacts (%)	91.03	77.64	91.89	73.52	89.38

Table A1.2. Double-blind identification of K-complex signals in 2 birds. K-complexes were identified by two human scorers (“Scorer 1” and “Scorer 2”) who had access to EEGs but not to videos of sleeping finches. These scorers were blind to the vigilance state of the birds. Sleep stages were manually labeled by an automated algorithm (“Automated Classification”) and a third human scorer (“Manual Classification”), both blind to the K-complex analysis. The third human scorer had also access to video and he labeled artifacts. Amplitudes were calculated by measuring the peak to peak voltage deflection of the K-complex signals. Average amplitudes and durations are given with the standard error of the mean. “Scorer X – Scorer Y Agreement” corresponds to the percentage of signals chosen by Scorer X which Scorer Y also designated as K-complex signals. Signals which were identified as a K-complex by Scorer X only are listed under “Scorer X Outlier(s)”. K-complexes were found to occur predominantly in NREM sleep as determined by both automated and manual classifications. Only 4 out of 102 signals were associated with artifacts.

Table A1.2 K-complex	W 147	F 1
Number of Signals	64	13
Average Duration (msec)	448.67 ± 1.65	468.25 ± 7.86
Average Amplitude (μV)	116.81 ± 4.69	123.36 ± 11.85
Automated Classification		
SWS	57	12
IS	5	1
REM	0	0
AWAKE	2	0
Manual Classification		
NREM	58	12
REM	4	1
AWAKE	0	0
ARTIFACT	2	0
Scorer 1 - Scorer 2 Agreement (%)	74.42	92.86
Scorer 2 - Scorer 1 Agreement (%)	96.97	100
Scorer 1 Outlier(s)		
Number of Signals	22	1
Average Duration (msec)	493.44 ± 4.16	440
Average Amplitude (μV)	104.93 ± 8.94	93.87
Automated Classification		
SWS	12	1
IS	6	0
REM	4	0
AWAKE	0	0
Manual Classification		
NREM	15	1
REM	6	0
AWAKE	0	0
ARTIFACT	1	0
Scorer 2 Outlier(s)		
Number of Signals	2	0
Average Duration (msec)	390.94 ± 38.23	N/A
Average Amplitude (μV)	89.57 ± 12.67	N/A
Automated Classification		
SWS	1	N/A
IS	0	N/A
REM	0	N/A
AWAKE	1	N/A
Manual Classification		
NREM	1	N/A
REM	0	N/A
AWAKE	0	N/A
ARTIFACT	1	N/A

Chapter A1 is, in full, being prepared for publication. Co-authors are S. Shank, T. Sejnowski and D. Margoliash. The dissertation author was responsible for the techniques described and main observations therein and was the primary investigator and author of this paper.

CHAPTER A2

Fine Structure of Human Sleep

Traditional analysis of human sleep stages requires several channels of data and is usually performed by human scorers. Here we show that by representing each temporal window or epoch in a single channel of EEG by the frequency with the highest normalized power across the length of the entire signal, a new map of brain activity throughout time is generated that exhibits new features, independent of raw power, and allows Slow Wave Sleep (SWS), Intermediate Sleep (IS) and Rapid Eye Movement (REM) sleep states as well as Wakefulness (W) to be automatically clustered, consistent with manual scoring by experts, with high resolution. This analysis reveals that human REM sleep is not “awake-like” and therefore not paradoxical. These results have been validated on data collected with different instruments, in different labs and manually scored by different personnel.

The discovery of brain electrical potentials in animals (1) and later in humans (2) have provided physiologists and clinicians with the challenge to classify brain activity in separate stages. In 1937, a taxonomy

of human sleep was devised (3). This 5 stage taxonomy did not include Rapid Eye Movement (REM) sleep which was discovered in 1953 (4). Five years later, Dement and Kleitman (5) provided a description of sleep encompassing REM sleep and 4 non-REM (NREM) stages. In 1968, a committee led by Rechtschaffen and Kales devised “A Manual of Standardized terminology, Techniques and Scoring System for Sleep Stages of Human Subject” (R-K) (6) which provided continuity with the prior description of sleep stages established by Dement and Kleitman (5). R-K classifies human sleep into two Slow Wave Sleep (SWS) stages (Stages III and IV), two Intermediate Sleep stages (Stages I and II) and REM sleep. In this classification, SWS EEG is composed of moderate to large amounts of high amplitude, slow wave activity; REM displays relatively low voltage, mixed frequency EEG in conjunction with episodic REMs (Rapid Eye Movements) and low-amplitude electromyogram (EMG); IS has a relatively low voltage, mixed frequency EEG with stage II further displaying 12-14 Hz oscillations and brief high amplitude K-complexes; Wake EEG contains alpha activity and/or low voltage, mixed frequency activity. This characterization of sleep and waking stages has been highly influential in guiding sleep research. Recently, rules provided

by R-K were amended (7) and the stages II/IV distinction was removed, leaving 3 NREM stages. While it is expected that sleep scorers will adapt to the new system, the precise number of sleep stages is still very much a topic of discussion (8-10).

Given the variability of sleep structure both across and within individuals as well as subjective nature of human scoring (11-13), it is a difficult exercise to find thresholds or state transition statistics to objectively segment a night of sleep into distinct stages based on a “fixed” interpretation of R-K (9); nor have techniques such as supervised and unsupervised classifiers been successful at automatic sleep stage classification across multiple data sets using a single channel of either human or animal brain activity (14-17).

Because human EEG recordings are low-pass filtered by the skull, higher frequency signals detected in intracranial animals studies, such as the interdigitation of high and low frequencies during Up and Down SWS states (18) or the gamma oscillation during REM (19) have not been readily observed, but have been detected using magnetic measurements (20). The scalp recordings further give human EEGs a poor spatial resolution. Thus it is not known whether human SWS and REM are

spatially “synchronized” and “desynchronized”, respectively, as suggested by animal studies (18, 21). In view of these open questions, we sought a new mathematical framework with high spectral and temporal resolution, in which sleep stage information could be rapidly and reliably extracted from a single channel of EEG.

One channel of EEG (C3-A2 derivation) from twenty-six nights (8 hours each) of sleep was obtained from twenty-six different polysomnographic recordings conducted in twenty-six healthy human subjects. The EEG data and manual scoring was provided by the UCSD VA hospital in San Diego, CA, USA (n=6) and the Max-Planck Institute (MPI) for Psychiatry in Munich, Germany (n=20). Experimental procedures were approved by the Institutional Review Boards at each institution.

EEG data were collected at 256 Hz and bandpassed at 0.3-100Hz with a 60 Hz notch filter (UCSD) or collected at 250 Hz and bandpassed at 0.53-70 Hz (MPI). These recordings were amplified at 10 K and manually scored in 30 sec epochs in accordance with R-K. For each recording, the whole night spectrogram (WS, Fig. A2.7a) was computed

over 2 orthogonal tapers on 30 sec epochs using a standard multitaper technique (22). The power information was then normalized by z-scoring for each frequency bin (from 1 to 100 Hz, 30 bins per Hz) across time. This normalized spectrogram (NS) thus weights each frequency band equally. Each 30 second segment can then be represented by the frequency with the largest z-score. In this preferred frequency space (PFS), sleep and waking states broadly separated into different patterns (Figs. A2.1, A2.14, A2.15, A2.16 a,c, A2.20 a,c). W was always characterized by a band in alpha (7-12 Hz) and sometimes by a band in beta (15-25 Hz). IS exhibited prominent activity in the spindle frequencies (12-15 Hz). Surprisingly, REM was defined by compact bands in theta (4-8 Hz) and sometimes beta (15-25 Hz) frequencies whereas SWS was dominated by delta activity. When computed over overlapping 3 sec windows and a 1 sec sliding window, similar trends were visible in the PFS except that beta activity emerged in REM (Fig. 2). At that resolution, REM appears more “awake-like” than at a 30 sec resolution. However, at that resolution, all the sleep states whether they were identified manually or automatically had distinct signatures in the PFS (Table A2.1A).

At each time point, using z-scoring, one can normalize the NS across frequencies to create a doubly normalized spectrogram. In this space, bands apparent in the PFS still had positive values whereas dark regions tended to have negative values. By adding the 2NS values of frequencies that show up as bands in the PFS and subtracting those that do not, filters can be constructed that maximally separate states. One maximizes W (‘W filter”), another separates NREM from W and REM (‘NREM filter’) and a third distinguishes IS from SWS (‘SWS filter’) (See ‘Materials & Methods’). The output of these three filters spans a space in which the three broad sleep stages and W tend to separate (Figs. A2.73, A2.22-A2.23).

Interestingly, Stage I did not cluster in either space and SWS formed only one cluster (rather than two, one for Stage III and one for Stage IV). The latter is in accordance with the recent revision of R-K which abandoned the Stage III/ IV distinction (7). Manual scoring of Stages I and III was done in 30 sec increments. At that resolution, epochs manually labeled as Stage III could not be disambiguated from epochs manually labeled as Stage II or Stage IV in the majority of recordings (Table A2.2) and epochs manually labeled as Stage I could not be

distinguished from epochs manually labeled as Stage II, REM or W in most recordings (Table A2.3) in the PFS. Thus it is conceivable that Stages I and III are not sleep states per se and should at best be thought of as transitional rather than stationary states. However REM was easily distinguishable from Waking (Table A2.4). Thus, human REM sleep should no longer be thought of as “awake-like” or “paradoxical”.

A K-means clustering algorithm (Scheme A2.1) was applied to the spaces above to classify sleep. Even though the VA and MPI data were filtered differently, the general position of the sleep and waking clusters was similar across sets. Moreover, while the algorithm was optimized on the MPI data set, it performed at 80.6% on the VA data, which is unprecedented using a single channel of data and is similar to the performance of other algorithms using many more channels (17). The standard error of the mean was also lower for the VA set than the MPI set even though the former had 6 subjects and the latter had 20 subjects (1.73% vs. 1.78%, respectively). The average agreement rate with human scoring on the full data set was 77.58% on 4 stages (Tables A2.1A and A2.8). This striking concordance can be visualized by overlapping

automated and manually derived hypnograms, plots depicting sleep staging for a given subject for a given night (Figs. A2.4-A2.5). In two out of twenty-six recordings, it appeared that the algorithm was mislabeling the data and in these cases. While that data appeared different when compared to the rest of the data set, visualization of the manual scoring on the preferred frequency map did however show separate signatures for sleep and waking stages. On the VA data, when the algorithm's performance was compared against data rescored by the same person or scored by a more experienced scorer, the average agreement rate with the algorithm increased and was in the 82.4-83.3% range (Table A2.1B).

Further normalizations in time and frequency can be applied to the whole night spectrogram, at both a 30 sec (Figs. A2.7 a,c, A2.8) and a 1 sec resolution (Figs. A2.7 b,d, A2.9-A2.10). Here sleep and waking stages tile the entire 1-100 Hz spectrum with REM, W and IS exhibiting broadband patterns (Figs. A2.8, A2.9-A2.10 c-d).

In this space, one can measure the average spread in normalized power across time (temporal fragmentation) (Figs. 4, A2.16-A2.20 b,d, A2.21.) (See "Materials & Methods"). This analysis revealed a bimodal distribution for REM sleep. This pattern persisted when the frequency

range was narrowed to 4-40HZ (data not shown). The unstable part of REM accounted for (mean ± s.e.m) 26.18 ± 1.7 % of REM at a rate of 37.42 ± 2.70 epochs per night lasting an average of 36.18 ± 1.27 seconds and separated by an average of 129.08 ± 11.04 seconds of stable REM (Table A2.5). These components of REM do not correspond to tonic and phasic REM (Table A2.6) and exhibit different spectral signatures (Fig. S21). The unstable part of REM sleep was more likely to be confused with stage II than the stable part (Tables S9-10). In these cases some spindles and K-complexes in the presence of REM caused these epochs to be scored as stage II (Figs. A2.1-A2.2, A2.16) even though they would have been scored as REM at a finer temporal resolution _ R-K rules are such that no spindles or K-complexes can be separated by less than 3 minutes in REM (6). While K-complexes and spindles can be found in REM, according to the analysis presented here, these signals are not responsible for the bimodal temporal fragmentation pattern observed in REM since manually scored REM, presumably devoid of spindles and K-complexes, still exhibits this pattern (Figs. A2.4 a-b, A2.16-A2.20c, A2.21a, Table A2.9 right columns). Moreover, REM still exhibited a bimodal distribution on a spectrum without spindle frequency power (Fig.

A2.25). The temporal fragmentation is a measure sensitive to sudden changes in normalized power. Such changes can also be brought about by artifacts and the changes they produce will be all the more consequent in the background of a low power EEG. Therefore the possibility that artifacts of some sort are responsible for most if not all of the bimodal temporal fragmentation of REM should not be excluded. When epochs adjacent to epochs known to contain movement artifacts were discarded from the analysis as well as any epoch having a preferred frequency greater than 25 Hz, the percentage of unstable REM epochs was diminished even if the bimodal pattern could still be seen (Fig. A2.26). The bimodal pattern was even less apparent when more artifacts were isolated (Fig. A2.27-A.2-28). However when these artifacts were included in the fragmentation analysis, in 4 out of 6 cases (5 out of 6 cases when REM was visually identified by a second scorer), they accounted for a higher percentage of the non-fragmented portion of REM (6 out of 6 for automated scoring) and in all but two cases for manual scoring (non-fragmented portion of REM _71.91 % in subject 9 and 50.73% and 52.24% in subject 20, depending on the scorer) and in all but one case for automated scoring (non-fragmented portion of REM _ 75.9% in subject

9), they accounted for less than 50% of either portion of REM (Table A2.11). A nearest-neighbor analysis was performed on epochs which did not themselves include artifacts (Table A2.12). The fragmented portion of REM had almost in all cases more neighbors which contained an artifact than the non-fragmented portion, according to manual scoring (5/6 subjects for one scorer 6/6 subjects for the other). When REM was detected automatically, in most subjects, the majority of both the fragmented and non-fragmented epochs were devoid of neighboring artifacts. High-resolution 1 sec automated and manual analysis of these data will be necessary to identify EEG grapho-elements which might be responsible for the observed patterns and possibly a new state of sleep. In the meantime, the temporal fragmentation provides yet another variable wherein REM tends to be easily distinguished from both W and Stage I (Table A2.7).

The new methods introduced here recovered both known and novel signatures of sleep stages automatically. High gamma activity during wakefulness was recently reported in human electrocorticograms (23) and is present in our scalp recordings as well (Figs. A2.8-A2.10) though

precise quantifications have yet to be made. Importantly we have shown that a single channel of EEG was sufficient to decouple sleep and waking stages and these are clearly separable.

This study provides guidance in the debate concerning the number of human sleep stages and refutes the belief that REM sleep is “awake-like” or “paradoxical.” Although REM is known to exhibit theta, the clear REM/W separation (Figs. A2.1-A2.4, A2.11, A2.15, A2.18-A2.23, Tables A2.4, A2.7-A2.8) as well as between other stages is not apparent by eye or by previous analysis from a single channel of human EEG. The bimodal temporal fragmentation pattern of REM sleep is also striking (Figs. A2.4, A2.16-A2.21, Tables A2.5-A2.7).

Alternative electrophysiological derivations and placement have been of interest to sleep researchers and clinicians (24-26). The results reported here appear to generalize beyond the C3-A1 EEG derivation to alternative derivations, including even a single channel of EOG (Figs. A2.11-A2.13). Finally, these methods presents a rapid, economic and quantitatively rigorous alternative to manually scored sleep staging in both clinical and comparative research and should find many new applications.

Materials & Methods

The filters used in Figure Scheme A2.1 are as follows.

sws_filter=mean(2NS(≤3 Hz));

w_filter=mean(2NS(9-12Hz));

nrem_filter=mean(2NS(60-100Hz))+mean(2NS(3-4Hz))-[mean(2NS(12-14Hz))+mean(2NS(25-60Hz))+mean(2NS(15-25Hz))];

AA= mean(2NS(12-14 Hz));

BB= mean(2NS(15-25 Hz));

CC=mean(WS(≤3 Hz));

DD=mean(2NS(9-12HZ);

WS and 2NS correspond to the raw and doubly normalized spectrograms, respectively. The temporal fragmentation corresponds to the zscore of the mean of the absolute value of the temporal gradient of the spectrum normalized throughout time and frequency and was computed on a 1-100Hz range unless otherwise noted.

Acknowledgements

This work was supported by a predoctoral fellowship from the Sloan-Swartz Center for Theoretical Neurobiology at the Salk Institute and the Swartz Foundation (PSL) and by the Howard Hughes Medical Institute (TJS). The authors are grateful to S. Drummond, from the UCSD VA hospital and to F. Holsboer, T. Wetter, L. Friess from the Max-Planck Institute for Psychiatry (MPI) who have generously provided the data and associated scores used in this analysis. Recordings: U. Ambrosius (MPI), S. Litzenmaier (MPI), A. Schlosser (VA), R. Wong (VA); 30 sec manual scoring: R. Wehrle (MPI), A. Schlosser (VA), R. Wong (VA); 1 sec manual scoring: H. Mien (VA/Salk), I. Spokoyny (VA/Salk); artifacting: A. Schlosser (VA), R. Wong (VA); analysis: P. Low (Salk/UCSD); text: P. Low (Salk/UCSD), T. Sejnowski (Salk/UCSD); figures and tables: Sleep Parametric EEG Automated Recognition System (SPEARS) algorithm. SPEARS was conceived and created by P. Low at the Salk Institute. The Salk Institute has filed patents covering this algorithm and is in licensing negotiations with NeuroVigil, Inc. a company founded by the authors.

References

1. R. Caton, *Br. Med. J.* 2 (1875).

2. H. Berger, Arch. *Psychiatr. Nervenkr.* **97**, 6 (1929).

3. A.L. Loomis, E. N. Harvey, G. A. Hobart, *J. Exper. Psychol.* **21**, 127 (1937).

4. E. Aserinsky, N. Kleitman, *Science* **118**, 273 (1953).

5. W. Dement, N. Kleitman, *Electroenceph. clin. Neurophysiol.* **9**, 673 (1957).

6. A. Rechstchaffen, A. Kales, R. J. Berger, W. C. Dement, A. Jacobson, L. C. Johnson, M. Jouvet, L. J. Monroe, I. Oswald, H.P. Roffwarg, B. R. Roth, R. D. Walter, in *A Manual of Standardized Terminology, Techniques, and Scoring System for Sleep Stages of Human Subjects,* A. Rechstchaffen, A. Kales, Eds. (U.S. Government Printing Office, Washington D.C., 1968).

7. C. Iber, S. Ancoli-Israel, A. L. Chesson, S. F. Quan, in *The AASM Manual for the Scoring of Sleep and Associated Events: Rules, Terminology, and Technical Specifications,* (American Academy of Sleep Medicine, Westchester, IL, 2007).

8. T. Hori, M. Hayashi, T. Morikawa, in *Sleep Onset: Normal and Abnormal Processes.* R. D. Ogilvie, J. R. Harsh, Eds. (APA, Washington, 1994).

9. S. L. Himanen, J. Hasan, *Sleep Med. Rev.* **4**, 149 (2000).

10. B. Müller, W. D. Gäbelein, H. Schulz, *Sleep* **29**, 967 (2006).

11. J. T. Kelly, K. Reed, E. L. Reilly, J. E. Overall, *Clin. Electroenceph.* **16**, 16 (1985).

12. H. Danker-Hopfe, D. Kunz, G. Gruber G. Klösch, J. L. Lorenzo, S. L. Himanen, B. Kemp, T. Penzel, J. Röschke, H. Dorn, A. Schlögl, E. Trenker, G. Dorffner, *J Sleep Res.* **13**, 63 (2004).

13. A. Chediak, B. Esparis, R. Isaacson, L. De la Cruz, J. Ramirez, J. F. Rodriguez, A. Abreu, *J. Clin. Sleep Med.* **2**, 427 (2006).

14. S. Roberts, L. Tarrassenko, *IEE Proceedings-F* **139**, 420 (1992).

15. D. Gervasoni, S. C. Lin, S. Ribeiro, E. S. Soares, J. Pantoja, M. A. Nicolelis, *J. Neurosci.* **24**, 11137 (2004).

16. P. Anderer, G. Gruber, S. Parapatics, M. Woertz, T. Miazhynskaia, G. Klosch, B. Saletu, J. Zeitlhofer, M. J. Barbanoj, H. Danker-Hopfe, S. L. Himanen, B. Kemp, T. Penzel, M. Grozinger, D. Kunz, P. Rappelsberger, A. Schlogl, G. Dorffner, *Neuropsychobiology*. **51**, 115 (2005).

17. A. Flexer, G. Gruber, G. Dorffner, *Artif Intell Med.* **33**, 199 (2005).

18. A. Destexhe, D. Contreras, M. Steriade, *J. Neurosci.* **19**, 4595 (1999).

19. C. Gottesmann, *Neurosci. Biobehav. Rev.* **20**, 367 (1996).

20. R. R. Llinás, U. Ribary, *Proc. Natl. Acad. Sci. USA* **90**, 2078 (1993).

21. A. Destexhe, T. J. Sejnowski, in *Thalamocortical Assemblies,* A. Destexhe, T. J. Sejnowski, Eds. (Oxford Univ. Press, Oxford, 2001) pp. 347-391.

22. D. J. Thomson, *Proc. IEEE* **70**, 1055 (1982).

23. R. T. Canolty, E. Edwards, S. S. Dalal, M. Soltani, S. S. Nagarajan, H. E. Kirsch, M. S. Berger, N. M. Barbaro, R. T. Knight, *Science* **313**, 1626 (2006).

24. R. J. Dyson, C. Thornton, C. J. Doré, *Sleep* **7**, 180 (1984).

25. B. van Sweden, B. Kemp, H.A. Kamphuisen, E.A.Van der Velde, *Sleep* **13**, 279 (1990).

26. J. Virkkala, J. Hasan, A. Värri, S. L. Himanen, M. Härmäet, *J. Neurosci. Methods* **163**, 137 (2007).

Figure A2.1. Preferred frequency space. The preferred frequency space was computed at a 30 sec resolution on two sleep recordings from two different subjects (a-b VA, c-d MPI). Each dot corresponds to 30 seconds of EEG. The labels were drawn either directly from the manual scoring (a,c) or the automated algorithm (b,d). SWS, IS, REM and W are depicted in white, cyan, red and yellow, respectively. The white diamonds correspond to epochs wherein movements were preventing the human scorers from assessing the sleep or waking state of the subject (legend the same throughout all figures unless otherwise specified). The algorithm is able to make such an assessment despite these artifacts. Notice the discrepancy between the human and automated scores towards the end of the night in the recording on the left panels. When this portion of the data was reanalyzed by visual inspection, the human scorer did find traces of REM, in accordance with the automated classification (in order to avoid any bias towards the automated method, the original human scores were used in comparisons between automated and manual scoring (Tables A2.1A and A2.8)).

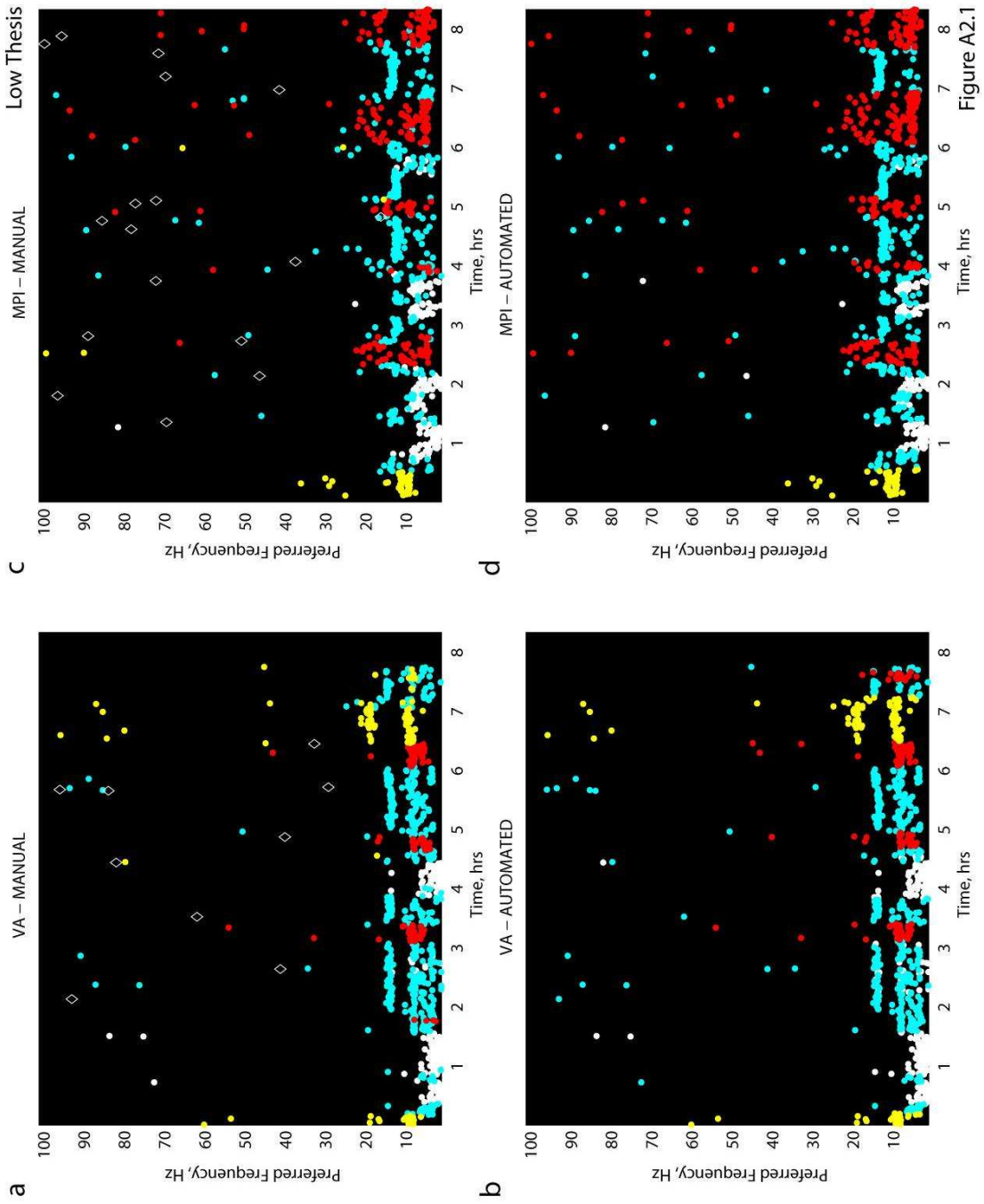
a
VA – MANUAL
b
VA – AUTOMATED
c
MPI – MANUAL
Low Thesis
d
MPI – AUTOMATED
Preferred Frequency, Hz
Time, hrs

Figure A2.1

Figure A2.2. Preferred frequency space (High Temporal Resolution). Same data as in Figure A2.1, computed at a 3 sec spectral resolution over 1 sec increments. Beta bands in REM are becoming visible in the VA data. Other features such as 60 Hz noise are also visible. These tend to be more visible when the EEG has less overall power.

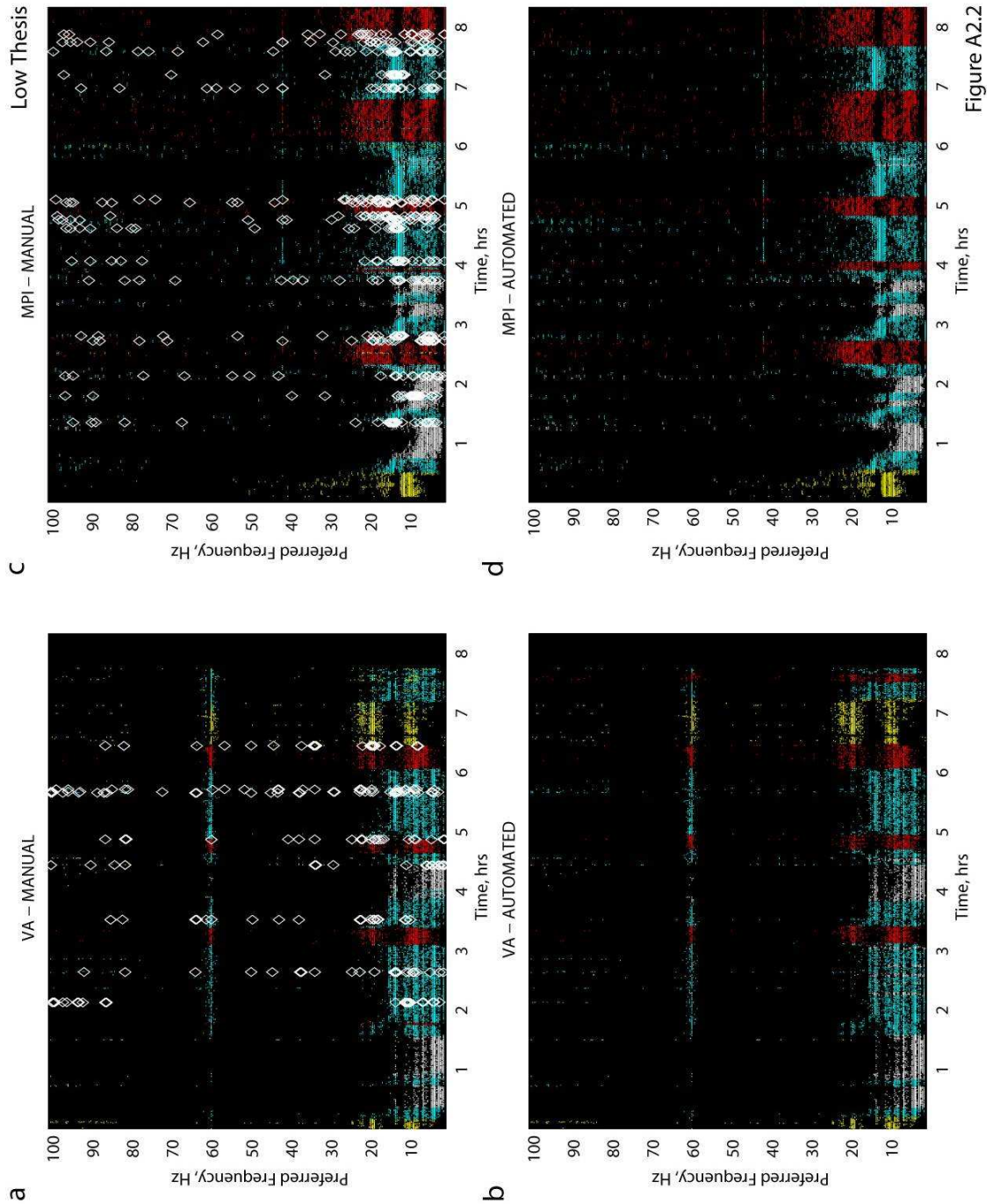
a
VA – MANUAL
b
VA – AUTOMATED
c
MPI – MANUAL
Low Thesis
d
MPI – AUTOMATED
Preferred Frequency, Hz
Time, hrs

Figure A2.2

Figure A2.3. Clustering subspace. A subspace of the clustering space is shown for two different sleep recordings from two different subjects (a-b, c-d). Each dot corresponds to 30 seconds of EEG. Labels are drawn from either manual (a,c) or automated (b,d) scoring. Sleep and waking stages tend to localize in different regions. The separation for the subject on the left is more apparent in Figure A2.23.

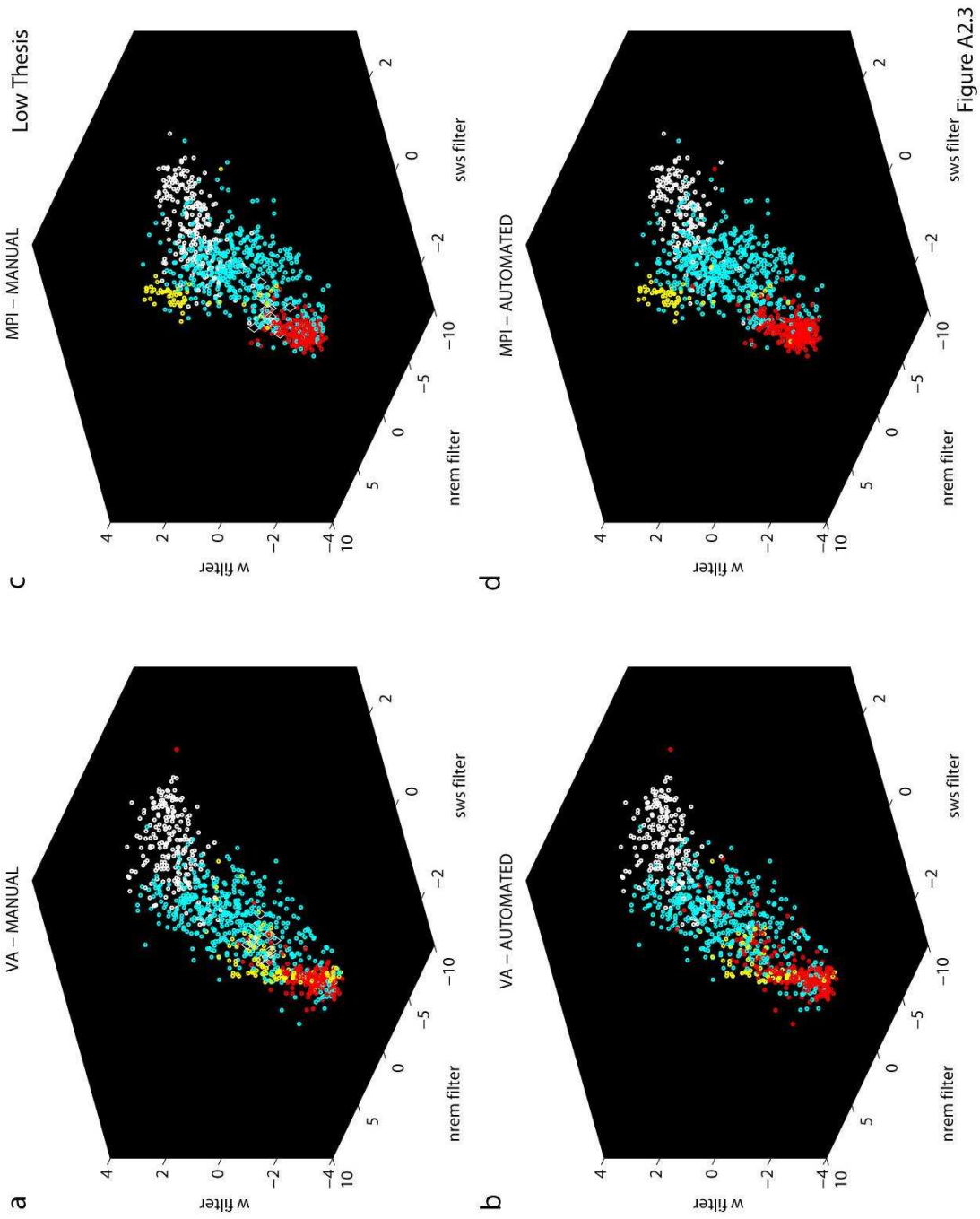
a
VA – MANUAL
b
VA – AUTOMATED
c
MPI – MANUAL
Low Thesis
d
MPI – AUTOMATED
w filter
nrem filter
sws filter

Figure A2.3

Figure A2.4. Bimodal Temporal Fragmentation of REM sleep. The temporal fragmentation was computed at a 30 second resolution for two different sleep recordings of two different subjects (a-b, c-d). Labels are drawn from either manual (a, c) or automated (b, d) scoring. REM sleep, in red, split into two different groups with either high or low temporal fragmentation. This was apparent here in both recordings, independently of whether the human or algorithm performed the scoring.

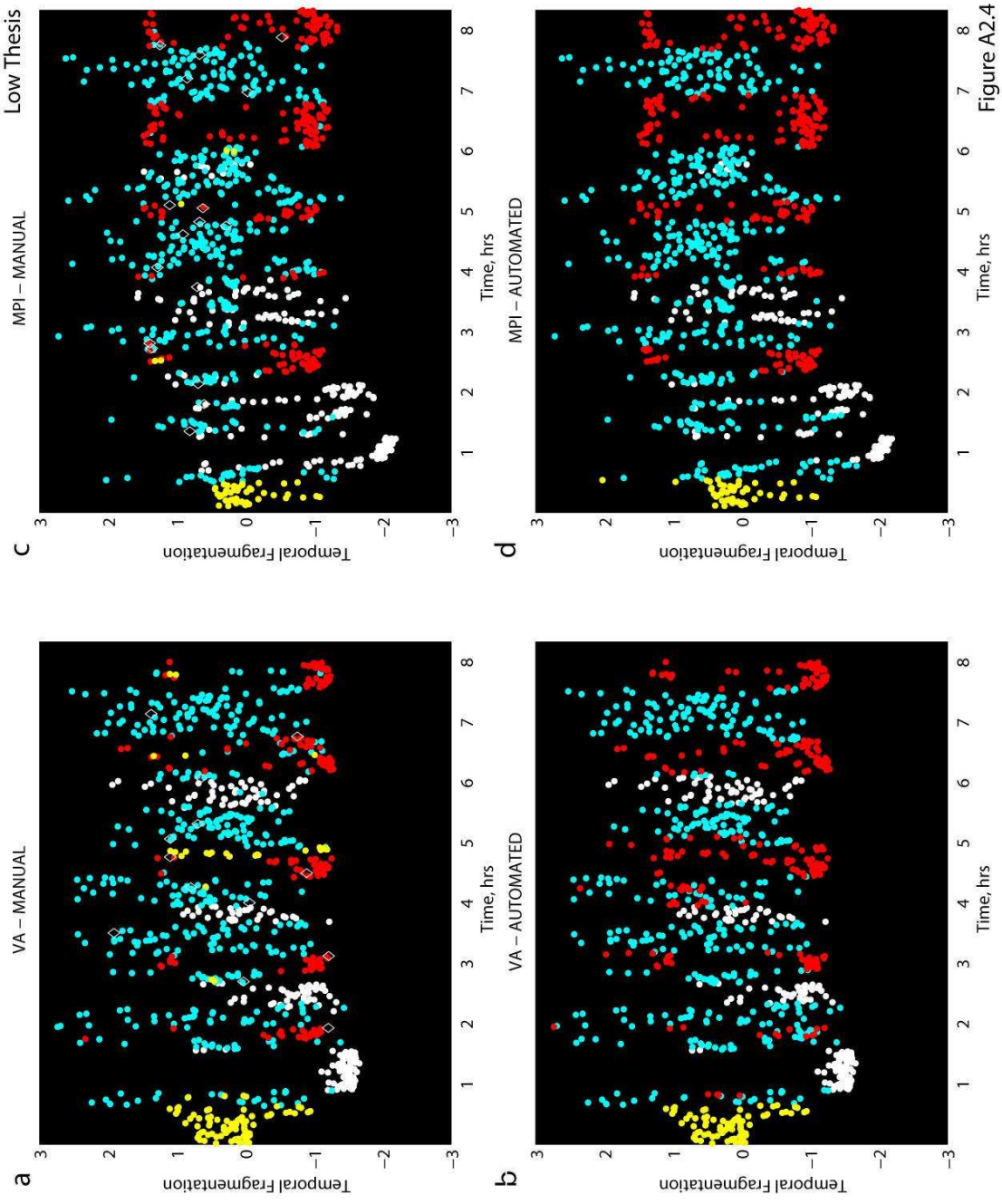
Low Thesis
a
VA – MANUAL
b
VA – AUTOMATED
c
MPI – MANUAL
d
MPI – AUTOMATED
Temporal Fragmentation
Time, hrs

Figure A2.4

Figure A2.5. Hypnograms. Hypnograms were computed for 4 different subjects (1 recording per panel). D and M correspond to times during which the subject was disconnected from the recording equipment or moving, respectively. The algorithm computed a W, REM, IS or SWS assignment instead of M. Manual and automated scoring are in red and blue, respectively. The red and blue hypnograms are mostly overlapping which signifies that the manual and automated scoring were in high agreement.

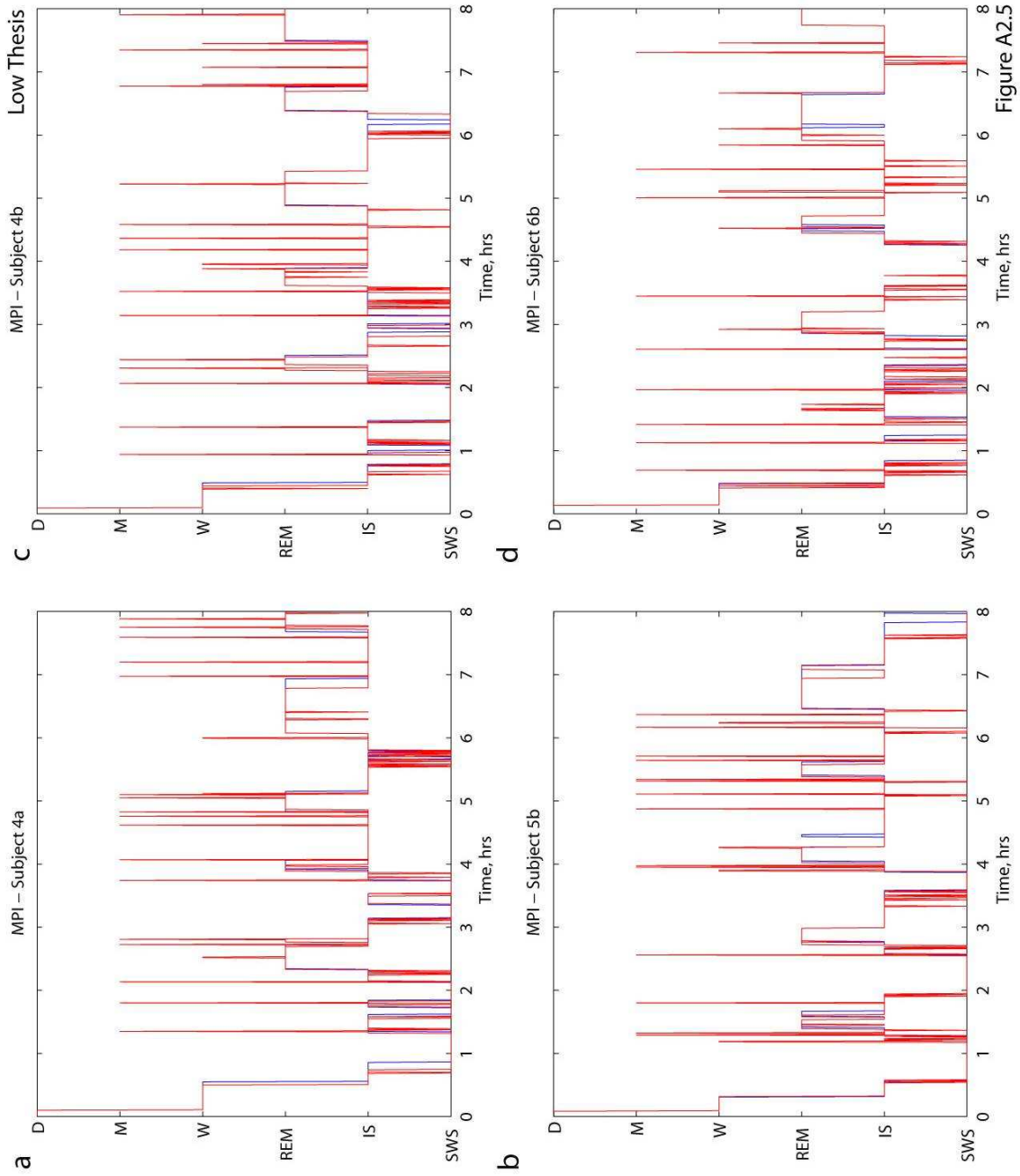
a
MPI – Subject 4a
c
MPI – Subject 4b
Low Thesis
b
MPI – Subject 5b
d
MPI – Subject 6b
D
M
W
REM
IS
SWS
Time, hrs
0
1
2
3
4
5
6
7
8

Figure A2.5

Figure A2.6. Hypnograms. Hypnograms were computed for 4 different subjects (1 recording per panel). D and M correspond to times during which the subject was disconnected from the recording equipment or moving, respectively. The algorithm computed a W, REM, IS or SWS assignment instead of M. Manual and automated scoring are in red and blue, respectively. The red and blue hypnograms are mostly overlapping which signifies that the manual and automated scoring were in high agreement. Note that because the automated procedure does not rely on fixed transition probabilities between states, it can perform well on unusual patterns such as the frequent awakenings presented by the subject in Figure A2.6d.

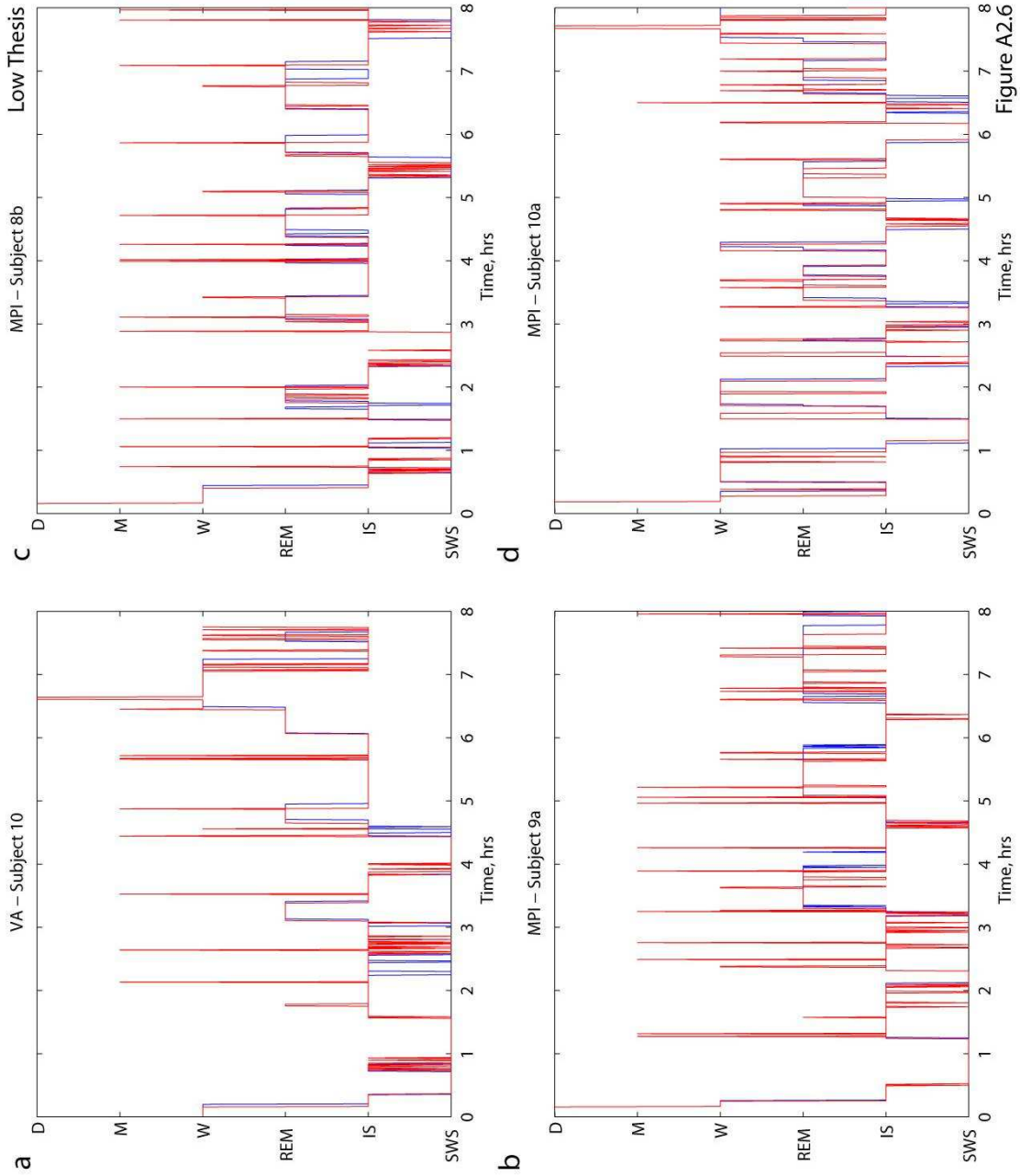
a
VA – Subject 10
b
MPI – Subject 9a
c
MPI – Subject 8b
Low Thesis
d
MPI – Subject 10a
D
M
W
REM
IS
SWS
0
1
2
3
4
5
6
7
8
Time, hrs

Figure A2.6

Figure A2.7: Raw and Normalized Spectrograms. Raw spectrogram were calculated at 30 sec (a) or at a 3 sec spectral resolution over 1 sec increments (b). Each spectrogram was then normalized across time and frequency several times yielding a normalized spectrogram at 30 sec resolution (c) and another one at a 3 sec spectral resolution over 1 sec increments (d). While only movement artifacts have high frequency (>20 Hz) content in the raw data (a-b), the normalized spectrograms have much more high frequency activity (c-d).

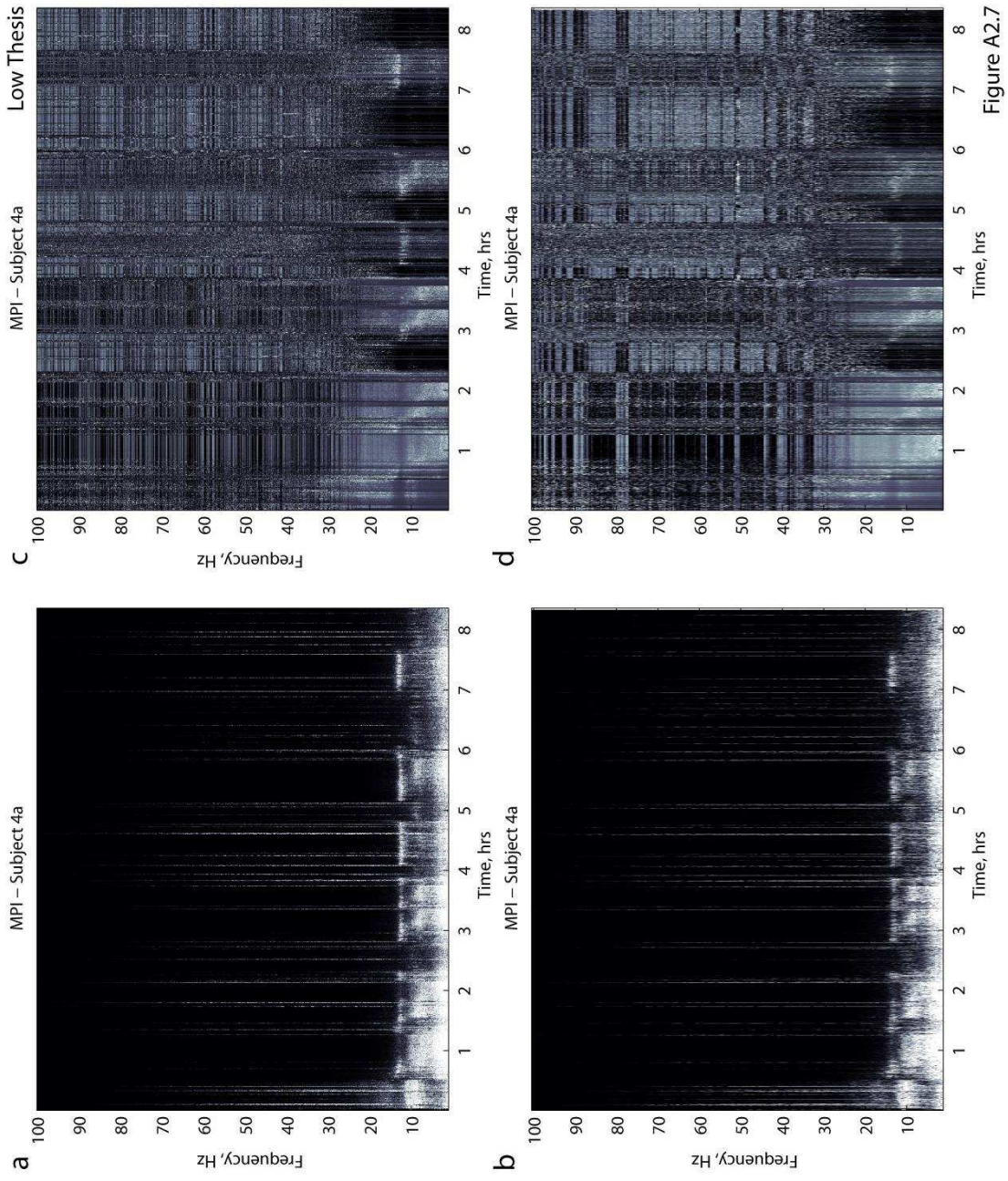
a
MPI – Subject 4a
Frequency, Hz
Time, hrs
b
MPI – Subject 4a
Frequency, Hz
Time, hrs
c
MPI – Subject 4a
Low Thesis
Frequency, Hz
Time, hrs
d
MPI – Subject 4a
Frequency, Hz
Time, hrs

Figure A2.7

Figure A2.8: Preferred frequency analysis over a spectrogram with multiple normalizations at high temporal resolution. a, b same as Fig. A2.3 b and d, respectively. The analyses from Figure A2.4 a and b were respectively applied to a and b to yield c and d, respectively. The trends observed in Fig. A2.4 are reinforced at this temporal resolution. High-frequency information is also visible for SWS.

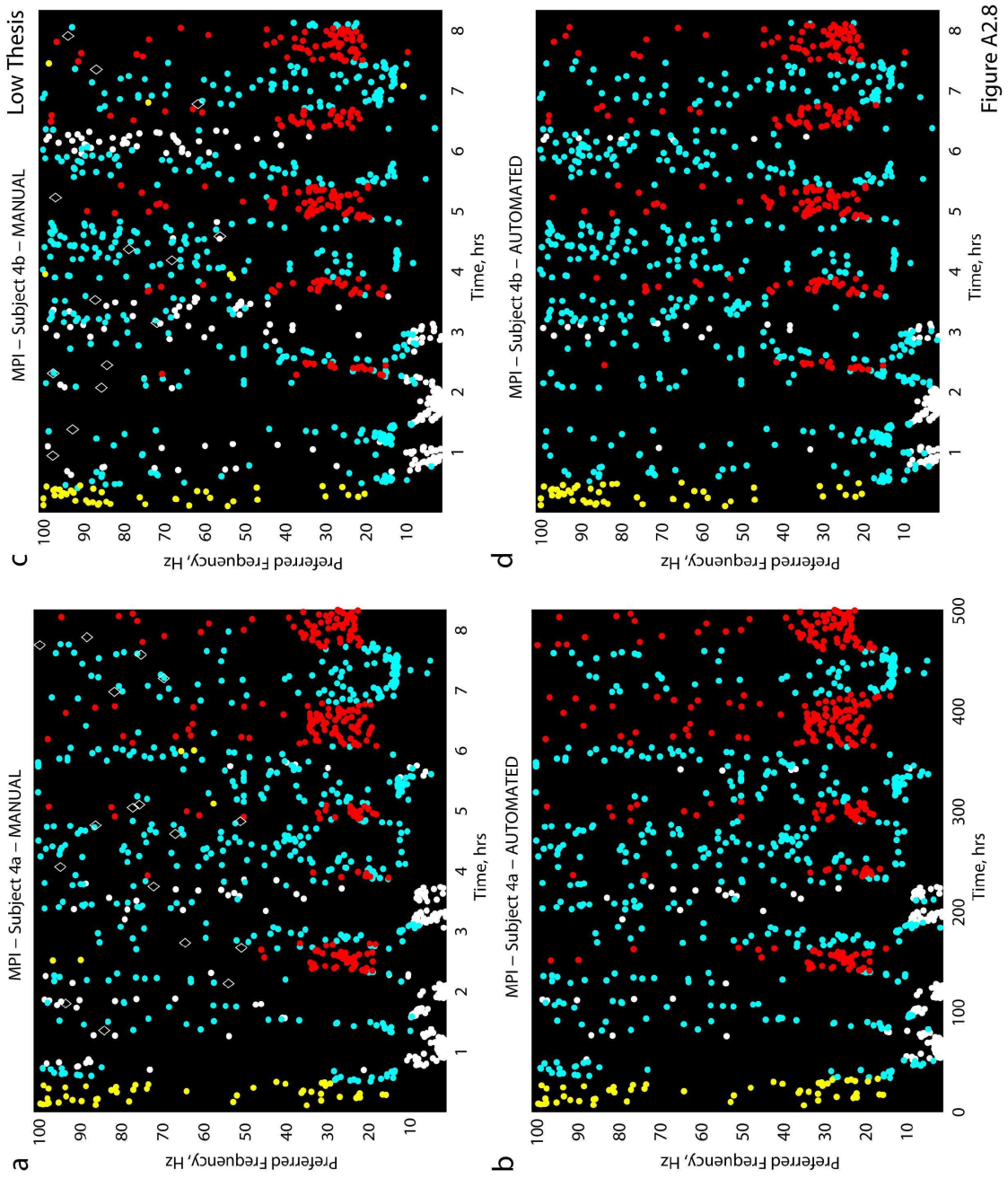
a
MPI – Subject 4a – MANUAL
Preferred Frequency, Hz
Time, hrs
b
MPI – Subject 4a – AUTOMATED
Preferred Frequency, Hz
Time, hrs
c
MPI – Subject 4b – MANUAL
Low Thesis
Preferred Frequency, Hz
Time, hrs
d
MPI – Subject 4b – AUTOMATED
Preferred Frequency, Hz
Time, hrs

Figure A2.8

Figure A2.9. Preferred frequency analysis over a spectrogram with multiple normalizations at high temporal resolution. a, b same as Figure A2.7 b and d, respectively. The analyses from Figure A2.8 a and b were respectively applied to a and b to yield c and d, respectively. The trends observed in Figure A2.8 are reinforced at this temporal resolution. High-frequency information is also visible for SWS.

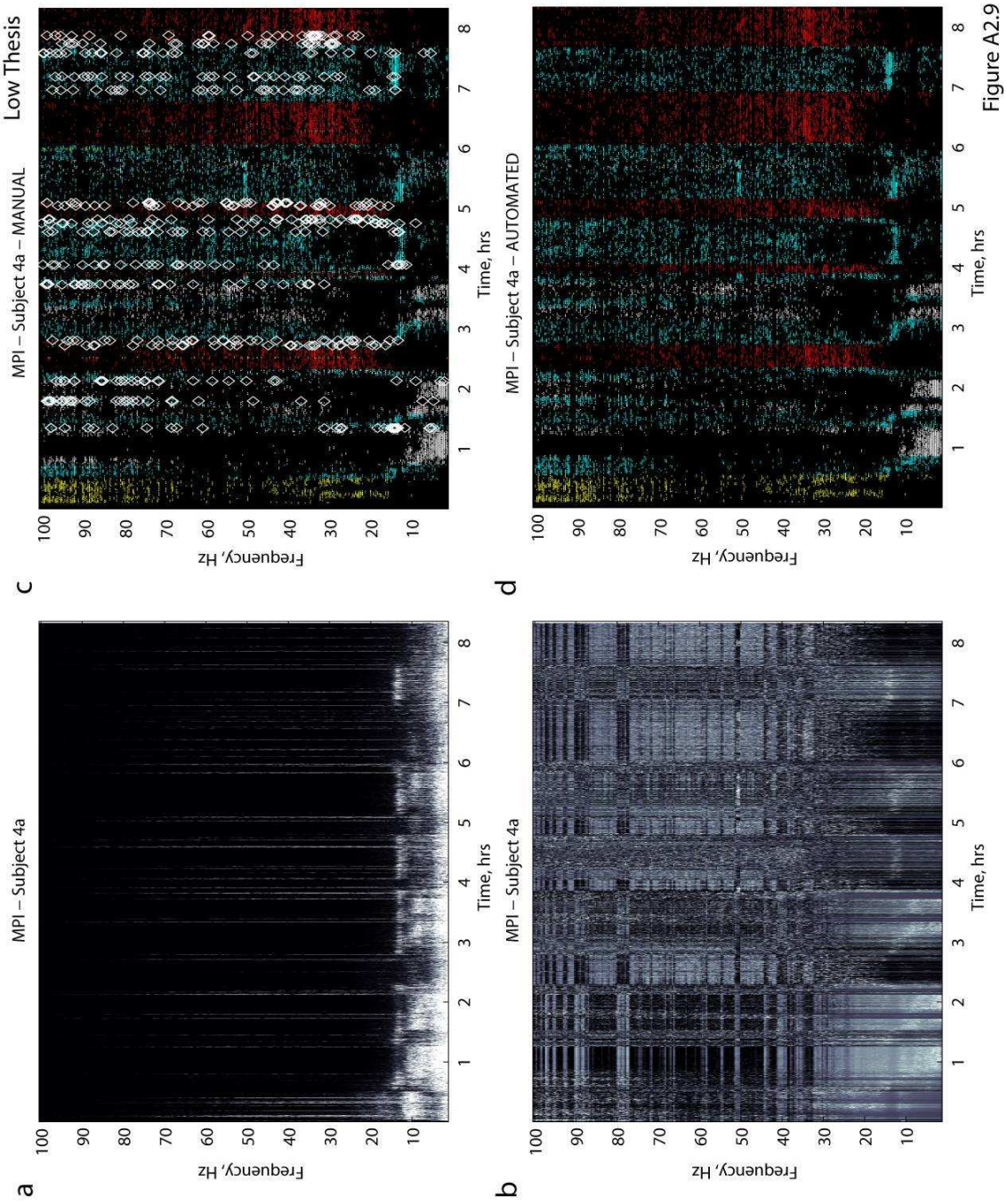
a
MPI – Subject 4a
Frequency, Hz
Time, hrs
b
MPI – Subject 4a
Frequency, Hz
Time, hrs
c
MPI – Subject 4a – MANUAL
Low Thesis
Frequency, Hz
Time, hrs
d
MPI – Subject 4a – AUTOMATED
Frequency, Hz
Time, hrs

Figure A2.9

Figure A2.10. Preferred frequency analysis over a spectrogram with multiple normalizations at high temporal resolution. Same analysis as in Figure A2.9 but for another subject. 60 Hz noise is visible.

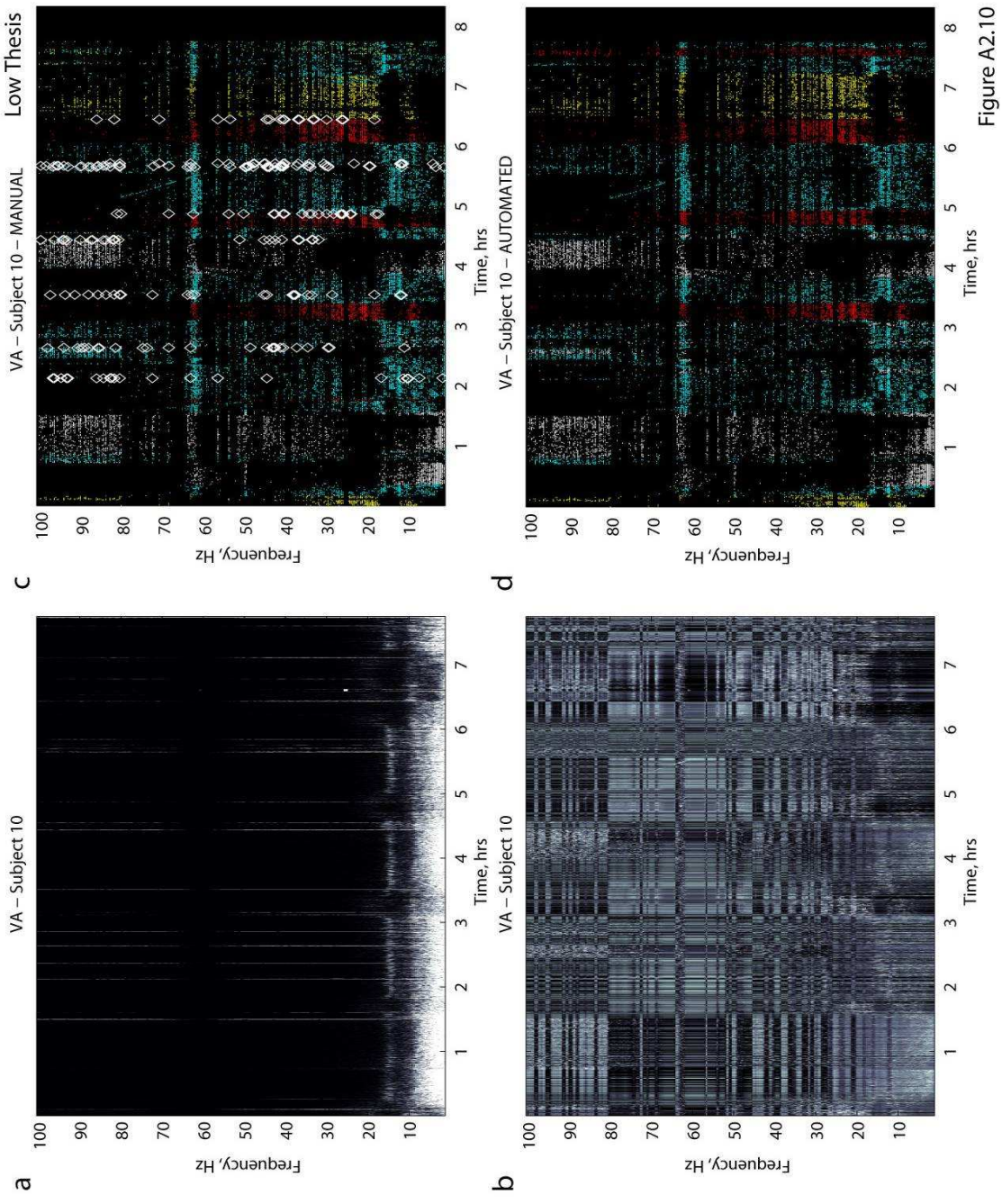
a
VA – Subject 10
Frequency, Hz
Time, hrs
b
VA – Subject 10
Frequency, Hz
Time, hrs
c
VA – Subject 10 – MANUAL
Low Thesis
Frequency, Hz
Time, hrs
d
VA – Subject 10 – AUTOMATED
Frequency, Hz
Time, hrs

Figure A2.10

Figure A2.11. Preferred Frequency Space on other data. PFS was computed for C3-A2 (a) as well as for left and right electrooculogram (EOG) (b,d), electromyogram (EMG) (c). Stage 1 is represented with cyan crosses and SWS is in black. SWS, IS, REM and W exhibited different patterns in the EEG and EOG PFS. (Courtesy NeuroVigil, Inc., La Jolla, CA).

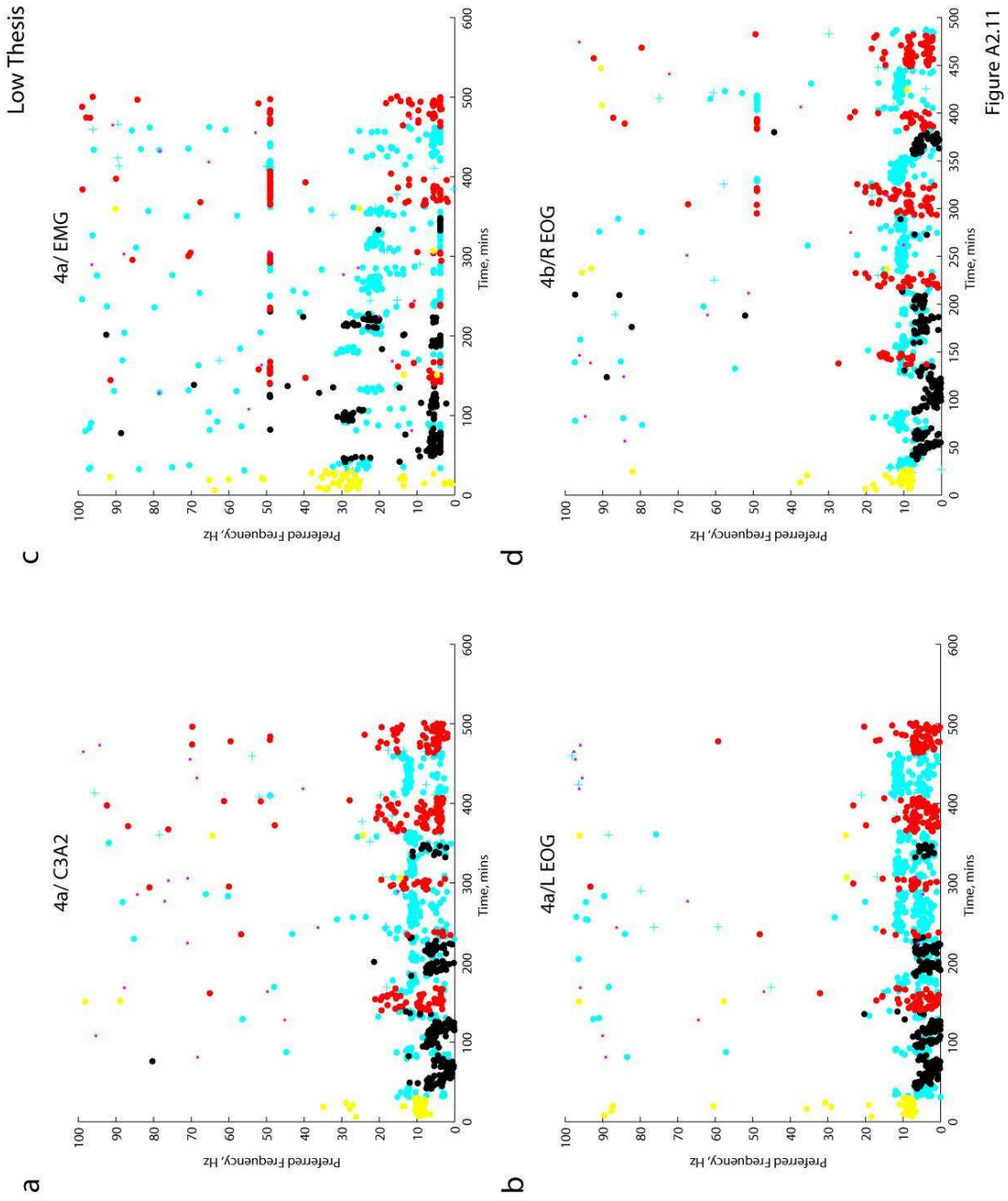
Low Thesis
a
4a/ C3A2
b
4a/L EOG
c
4a/ EMG
d
4b/R EOG
Preferred Frequency, Hz
Time, mins

Figure A2.11

Figure A2.12. Preferred Frequency Space on other data. PFS was computed for other EEG derivations. Stage 1 is represented with cyan crosses and SWS is in black. SWS, IS, REM and W exhibited different patterns in the PFS. (Courtesy NeuroVigil, Inc., La Jolla, CA).

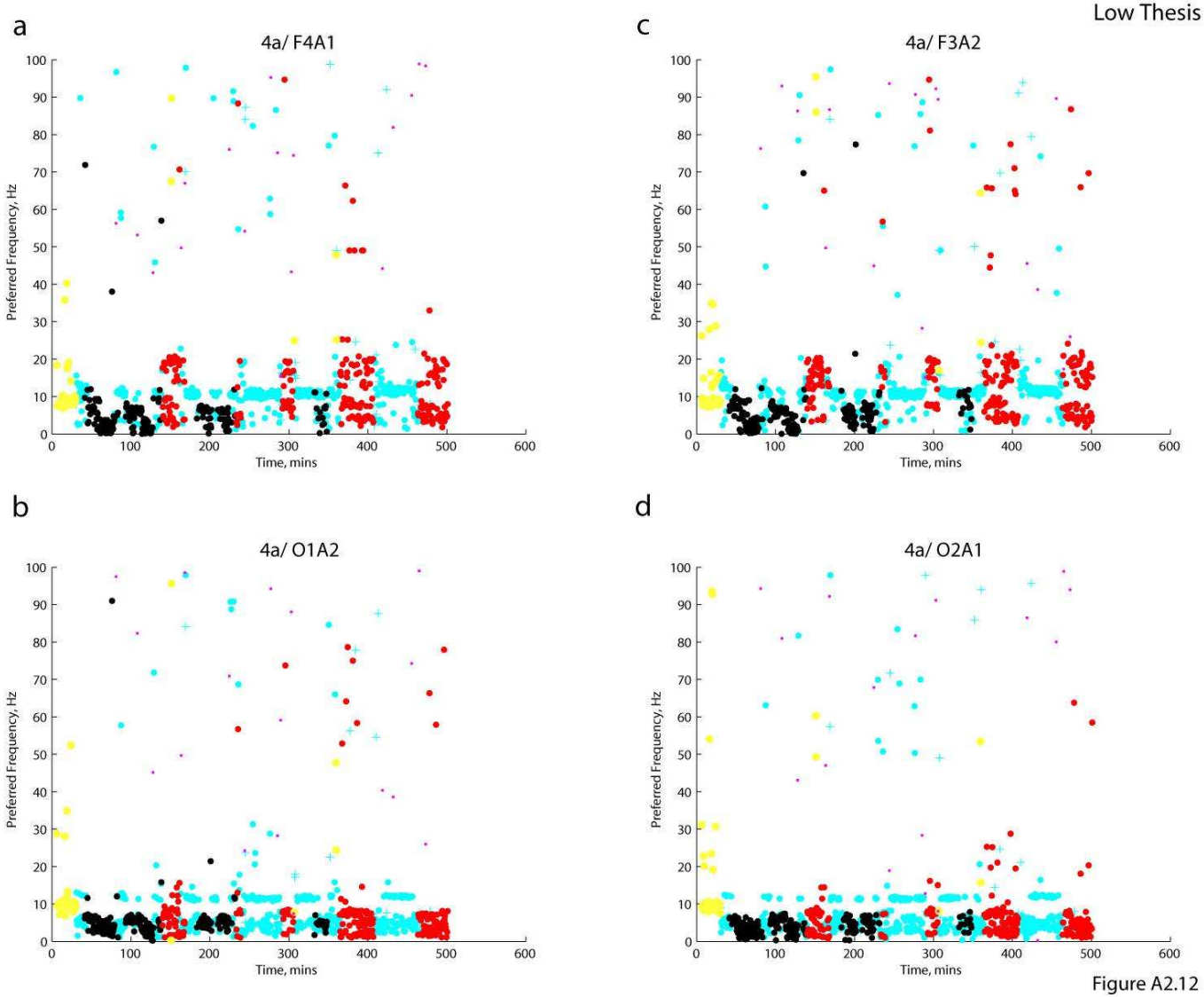
a
4a/ F4A1
c
4a/ F3A2
b
4a/ O1A2
d
4a/ O2A1
Preferred Frequency, Hz
Time, mins
0
10
20
30
40
50
60
70
80
90
100
0
100
200
300
400
500
600

Figure A2.12

Figure A2.13. Preferred Frequency Space on other data. PFS was computed for other EEG derivations. Stage 1 is represented with cyan crosses and SWS is in black. SWS, IS, REM and W exhibited different patterns in the PFS. (Courtesy NeuroVigil, Inc., La Jolla, CA).

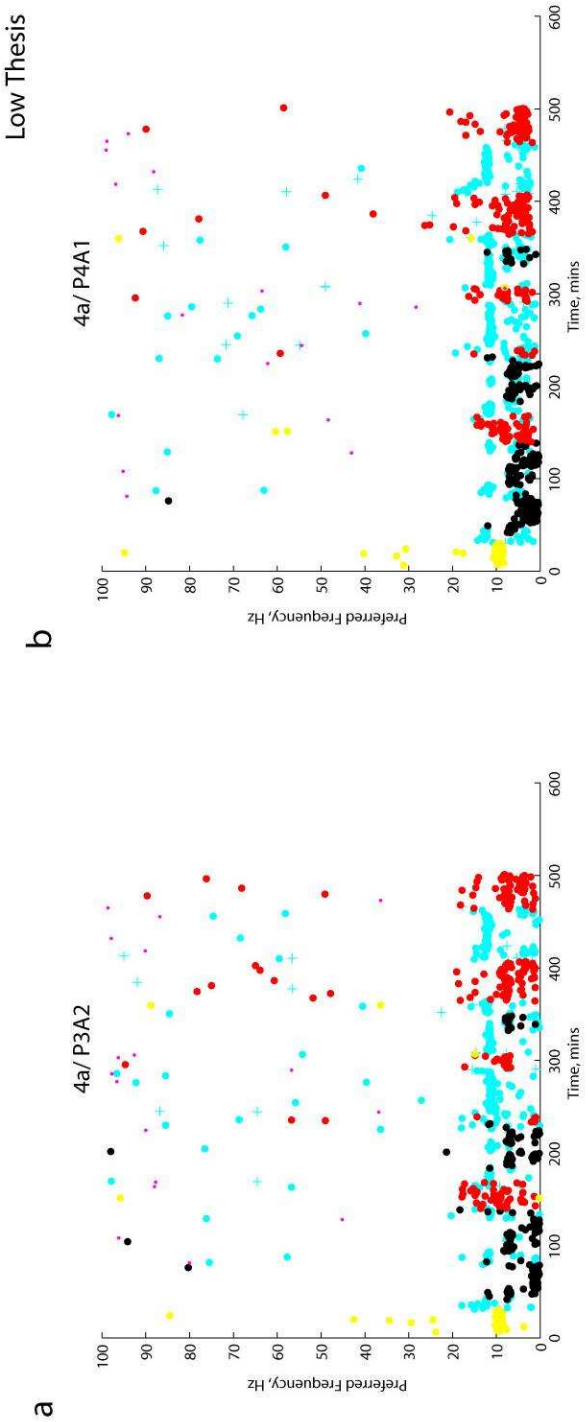
Low Thesis
b
4a/ P4A1
Preferred Frequency, Hz
Time, mins
a
4a/ P3A2
Preferred Frequency, Hz
Time, mins

Figure A2.13

Figure A2.14. Some discrepancies between automated and manual scoring.
Only about 36% (Table A2.8) of the epochs scored as SWS by the algorithm (white, panel b) were given the same designation by the human scorer (white, panel a). The rest were scored as IS (cyan, panel a), yielding an agreement rate of 76.95% (Table A2.1).

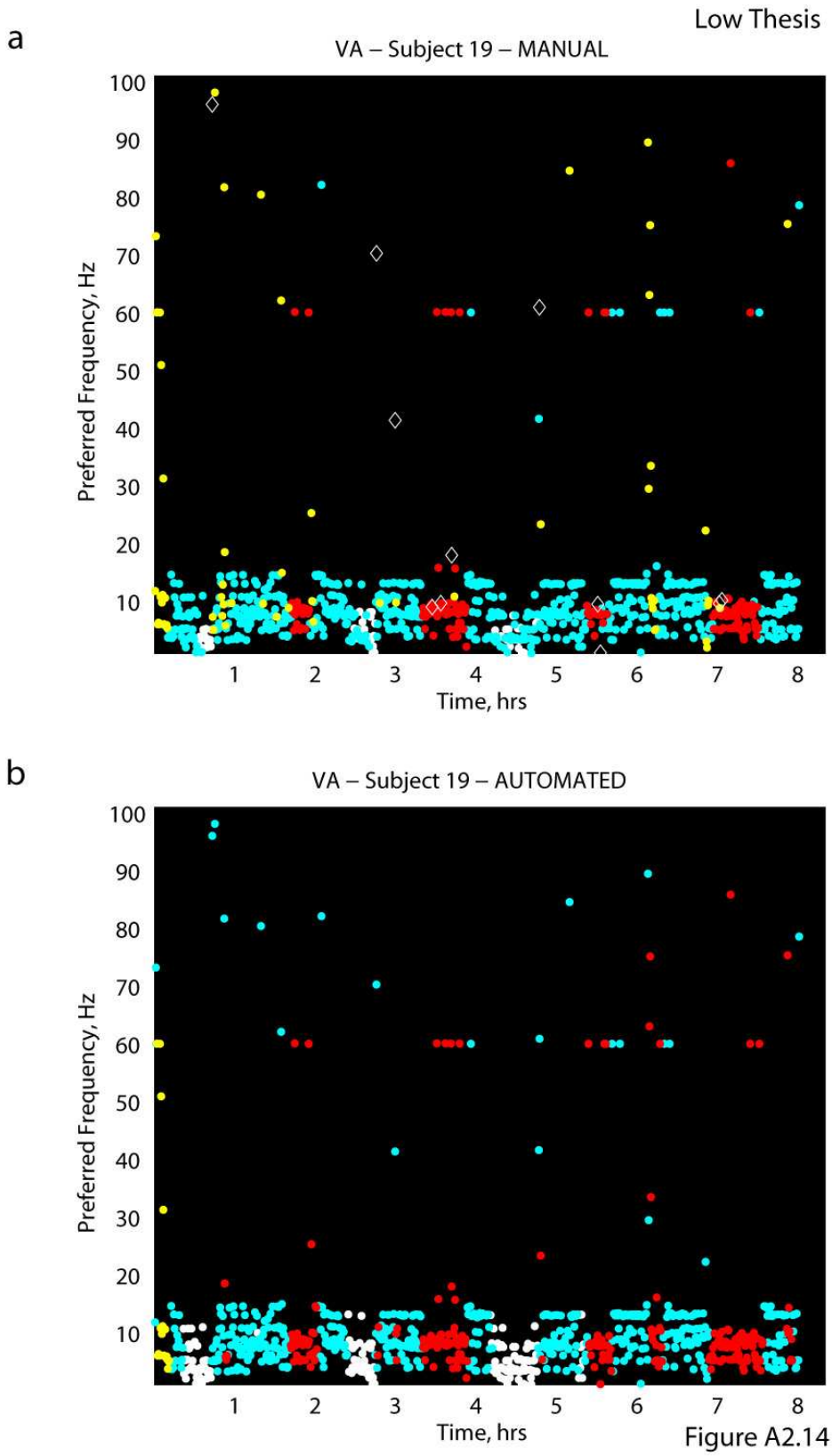
a
VA – Subject 19 – MANUAL
Preferred Frequency, Hz
100
90
80
70
60
50
40
30
20
10
1
2
3
4
5
6
7
8
Time, hrs
b
VA – Subject 19 – AUTOMATED
Preferred Frequency, Hz
100
90
80
70
60
50
40
30
20
10
1
2
3
4
5
6
7
8
Time, hrs

Figure A2.14

Figure A2.15. Some discrepancies between automated and manual scoring.
Manual (a) and automated (b) analyses have an agreement of 80.53% (Table A2.1) but over a quarter of the epochs scored by the human as SWS (white, a) are scored as IS (cyan, b) by the algorithm (Table A2.8).

a

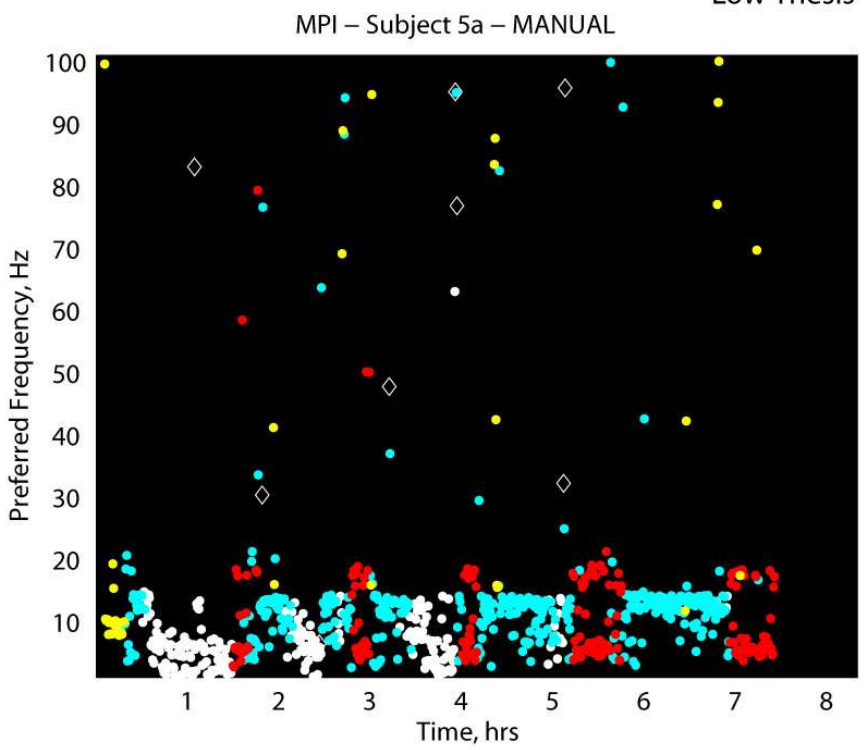

b

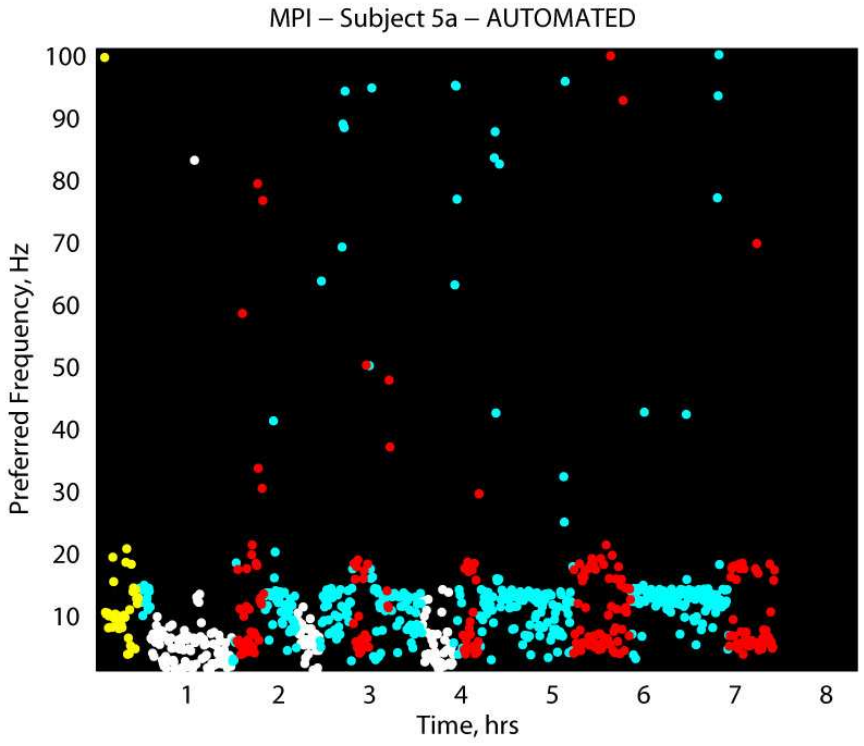

Figure A2.15

Figure A2.16. Some discrepancies between automated and manual scoring.
The overall agreement rate was 76.97% (Table A2.1) but half of the epochs scored by the human as IS (a, c, cyan) were found to be REM by the algorithm (b,d, red) (Table A2.8). These epochs had a signature closer to that of REM than IS in both the PFS (a-b) and the temporal fragmentation space (c-d), especially the second sets of epochs, occurring approximately after 2.5 hours of sleep. Reexamination of these epochs by the human scorer as well as by a second scorer did find traces of REM. Manual scores were left unchanged.

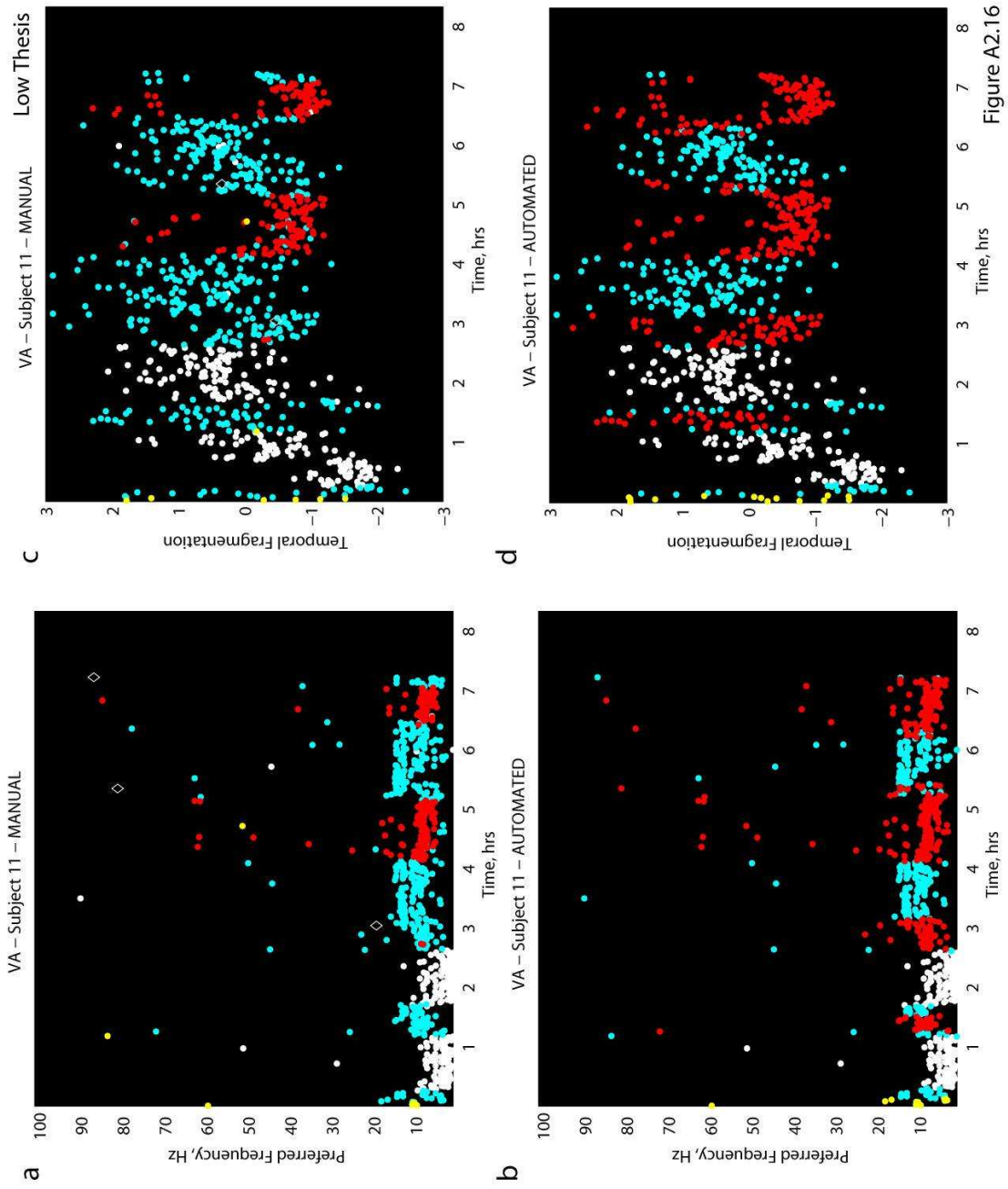
a
VA – Subject 11 – MANUAL
Preferred Frequency, Hz
Time, hrs
b
VA – Subject 11 – AUTOMATED
Preferred Frequency, Hz
Time, hrs
c
VA – Subject 11 – MANUAL
Low Thesis
Temporal Fragmentation
Time, hrs
d
VA – Subject 11 – AUTOMATED
Temporal Fragmentation
Time, hrs

Figure A2.16

Figure A2.17. PFS and Temporal Fragmentation. Same type of figure as A2.16. The overall agreement rate between automated and manual scoring for is 83.8%.

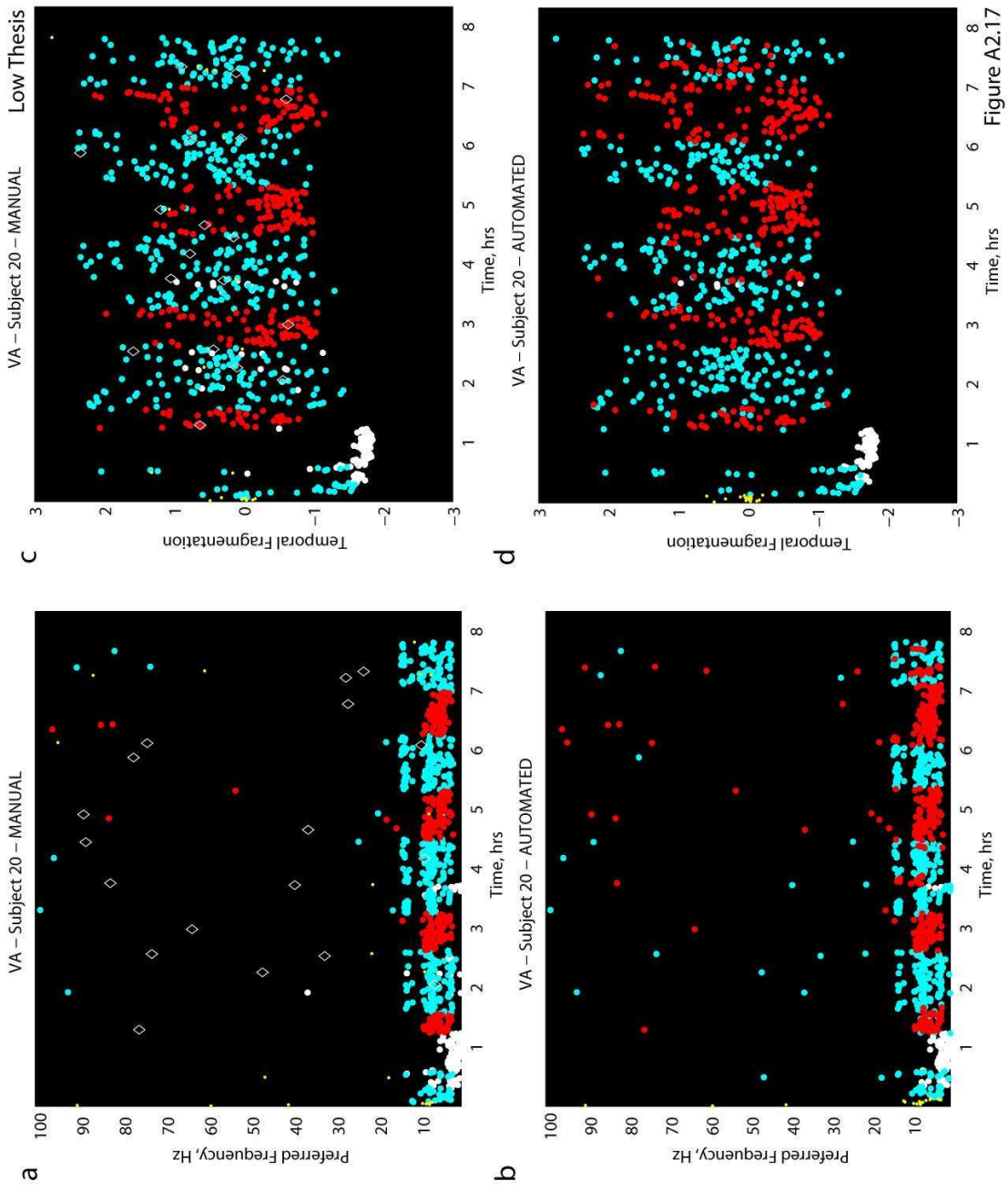
a
VA – Subject 20 – MANUAL
Low Thesis
Preferred Frequency, Hz
Time, hrs
b
VA – Subject 20 – AUTOMATED
c
VA – Subject 20 – MANUAL
Temporal Fragmentation
d
VA – Subject 20 – AUTOMATED

Figure A2.17

Figure A2.18. PFS and Temporal Fragmentation. Same type of figure as A2.16-A2.17. The overall agreement rate between automated and manual scoring is 75.74%.

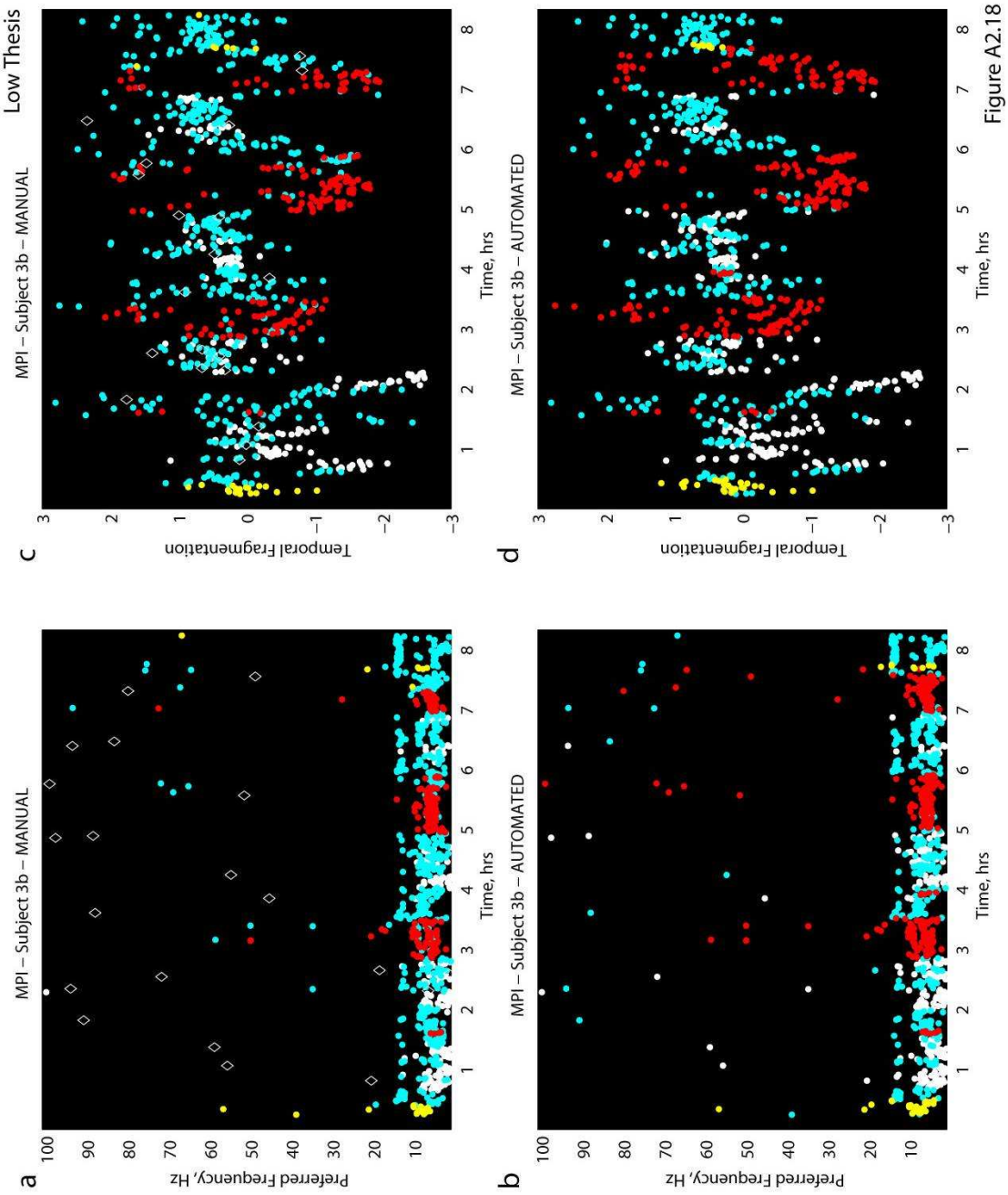
a
MPI – Subject 3b – MANUAL
Preferred Frequency, Hz
Time, hrs
b
MPI – Subject 3b – AUTOMATED
Preferred Frequency, Hz
Time, hrs
c
MPI – Subject 3b – MANUAL
Low Thesis
Temporal Fragmentation
Time, hrs
d
MPI – Subject 3b – AUTOMATED
Temporal Fragmentation
Time, hrs

Figure A2.18

Figure A2.19. PFS and Temporal Fragmentation. Same type of figure as A2.16-A2.18. The overall agreement rate between automated and manual scoring is 83.58%.

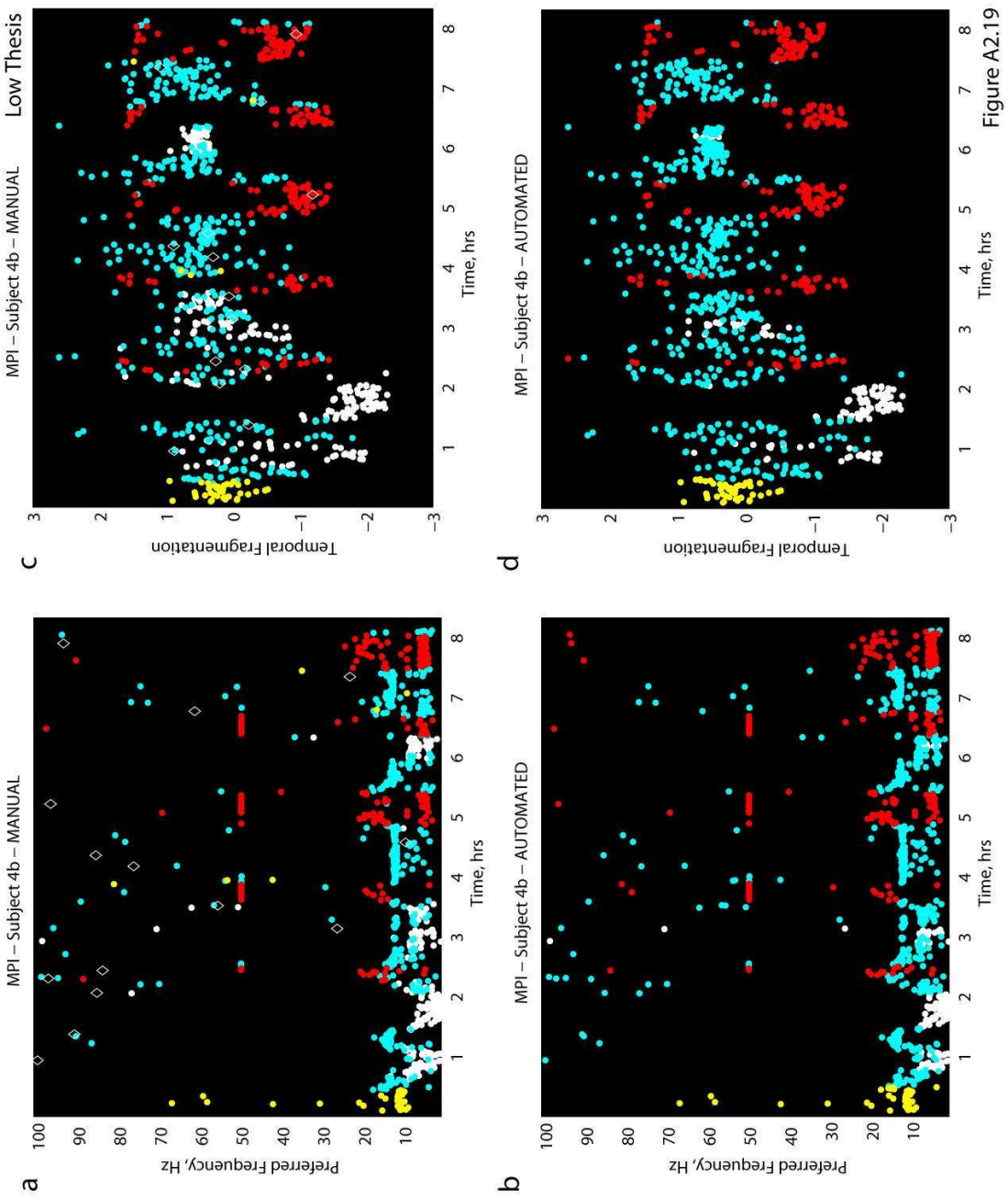
a
MPI – Subject 4b – MANUAL
Preferred Frequency, Hz
Time, hrs
b
MPI – Subject 4b – AUTOMATED
Preferred Frequency, Hz
Time, hrs
c
MPI – Subject 4b – MANUAL
Low Thesis
Temporal Fragmentation
Time, hrs
d
MPI – Subject 4b – AUTOMATED
Temporal Fragmentation
Time, hrs

Figure A2.19

Figure A2.20. PFS and Temporal Fragmentation. Same type of figure as A2.16-A2.19. The overall agreement rate between automated and manual scoring is 86.26%.

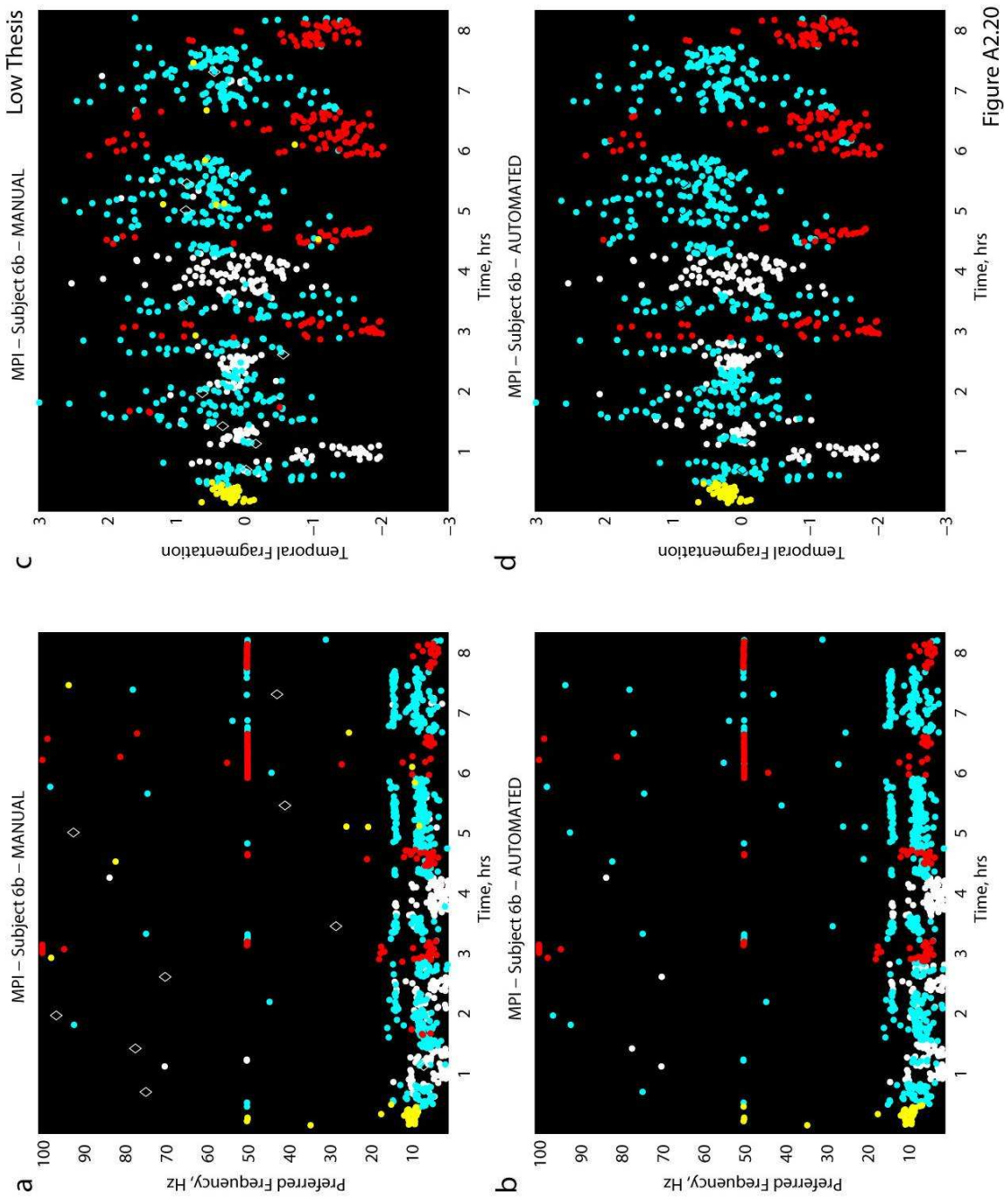
a
MPI – Subject 6b – MANUAL
Preferred Frequency, Hz
Time, hrs
b
MPI – Subject 6b – AUTOMATED
Preferred Frequency, Hz
Time, hrs
c
MPI – Subject 6b – MANUAL
Low Thesis
Temporal Fragmentation
Time, hrs
d
MPI – Subject 6b – AUTOMATED
Temporal Fragmentation
Time, hrs

Figure A2.20

Figure A2.21. Temporal Fragmentation. Temporal Fragmentation over time in the same recording in a subject with multiple awakenings. This is the same subject as the one represented in Figure A2.6d. Note the strikingly different signatures of REM (red), IS (cyan) and W (yellow) in both the manual (a) and automated (b) labels. A Kolmogorov-Smirnov test sharply rejects the null hypothesis that REM is “awake-like” or similar to Stage I (Table A2.7).

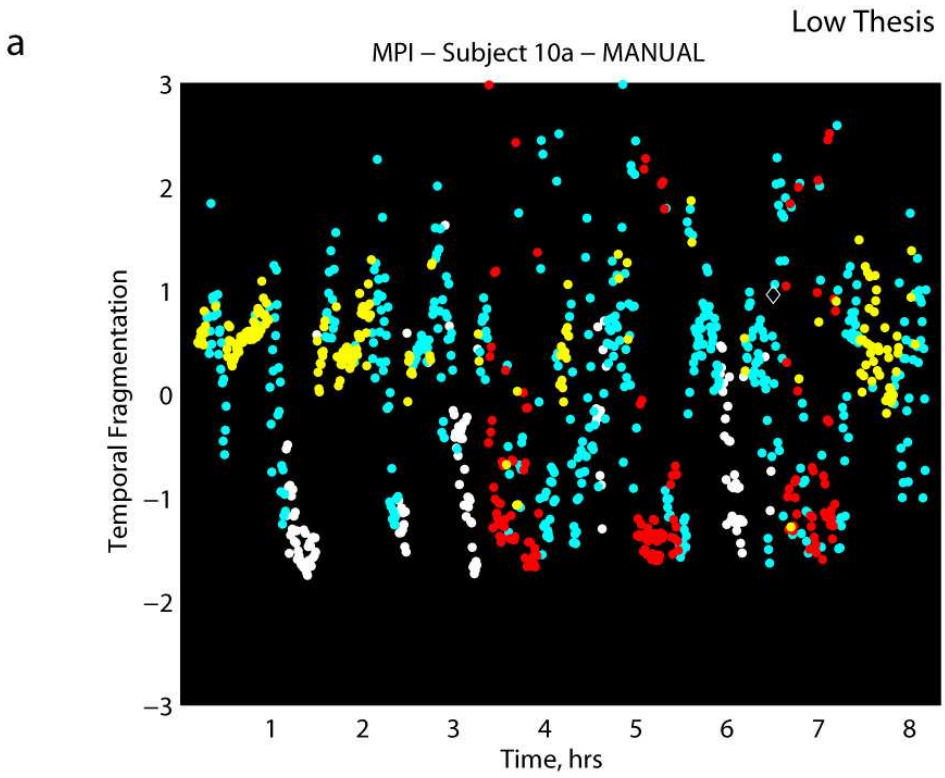
a
Low Thesis
MPI – Subject 10a – MANUAL
Temporal Fragmentation
Time, hrs
3
2
1
0
−1
−2
−3
1
2
3
4
5
6
7
8

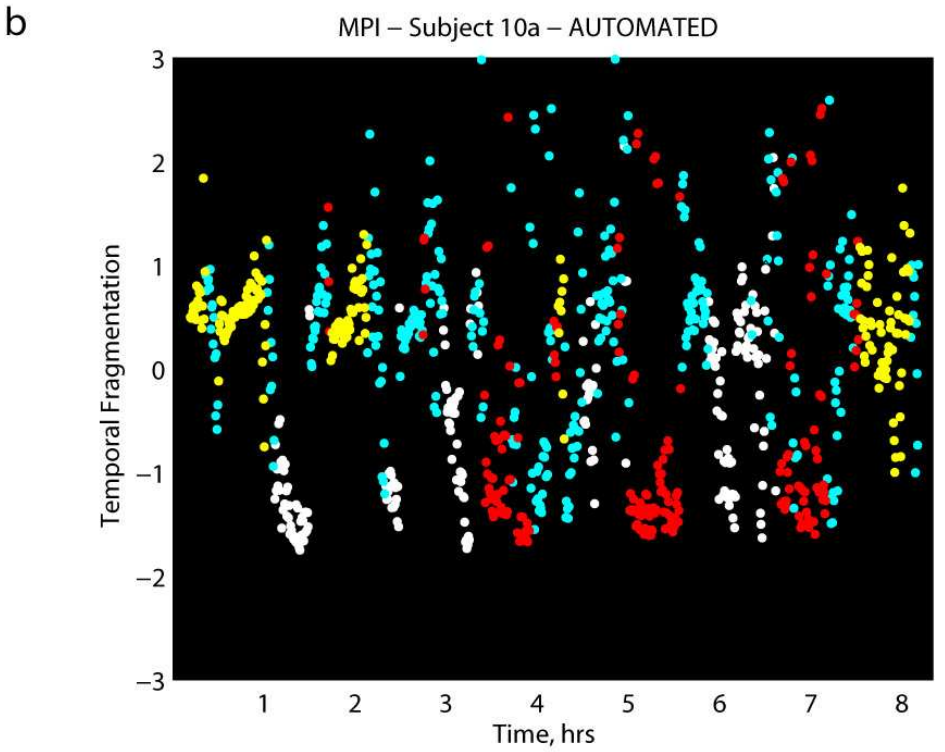
b
MPI – Subject 10a – AUTOMATED
Temporal Fragmentation
Time, hrs
3
2
1
0
−1
−2
−3
1
2
3
4
5
6
7
8

Figure A2.21

Figure A2.22. Clustering subspace. Same analysis as in Figure A2.3 on three different subjects. Labels are drawn either from manual (top) or automated scoring (bottom).

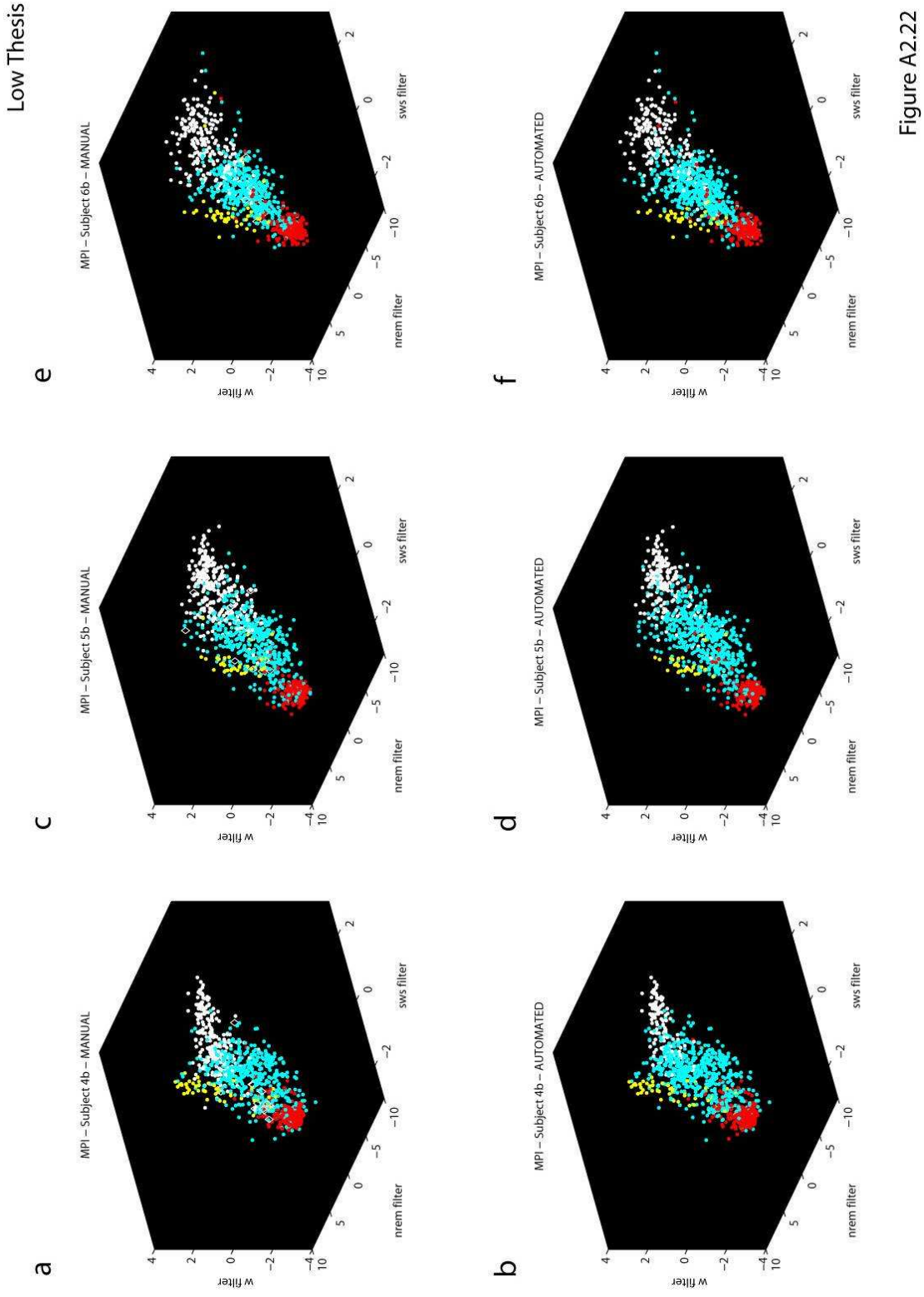
Low Thesis
a
MPI – Subject 4b – MANUAL
c
MPI – Subject 5b – MANUAL
e
MPI – Subject 6b – MANUAL
b
MPI – Subject 4b – AUTOMATED
d
MPI – Subject 5b – AUTOMATED
f
MPI – Subject 6b – AUTOMATED
w filter
nrem filter
sws filter

Figure A2.22

Figure A2.23. Clustering subspace. More advanced separation is possible using the kinds of methods provided here. This analysis is for the subject in Figure 3 and b. We show a similar clustering subspace in a and c as in Figures A2.3 and A2.22. Another subpace based on principal and independent component analysis (PCA and ICA) is shown. Epochs manually designated as Stage I are depicted in triangles and movements are in fuchsia. Stage I does not cluster in either space, in agreement with the hypothesis that is not a sleep state per se (see text and Table A2.3). The manual (a-b) and automated scoring (c-d) now have an agreement of 91.14% for this subject (Courtesy NeuroVigil, Inc., La Jolla, CA).

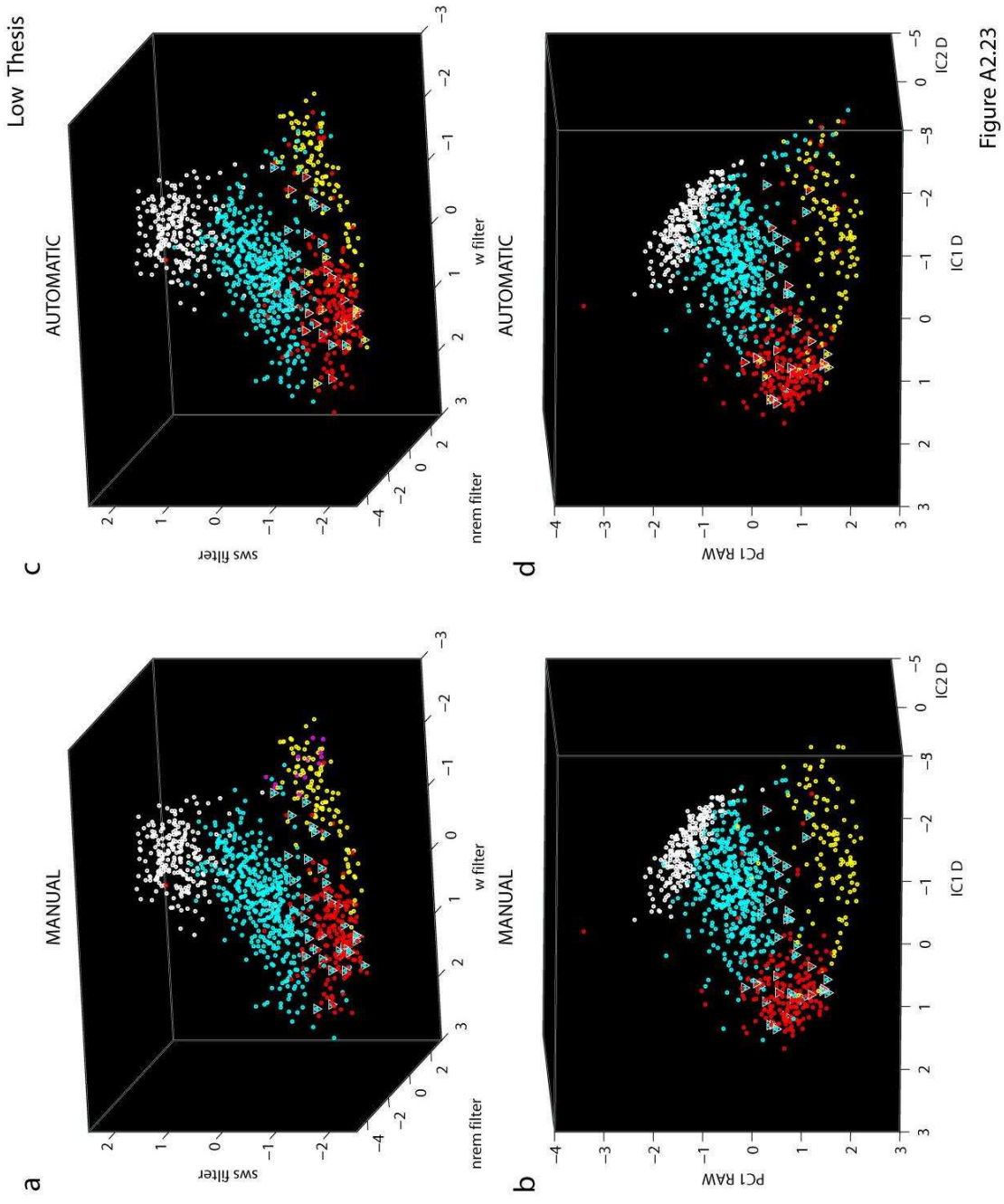
Low Thesis
a
MANUAL
sws filter
w filter
nrem filter
c
AUTOMATIC
sws filter
w filter
nrem filter
b
MANUAL
PC1 RAW
IC1 D
IC2 D
d
AUTOMATIC
PC1 RAW
IC1 D
IC2 D

Figure A2.23

Figure A2.24. Spectra in the normalized space with iterated normalizations (the spectrogram was normalized in time and frequency 19 times). REM sleep was manually scored. The stable and unstable components were isolated with a K-means clustering algorithm. The averages of the spectra for the stable (red) and unstable (green) components are shown in the space with multiple normalizations across time and frequency over multiple recordings (a-b VA, c-d, MPI). Note the elevated relative power at low frequencies for the unstable part of REM sleep as opposed to the stable part. The depression at 60 Hz is the VA data is most likely due to the use of a 60 Hz notch filter.

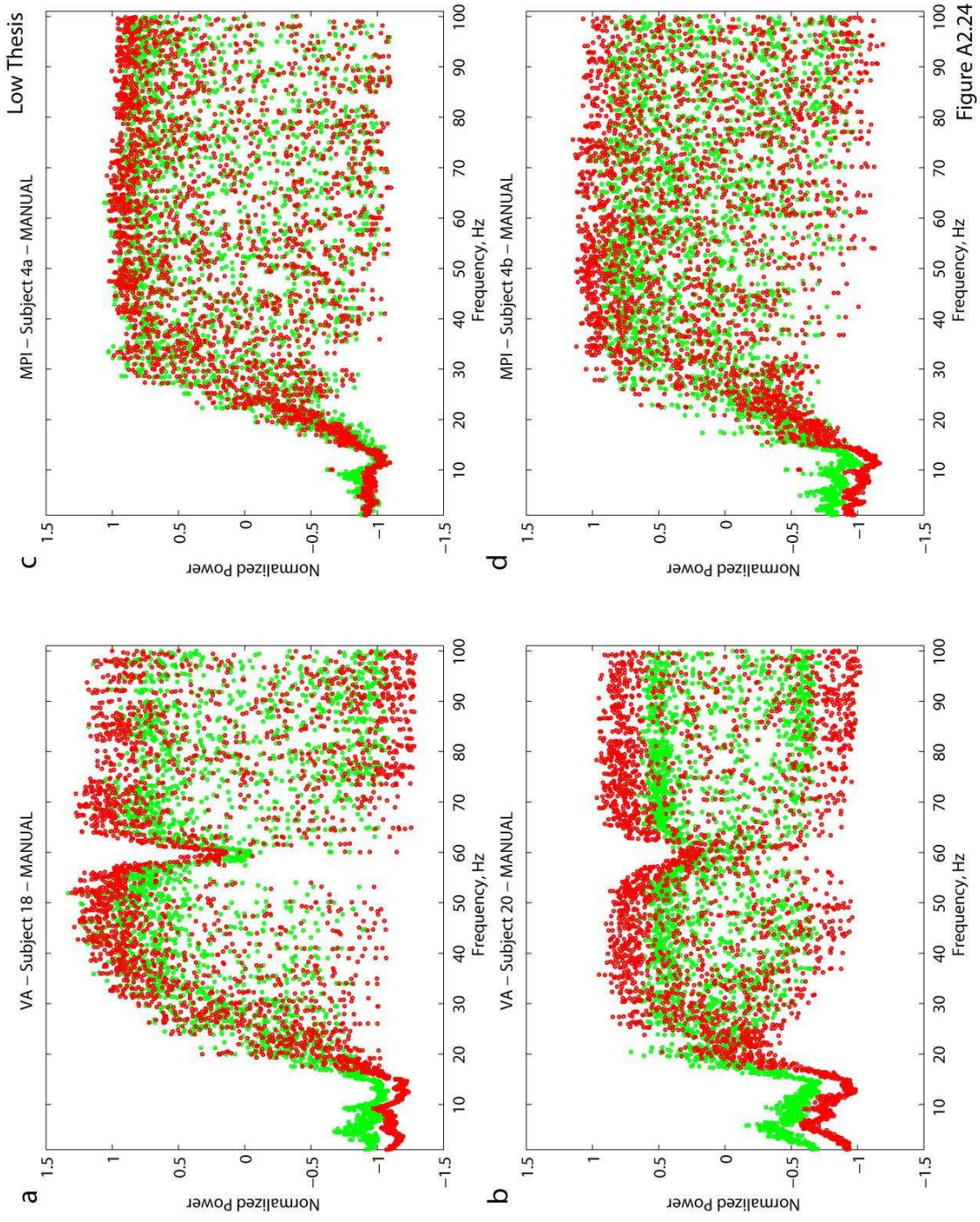
Low Thesis
a
VA – Subject 18 – MANUAL
b
VA – Subject 20 – MANUAL
c
MPI – Subject 4a – MANUAL
d
MPI – Subject 4b – MANUAL
Normalized Power
Frequency, Hz

Figure A2.24

Figure A2.25. Bimodal Temporal Fragmentation without power in the spindle range. The temporal fragmentation was displayed for the recordings in A.24, with the 10-15 Hz (encompassing the spindles range) portion of the spectrum removed. The bimodal temporal fragmentation pattern was still apparent.

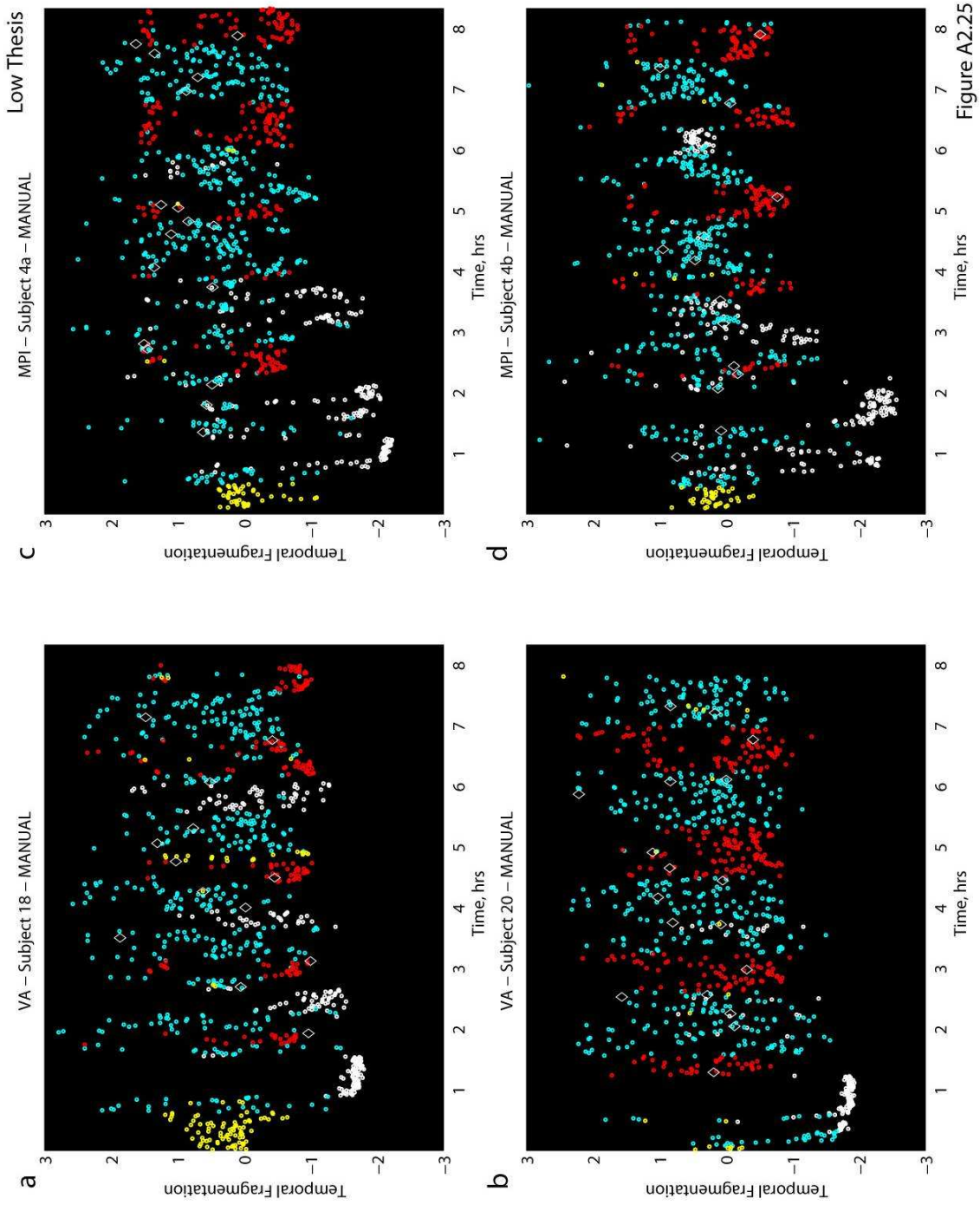
Low Thesis
a
VA – Subject 18 – MANUAL
b
VA – Subject 20 – MANUAL
c
MPI – Subject 4a – MANUAL
d
MPI – Subject 4b – MANUAL
Temporal Fragmentation
Time, hrs

Figure A2.25

Figure A2.26. Movement Artifact Analysis. For the recordings shown in A2.24-A2.25, epochs manually labeled as containing one or more artifacts, their immediate neighbors as well as any epoch with a preferred frequency over the normalized spectrum (1 normalization across time as in Figures 1 and 2) exceeding 25 Hz, were excluded. When the temporal fragmentation was calculated, the bimodal pattern was present, yet less visible.

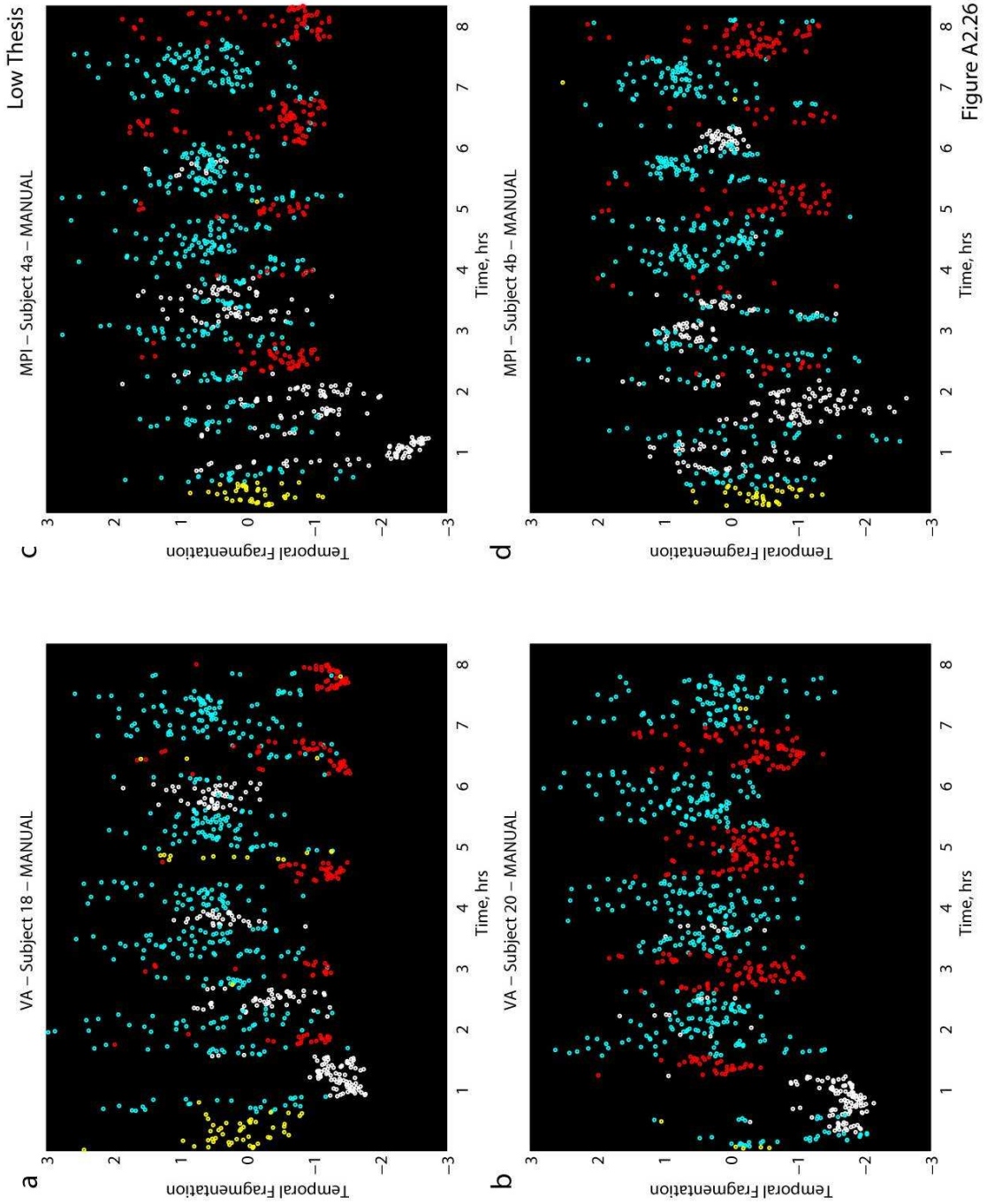
Low Thesis
a
VA – Subject 18 – MANUAL
b
VA – Subject 20 – MANUAL
c
MPI – Subject 4a – MANUAL
d
MPI – Subject 4b – MANUAL
Temporal Fragmentation
Time, hrs

Figure A2.26

Figure A2.27. Extended Artifact Analysis. On the VA recordings, an extensive artifact analysis was performed, which identified high and low frequency artifacts as well eye intrusions. The temporal fragmentation was far less bimodal when these artifacts and movement artifacts were excluded from the analysis, with higher REM fragmentation values typically occurring at the edges of REM. Though the artifact analysis was usually limited to REM epochs, sometimes NREM epochs were also discarded (d).

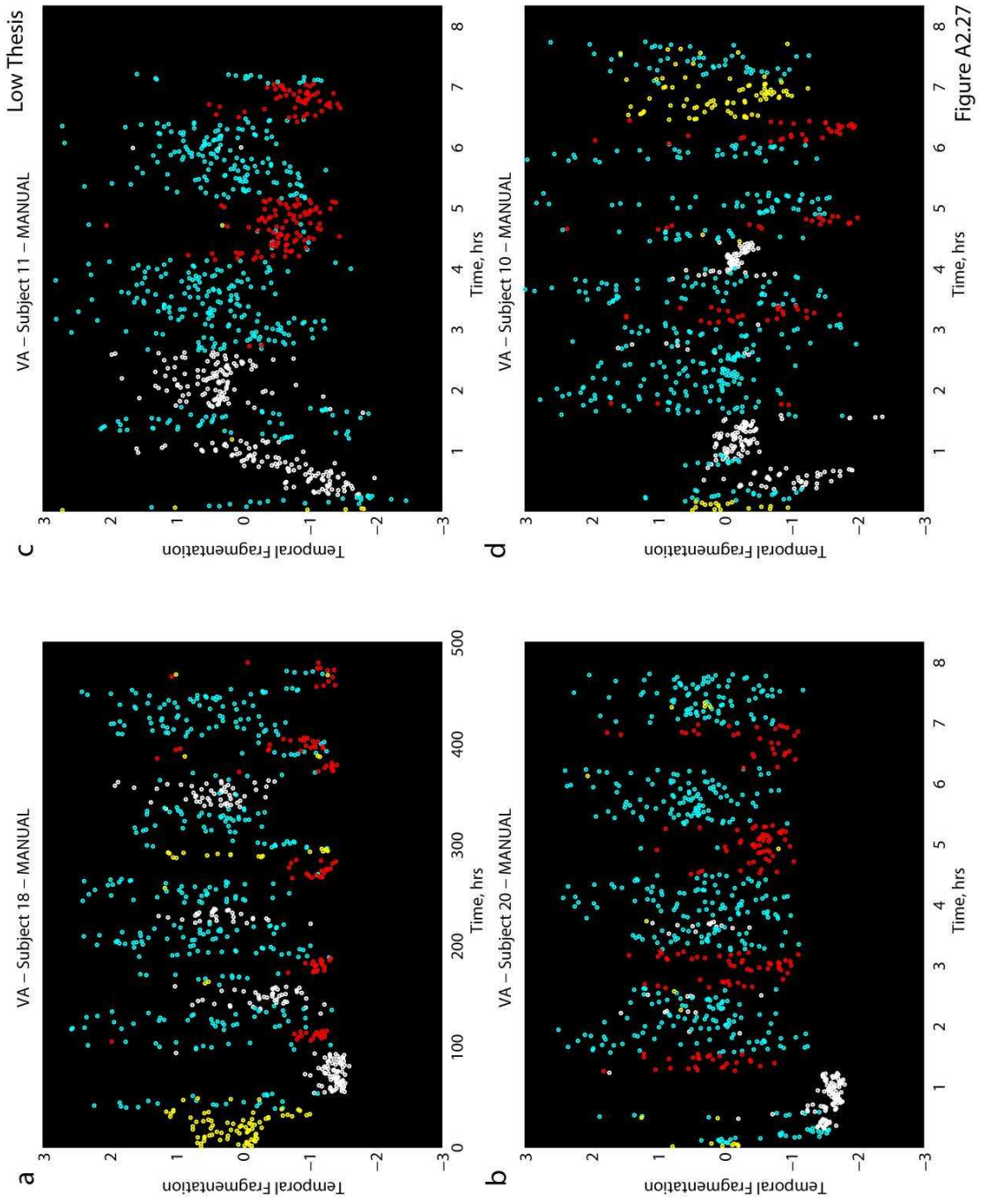
Low Thesis
a
VA – Subject 18 – MANUAL
Temporal Fragmentation
Time, hrs
b
VA – Subject 20 – MANUAL
Temporal Fragmentation
Time, hrs
c
VA – Subject 11 – MANUAL
Temporal Fragmentation
Time, hrs
d
VA – Subject 10 – MANUAL
Temporal Fragmentation
Time, hrs

Figure A2.27

Figure A2.28. Extended Artifact Analysis. On the VA recordings, an extensive artifact analysis was performed, which identified high and low frequency artifacts as well eye intrusions. The temporal fragmentation was far less bimodal when these artifacts and movement artifacts were excluded from the analysis, with higher REM fragmentation values typically occurring at the edges of REM.

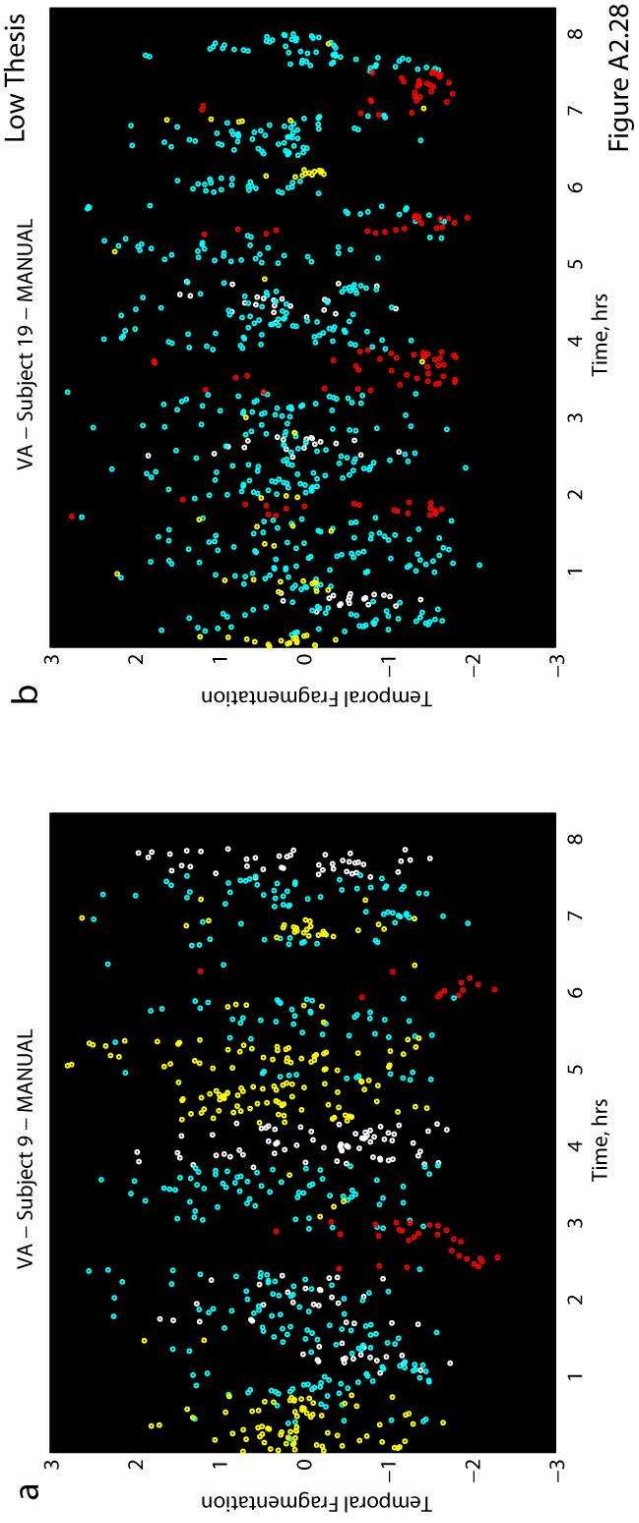
a
VA – Subject 9 – MANUAL
Temporal Fragmentation
Time, hrs
b
VA – Subject 19 – MANUAL
Low Thesis
Temporal Fragmentation
Time, hrs

Figure A2.28

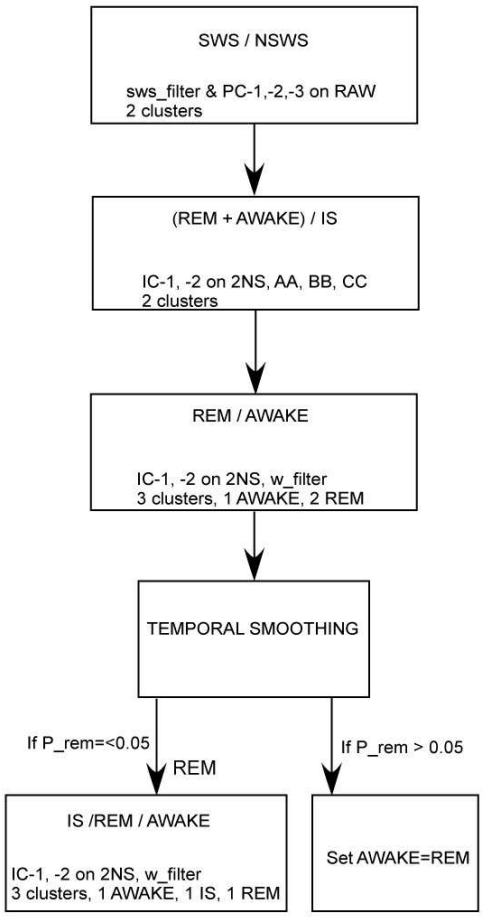

Scheme A2.1. Algorithm. The algorithm serially identifies SWS, IS, REM and W using variables described in Materials and Methods. The data is then smoothed in time. The REM/W separation is measured again by computing a P value for the REM distribution. If the latter exceeds a fixed value, REM is rejected and replaced by W. If REM is accepted, it is split in W, REM and W. One can choose as a precaution to label REM-like events occurring at the very beginning of the night as W. The increases in performance are slim as REM and W tend to form different clusters.

Table A2.1A. Performance and Separation. 1st column: Same algorithm was used on US and German data sets. 2nd column: human/algorithm agreement. This agreement was assessed only on epochs for which the human scorer could provide a sleep or waking designation, i.e. the human was not penalized for calling an epoch "M" because of movement artifacts. 3rd column: each manually and automatically determined state was respectively assessed against every other manually and automatically defined states, in the 1-100 Hz PFS using a Kolmogorov-Smirnov test (KS) over 1 sec increments computed over 3 sec windows. The numbers shown in this column correspond to the maximum of the largest p-value corresponding to a rejection of the null hypothesis and 0.001. At this resolution, the null hypothesis was rejected for all of the automatically scored data and was rejected for all but four nights for the manually scored data (P values for the rejections are showed in the table: *P_StageII_W=0.0605 and P_StageI_REM= 0.073; † P_StageIII_StageIV=0.0561; ‡P_StageI_StageII=0.1499 and P_StageIII_StageIV=0.2593; € P_StageI_W=0.0531).

TABLE A2.1A- PERFORMANCE		
	Overall (%)	**KS (3s-1s)**
VA		
S_9	**76.4021**	**0.001**
S_10	**85.5895**	**0.001**
S_11	**76.9676**	**0.0365**
S_18	**83.8608**	**0.001**
S_19	**76.9474**	**0.0483**
S_20	**83.8043**	**0.0483**
Mean	**80.59528**	
MPI		
S_2a	**79.9582**	**0.001***
S_2b	**76.096**	**0.0161**
S_3a	**77.5899**	**0.0208**
S_3b	**75.7447**	**0.002**
S_4a	**84.9949**	**0.001**
S_4b	**83.5789**	**0.001**
S_5a	**80.5269**	**0.001**
S_5b	**84.0549**	**0.0119**
S_6a	**86.3114**	**0.001†**
S_6b	**86.2643**	**0.001**
S_7a	**70.0315**	**0.0022**
S_7b	**66.7368**	**0.0016**
S_8a	**54.5738**	**0.001**
S_8b	**77.0285**	**0.001‡**
S_9a	**81.7801**	**0.0013**
S_9b	**79.7495**	**0.001€**
S_10a	**73.5572**	**0.001**
S_10b	**78.2881**	**0.0022**
S_11a	**69.3122**	**0.0131**
S_11b	**67.2632**	**0.0048**
Mean	**76.67205**	

Table A2.1B. Performance against multiple reviews by multiple scorers. On the VA data, the performance of the algorithm was assessed against two human scorers (S-1, S-2), who examined the data twice (a, b). S-1a and S-2a correspond to scoring which was done independently of the algorithm. S-1 b corresponds to scores derived when S-1 had a chance to revise his scores in light of results by the algorithm, while S-2 b corresponds to scores derived after S-2 viewed S-1's original scores. S-1 had 15 years of experience scoring EEGs at the time of his initial scoring and 17 years of experience by the time of his second scoring. S-2 had 23 years of experience at the time of both of her scorings.

TABLE A2.1 B	**S-1 a**	**S-1 b**	**S- 2 a**	**S-2 b**
VA				
S_9	**76.4021**	**73.1217**		**76.9312**
S_10	**85.5895**	**85.5895**	**84.7162**	**84.4978**
S_11	**76.9676**	**77.1991**	**80.3241**	**79.9769**
S_18	**83.8608**	**83.8608**	**84.3882**	**83.7014**
S_19	**76.9474**	**75.5789**		**76.7368**
S_20	**83.8043**	**83.532**	**83.4056**	**81.4735**
Mean	**80.59528**	**82.54535**	**83.20853**	**82.4124**

Table A2.2. Stage III. KS tests were performed on the PFS on the full spectrum (1-100 Hz) to determine the similarity between Stage III and stages IV and II. An H value of 0 or 1 means that the null hypothesis was respectively accepted or rejected with a corresponding P value in the adjoining column. In the majority of recordings, the null hypothesis (stage III and the compared state are not statistically different) was accepted in at least one condition, i.e. Stage III was not disambiguated from SWS or Stage II in the PFS.

TABLE A2.2 – STAGE III				
	H-SWS	P-SWS	H-SII	P-SII
VA				
S_9	0	0.1334	1	4.95E-09
S_10	1	0.0015	1	1.50E-46
S_11	1	5.76E-08	0	0.1269
S_18	1	0.0013	1	1.18E-06
S_19	0	0.418	1	1.16E-17
S_20	1	1.69E-06	0	1.10E-01
MPI				
S_2a	1	1.32E-05	1	0.0043
S_2b	1	0.0137	1	3.55E-04
S_3a	0	0.8531	1	0.0016
S_3b	0	0.1527	0	0.3381
S_4a	1	0.0018	1	1.27E-06
S_4b	1	3.76E-06	1	2.30E--3
S_5a	1	4.01E-04	1	8.88E-16
S_5b	1	4.53E-05	1	2.82E-10
S_6a	0	0.502	1	4.43E-07
S_6b	0	0.0654	1	2.19E-10
S_7a	0	0.7484	1	1.03E-23
S_7b	0	0.849	1	1.10E-14
S_8a	NaN	NaN	0	3.07E-01
S_8b	0	0.2658	1	8.36E-05
S_9a	1	1.01E-09	1	1.56E-04
S_9b	0	0.9592	1	1.75E-15
S_10a	1	0.0105	1	4.89E-05
S_10b	0	0.3407	1	1.21E-08
S_11a	0	0.5496	1	3.86E-06
S_11b	0	0.3837	1	3.39E-02

Table A2.3. Stage I. Similar analysis as in the previous table, comparing Stage I with Stage II, REM and Waking (W). In all 22 out of 26 recordings, the null hypothesis was accepted in at least one condition.

TABLE A2.3 - STAGE I						
	H-SII	P-F-SII	H-F-REM	P-F-REM	H-F-W	P-F-W
VA						
S_9	1	5.96E-10	1	1.85E-08	1	1.63E-09
S_10	0	0.5993	1	0.0065	0	0.3241
S_11	0	0.4964	0	0.4579	0	0.066
S_18	1	2.91E-04	1	0.0194	1	2.57E-07
S_19	0	0.7925	0	0.402	0	0.2943
S_20	0	0.3791	1	6.10E-07	0	0.3292
MPI						
S_2a	1	0.005	1	0.0046	0	0.0786
S_2b	0	0.1743	0	0.166	0	0.5593
S_3a	1	0.0443	0	0.062	0	0.7146
S_3b	1	1.24E-05	1	0.0107	1	0.0214
S_4a	0	0.0814	0	0.1615	1	0.015
S_4b	1	3.10E-03	1	0.0293	1	0.0197
S_5a	0	0.1308	0	0.8425	0	0.1457
S_5b	0	9.78E-01	0	0.2074	0	0.24
S_6a	1	0.0177	0	0.23	1	0.0095
S_6b	0	1.44E-01	1	0.0024	0	0.8589
S_7a	0	0.1186	1	0.0118	0	0.5723
S_7b	0	9.99E-01	0	0.9606	0	0.3975
S_8a	0	0.2488	0	0.079	0	0.3351
S_8b	0	2.58E-01	0	0.172	0	0.4921
S_9a	0	0.3047	0	0.4271	0	0.5964
S_9b	0	1.18E-01	0	0.5353	0	0.6615
S_10a	0	0.191	1	0.0131	1	5.30E-05
S_10b	0	0.056	0	0.1773	0	0.9267
S_11a	0	0.1886	0	0.3219	0	0.3275
S_11b	0	0.4501	0	0.2254	1	3.04E-06

Table A2.4. REM & Wakefulness. Similar analysis as in the previous tables with the inclusion of an analysis for automated scores in the last two columns. The null hypothesis for REM and W was rejected by both the manual scoring and the algorithm in two recordings.

TABLE A2.4 - REM & Wakefulness				
	H-REM	P-REM	H-REM_AUT	PREM_AUT
VA				
S_9	1	1.75E-19	1	5.25E-12
S_10	1	5.30E-15	1	1.41E-14
S_11	1	2.16E-04	1	0.0045
S_18	1	5.01E-10	1	9.94E-12
S_19	1	1.06E-04	0	9.03E-02
S_20	1	3.50E-03	1	3.50E-03
MPI				
S_2a	0	0.2188	1	0.0016
S_2b	0	0.6451	0	0.1276
S_3a	0	0.2267	1	3.19E-04
S_3b	1	3.25E-08	1	2.59E-05
S_4a	1	0.0022	1	1.24E-04
S_4b	1	5.33E-04	1	4.91E-06
S_5a	1	9.71E-06	1	3.14E-05
S_5b	1	3.70E-03	1	6.19E-09
S_6a	1	4.52E-02	1	1.26E-05
S_6b	1	5.70E-04	1	3.99E-07
S_7a	1	6.9360e-04	NaN	NaN
S_7b	0	1.28E-01	1	3.70E-05
S_8a	1	1.54E-02	1	1.00E-05
S_8b	0	5.84E-01	1	3.50E-06
S_9a	0	3.72E-01	1	3.96E-02
S_9b	0	5.58E-01	0	1.30E-01
S_10a	1	1.20E-11	1	1.17E-33
S_10b	0	2.24E-01	1	6.92E-06
S_11a	0	5.57E-02	NaN	NaN
S_11b	1	6.08E-09	0	1.95E-01

Table A2.5. Statistics on temporally fragmented part of REM sleep. The percentage of REM, number of episodes, their mean duration and separation is represented in each recording from both data sets.

TABLE A2.5 - TOP REM				
	%REM	Number	Mean Duration (s)	Mean Separation (s)
VA				
S_9	25.2101	25	33.6	109.0909
S_10	36.036	23	48.2609	102.6316
S_11	11.1732	21	30	87.5
S_18	15.1351	21	35.7143	163.6364
S_19	35.9551	46	33.2609	96.7742
S_20	29.0657	53	43.5849	137.0455
MPI				
S_2a	37.6471	63	44.2857	70.4348
S_2b	41.8251	68	46.7647	74.6809
S_3a	25.3086	25	44.4	169.4118
S_3b	22.7513	37	30	111.25
S_4a	24.2553	48	31.875	119.1176
S_4b	17.9724	33	29.0909	187.1429
S_5a	15.1685	21	30	312
S_5b	13.4503	20	28.5	266.6667
S_6a	17.1123	30	28	136.9565
S_6b	16.2679	32	27.1875	161.0526
S_7a	34.8958	54	31.1111	80.9091
S_7b	31.7647	51	42.3529	97.5
S_8a	25.2475	33	42.7273	140
S_8b	34.2723	49	37.3469	120
S_9a	30.1508	45	38	95.2941
S_9b	33.3333	39	42.3077	86.5385
S_10a	15.8621	21	31.4286	125
S_10b	32.2034	41	38.0488	102.8571
S_11a	29.3785	41	32.9268	104.4828
S_11b	29.3413	33	40	98.1818

Table A2.6. The fragmented and no-fragmented portions of REM sleep do not correspond to phasic or tonic REM. In the VA data only, REM was subdivided into epochs without eye movements (tonic REM) and epochs with 0-25%, 25-50%, 50-75%, 75-100% eye movements (phasic REM). For each subject, the percentage of times one of the substates listed above occurs in the unstable portion of REM is reported. Both tonic REM and phasic REM take place in the unstable part of REM.

TABLE A2.6 - Eye Movements					
	Tonic	**Phasic**			
	no eye mvmts	**0-25%**	**25-50%**	**50-75%**	**75-100%**
VA					
S_9	**31.8182**	**34.2105**	**16.6667**	**15.7895**	**20**
S_10	**43.1818**	**35.0877**	**11.1111**	**0**	**NaN**
S_11	**8.046**	**15.2941**	**0**	**NaN**	**NaN**
S_18	**21.2766**	**16.092**	**9.375**	**5.5556**	**0**
S_19	**38.8889**	**34.2857**	**26.6667**	**33.3333**	**NaN**
S_20	**44.4444**	**26.5487**	**10.2564**	**14.2857**	**20**

Table A2.7. REM has a unique temporal fragmentation pattern which distinguishes it from Stage I and W. A KS analysis at a 30 second resolution as in Tables A2.2 and A2.3 is performed. The null hypothesis was rejected for REM vs Stage I (left columns) in 23 out 26 recordings and for REM vs. W (right columns) 24 out of 26 recordings, as defined by manual scoring.

TABLE A2.7 - Fragmentation				
	H_IS-1_REM	P_IS-1-REM	H_W-REM	P_W-REM
VA				
S_9	1	6.89E-13	1	1.43E-29
S_10	1	2.83E-02	1	6.91E-08
S_11	1	0.0035	1	2.65E-02
S_18	1	1.15E-12	1	1.88E-27
S_19	1	6.27E-08	1	2.27E-17
S_20	1	5.78E-11	1	7.53E-06
MPI				
S_2a	1	1.40E-04	1	0.0041
S_2b	0	0.2307	0	0.1047
S_3a	1	0.0054	1	1.62E-04
S_3b	1	5.41E-06	1	1.51E-07
S_4a	1	4.41E-06	1	5.94E-12
S_4b	1	9.02E-10	1	5.88E-19
S_5a	1	1.02E-04	1	4.99E-15
S_5b	1	2.11E-06	1	2.12E-20
S_6a	1	1.81E-07	1	7.93E-28
S_6b	1	5.97E-07	1	2.14E-20
S_7a	0	0.1648	1	3.17E-02
S_7b	1	1.84E-02	0	2.07E-01
S_8a	1	1.18E-13	1	1.88E-19
S_8b	1	1.17E-06	1	4.68E-12
S_9a	1	5.40E-03	1	6.00E-07
S_9b	0	0.8904	1	4.07E-04
S_10a	1	7.27E-16	1	9.06E-49
S_10b	1	1.04E-06	1	1.47E-11
S_11a	1	2.50E-03	1	5.75E-11
S_11b	1	8.12E-06	1	4.44E-04

Table A2.8. Agreement matrices for each recording. For each recording, two matrices are presented, one to the left and one to the right. Matrices on the left should be read column-wise. Each box corresponds to the percentage of the stage listed above, as derived by automated classification, to be listed to belong to the stage on the left, as derived by manual scoring. The columns do not always add up 100% because some the epochs were scored as M by the human scorer. Matrices on the right should be read row-wise, for each box corresponds to the percentage of times an epoch manually labeled as the stage to the left was automatically classified as the stage above. Since all the data is scored by the algorithm, the rows add up to 100%. The last set of matrices displays in each box an average of all of the preceding values in that particular box. This is not a precise estimate, as it is not weighed by the number of epochs scored as particular stage. In certain cases for example, a single epoch per state was found leading to either 0% or 100% agreement*****.

Table A2.8 - Agreement Matrix

MPI - 2a	Automated			
Human	SWS	IS	REM	W
SWS	**96.8153**	10.2439	0.2584	0
IS	3.1847	**85.6098**	32.8165	18.75
REM	0	1.2195	**64.5995**	0
W	0	0.4878	1.8088	**81.25**

	Automated			
Human	SWS	IS	REM	W
SWS	**77.9487**	21.5385	0.5128	0
IS	1.0288	**72.2222**	26.1317	0.6173
REM	0	1.9608	**98.0392**	0
W	0	9.0909	31.8182	**59.0909**

MPI - 2b	Automated			
Human	SWS	IS	REM	W
SWS	**82.7586**	3.125	0	0
IS	15.0862	**84.6591**	33.871	69.2308
REM	0	7.9545	**63.172**	0
W	0.431	2.5568	2.6882	**30.7692**

	Automated			
Human	SWS	IS	REM	W
SWS	**94.5813**	5.4187	0	0
IS	7.4786	**63.6752**	26.9231	1.9231
REM	0	10.6464	**89.3536**	0
W	4.1667	37.5	41.6667	**16.6667**

MPI - 3a	Automated			
Human	SWS	IS	REM	W
SWS	**69.145**	1.432	0	0
IS	27.881	**93.5561**	39.2857	55
REM	0	3.58	**58.3333**	0
W	0	0.4773	1.5873	**45**

	Automated			
Human	SWS	IS	REM	W
SWS	**96.875**	3.125	0	0
IS	12.9983	**67.9376**	17.1577	1.9064
REM	0	9.2593	**90.7407**	0
W	0	13.3333	26.6667	**60**

Table A2.8, continued

MPI - 3b	Automated			
Human	SWS	IS	REM	W
SWS	**63.8889**	6.3882	0	0
IS	31.3492	**87.9607**	31.9549	45.7143
REM	0.7937	3.1941	**65.4135**	0
W	0	0.9828	1.1278	**54.2857**

	Automated			
Human	SWS	IS	REM	W
SWS	**86.0963**	13.9037	0	0
IS	14.684	**66.5428**	15.7993	2.974
REM	1.0582	6.8783	**92.0635**	0
W	0	15.3846	11.5385	**73.0769**

MPI - 4a	Automated			
Human	SWS	IS	REM	W
SWS	**93.2927**	12.8364	0	0
IS	5.4878	**82.8157**	19.0311	11.1111
REM	0	1.8634	**78.2007**	0
W	0	0.4141	1.0381	**88.8889**

	Automated			
Human	SWS	IS	REM	W
SWS	**71.1628**	28.8372	0	0
IS	1.9149	**85.1064**	11.7021	1.2766
REM	0	3.8298	**96.1702**	0
W	0	3.7736	5.6604	**90.566**

MPI - 4b	Automated			
Human	SWS	IS	REM	W
SWS	**99.2248**	20.471	0	0
IS	0	**75.3623**	9.3617	14.5833
REM	0	1.4493	**88.9362**	0
W	0	0.9058	0.4255	**85.4167**

	Automated			
Human	SWS	IS	REM	W
SWS	**53.112**	46.888	0	0
IS	0	**93.4831**	4.9438	1.573
REM	0	3.6866	**96.3134**	0
W	0	10.6383	2.1277	**87.234**

Table A2.8, continued

MPI - 5a	Automated			
Human	SWS	IS	REM	W
SWS	**98.8764**	16.4384	0	0
IS	0	**76.484**	21.8182	46.6667
REM	0	2.2831	**76.3636**	0
W	0	3.8813	0.9091	**53.3333**

MPI - 5b	Automated			
Human	SWS	IS	REM	W
SWS	**95.3917**	15.0476	0	0
IS	3.2258	**77.7143**	18.75	0
REM	0	3.2381	**80.2083**	0
W	0.9217	1.5238	1.0417	**100**

MPI - 6a	Automated			
Human	SWS	IS	REM	W
SWS	**80.695**	4.7009	0	0
IS	16.6023	**88.2479**	4.0201	26.6667
REM	0	3.4188	**85.9296**	0
W	0	2.1368	10.0503	**73.3333**

	Automated			
Human	SWS	IS	REM	W
SWS	**70.9677**	29.0323	0	0
IS	0	**82.9208**	11.8812	5.198
REM	0	5.618	**94.382**	0
W	0	39.5349	4.6512	**55.814**

	Automated			
Human	SWS	IS	REM	W
SWS	**72.3776**	27.6224	0	0
IS	1.5521	**90.4656**	7.9823	0
REM	0	9.9415	**90.0585**	0
W	5.1282	20.5128	5.1282	**69.2308**

	Automated			
Human	SWS	IS	REM	W
SWS	**90.4762**	9.5238	0	0
IS	9.0336	**86.7647**	1.6807	2.521
REM	0	8.5561	**91.4439**	0
W	0	15.873	31.746	**52.381**

Table A2.8, continued

MPI - 6b	Automated			
Human	SWS	IS	REM	W
SWS	**84.4221**	10.7345	0	0
IS	14.0704	**82.6742**	4.5226	17.0732
REM	0	3.9548	**94.4724**	0
W	0	1.5066	1.005	**82.9268**

MPI - 7a	Automated			
Human	SWS	IS	REM	W
SWS	**68.5393**	1.6787	0	NaN
IS	31.4607	**86.3309**	46.8665	NaN
REM	0	1.9185	**50.1362**	NaN
W	0	8.1535	2.1798	**NaN**

MPI - 7b	Automated			
Human	SWS	IS	REM	W
SWS	**99.1935**	1.7654	0	0
IS	0.8065	**63.0517**	90	50
REM	0	32.1564	**0**	0
W	0	2.1438	0	**50**

	Automated			
Human	SWS	IS	REM	W
SWS	**74.6667**	25.3333	0	0
IS	5.7971	**90.8903**	1.8634	1.4493
REM	0	10.0478	**89.9522**	0
W	0	18.1818	4.5455	**77.2727**

	Automated			
Human	SWS	IS	REM	W
SWS	**94.5736**	5.4264	0	0
IS	9.5238	**61.2245**	29.2517	0
REM	0	4.1667	**95.8333**	0
W	0	80.9524	19.0476	**0**

	Automated			
Human	SWS	IS	REM	W
SWS	**89.781**	10.219	0	0
IS	0.1887	**94.3396**	3.3962	2.0755
REM	0	100	**0**	0
W	0	60.7143	0	**39.2857**

Table A2.8, continued

MPI - 8a	Automated			
Human	SWS	IS	REM	W
SWS	**28.1818**	0.6696	0	0
IS	71.8182	**74.5536**	48.9627	56.6667
REM	0	22.0982	**42.7386**	0
W	0	1.5625	7.4689	**43.3333**

	Automated			
Human	SWS	IS	REM	W
SWS	**95.3846**	4.6154	0	0
IS	24.5342	**51.8634**	18.323	5.2795
REM	0	49.0099	**50.9901**	0
W	0	13.7255	35.2941	**50.9804**

MPI - 8b	Automated			
Human	SWS	IS	REM	W
SWS	**61.1111**	1.7857	0	0
IS	38.4259	**88.3929**	28.6792	14.7059
REM	0	8.7054	**65.6604**	0
W	0	0	2.6415	**85.2941**

	Automated			
Human	SWS	IS	REM	W
SWS	**94.2857**	5.7143	0	0
IS	14.8214	**70.7143**	13.5714	0.8929
REM	0	18.3099	**81.6901**	0
W	0	0	19.4444	**80.5556**

MPI - 9a	Automated			
Human	SWS	IS	REM	W
SWS	**95.7983**	6.4579	0	0
IS	4.2017	**90.411**	34.8765	8.3333
REM	0	0.9785	**59.8765**	0
W	0	0.5871	4.321	**91.6667**

	Automated			
Human	SWS	IS	REM	W
SWS	**77.551**	22.449	0	0
IS	0.8606	**79.5181**	19.4492	0.1721
REM	0	2.5126	**97.4874**	0
W	0	10.7143	50	**39.2857**

Table A2.8, continued

MPI - 9b	Automated			
Human	SWS	IS	REM	W
SWS	**95.5696**	4.5064	0	0
IS	4.4304	**92.7039**	42.6866	0
REM	0	1.7167	**53.1343**	0
W	0	0.8584	3.2836	**100**

	Automated			
Human	SWS	IS	REM	W
SWS	**87.7907**	12.2093	0	0
IS	1.2027	**74.2268**	24.5704	0
REM	0	4.3011	**95.6989**	0
W	0	22.2222	61.1111	**16.6667**

MPI - 10a	Automated			
Human	SWS	IS	REM	W
SWS	**62.6794**	1.462	0	0
IS	34.9282	**85.9649**	19.9005	28.7129
REM	0	3.8012	**65.6716**	0
W	1.9139	8.7719	14.4279	**71.2871**

	Automated			
Human	SWS	IS	REM	W
SWS	**96.3235**	3.6765	0	0
IS	15.6989	**63.2258**	8.6022	12.4731
REM	0	8.9655	**91.0345**	0
W	1.9324	14.4928	14.0097	**69.5652**

MPI - 10b	Automated			
Human	SWS	IS	REM	W
SWS	**61.9048**	0.2028	0	0
IS	37.619	**91.0751**	24.5614	51.6129
REM	0	4.2596	**68.4211**	0
W	0	4.2596	6.1404	**48.3871**

	Automated			
Human	SWS	IS	REM	W
SWS	**99.2366**	0.7634	0	0
IS	13.1667	**74.8333**	9.3333	2.6667
REM	0	11.8644	**88.1356**	0
W	1.9324	14.4928	14.0097	**69.5652**

Table A2.8, continued

MPI - 11a	Automated			
Human	SWS	IS	REM*	W
SWS	**91.7431**	2.8015	0	0
IS	8.2569	**65.8952**	0	26.3158
REM	0	21.5591	**0**	73.6842
W	0	8.8916	100	**0**

	Automated			
Human	SWS	IS	REM	W
SWS	**81.3008**	18.6992	0	0
IS	1.6216	**97.4775**	0	0.9009
REM	0	100	**0**	0
W	0	81.1111	3.3333	**15.5556**

MPI -11b	Automated			
Human	SWS	IS	REM	W*
SWS	**64.557**	0.3854	0	0
IS	32.2785	**76.4933**	47.8873	100
REM	3.1646	4.2389	**49.2958**	0
W	0	17.341	1.4085	**0**

	Automated			
Human	SWS	IS	REM	W
SWS	**98.0769**	1.9231	0	0
IS	8.7179	**67.8632**	23.2479	0.1709
REM	2.994	13.1737	**83.8323**	0
W	0	95.7447	4.2553	**0**

VA - 9	Automated			
Human	SWS	IS	REM	W
SWS	**69.3617**	2.3102	0	0
IS	30.2128	**86.4686**	10.7914	28.7313
REM	0	4.2904	**76.259**	0
W	0.4255	6.9307	12.9496	**71.2687**

	Automated			
Human	SWS	IS	REM	W
SWS	**95.8824**	4.1176	0	0
IS	16.7059	**61.6471**	3.5294	18.1176
REM	0	10.9244	**89.0756**	0
W	0.4329	9.0909	7.7922	**82.684**

Table A2.8, continued

VA - 10	Automated			
Human	SWS	IS	REM	W
SWS	**81.1475**	2.5057	0	0
IS	18.4426	**91.344**	18.9394	19.0909
REM	0	3.4169	**72.7273**	0
W	0	1.3667	6.8182	**80.9091**

	Automated			
Human	SWS	IS	REM	W
SWS	**94.7368**	5.2632	0	0
IS	9.1463	**81.5041**	5.0813	4.2683
REM	0	13.5135	**86.4865**	0
W	0	5.7692	8.6538	**85.5769**

VA - 11	Automated			
Human	SWS	IS	REM	W
SWS	**98.6047**	5.2817	0.2833	0
IS	1.3953	**94.0141**	48.1586	53.3333
REM	0	0	**50.7082**	0
W	0	0.3521	0.2833	**46.6667**

	Automated			
Human	SWS	IS	REM	W
SWS	**92.9825**	6.5789	0.4386	0
IS	0.6696	**59.5982**	37.9464	1.7857
REM	0	0	**100**	0
W	0	5.7692	8.6538	**85.5769**

VA - 18	Automated			
Human	SWS	IS	REM	W
SWS	**95.6098**	4.0767	0	0
IS	3.9024	**87.2902**	26.4368	2.5641
REM	0	6.235	**60.9195**	0
W	0	1.199	9.9617	**97.4359**

	Automated			
Human	SWS	IS	REM	W
SWS	**92.0188**	7.9812	0	0
IS	1.8059	**82.167**	15.5756	0.4515
REM	0	14.0541	**85.9459**	0
W	0	4.6729	24.2991	**71.028**

Table A2.8, continued

VA - 19	Automated			
Human	SWS	IS	REM	W
SWS	**36.1963**	0.5814	0	0
IS	63.8037	**93.0233**	22.8137	15.7895
REM	0	0.3876	**66.9202**	0
W	0	5.2326	7.6046	**84.2105**

	Automated			
Human	SWS	IS	REM	W
SWS	**95.1613**	4.8387	0	0
IS	16.0742	**74.1886**	9.2736	0.4637
REM	0	1.1236	**98.8764**	0
W	0	42.8571	31.746	**25.3968**

VA - 20	Automated			
Human	SWS	IS	REM	W
SWS	**98.9474**	7.4492	0	0
IS	1.0526	**87.3589**	22.9167	50
REM	0	1.5801	**73.4375**	0
W	0	1.5801	1.3021	**50**

	Automated			
Human	SWS	IS	REM	W
SWS	**74.0157**	25.9843	0	0
IS	0.2066	**79.9587**	18.1818	1.6529
REM	0	2.4221	**97.5779**	0
W	0	35	25	**40**

Average	Automated			
Human	SWS	IS	REM	W
SWS	**79.75599**	5.589931	0.020835	0
IS	19.2278	**84.20983**	28.84266	32.42611
REM	0.152242	5.749927	**61.98213**	2.947368
W	0.142004	3.234758	7.787419	**64.62652**

	Automated			
Human	SWS	IS	REM	W
SWS	**86.43716**	13.52625	0.036592	0
IS	7.285862	**75.93688**	14.0538	2.723462
REM	0.155854	16.33716	**83.50699**	0
W	0.522792	26.19818	18.93074	**54.3483**

Table A2.9. Agreement matrices for REM components. For each subject, two matrices as in Table A2.8 are presented. The matrices on the left and right should be read column-wise and row-wise, respectively. Each box in the left matrix corresponds to the percentage of times an epoch of the stage listed above as either the fragmented (REM UP) or stable (REM DOWN) components of REM as defined by the automated algorithm has been labeled as the stage on the left as defined by the human scorer. M corresponds to epochs labeled as movement. Each box in the right matrix corresponds to the percentage of time an epoch on the left, as defined by an automatic separation of manually identified REM is listed as the epoch above as defined by the algorithm. The REM UP/DOWN distinction is always done by a K-means algorithm on REM data, whether it is identified by the human scorer or the algorithm. Average percentage agreements were also computed for VA subjects, MPI subjects and both data sets, respectively. These matrices exclude three cases, where inspection of the preferred frequency map shows suspicious performance on the part of either the algorithm (MPI 7b and 11a) or the human scorer (MPI 8a). Most manually labeled REM components fall into the same automatically labeled REM components (right matrices). The unstable portion of REM as defined by the algorithm is most likely to be confused with stage II by the human when it is not scored as REM (left matrices).

Table A2.9 - Agreement Matrix - REM

VA - 9	**Automated**	
Human	REM UP	REM DOWN
SWS-4	0	0
SWS-3	0	0
IS-2	12.5	1.2048
IS-1	10.7143	1.2048
REM UP	**48.2143**	0
REM DOWN	0	**95.1807**
W	28.5714	2.4096
M	0	0

	Automated				
Human	SWS	IS	REM UP	REM DOWN	W
REM UP	0	10	**90**	0	0
REM DOWN	0	11.236	0	**88.764**	0

VA - 10	**Automated**	
Human	REM UP	REM DOWN
SWS-4	0	0
SWS-3	0	0
IS-2	14	15.8537
IS-1	8	1.2195
REM UP	**58**	0
REM DOWN	0	**81.7073**
W	18	0
M	2	1.2195

	Automated				
Human	SWS	IS	REM UP	REM DOWN	W
REM UP	0	27.5	**72.5**	0	0
REM DOWN	0	5.6338	0	**94.3662**	0

VA - 11	**Automated**	
Human	REM UP	REM DOWN
SWS-4	0	0.3861
SWS-3	0	0
IS-2	74.4681	36.2934
IS-1	3.1915	1.1583
REM UP	**21.2766**	0
REM DOWN	0	**61.39**
W	0	0.3861
M	1.0638	0.3861

	Automated				
Human	SWS	IS	REM UP	REM DOWN	W
REM UP	0	0	**100**	0	0
REM DOWN	0	0	0	**100**	0

Table A2.9, continued

VA - 18	**Automated**	
Human	REM UP	REM DOWN
SWS-4	0	0
SWS-3	0	0
IS-2	34.0909	8.0925
IS-1	15.9091	6.3584
REM UP	**29.5455**	0
REM DOWN	0	**76.8786**
W	17.0455	6.3584
M	3.4091	2.3121

	Automated				
Human	SWS	IS	REM UP	REM DOWN	W
REM UP	0	7.1429	**92.8571**	0	0
REM DOWN	0	15.2866	0	**84.7134**	0

VA - 19	**Automated**	
Human	REM UP	REM DOWN
SWS-4	0	0
SWS-3	0	0
IS-2	21.6	12.3188
IS-1	10.4	2.1739
REM UP	**49.6**	0
REM DOWN	0.8	**81.8841**
W	16	0
M	1.6	3.6232

	Automated				
Human	SWS	IS	REM UP	REM DOWN	W
REM UP	0	3.125	**96.875**	0	0
REM DOWN	0	0	0.8772	**99.1228**	0

VA - 20	**Automated**	
Human	REM UP	REM DOWN
SWS-4	0	0
SWS-3	0	0
IS-2	25	13.8462
IS-1	6.4516	5
REM UP	**60.4839**	1.5385
REM DOWN	0	**78.0769**
W	3.2258	0.3846
M	4.8387	1.1538

	Automated				
Human	SWS	IS	REM UP	REM DOWN	W
REM UP	0	5.9524	**89.2857**	4.7619	0
REM DOWN	0	0.9756	0	**99.0244**	0

Table A2.9, continued

Average VA	**Automated**	
Human	REM UP	REM DOWN
SWS-4	0	0.06435
SWS-3	0	0
IS-2	30.2765	14.60157
IS-1	9.111083	2.852483
REM UP	**44.52005**	0.256417
REM DOWN	0.133333	**79.18627**
W	13.80712	1.589783
M	2.151933	1.449117

	Automated				
Human	SWS	IS	REM UP	REM DOWN	W
REM UP	0	8.953383	**90.25297**	0.79365	0
REM DOWN	0	5.522	0.1462	**94.3318**	0

MPI -2a	**Automated**	
Human	REM UP	REM DOWN
SWS-4	0	0
SWS-3	0.6135	0
IS-2	27.6074	24.5536
IS-1	11.0429	4.0179
REM UP	**56.4417**	1.3393
REM DOWN	0	**69.1964**
W	3.681	0.4464
M	0.6135	0.4464

	Automated				
Human	SWS	IS	REM UP	REM DOWN	W
REM UP	0	1.0417	**95.8333**	3.125	0
REM DOWN	0	2.5157	0	**97.4843**	0

MPI -2b	**Automated**	
Human	REM UP	REM DOWN
SWS-4	0	0
SWS-3	0	0
IS-2	22.695	31.1688
IS-1	6.383	5.6277
REM UP	**67.3759**	0
REM	0	**60.6061**

	Automated				
Human	SWS	IS	REM UP	REM DOWN	W
REM UP	0	13.6364	**86.3636**	0	0
REM DOWN	0	8.4967	0	**91.5033**	0

Table A2.9, continued

DOWN		
W	3.5461	2.1645
M	0	0.4329

MPI -3a	**Automated**	
Human	REM UP	REM DOWN
SWS-4	0	0
SWS-3	0	0
IS-2	24	23.7288
IS-1	22.6667	12.4294
REM UP	**48**	0
REM DOWN	0	**62.7119**
W	4	0.565
M	1.3333	0.565

	Automated				
Human	SWS	IS	REM UP	REM DOWN	W
REM UP	0	12.1951	**87.8049**	0	0
REM DOWN	0	8.2645	0	**91.7355**	0

MPI -3b	**Automated**	
Human	REM UP	REM DOWN
SWS-4	0	0
SWS-3	0	0
IS-2	25.6757	18.75
IS-1	20.2703	7.8125
REM UP	**48.6486**	0.5208
REM DOWN	0	**71.3542**
W	2.7027	0.5208
M	2.7027	1.0417

	Automated				
Human	SWS	IS	REM UP	REM DOWN	W
REM UP	2.3256	11.6279	**83.7209**	2.3256	0
REM DOWN	0.6849	5.4795	0	**93.8356**	0

MPI -4a	**Automated**	
Human	REM UP	REM DOWN
SWS-4	0	0
SWS-3	0	0
IS-2	15.5556	10.5528
IS-1	13.3333	4.0201
REM UP	**62.2222**	0
REM DOWN	1.1111	**84.9246**

	Automated				
Human	SWS	IS	REM UP	REM DOWN	W
REM UP	0	1.7544	**98.2456**	0	0
REM DOWN	0	4.4944	0.5618	**94.9438**	0

Table A2.9, continued

W	3.3333	0
M	4.4444	0.5025

MPI -4b	**Automated**	
Human	REM UP	REM DOWN
SWS-4	0	0
SWS-3	0	0
IS-2	7.1429	6.7358
IS-1	9.5238	1.0363
REM UP	**78.5714**	0
REM DOWN	0	**91.1917**
W	2.381	0
M	2.381	1.0363

	Automated				
Human	SWS	IS	REM UP	REM DOWN	W
REM UP	0	15.3846	**84.6154**	0	0
REM DOWN	0	1.1236	0	**98.8764**	0

MPI -5a	**Automated**	
Human	REM UP	REM DOWN
SWS-4	0	0
SWS-3	0	0
IS-2	51.8519	9.0361
IS-1	1.8519	2.4096
REM UP	**38.8889**	0
REM DOWN	0	**88.5542**
W	3.7037	0
M	3.7037	0

	Automated				
Human	SWS	IS	REM UP	REM DOWN	W
REM UP	0	22.2222	**77.7778**	0	0
REM DOWN	0	2.649	0	**97.351**	0

MPI -5b	**Automated**	
Human	REM UP	REM DOWN
SWS-4	0	0
SWS-3	0	0
IS-2	17.2414	14.7239
IS-1	10.3448	2.454
REM UP	**62.069**	0
REM DOWN	3.4483	**82.8221**

	Automated				
Human	SWS	IS	REM UP	REM DOWN	W
REM UP	0	21.7391	**78.2609**	0	0
REM DOWN	0	8.1081	0.6757	**91.2162**	0

Table A2.9, continued

W	6.8966	0
M	0	0

MPI -6a	**Automated**	
Human	REM UP	REM DOWN
SWS-4	0	0
SWS-3	0	0
IS-2	8.5106	1.9737
IS-1	2.1277	0
REM UP	**46.8085**	0
REM DOWN	4.2553	**96.7105**
W	38.2979	1.3158
M	0	0

	Automated				
Human	SWS	IS	REM UP	REM DOWN	W
REM UP	0	31.25	**68.75**	0	0
REM DOWN	0	3.871	1.2903	**94.8387**	0

MPI -6b	**Automated**	
Human	REM UP	REM DOWN
SWS-4	0	0
SWS-3	0	0
IS-2	0	4.023
IS-1	4	0.5747
REM UP	**88**	0
REM DOWN	4	**94.8276**
W	4	0.5747
M	0	0

	Automated				
Human	SWS	IS	REM UP	REM DOWN	W
REM UP	0	35.2941	**64.7059**	0	0
REM DOWN	0	5.1429	0.5714	94.2857	0

MPI -7a	**Automated**	
Human	REM UP	REM DOWN
SWS-4	0	0
SWS-3	0	0
IS-2	25.5474	26.9565
IS-1	24.0876	18.2609
REM UP	**45.2555**	0
REM DOWN	0	**53.0435**

	Automated				
Human	SWS	IS	REM UP	REM DOWN	W
REM UP	0	7.4627	**92.5373**	0	0
REM DOWN	0	2.4	0	**97.6**	0

Table A2.9, continued

W	2.9197	1.7391
M	2.1898	0

MPI -7b	**Automated**	
Human	REM UP	REM DOWN
SWS-4	0	0
SWS-3	0	0
IS-2	90	80
IS-1	0	10
REM UP	**0**	0
REM DOWN	0	**0**
W	0	0
M	10	10

	Automated				
Human	SWS	IS	REM UP	REM DOWN	W
REM UP	0	100	**0**	0	0
REM DOWN	0	100	0	**0**	0

MPI -8a	**Automated**	
Human	REM UP	REM DOWN
SWS-4	0	0
SWS-3	0	0
IS-2	59.854	7.6923
IS-1	16.7883	4.8077
REM UP	**8.7591**	0
REM DOWN	0.7299	**86.5385**
W	12.4088	0.9615
M	1.4599	0

	Automated				
Human	SWS	IS	REM UP	REM DOWN	W
REM UP	0	76.4706	**23.5294**	0	0
REM DOWN	0	39.7351	0.6623	**59.6026**	0

MPI -8b	**Automated**	
Human	REM UP	REM DOWN
SWS-4	0	0
SWS-3	0	0
IS-2	26.2626	18.0723
IS-1	13.1313	4.2169
REM UP	**44.4444**	0
REM DOWN	1.0101	**77.7108**

	Automated				
Human	SWS	IS	REM UP	REM DOWN	W
REM UP	0	39.726	**60.274**	0	0
REM DOWN	0	7.1429	0.7143	**92.1429**	0

Table A2.9, continued

W	7.0707	0
M	8.0808	0

MPI -9a	**Automated**	
Human	REM UP	REM DOWN
SWS-4	0	0
SWS-3	0	0
IS-2	17.2727	18.6916
IS-1	22.7273	13.5514
REM UP	**50.9091**	0
REM DOWN	0	**64.486**
W	8.1818	2.3364
M	0.9091	0.9346

	Automated				
Human	SWS	IS	REM UP	REM DOWN	W
REM UP	0	6.6667	**93.3333**	0	0
REM DOWN	0	0.7194	0	**99.2806**	0

MPI -9b	**Automated**	
Human	REM UP	REM DOWN
SWS-4	0	0
SWS-3	0	0
IS-2	17.6991	16.2162
IS-1	24.7788	26.5766
REM UP	**48.6726**	0
REM DOWN	0	**55.4054**
W	7.0796	1.3514
M	1.7699	0.4505

	Automated				
Human	SWS	IS	REM UP	REM DOWN	W
REM UP	0	11.2903	**88.7097**	0	0
REM DOWN	0	0.8065	0	**99.1935**	0

MPI -10a	**Automated**	
Human	REM UP	REM DOWN
SWS-4	0	0
SWS-3	0	0
IS-2	7.0175	11.1111
IS-1	12.2807	9.0278
REM UP	**28.0702**	0
REM	8.7719	**77.0833**

	Automated				
Human	SWS	IS	REM UP	REM DOWN	W
REM UP	0	30.4348	**69.5652**	0	0
REM DOWN	0	4.918	4.0984	**90.9836**	0

Table A2.9, continued

DOWN		
W	43.8596	2.7778
M	0	0

MPI - 10b	**Automated**	
Human	REM UP	REM DOWN
SWS-4	0	0
SWS-3	0	0
IS-2	6.8966	2.8369
IS-1	27.5862	15.6028
REM UP	**50.5747**	0
REM DOWN	0	**79.4326**
W	13.7931	1.4184
M	1.1494	0.7092

	Automated				
Human	SWS	IS	REM UP	REM DOWN	W
REM UP	0	22.807	**77.193**	0	0
REM DOWN	0	6.6667	0	**93.3333**	0

MPI - 11a	**Automated**	
Human	REM UP	REM DOWN
SWS-4	0	0
SWS-3	0	0
IS-2	0	0
IS-1	0	0
REM UP	**0**	0
REM DOWN	0	**0**
W	100	100
M	0	0

	Automated				
Human	SWS	IS	REM UP	REM DOWN	W
REM UP	0	0	**100**	0	0
REM DOWN	0	0	100	**0**	0

MPI - 11b	**Automated**	
Human	REM UP	REM DOWN
SWS-4	0	0
SWS-3	0	0
IS-2	53.4351	26.7974
IS-1	7.6336	9.8039
REM	**29.771**	0

	Automated				
Human	SWS	IS	REM UP	REM DOWN	W
REM UP	0	20.4082	**79.5918**	0	0
REM DOWN	4.2373	10.1695	6.7797	**78.8136**	0

Table A2.9, continued

UP		
REM DOWN	6.1069	**60.7843**
W	2.2901	0.6536
M	0.7634	1.9608
average MPI	**Automated**	
Human	REM UP	REM DOWN
SWS-4	0	0
SWS-3	0.036088	0
IS-2	20.84774	15.64285
IS-1	13.751177	8.083676
REM UP	**52.63081**	0.109418
REM DOWN	1.688447	**74.7556**
W	9.278641	0.933171
M	1.767118	0.475288
average ALL	**Automated**	
Human	REM UP	REM DOWN
SWS-4	0	0.016787
SWS-3	0.026674	0
IS-2	23.30741	15.37121
IS-1	12.54071	6.719017
REM UP	**50.51496**	0.147765
REM DOWN	1.282765	**75.91143**
W	10.45998	1.104461
M	1.867504	0.72933

	Automated				
Human	SWS	IS	REM UP	REM DOWN	W
REM UP	0.1368	17.93772	**81.60486**	0.320624	0
REM DOWN	0.289541	4.880494	0.864212	**93.96576**	0

	Automated				
Human	SWS	IS	REM UP	REM DOWN	W
REM UP	0.101113	15.59398	**83.86089**	0.444022	0
REM DOWN	0.214009	5.047843	0.676904	**94.06125**	0

Table A2.10. REM outliers. On 4 VA subjects, 1 sec manually scored Stage II revealed that most of the spindles or K-complex, which were scored as REM by the algorithm did take place in the unstable part. The same was true for baseline Stage II without spindles or K-complexes, in 3 out of 4 subjects (left columns, the exception being subject 10.

Table A2.10 - REM Outliers											
	Stage II				Spindles				K-complex		
	events	TOP (%)	DOWN (%)		events	TOP (%)	DOWN (%)		events	TOP (%)	DOWN (%)
VA - 9	185	96.2162	3.7838		16	93.75	6.25		4	100	0
VA - 10	550	33.6364	66.3636		34	55.8824	44.1176		10	50	50
VA - 18	1123	66.4292	33.5708		126	76.1905	23.8095		12	66.6667	33.3333
VA - 19	1290	61.0078	38.9922		27	74.0741	25.9259		3	100	0

Table A2.11. Artifact and K-complex analysis. On the VA subjects, high and low frequency artifacts, movement artifacts with and without high frequency artifacts, eye intrusions (counted here as artifacts), times during which electrodes were disconnected and K-complexes were identified by two scorers (1 row per scorer), during manually labeled REM and sometimes in NREM. The percentage of fragmented ('TOP') and non-fragmented ('DOWN') REM composed by K-complexes ('K') and artifacts ('ART') is displayed for manually ('Manual') and automatically ('Automated') scored REM. Results for VA-9 are the same across both scorers because the discrepancy of their scoring was limited to NREM stages. Differences in the automated results in terms of percentages of artifacts present in each portion of REM for subjects 18 and 20 are due to one scorer identifying more movement artifacts than the to other scorer in these subjects.

Table A2.11 - Artifact Analysis									
	Manual					Automated			
	%K,TOP	%K,DOWN	%ART,TOP	%ART,DOWN		%K,TOP	%K,DOWN	%ART,TOP	%ART,DOWN
VA - 9	3.3333	2.2472	46.6667	71.9101		0	2.4096	39.2857	75.9036
VA - 9	3.3333	2.2472	46.6667	71.9101		0	2.4096	39.2857	75.9036
VA - 10	7.5	4.2254	25	33.8028		0	1.2195	30	32.9268
VA - 10	15.5556	7.8947	22.2222	32.8947		0	1.2195	30	32.9268
VA - 11	5	8.805	25	20.1258		3.1915	8.4942	12.766	16.6023
VA - 11	10	12.5714	20	20		3.1915	8.4942	12.766	16.6023
VA - 18	10.7143	2.5478	35.7143	49.6815		2.2727	2.3121	36.3636	47.3988
VA - 18	12.9032	3.0303	32.2581	48.4848		2.2727	2.3121	35.2273	46.2428
VA - 19	1.5625	0	37.5	35.9649		0.8	0	32	34.7826
VA - 19	1.5873	0	39.6825	36.2832		0.8	0	32	34.7826
VA - 20	13.0952	4.3902	33.3333	50.7317		10.4839	3.8462	30.6452	43.4615
VA - 20	18.4211	4.4776	34.2105	52.2388		10.4839	3.8462	29.8387	43.0769

Table A2.12. Nearest neighbor analysis. In the same subjects as in the previous table, epochs devoid of artifacts were identified to establish whether proximity to an artifact could be responsible for the fragmented portion of REM. %XY means percentage of neighbors of Y (TOP or DOWN) composed of X (0=no artifact in either neighbor, 1=one neighbor is an artifact, 2=both neighbors are artifacts). As in the previous table, each row corresponds to a different scorer. Similarities and differences observed within results for subject 9, 18 and 20 are explained in the previous legend. Subjects 9 and 19 have respectively 18/34 and 45/85 epochs in the fragmented part of automatically identified REM which do not have any neighboring artifacts, leading to the same percentage in both cases.

Table A2.12 - Nearest Neighbor Analysis													
	Manual							Automated					
	%0, TOP	%1, TOP	%2, TOP	%0, DOWN	%1, DOWN	%2, DOWN		%0, TOP	%1, TOP	%2, TOP	%0, DOWN	%1, DOWN	%2, DOWN
VA - 9	12.5	62.5	25	36	24	40		52.9412	32.3529	14.7059	25	25	50
VA - 9	12.5	62.5	25	36	24	40		52.9412	32.3529	14.7059	25	25	50
VA -10	36.6667	50	13.3333	53.1915	40.4255	6.383		37.1429	51.4286	11.4286	58.1818	36.3636	5.4545
VA -10	42.8571	45.7143	11.4286	56.8627	37.2549	5.8824		37.1429	51.4286	11.4286	58.1818	36.3636	5.4545
VA -11	20	60	20	67.7165	29.1339	3.1496		63.4146	31.7073	4.878	76.3889	21.2963	2.3148
VA -11	33.3333	50	16.6667	70	27.1429	2.8571		63.4146	31.7073	4.878	76.3889	21.2963	2.3148
VA -18	27.7778	61.1111	11.1111	48.1013	44.3038	7.5949		48.2143	46.4286	5.3571	57.1429	36.2637	6.5934
VA -18	38.0952	57.1429	4.7619	49.4118	43.5294	7.0588		54.386	42.1053	3.5088	58.0645	35.4839	6.4516
VA -19	30	57.5	12.5	68.4932	28.7671	2.7397		52.9412	38.8235	8.2353	75.5556	22.2222	2.2222
VA -19	28.9474	57.8947	13.1579	68.0556	29.1667	2.7778		52.9412	38.8235	8.2353	75.5556	22.2222	2.2222
VA -20	55.3571	35.7143	8.9286	53.4653	33.6634	12.8713		61.6279	32.5581	5.814	64.6259	24.4898	10.8844
VA -20	52	36	12	53.125	33.3333	13.5417		64.3678	29.8851	5.7471	64.1892	24.3243	11.4865

Chapter A2 is, in part, being prepared for publication. The co-author is T. Sejnowski. The dissertation author was responsible for the techniques described and main observations therein and was the primary investigator and author of this paper.

CHAPTER A3

REM REVISITED

The recently discovered phenomenon of Disuse Hypersensitivity (1-3) shows that neurons, especially immature neurons, whose activity has been suppressed will progressively become more excitable. If this is true in vivo, and there is some evidence for this, then what happens to networks which are not sufficiently activated during wakefulness? Could such unused networks be stabilized by excitation during sleep?

Several studies show that Slow Wave Sleep is associated with a replay of awake patterns of activity (4-5). It is during REM sleep that patterns which have not been used much or at all during wakefulness can be activated (not necessarily in exclusivity). The reduced synchrony that occurs during this phase makes it especially appropriate for such a task: the less synchrony, the more neurons can be co-activated without triggering instabilities. Thus REM pressure corresponds, in this view, to a response to reduced activity rather than to an overload of information during wakefulness.

This simple hypothesis could explain certain phenomena. For example, in this framework, one would expect that REM enhancement reduces the probability of epileptic seizures and that, conversely, REM deprivation would have the opposite effect. Both are true (6-7). This hypothesis can also offer an explanation as to why clinically depressed patients have more REM sleep and why REM deprivation helps reduce depression (8-9). If one associates depression with an obsessive rehearsal of negative events, and treat such a rehearsal as a stimulation of the same cortical networks at the expense of others, then larger neural populations would need to be stabilized via excitation during REM sleep, making REM more prominent in the sleep architecture. On the other hand, REM deprivation, would lead to large neural populations being increasingly excitable during subsequent awake states, which would interfere with the repetitive stimulation underlying the rehearsal.

Furthermore, one might also understand why there is less REM in the prefrontal cortex (PFC) than in other parts of the cortex (10): multiplexing in the PFC reduces the probability of having large populations of disused synapses in the awake state, thus limiting the need for subsequent REM sleep in that area.

Implications

Most of our dreams occur in REM sleep (11). If REM activity corresponds to, as suggested, a global stabilization of disused networks via excitation, then information that was suppressed by attention during wakefulness will be likely to appear during REM sleep. This can be understood in light of the observation that attentive mechanisms can reduce the activity of neurons which tend to preferentially respond to an unattended stimulus. Thus we would expect that if a V4 neuron is not upregulated by attention during wakefulness (12-13), its spontaneous activity during REM should be greater than in NREM whereas the opposite would be predicted for V4 neurons which were upregulated by an attentive mechanism during wakefulness.

It seems possible that this putative REM related activity of disused neurons, could very well trigger attention related activity during sleep so that our dreams would engage our attention at the expense of surrounding stimuli, such as sounds. In this sense, REM can be thought of as a sleep promoting phase so that the body can rest following intense hormonal activity during other phases of sleep. In this paradigm, REM is not treated

as a simple sleep-awake transition phase, especially since it is not restricted to the final hours of sleep. If dreams are for the most part necessary to maintain sleep, then we would expect other species to be selected by evolution to dream as well. We would therefore expect them to have subjective experiences.

This hypothesis concerning dreams would explain why we tend not to remember our dreams: disused neurons are have been stabilized and their spontaneous activity during subsequent wakefulness is reduced.

Back to the Crick-Mitchison theory

The Crick-Mitchison (C-M) theory of REM sleep (14) posits that during REM sleep, a reverse learning mechanism modifies cortical networks in order to reduce the likelihood of parasitical modes during subsequent wakefulness. In the present hypothesis, large scale excitation of the hyperexcitable and parasitical neurons corresponds to this reverse learning mechanism.

However, as mentioned before, the parasitical modes would stem from reduced neural activity, not overload. Neural overload is likely to be linked to sleep deprivation which we know gives rise to more subsequent Slow Wave Sleep (15).

A revised version of C-M can account for unsolved issues in the original version. For example, one could see why antidepressants can knock out REM sleep without any perceivable associated cognitive deficit: REM deprivation increases the subsequent neural load and any overload will be palliated in SWS.

Finally we can now understand why fetuses in the womb have REM sleep: their cortical wiring is very limited, leading large neural populations to be disused and excitable, which strongly increases REM pressure.

References

1. V. N. Murthy, T. Schikorski, C. F. Stevens, Y. Zhu, *Neuron* **32**, 673 (2001).

2. V. Kilman, M. C. van Rossum, G. G. Turrigiano, *J. Neurosci.* **22**, 1328 (2002).

3. N. S. Desai, R. H. Cudmore, S. B. Nelson, G. G. Turrigiano, *Nat.Neurosci.* **5**,783 (2002).

4. R. Stickgold, J. A. Hobson, R. Fosse , M. Fosse, *Science* **294**, 1052 (2001).

5. M. A. Wilson, B. L. McNaughton, *Science* **265**, 676 (1994).

6. P. Kumar, T. R. Raju, *Brain Research* **922**, 299 (2001).

7. H. M. de Paula, K. Hoshino**,** *Brain Res.* **926**, 80 (2002).

8. H. P. Landolt, J. C. Gillin, *Neuropsychopharmacology* **27**, 462 (2002).

9. H. P. Landolt, E. B. Raimo, B. J. Schnierow, J. R. Kelsoe, M. H. Rapaport, J. C., *Arch. Gen. Psychiatry* **58,** 268 (2001).

10. L. De Gennaro, M. Ferrara, G. Curcio, R. Cristiani, M. Bertini, *Clin. Neurophysiol.* **113**, 561 (2002).

11. W. Dement, N. Kleitman, *Electroenceph. Clin. Neurophysiol.* **9**,673 (1957).

12 J. H. Reynolds, T. Pasternak, R. Desimone, *Neuron* **26**, 703 (2000).

13. P. Fries, J. H. Reynolds, A. E. Rorie, R. Desimone,

Science **291**,1560 (2001).

14. F. Crick, G. Mitchison, *Nature* **304**,111 (1983).

15. D. P. Brunner, D. J. Dijk, I. Tobler, A. A. Borbély, *Electroenceph. Clin. Neurophysiol.* **75**,492 (1990).

CHAPTER A4

PATENTS

A. PCT Patent Application Serial No. US2005/027562 filed August 2, 2005, entitled "Dynamic Signal Processing"

Inventors: Philip Low and Terrence Sejnowski

(12) INTERNATIONAL APPLICATION PUBLISHED UNDER THE PATENT COOPERATION TREATY (PCT)

(19) World Intellectual Property Organization
International Bureau

(43) International Publication Date
16 November 2006 (16.11.2006)

PCT

(10) International Publication Number
WO 2006/121455 A1

(51) International Patent Classification:
G06F 7/06 (2006.01)

(21) International Application Number:
PCT/US2005/027562

(22) International Filing Date: 2 August 2005 (02.08.2005)

(25) Filing Language: English

(26) Publication Language: English

(30) Priority Data:
60/679,951 10 May 2005 (10.05.2005) US

(71) Applicant *(for all designated States except US)*: **THE SALK INSTITUTE FOR BIOLOGICAL STUDIES** [US/US]; Office of Technology Management, 10010 North Torrey Pines Road, La Jolla, CA 92037 (US).

(72) Inventors; and

(75) Inventors/Applicants *(for US only)*: **LOW, Philip, S.** [CA/US]; Apartment 214, 8870 Villa La Jolla Drive, La Jolla, CA 92037 (US). **SEJNOWSKI, Terrence, J.** [US/US]; 672 San Mario Drive, Solana Beach, CA 92075 (US).

(74) Agents: **HARRIS, Scott, C.** et al.; Fish & Richardson P.C., P.O. Box 1022, Minneapolis, MN 55440-1022 (US).

(81) Designated States *(unless otherwise indicated, for every kind of national protection available)*: AE, AG, AL, AM, AT, AU, AZ, BA, BB, BG, BR, BW, BY, BZ, CA, CH, CN, CO, CR, CU, CZ, DE, DK, DM, DZ, EC, EE, EG, ES, FI, GB, GD, GE, GH, GM, HR, HU, ID, IL, IN, IS, JP, KE, KG, KM, KP, KR, KZ, LC, LK, LR, LS, LT, LU, LV, MA, MD, MG, MK, MN, MW, MX, MZ, NA, NG, NI, NO, NZ, OM, PG, PH, PL, PT, RO, RU, SC, SD, SE, SG, SK, SL, SM, SY, TJ, TM, TN, TR, TT, TZ, UA, UG, US, UZ, VC, VN, YU, ZA, ZM, ZW.

(84) Designated States *(unless otherwise indicated, for every kind of regional protection available)*: ARIPO (BW, GH, GM, KE, LS, MW, MZ, NA, SD, SL, SZ, TZ, UG, ZM, ZW), Eurasian (AM, AZ, BY, KG, KZ, MD, RU, TJ, TM), European (AT, BE, BG, CH, CY, CZ, DE, DK, EE, ES, FI, FR, GB, GR, HU, IE, IS, IT, LT, LU, LV, MC, NL, PL, PT, RO, SE, SI, SK, TR), OAPI (BF, BJ, CF, CG, CI, CM, GA, GN, GQ, GW, ML, MR, NE, SN, TD, TG).

[Continued on next page]

(54) Title: DYNAMIC SIGNAL PROCESSING

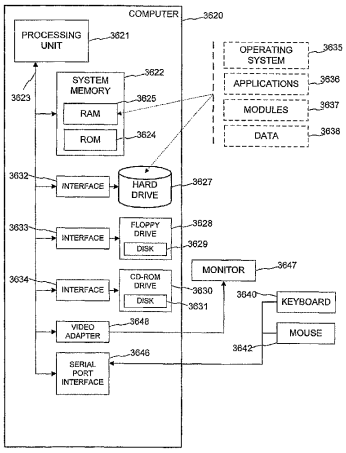

(57) Abstract: Technologies presented can determine low power frequency range information from spectral data. Raw signal data can be adjusted to increase dynamic range for power within low power frequency ranges as compared to higher-power frequency ranges to determine adjusted source data valuable for acquiring low power frequency range information. Low power frequency range information can be used in the analysis of a variety of raw signal data. For example, low power frequency range information within electroencephalography data for a subject from a period of sleep can be used to determine sleep states. Similarly, automated full-frequency spectral electroencephalography signal analysis can be useful for customized analysis including assessing sleep quality, detecting pathological conditions, and determining the effect of medication on sleep states.

WO 2006/121455 A1

Declaration under Rule 4.17:
— *of inventorship (Rule 4.17(iv))*

Published:
— *with international search report*

For two-letter codes and other abbreviations, refer to the "Guidance Notes on Codes and Abbreviations" appearing at the beginning of each regular issue of the PCT Gazette.

DYNAMIC SIGNAL PROCESSING

REFERENCE TO RELATED APPLICATIONS

This application claims the benefit of U.S. Provisional Patent Application No. 60/679,951, entitled, "DYNAMIC SIGNAL PROCESSING," filed May 10, 2005, which is hereby incorporated by reference herein.

FIELD

The field relates to digital signal processing.

BACKGROUND

Raw signal data can commonly overrepresent certain frequencies due to high power signals received from select frequency ranges in a frequency spectrum. In turn, in many fields of study, low power frequency range information is disregarded or ignored when valuable information exists within those frequencies in the raw signal. Within the medical and biological sciences there are many signals analyzed to assess clinical states, pathological conditions, and the like. In particular, sleep is commonly analyzed via electroencephalography (EEG) signals; signals which normally over represent the low frequency ranges. However, the details of sleep reside within the full spectrum of frequency information in the signal. As a person falls asleep, brain activity is modulated and there is a progressive increase in the depth of sleep. A typical night's sleep for a normal person quickly transitions to a sleep stage known as slow wave sleep (SWS) characterized by low frequency, high power EEG activity. At intervals during the night, sleep lightens into intermediate sleep stages and can enter a sleep state known as rapid eye movement (REM) sleep characterized by high frequency, low power EEG activity. EEGs follow a 1/f distribution where the higher frequency signals tend to have lower amplitudes and therefore lower power. The current gold-standard for analyzing EEG signals for sleep stage determination is the Rechtschaffen-Kales method. This method can rely on manually scoring sleep EEG signals due to the low power frequency limitations of automated signal analysis techniques. The Rechtschaffen-Kales method can be both highly unreliable and time consuming because statistically significant shifts at high frequencies are usually not detectable by a human scorer due to the very low amplitudes. Further, the Rechtschaffen-Kales method tends to have poor temporal and spatial resolution, does not make all of its variables known, and commonly leads to low inter-user agreement rates across manual as well as automated scorers. Unfortunately, alternative sleep state determination methods, including artificial neural network classifiers, tend to emulate human performance, thereby improving the time of determination without drastically improving quality. There remains a need with the sleep sciences for a fast and quantitatively

rigorous alternative to current EEG signal analysis methods. Accordingly, there also remains a clear need to better analyze any signal data to elucidate valuable low power frequency range data that is otherwise disregarded or ignored due to over represented high power frequency range data.

SUMMARY

Raw signal data can be adjusted to increase dynamic range for power within low power frequency ranges as compared to higher power frequency ranges to determine adjusted source data valuable for acquiring low power frequency range information. Low power frequency range information can be used in the analysis of a variety of raw signal data. For example, low power frequency range information within electroencephalography data for a subject from a period of sleep can be used to determine sleep states. Similarly, automated full-frequency spectral electroencephalography signal analysis can be useful for customized medical analysis including assessing sleep quality, detecting pathological conditions, and determining the effect of medication on sleep states.

The techniques described herein can be applied to any number of signal types where determining low power frequency information from source data is desired.

Additional features and advantages of the technologies described herein will be made apparent from the following detailed description of illustrated embodiments, which proceeds with reference to the accompanying drawings.

BRIEF DESCRIPTION OF THE DRAWINGS

FIG. 1 is a block diagram of an exemplary system for determining low power frequency information from source data with at least one low power frequency range.

FIG. 2 is a flowchart showing an exemplary method for adjusting source data.

FIG. 3 is a flowchart showing an exemplary method for adjusting source data to account for differences in power over a spectrum of frequencies over time.

FIG. 4 is a block diagram of an exemplary system for determining sleep state information for a subject.

FIG. 5 is a block diagram of another exemplary system for determining sleep state information for a subject.

FIG. 6 is a flowchart showing an exemplary method for determining sleep states in a subject.

FIG. 7 is a flowchart showing an exemplary method for classifying sleep states in a subject.

FIG. 8 is a block diagram of an exemplary system for determining a pathological condition of a subject from sleep states.

FIG. 9 is a flowchart showing an exemplary computer-implemented method for determining a pathological condition for a subject based on sleep states.

FIG. 10 is a block diagram of an exemplary system for dynamically determining customized sleep scores for a subject.

FIG. 11 is a screen shot of an exemplary whole night EEG source data frequency power spectrogram.

FIG. 12 is a screen shot of the exemplary whole night EEG source data shown in FIG.11 after an exemplary adjustment technique has been applied.

FIG. 13 is a screen shot of a two hour time frame of the exemplary adjusted whole night EEG source data shown in FIG.12.

FIG. 14 is a screen shot of an exemplary visualization of high and low power frequency bands within the whole night EEG spectrogram shown in FIG. 12.

FIG. 15 is a screen shot of a two hour and forty minutes time frame of the exemplary visualization of high and low power frequency bands within the whole night spectrogram shown in FIG. 14.

FIG. 16 is a screen shot of an exemplary five-dimensional parameter space visualization of the whole night EEG spectrogram of FIG. 12.

FIG. 17 is a screen shot of a two hour time frame of the exemplary five-dimensional parameter space visualization of the whole night EEG visualization shown in FIG.16.

FIG. 18 is a screen shot of an exemplary visualization of classified sleep states based on EEG spectrogram data.

FIG. 19 is a screen shot of another exemplary visualization of classified sleep states based on EEG spectrogram data.

FIG. 20 is a screen shot of yet another exemplary visualization of classified sleep states based on EEG spectrogram data.

FIG. 21 is screen shot from another vantage point of the exemplary visualization of classified sleep states based on EEG spectrogram data of FIG. 20.

FIGS. 22, 23, 24, and 25 are screen shots of canonical spectra representative of frequency weighted epochs designated as distinct sleep states in a subject for a period of time.

FIG. 26 is a screen shot of a canonical spectra representative of a frequency weighted epoch that displays a transient sleep state having characteristics of more than one sleep state.

FIGS. 27 is a screen shot of an exemplary visualization of the degree of sleep stage separation that distinguishes representative canonical spectra of distinct sleep states.

FIG. 28, 29, 30, 31, and 32 are screen shots of exemplary visualizations of sleep state statistics for a subject according to sleep state designations of one or more epochs.

FIG. 33 is a screenshot of an exemplary visualization of classified anesthesia states of an anesthetized cat based on EEG spectrogram data.

FIGS. 34 is a screenshots of an exemplary visualization of classified sleep states of a human subject based on EEG spectrogram data.

FIG. 35 is flowchart showing yet another exemplary method for classifying sleep states in a subject that can be implemented with the described technologies.

FIG. 36 is an exemplary computer system that can be implemented with the described technologies.

FIG. 37 is a screenshot of an exemplarly visualization of independent component analysis applied on a normalized spectorogram to further determine appropriate frequency windows for extracting information.

FIG. 38 is a screenshot of an exemplary visualization of independent components of FIG. 37 throughout time.

FIG. 39 is a screen shot of a six and a half hour time frame of an exemplary five-dimensional parameter space visualization of frequency bands of the whole night EEG visualization from a human subject with Alzheimer's.

FIG. 40 is a screen shot of an exemplary visualization of classified unihemispheric sleep from a bird.

DETAILED DESCRIPTION

Overview of Technologies

The techniques described herein can be used in any variety of scenarios in which analyzing source data for determining low power frequency information is useful.

Low power frequency information includes any information extracted from frequencies in source data that exhibit low power relative to other frequencies within the source data frequency spectrum. For example, data representing high frequency signals having low power within the frequency spectrum of source data can be low power frequency information.

An *epoch* includes any time series increment (e.g., time segment) of data. For example, data can be segmented into one or more epochs for analyzing. Further, for example, epochs can be determined via segmenting data by scanning a length of time of data via a scanning window and moving along the data time domain in increments via a sliding window. For example, neighboring epochs can have overlapping time series data when a sliding window is less than a scanning window or non-overlapping time series data when a sliding window is greater than or equal to a scanning window. Alternatively, an epoch can span an entire (e.g., whole) time series when a scanning window and sliding window both cover the length of the entire time series..

A *scanning window* includes any set period of time for use in capturing discrete time series of data. For example, a one minute time frame of received signal data can be scanned in increments of ten seconds (e.g., a scanning window of ten seconds), resulting in six discrete time series segments of the data.

A *sliding window* includes any set period of time for use in setting the starting time point of a scanning window. For example, a one minute time frame of received signal data can be scanned with a ten-second scanning window that begins every five seconds (e.g., a sliding window of five seconds) resulting in ten-second epochs that overlap by five seconds.

A *frequency weighted epoch* includes any epoch which has been normalized. For example, an epoch that has undergone any normalization process to account for differences in frequency power of the one or more epochs across time in data can be a frequency weighted epoch.

A *sleep state* includes any distinguishable period of sleep or wakefulness representative of certain behavioral, physical, or signal characteristics. For example, slow wave sleep (SWS), rapid eye movement sleep (REM), and intermediate (INTER or IS) sleep states (e.g., intermediate sleep states I and II) and awake state can be sleep states. Awake states can be further categorized into vigilance (e.g., attentiveness or levels of alertness) states.

A *sleep state designation* includes any sleep state label or term for describing an epoch. For example, sleep state designations can include slow wave sleep (SWS), non-slow wave sleep (NSWS), rapid eye movement sleep (REM), non-rapid eye movement sleep (NREM), intermediate I sleep, (INT I), intermediate II sleep (INT II), transient (e.g., spindles and K-complexes), outlier, artifact, awake, and the like. Similarly, numbers can be used to represent sleep states (e.g., 0 for SWS and 1 for non-SWS sleep or vice versa). In such a way, computational methods can be used to average neighboring epochs during the sleep state designation process.

An *artifact* includes any data that misrepresents the data intended to be received. For example, movement data in an EEG can be an artifact.

Movement data includes any data representing movement in a subject during the acquisition of source data. For example, movement data can be data representing a muscle twitch or the like.

Dynamic range includes any range of intensity measurement. For example, dynamic range for power can be determined for frequency ranges within a frequency spectrum and compared, resulting in a lower dynamic range for one frequency range versus another.

Segmenting includes separating, dividing or splitting information into components or consitituents. The terms "segmenting" and "separating" can be used interchangeably. For example, source data can be segmented (e.g. separated) into a plurality of time segments (e.g., epochs).

Example 1 - Exemplary Source Data

In any of the technologies described herein, a variety of source data can be analyzed including electroencephalography (EEG) data, electrocardiography data (EKG), electrooculography data (EOG), electromyography data (EMG), wave data including sound and pressure waves, and any data exhibiting a 1/f nature where there are differences in dynamic range of power for various frequencies across a frequency spectrum of the data. Source data can include encoded data stored at low power frequency within source data.

Example 2 - Exemplary System for Determining Low Power Frequency Information from Source Data with at Least One Low Power Frequency Range

FIG. 1 shows an exemplary system 100 for determining low power frequency information from source data with at least one low power frequency range.

Source data with at least one low power frequency range 102 is obtained and input into software 104 to determine low power frequency information 106.

The software 104 can employ any combination of technologies, such as those described herein, to determine low power frequency information 106 for the source data.

Methods for determining low power frequency information from source data with at least one low power frequency range are described in detail below.

Example 3 - Exemplary Method for Adjusting Source Data

FIG. 2 shows an exemplary method 200 for adjusting source data. For example, the method 200 can be implemented within system 100 of FIG. 1.

At 202, source data with at least one low power frequency range is received. For example, electroencephalography source data for a subject can be received. Source data can be received via a single channel or multiple channels.

At 204, source data is adjusted to increase the dynamic range for power within at least one low power frequency range of the frequency spectrum of the source data as compared to a second higher power frequency range. Any of the adjustment techniques described herein (e.g., normalization, frequency weighting, and the like) can be used. For example, electroencephalography source data can be analyzed to increase the low power, higher frequency range data relative to the higher power, lower frequency range data.

After the source data is adjusted, various other processing can be done. For example, a visualization of the adjusted source data can be presented. Further, low power frequency information can be extracted from the adjusted source data. For example, low power frequency information can be extracted from adjusted electroencephalography source data. Higher power frequency information can also be extracted from the adjusted source data.

The method described in this or any of the other examples can be a computer-implemented method performed via computer-executable instructions in one or more computer-readable media. Any of the actions shown can be performed by software incorporated within a signal processing system or any other signal data analyzer system.

Example 4 -Exemplary Method for Adjusting Source Data to Account for Differences in Power over a Spectrum of Frequencies over Time

FIG. 3 shows an exemplary method 300 for adjusting source data to account for differences in power over a spectrum of frequencies over time. For example, the method 300 can be implemented within system 100 of FIG. 1.

At 302, source data with at least on low power frequency range is received. For example, electroencephalography data with at least one low power frequency range can be received. Artifacts in the data can be removed from the source data. For example, artifact data can be manually removed

from the source data or automatically filtered out of source data via a filtering (e.g., direct current filtering) or data smoothing technique.

At 304, the source data is segmented into one or more epochs. For example, the source data can be segmented in a plurality of time segments via a variety of separating techniques. Scanning windows and sliding windows can be used to separate the source data into time series increments. The source data can also be filtered via direct current filtering during or prior to segmentation. The source data can also be pretreated with component analysis.

At 306, the one or more epochs can be normalized to account for differences in power of the one or more epochs across time. For example, the power of each epoch at one or more frequencies can be normalized across time to determine appropriate frequency windows for extracting information. Such normalization can reveal low power, statistically significant shifts in power at one or more frequencies (e.g., Delta, Gamma, and the like). Any frequency range can be revealed and utilized for analysis. Information can be calculated for each of the one or more epochs after appropriate frequency windows have been established. Such information can include low frequency power (e.g., Delta power), high frequency power (e.g., Gamma power), standard deviation, maximum amplitude (e.g., maximum of the absolute value of peaks) and the sort. Further calculations can be done on the information calculated for each of the one or more epochs creating information such as Gamma power/Delta power, time derivative of Delta, time derivative of Gamma power/Delta power and the like. Time derivatives can be computed over preceding and successive epochs. After calculating the information, it can then be normalized across the one or more epochs. A variety of data normalization techniques can be conducted including z-scoring and the like.

At 308, results of the adjustment of source data to account for differences in power over a spectrum of frequencies over time can be presented as one or more epochs of data. For example, frequency weighted epochs can be presented as adjusted source data.

Example 5 - Exemplary System for Determining Sleep State Information for a Subject

FIG. 4 shows an exemplary system 400 for determining sleep state information for a subject.

Electroencephalography data for a subject 402 is obtained and input into software 404 to determine sleep state information for the subject 406.

The software 404 can employ any combination of technologies, such as those described herein, to determine sleep state information for the subject 406.

Methods for determining sleep state information for a subject are described in detail below.

Example 6 - Another Exemplary System for Determining Sleep State Information for a Subject

FIG. 5 shows an exemplary system 500 for determining sleep state information for a subject.

Electroencephalography data for a subject 502 is obtained and input into segmenter 504 to segment the data into one or more epochs. In practice, epochs are of similar (e.g., the same) length. Epoch length can be adjusted via a configurable parameter. The one or more epochs, in turn, are input into normalizer 506 to normalize frequency data in the one or more epochs across time, thereby frequency weighting the one or more epochs of electroencephalography data. The one or more frequency weighted epochs are then input into classifier 508 to classify the data into sleep states, thereby generating sleep state information for the subject 510.

Methods for determining sleep state information for a subject are described in detail below.

Example 7 - Exemplary Method for Determining Sleep States in a Subject

FIG. 6 shows an exemplary method 600 for determining sleep states in a subject. For example, the method 600 can be implemented within system 500 of FIG. 5 or system 400 of FIG. 4.

At 602, electroencephalography (EEG) data for a subject is received. For example, electroencephalography data which exhibits lower dynamic range for power in at least one low power first frequency range in a frequency spectrum as compared to a second frequency range in the frequency spectrum can be received.

At 604, the electroencephalography data for the subject is segmented into one or more epochs. For example, the EEG data can be segmented into one or more epochs via a variety of separating techniques. Scanning windows and sliding windows can be used to separate the EEG data into one or more epochs. The source data can also be filtered via direct current filtering during, prior to, or after segmenting. The source data can also be pretreated with component analysis (e.g., principle or independent component analysis). FIG. 11 is a screen shot of an exemplary whole night EEG source data frequency power spectrogram for a subject that has been segmented over three second epochs spaced in 1 second increments. Power range is indicated in the shading, where white shaded regions are higher in power than dark shaded regions. The higher frequencies (e.g., Gamma) therefore exhibit lower power than the lower frequencies (e.g., Delta, Theta and the like) in the whole night EEG data.

At 606, frequency power of the one or more epochs is weighted across time. For example, the power of each epoch at one or more frequencies can be normalized across time to determine appropriate frequency windows for extracting information. Such normalization can reveal low power, statistically significant shifts in power at one or more frequencies (e.g., Delta, Gamma, and the like). Additionally, each epoch can be represented by the frequency with the highest relative power over time to determine appropriate frequency windows for extracting information. Alternatively, component analysis (e.g., principle component analysis (PCA) or independent component analysis (ICA)) can be utilized after normalization to further determine appropriate frequency windows for extracting information. For example, FIGS. 37 and 38 are screen shots of component analysis utilized after normalization to suggest filters (e.g., screen shot 3700) and express independent components

throughout time (e.g., screen shot 3800). Any frequency range can be revealed and utilized for analysis.

Information can be calculated for each of the one or more epochs after appropriate frequency windows have been established (e.g., after weighting frequency). Such information can include low frequency power (e.g., Delta power), high frequency power (e.g., Gamma power), standard deviation, maximum amplitude (e.g., maximum of the absolute value of peaks) and the sort. Further calculations can be done on the information calculated for each of the one or more epochs creating information such as Gamma power/Delta power, time derivative of Delta, time derivative of Gamma power/Delta power and the like. Time derivatives can be computed over preceding and successive epochs. After calculating the information, it can then be normalized across the one or more epochs. A variety of data normalization techniques can be conducted including z-scoring and the like.

FIG. 12 is a screen shot of the exemplary whole night EEG source data shown in FIG.11 after an exemplary frequency power of the one or more epochs has been weighted across time. The higher frequency data is now more clearly visible. FIG. 13 is a screen shot of a two hour time frame of the exemplary adjusted whole night EEG source data shown in FIG.12. FIG. 14 is a screen shot of an exemplary visualization of high (e.g., Gamma) and low (e.g., Delta) power frequency bands within the whole night EEG spectrogram shown in FIG. 12. FIG. 15 is a screen shot of a two hour and forty minutes time frame of the exemplary visualization of high and low power frequency bands shown in FIG. 14.

FIG. 16 is a screen shot of an exemplary five-dimensional parameter space visualization of the whole night EEG spectrogram of FIG. 12. The five parameters (e.g., variables) are information calculated for each of the one or more epochs after weighting frequency. FIG. 17 is a screen shot of a two hour time frame of the exemplary five-dimensional parameter space visualization of the whole night EEG visualization shown in FIG.16.

At 608, sleep states in the subject are classified based on the one or more frequency weighted epochs. For example, the one or more frequency weighted epochs can be clustered by any variety of clustering techniques including k-means clustering. The clustering can be done on information calculated from the epochs (e.g., Delta power, Gamma power, standard deviation, maximum amplitude (Gamma/Delta), time derivative of Delta, time derivative of (Gamma /Delta), and the sort). Component analysis (e.g., PCA or ICA) can be used to determine the parameter space (e.g., types of information used) in the clustering. Subsequent to clustering, sleep state designations can be assigned to the epochs. Sleep state designated epochs can then be presented as representations of sleep states in the subject for the period of time represented by the epoch. Classification can also incorporate manually determined sleep states (e.g., manually determined "awake" versus "sleeping" sleep states). Additionally, artifact information (e.g. movement data, poor signal data, or the like) can be utilized in the classification.

Example 8 - Exemplary Sleep State Classification Techniques

Epochs can be classified according to a number of sleep states. An epoch can be classified according to normalized variables (e.g., information calculated for an epoch) based on high frequency information, low frequency information, or both high and low frequency information. For example, REM sleep state epochs can have higher relative power than SWS at higher frequencies and lower relative power than SWS at lower frequencies. Similarly, SWS sleep state epochs can have lower relative power than REM at higher frequencies and higher relative power than REM at lower frequencies. Additionally, epochs initially classified as both NREM and NSWS sleep (e.g., epochs having low relative power at both higher and lower frequencies) can be classified as intermediate sleep and epochs classified as both REM and SWS sleep (e.g., epochs having high relative power at both higher and lower frequencies) can be classified as outliers. Further, epochs initially classified as both NREM and NSWS sleep can be classified as intermediate stage I sleep and epochs initially classified as both REM and SWS sleep can be classified as intermediate stage II sleep. Additionally, sleep states can be split in the classifying to look for spindles, k-complexes, and the like. Any group of epochs initially classified as one sleep state can be split into multiple sub-classified sleep states according to increasing levels of classification detail. For example, a group of epochs classified as SWS can be reclassified as two distinct types of SWS.

Example 9 - Exemplary Artifact Classification Techniques

Artifact data (e.g. movement data, poor signal data, and the like) can also be used in sleep state classification. For example, artifacts can be used to analyze whether epochs initially assigned a sleep state designation should be reassigned a new sleep state designation due to neighboring artifact data. For example, an epoch assigned a sleep state designation of REM that has a preceding movement artifact or awake epoch can be reassigned a sleep state designation of awake. Further, for example, an artifact epoch that has a succeeding SWS epoch can be reassigned a sleep state designation of SWS because there is a high likelihood that the epoch represents a large SWS sleep epoch rather than a large movement artifact which is more common during wakefulness. In such ways, for example, artifact data can be utilized in a data smoothing technique.

Example 10 - Exemplary Smoothing Techniques

Any variety of data smoothing techniques can be used during the assigning of sleep states. For example, numbers (e.g., 0 and 1) can be used to represent designated sleep states. Neighboring epochs' sleep state designation numbers can then be averaged to determine if one of the epochs is inaccurately assigned a sleep state designation. For example, abrupt jumps from SWS-NSWS-SWS (and REM-NREM-REM) are rare in sleep data. Therefore, should a group of epochs be assigned sleep state designations representing abrupt jumps in sleep states, smoothing techniques can be applied to improve the accuracy of the assigning.

For example, in a scenario in which 0 represents SWS, 1 represents NSWS and the following sleep state designations existed for five neighboring epochs, 00100, then an average of the five sleep states would be 0.2. In such an instance, the middle epoch initially assigned a sleep designation of 1 (SWS) would be reassigned a sleep state designation of 0 (NSWS). The same technique could be used for REM versus NREM where a second set of sleep designations for the same five neighboring epochs is determined. For example, 1 can represent REM, 0 can represent NREM, and the following designations can exit for the five neighboring epochs, 00100. Again, the average of the five sleep states would be 0.2. Again, the middle epoch initially assigned a designation of 1 (REM) would be reassigned a sleep state designation of 0 (NREM). Such smoothing techniques can improve the accuracy of assigning sleep state designations.

Example 11 - Exemplary Method for Classifying Sleep States in a Subject

FIG. 7 shows an exemplary method 700 for classifying sleep states in a subject. For example, the method 700 can be implemented within system 500 of FIG. 5, system 400 of FIG. 4 or within the classifying 608 of method 600.

At 702, one or more frequency weighted epochs are received. For example, frequency weighted epochs determined from the weighting 606 of method 600 can be received.

At 704, the one or more frequency weighted epochs are clustered. For example, the one or more frequency weighted epochs can be clustered by any variety of clustering techniques including k-means clustering. The clustering can be done on information calculated from the epochs (e.g., Delta power, Gamma power, standard deviation, maximum amplitude (Gamma/Delta), time derivative of Delta, time derivative of Gamma /Delta, and the sort). Exemplary visualizations of clustered sleep states are shown in FIGS. 18 and 19. FIG. 18 shows epochs clustered via Delta, Gamma/Delta, and the time derivative of Delta. In such a manner, REM-like epochs form a visual spear point shape. FIG. 19 shows epochs clustered via Delta, Gamma/Delta, and the time derivative of (Gamma/Delta). In such a manner, SWS-like epochs form a visual spear point shape. Additional exemplary visualizations of clustered sleep states are shown in FIGS. 20 and 21, in which clustering was done using parameters (e.g., variables) derived via principle component analysis.

At 706, the one or more clustered, frequency weighted epochs are assigned sleep state designations. For example, an epoch with significant relative power at low frequency can be assigned a slow wave sleep designation and an epoch with significant relative power at high frequency can be assigned a rapid eye movement sleep designation. For example, REM sleep can have higher Gamma/Delta and a higher absolute value of the time derivative of (Gamma/Delta) compared to SWS, whereas SWS can have higher delta and a higher absolute value of the time derivative of delta than REM sleep. Further, for example, standard deviation can be used in assigning sleep state designations. It is possible for the same epoch to be assigned both a slow wave sleep designation and a rapid eye movement sleep designation. In such cases, the epoch can be reassigned a new sleep state designation of outlier or intermediate stage II sleep. Alternatively, an epoch can be assigned both a

non-slow wave sleep designation and a non-rapid eye movement sleep designation. In such cases, the epoch can be reassigned a new sleep state designation of intermediate sleep or intermediate stage I sleep. For example, when high frequency is expressed by dividing it by Delta and the parameter space Delta, Gamma/Delta, abs(derivative(Delta)), abs(derivative(Gamma/Delta)), and ,optionally, standard deviation, then intermediate sleep designation can be the intersection between NREM and NSWS while outlier designation can be the intersection between REM and SWS. Alternatively, for example, if Delta alone or with standard deviation is used to determine SWS from NSWS and gamma alone or with abs(derivative(Delta)) alone or with standard deviation is used to determine REM from NREM, then intermediate stage I sleep designation can be the intersection between NREM and NSWS while intermediate stage II sleep designation can be the intersection between REM and SWS. Any variety of data smoothing techniques can be used during the assigning of sleep states. Artifact data can also be used during the assigning of sleep states.

At 708, sleep state designations are presented as indicative of sleep states for the period of time represented by the one or more epochs. The sleep states can be presented in the form of sleep statistics across time. For example, FIGS. 28, 29, 30, 31, and 32 depict presentations of sleep statistics for sleep state designated epochs as a function of time. For example in FIG. 28, a screen shot 2800 depicts sleep state density as a percentage for each sleep state type per hour during a night of electroencephalography data for a subject. In FIG. 29, a screen shot 2900 depicts average episode length for each sleep stage across every hour. In FIG. 30, a screen shot 3000 depicts number of episodes for each sleep stage across every hour. In FIG. 31, a screen shot 3100 depicts average time intervals between successive REM sleep state intervals for each hour. In FIG. 32, a screen shot 3200 depicts stage transitions across the night.

Additionally, one or more frequency weighted epochs can be presented as canonical spectra representative of the sleep state in the subject for the period of time represented by the one or more epochs having similar sleep state designations. For example, an epoch within the middle of a group of epochs designated as having the same sleep state designations can be selected and its spectra presented as canonical spectra representative of the sleep state. Alternatively, an epoch having a weighted power closest to the average weighted power of one or more epochs having similar sleep state designations can be selected and its spectra presented as canonical spectra representative of the sleep state. For example, FIGS. 22, 23, 24, 25, and 26 are screen shots of exemplary visualizations of epochs for various sleep states in a subject (e.g., screen shot 2200 is SWS, screen shot 2300 is REM sleep, screen shot 2400 is Intermediate sleep, screen shot 2500 is awake, and screen shot 2600 is transient) based on EEG spectrogram data analysis.

Additionally, sleep state designations can be presented as a function of success versus manual scoring and quality measures can be presented (e.g., sleep state designation separation statistics including single variable and multivariable one-way ANOVAs, regression coefficients calculated for each stage for sleep densities, number of episodes, average episode length, cycle time, and the like). An exemplary visualization of presenting quality measures is shown in FIG. 27. A

screen shot 2700 depicts an exemplary visualization of the degree of sleep stage separation that distinguishes representative canonical spectra of distinct sleep states. For example, independent component analysis (ICA) can be used to establish the quality of sleep stage separation in the presented sleep states by applying ICA to canonical spectra or average spectra for each sleep state presented. Any variety of classifying techniques can be used to determine the quality of initially sleep stage classification.

Example 12 - Exemplary System for Determining a Pathological Condition of a Subject from Sleep States

FIG. 8 shows an exemplary system 800 for determining a pathological condition of a subject from sleep states.

Electroencephalography data for a subject 802 is obtained and input into sleep state analyzer 804 to determine a pathological condition of the subject 806.

Methods for determining a pathological condition of a subject from sleep states exhibited by a subject, as determined from analyzing electroencephalography data, are described in detail below.

Example 13 - Exemplary Computer-Implemented Method for Determining a Pathological Condition for a Subject from Sleep States

FIG. 9 shows an exemplary computer-implemented method 900 for determining a pathological condition for a subject from sleep states. The computer-implemented method 900 can be utilized in system 800 of FIG. 8.

At 902, electroencephalography data for a subject is received. For example, electroencephalography data which exhibits lower dynamic range for power in at least one low power first frequency range in a frequency spectrum as compared to a second frequency range in the frequency spectrum can be received.

At 904, the electroencephalography data is analyzed with frequency analysis. For example, frequency analysis can be the adjusting 204 of method 200.

At 906, sleep states in the subject are assigned based on the frequency analysis. For example, method 700 for classifying sleep states of FIG. 7 can be used to assign sleep states in the subject.

At 908, a pathological condition can be detected in a subject based on the sleep states. For example, sleep states can be acquired for an individual and analyzed to determine whether the sleep states represent normal sleep or abnormal sleep. Abnormal sleep could indicate a pathological condition. For example, sleep states can be acquired from individuals with pathological conditions and analyzed for common attributes to generate an exemplary distinctive "pathological condition" sleep state profile and/or sleep state statistics representative of having the pathological condition. Such a profile or statistics can be compared to sleep states determined for a subject in order to detect whether the subject has the pathological condition or any early indicators of the pathological condition. Any variety of pathological conditions can be detected and/or analyzed. For example

sleep related pathological conditions can include epilepsy, Alzheimer's disease, depression, brain trauma, insomnia, restless leg syndrome, and sleep apnea. For example, polysomnographically, subjects with Alzheimer's can show decreased rapid eye movement sleep in proportion to the extent of their dementia.

5

Example 14 - Exemplary System for Dynamically Determining Customized Sleep Scores for a Subject

FIG. 10 shows an exemplary system for dynamically determining customized sleep scores for a subject

10 A data collector 1002 can obtain electroencephalography data for a subject from a period of sleep.

A data normalizer 1004 can assess the electroencephalography data to determine low power frequency information.

A data presenter 1006 can present sleep states for the subject based at least on the low power

15 frequency information.

Methods for dynamically determining customized sleep scores for a subject are described herein, including method 500 of FIG. 5, method 600 of FIG. 6, and method 700 of FIG. 7.

Example 15 - Exemplary Pathological Conditions

20 In any of the technologies described herein, a variety of pathological conditions can be determined from source data obtained for a subject. For example, depression, brain trauma, epilepsy, and Alzheimer's disease can be pathological conditions determined from sleep states determined from source data obtained for a subject. For example, FIG. 39 is a screenshot 3900 of an application of the technologies described herein to determine sleep states indicative of characterizations of Alzheimer's

25 disease from a whole night EEG from a human subject with Alzheimer's.

Example 16 - Exemplary Medications and Chemicals that can Affect Sleep

In any of the technologies described herein, the effect of medications and chemicals on sleep states of a subject can be determined via analyzing source data obtained for a subject. For example,

30 sleep states can be modified by alcohol, nicotine, and cocaine use. Exemplary medications that affect sleep include steroids, theophylline, decongestants, benzodiazepines, antidepressants, monoamine oxidase inhibitors (e.g., Pheneizine and Moclobemide), selective serotonin reuptake inhibitors (e.g., Fluoxetine (distributed under the Prozac® name) and Sertralie (distributed under the Zoloft® name), thyroxine, oral contraceptive pills, antihypertensives, antihistamines, neuroleptics, amphetamines,

35 barbiturates, anesthetics, and the like.

Example 17 - Exemplary Sleep Statistics

In any of the technologies described herein, any variety of statistics can be generated from

adjusted source data. For example, sleep statistics can be generated from adjusted source EEG data that has been classified into sleep states. Exemplary sleep statistics can include information including sleep stage densities, number of sleep stage episodes, sleep stage average duration, cycle time, interval time between sleep stages, sleep stage separation statistics, onset of sleep, rapid eye movement sleep latency, regression coefficients of trends, measures of statistical significance of trends, and the like.

Example 18 - Exemplary Implementation of a Method of Determining Sleep States in a Subject over a Period of Time

Sleep is common and may be ubiquitous in all major taxa of the animal kingdom, but it is poorly understood. There is growing evidence from human studies from a variety of low-level psychophysical perceptual and motor tasks that sleep helps to remediate performance loss that is otherwise observed following task learning (Karni et al. 1994; Mednick et al. 2002; Mednick et al. 2003; Fenn et al. 2003). Animal studies have provided evidence of 'replay' during sleep, which may be a central component of the sleep process involved in consolidation of performance.

Recently, it has been shown that during sleep, robustus archistriatalis (RA) neurons of the zebra finch, *Taeniopygia guttata*, song system rehearse song patterns spontaneously and respond to playback of the bird's own song (Dave & Margoliash, 2000). During song development in zebra finches, juvenile birds start changing singing patterns the day following exposure to new vocal material from tutors (Tchernichovski et al. 2001). There is no conclusive evidence though that song learning in juveniles or song maintenance in adult birds requires or benefits from sleep.

Investigation of the possible role of sleep in song learning or maintenance is hampered by the limited knowledge of sleep states in passerine birds. Previous studies have not reported different phases of sleep in the zebra finch (Nick & Konishi, 2002; Hahnloser et al., 2002). In contrast, studies in other birds, including passerine birds (Ayala-Guerrero et al., 1988; Szymczak et al., 1993; Rattenborg et al., 2004), have reported REM sleep in this phylum. Moreover, in rat hippocampus different patterns of neuronal replay are known to take place during different phases of sleep (Buzsaki, 1989; Wilson & McNaughton, 1994; Louie & Wilson, 2001). Therefore, staging of sleep in zebra finches was investigated.

In order to determine the type, arrangement and location of electrodes, a series of acute experiments with birds anesthetized with urethane (20%, circa 90 µl over 1 hr) was first conducted. Optimal EEG recordings, as judged by amplitude and reliability of signals, were obtained using differentially paired thick platinum electrodes (A-M systems, WA) touching the dura mater, with an additional ground over the cerebellum. The stereotaxic coordinates for the recording and ground electrodes were respectively: (1.5R, 3L), (3R, 2L) and (0.5C, 0L).

Five birds were then anesthetized and implanted with 3 mm long L-shaped platinum electrodes at the aforementioned locations with the last 2 mm of the electrodes tangential to the dura mater along the medial-lateral axis. The electrode impedance was 0.15 Ohms. In order to assess

unihemispheric sleep, three birds were implanted with bilateral EEG electrodes. Electrodes were secured at their base with dental acrylic and attached with fine copper wire (A-M systems, WA) to a head connector. Birds were given 3 days to recover from the surgery and to habituate to the recording environment.

During recordings, a light cable was attached linking the bird's head to an overhead mercury commutator (Drangonfly Inc, WV). This setup allowed the bird relative freedom of movement within the cage and is preferable to restraining the animal since restraint-induced stress is known to modify sleep architecture (Altman et al., 1972). During the dark phase of the 16:8 light/dark cycle, electrophysiological recordings with direct observation of sleeping birds were combined. Birds were bathed in infrared (IR) light and monitored with an IR camera (Ikegama, Japan). Strategically placed mirrors facilitated detection of eye, head, and body movements. EEGs were amplified by 1K, sampled at 1 kHz and filtered at 1-100 Hz. In one bird, which exhibited low frequency artifacts, the data was filtered at 2-100 Hz. A 60Hz notch filter was also used to improve the signal-to-noise ratio.

In order to establish high confidence in the data analysis, the data was scored both manually as well as automatically. Manual scoring relied on visual inspection of 3 seconds EEG epochs in parallel with scoring of overt behaviors such as eye, head and body movements. Manual scoring classified each epoch as either REM, NREM (non-REM) or awake, including the artifacts. Automated scoring was restricted to the sleep data. The Sleep Parametric EEG Automated Recognition System (SPEARS) for stage separation and quantification of single channel EEG data was used. EEGs were downsampled to 200 Hz, DC filtered, and analyzed over 3 seconds epochs using a 1 second sliding window to combine high spectral, temporal and statistical resolutions. In order to minimize spectral leakage and to increase statistical resolution in the frequency domain, EEG power spectra were computed over 2 orthogonal tapers following a standard multi-taper estimation technique (Thomson, 1982).

The 1-4 Hz (Delta) and 30-55 Hz (Gamma) frequency bands were selected for the stage classification. Delta and Gamma/Delta were respectively used to separate SWS from NSWS (Non-SWS) and REM from NREM. The separation was done with a k-means clustering algorithm and refined by the inclusion of additional variables: the standard deviation and the absolute values of the time derivative of Delta and of (Gamma/Delta). For each epoch, the time derivative was computed over the preceding and successive epochs, using the Matlab "gradient" function. The initial separation was done over the artifact free sleep data. Thereafter, sleep artifacts were attributed the same score as the first non-artifact epoch immediately following it, unless it was an awake epoch in which case the sleep artifact was given the score of the first preceding artifact free epoch (which could not be an awake epoch for otherwise the artifact would have been labeled as an awake artifact by manual scoring). This convention did not significantly reduce the agreement rate with manual scoring (TABLE 1). It was important to include the sleep artifacts since removing or not scoring them would respectively shrink or puncture sleep episodes and thereby change the calculated density, average number of epochs and length for each stage.

Following initial separation, the score of each epoch was smoothed using a 5 second window in order to minimize the score contamination by brief artifacts which might not have been isolated by manual scoring. Epochs that were scored neither as REM nor as SWS were labeled as intermediate (INTER). Conversely, any epoch that had been labeled as belonging to both REM and SWS was relabeled as an outlier. There were very few outliers in the data (TABLE 1).

The REM, SWS and intermediate epochs can be visualized in a 3-dimensional space (FIGS. 20-21) defined by the principal components of the 5 dimensional space defined by Delta, Gamma/Delta, the standard deviation and the derivatives of Delta and (Gamma/Delta) (FIGS. 16-17). In each bird, a multivariate ANOVA on the 5-dimensional clustering space yielded a $P < 0.001$ for the separation of REM, SWS and the intermediate stage.

Using the MATLAB "silhouette" function, the most representative examples for the SWS, REM, intermediate and awake epochs were automatically generated (FIGS. 22, 23, 24, 25, and 26).

The agreement between manual and automated scoring was calculated by classifying each epoch scored as REM by only the manual or the automated scoring as an error. The general agreement rate was remarkably high given the high temporal resolution of the manual and automated scoring (TABLE 1).

Based on the automated analysis, the stage density (FIG. 28), average episode number (FIG. 30) and duration (FIG. 29), inter REM interval (FIG. 31) and stage transitions (FIG. 32) were computed (TABLE 1). All analyses were conducted in Matlab (MathWorks Inc, MA).

Table 1. Stage statistics for 5 nights of sleep in 5 birds.

Stage density, average episode duration and number and stage transitions were determined. The percentage of transitions out of each stage towards the intermediate stage and the percentage of transitions out of the intermediate stage towards the other stages are shown. For the bihemispherically implanted birds (Animals 1-3), unihemispheric sleep is reported and the other statistics were computed over the hemisphere with the most reliable data as determined by visual inspection of the EEG and video and the absence of outliers. The coefficient of regression was computed over the stage densities and inter-REM intervals for each hour and reflect the circadian distribution of SWS and REM (* = [$r^2 > 0.5$ and $p < 0.05$], § = [$r^2 > 0.5$ and $p = 0.05$], £ for values calculated for hours 2-8, € for values calculated for hours 1-7). The agreement rate between automated and manual scoring was determined with and without artifact rejection.

TABLE 1	Animal 1	Animal 2	Animal 3	Animal 4	Animal 5
Stage Density (%)					
SWS	44.44	30.14	41.03	25.71	36.59
INTER	30.96	30.34	37.46	31.70	37.49
REM	21.06	30.51	15.79	30.77	15.12
AWAKE	3.54	8.94	5.73	11.83	10.80
UNIHEM	0.09	0.59	0.65	N/A	N/A
OUTLIER	0.00	0.08	0.00	0.00	0.00
Average Episode Duration (sec)					
SWS	14.11	12.54	10.84	10.90	9.11
INTER	5.95	6.05	6.67	8.07	6.62
REM	9.84	10.11	8.53	16.98	9.21
AWAKE	11.37	12.10	9.30	16.11	12.02
UNIHEM	3.38	3.84	3.19	N/A	N/A
OUTLIER	N/A	2.22	N/A	N/A	N/A
Number of Episodes					
SWS	835	704	1092	629	1073
INTER	1378	1482	1623	1137	1601
REM	599	853	541	572	557
AWAKE	85	113	159	65	100
UNIHEM	8	44	59	N/A	N/A
OUTLIER	0	9	0	0	0
Transitions					
SWS-INTER (% SWS)	97.57	88.54	95.21	93.93	97.05
REM-INTER (% REM)	85.49	90.34	86.06	92.64	83.75
AWAKE-INTER (% AWAKE)	60.49	71.94	72.15	27.79	64.16
OUT-INTER (% OUT)	N/A	25.00	N/A	N/A	N/A
INTER-SWS (% INTER)	56.57	43.06	63.23	51.31	66.49
INTER-REM (% INTER)	38.55	49.33	29.52	43.72	26.78
INTER-AWAKE (% INTER)	4.88	7.61	7.25	4.97	6.73
INTER-OUT (% INTER)	N/A	0.00	N/A	N/A	N/A
Regression coefficients					
Stage Density per hour					
SWS	-6.20	-1.11	0.10	-5.46	-2.94
INTER	1.57	1.93	-0.29	4.21	4.09
REM	4.89	3.16	2.44	8.08	4.77
AWAKE	-0.25	-3.99	-2.25	-6.83	-5.92
OUTLIER	N/A	0.01	N/A	N/A	N/A
Average Episode Duration per hour					
SWS	-1.44	-0.37	0.59	-6.08	-1.11
INTER	0.05	0.24	0.21	1.37	0.31
REM	0.90	0.80	1.06	2.77	0.53
AWAKE	-0.74	-0.89	-0.21	-6.34	-0.92
OUTLIER	N/A	N/A	N/A	N/A	N/A
Number of Episodes per hour					
SWS	-3.93	-1.07	-6.13	-3.61	0.82
INTER	8.00	5.29	-8.11	2.93	14.46
REM	13.82	5.68	2.01	6.93	16.21
AWAKE	-0.29	-1.54	-6.05	0.18	-1.61
OUTLIER	N/A	-0.04	N/A	N/A	N/A
Inter-REM-interval per hour	-7.56	-2.66	-2.27	-0.75	-15.10
Cycle Time per hour	10.45	21.50	4.88	93.51	1.45
Agreement Rate (%)	89.94	76.75	90.52	73.23	88.44
Agreement Rate - No artifacts (%)	90.08	76.93	91.52	73.91	88.28

The analysis of the recordings indicate that zebra finches exhibit at least three distinct phases of sleep: SWS, REM and intermediate sleep. SWS had a high amplitude EEG signal with significant power in the Delta range (FIGS.14-17). REM was characterized by a very low amplitude "awake-like" EEG signal (FIG. 23), typically about ±30 μV with higher power in Gamma (FIGS. 14 and 15) than NREM, a feature that up to now had only been detected in mammals (Maloney et al., 1997; Cantero et al., 2004). The intermediate epochs had highly variable amplitudes, centered around ±50 μV and did not have significant power in either the Delta or Gamma ranges (FIGS. 14, 15 and 24). The intermediate stage has previously only been observed in mammals (Gottesmann et al., 1984; Glin et al., 1991; Kirov & Moyanova, 2002). Both birds on normal circadian patterns and shifted circadian schedules displayed these three sleep stages.

SWS epochs were longer than REM and intermediate episodes early in the night and would, following a mammalian-like distribution, decrease in duration (FIG. 29) throughout the night, leading to an overall decrease in stage density (FIG. 28) (TABLE 1).

During NREM birds breathe slowly and regularly; eye and head movements do not follow a stereotypical pattern and are quite distinct from those in REM. We observed several instances when one eye was open and the other was closed. The hemisphere contralateral to the open eye displayed a low amplitude and high frequency EEG while the hemisphere contralateral to the closed eye displayed SWS oscillations. These instances of unihemispheric sleep would usually account for less than 5% of the dark cycle (TABLE 1) and were more frequent in the light cycle. Such patterns of unihemispheric sleep have been previously detected in other species of birds, cetaceans and other marine mammals (Mukhametov et al., 1984; Mukhametov, 1987; Szymczak et al., 1996; Rattenborg et al., 1999; Lyamin et al., 2002).

REM episodes were typically brief early in the night and would become longer throughout the night (FIG. 29) as the number of episodes would increase as well (FIG. 30), leading the Inter-REM intervals to exhibit a downward "mammalian-like" trend throughout the night (FIG. 31) (TABLE 1). REM occurred reliably in conjunction with eye and subtle twitching head movements, as seen in other species (Siegel et al., 1999). The eye movements were on the order of one saccade per second. The head movements were not as reliable, but tended to follow the directional movement of the eyes when present. Head movements were not the result of displacement of the head by the weight of the attached cable during REM neck muscle atonia because the head movements were observed in conjunction with eye movements in intact, un-tethered animals.

The intermediate epochs were brief and numerous. The intermediate state was usually more stable throughout the night, in term of density (FIG. 28), average epoch duration (FIG. 29) and average number of episodes per hour (FIG.30) than REM and SWS. As is the case in mammals, the intermediate stage consistently acted as -but was not limited to- a transition phase between SWS and REM (FIG. 32) (TABLE 1).

In all birds, large peak-to-peak EEG transients lasting approximately 500 milliseconds were detected in NREM (FIG. 26). These signals are reminiscent of the description of mammalian K-

complexes (Rowan & Tolunsky, 2003). K-complexes have likely never been previously observed in a non-mammalian species.

In previous studies of zebra finch sleep EEG, only SWS has been reported. In addition to finding a suitable location over which to implant EEG electrodes, this study was successful in detecting NSWS (REM and the intermediate stage) presumably because the nature of the chronic recording setup did not restrain the animals and obviated the need of pharmacological agents such as melatonin to induce sleep. In one study (Mintz et al., 1998), infusion of melatonin was shown to induce SWS in pigeons. It is possible that melatonin might have a similar effect in zebra finches, thus reducing the amount of observable NSWS at night (Hahnloser et al. 2002).

The data analysis technique we used enabled us to resolve changes in power at the lower power, high frequencies, which was a key differentiating factor for REM sleep detection. Moreover, the automated analysis restricted manual scoring to the awake state and artifacts, which are easily detectable to a human scorer. Additionally, automated EEG scoring relied on whole night statistics (Gervasoni et al.) rather than on arbitrarily defined threshold, maximum likelihood methods or supervised nonlinear classifiers all of which tend to reflect and impose a human bias on the data analysis.

The results imply that mammalian-like sleep features have evolved in parallel in both mammals and birds. The basic pattern of interdigitation between Delta and Gamma power activation described herein (FIGS. 14 and 15) is highly similar to the one observed in the mammalian cortex during sleep (Destexhe, Contreras & Steriade, 1999). Furthermore, some of the signals we have observed have been specifically attributed to the mammalian cortex (Amzica & Steriade, 1998). Birds are however devoid of a large laminar cortex, raising the possibility that the cortex might be at best sufficient but not necessary for the development of mammalian-like sleep features. Conversely, it is conceivable that birds do indeed possess a mammalian cortex homolog in a non-laminar form (Karten, 1997). Future work at the cellular and molecular levels will be needed to assess which of these highly intriguing possibilities proves to be correct.

References cited:

Altman et al. Psychon. Sci. 26 (1972), pp. 152-154.

Amzica & Steriade. Neuroscience. 1998 Feb;82(3):671-86.

Ayala-Guerrero et al. Physiol Behav. 1988;43(5):585-9.

Buzsaki. Neuroscience. 1989;31(3):551-70.

Cantero et al. Neuroimage. 2004 Jul;22(3):1271-80.

Dave & Margoliash. Science. 2000 Oct 27;290(5492):812-6.

Destexhe, Contreras & Steriade. 1999 Jun 1;19(11):4595-608.

Fenn et al. Nature. 2003 Oct 9;425(6958):614-6.

Gervasoni et al. J Neurosci. 2004 Dec 8;24(49):11137-47.

Glin et al. Physiol Behav. 1991 Nov;50(5):951-3.

Gottesmann et al. J Physiol (Paris). 1984;79(5):365-72.

Hahnloser et al. Nature. 2002 Sep 5;419(6902):65-70.

Karni et al. Science. 1994 Jul 29; 265(5172):679-682

Karten. Proc Natl Acad Sci U S A. 1997 Apr 1;94(7):2800-4.

Khazipov et al. Society for Neuroscience Abstracts 2004.

Kirov & Moyanova. Neurosci Lett. 2002 Apr 5;322(2):134-6.

Louie & Wilson. Neuron. 2001 Jan;29(1):145-56.

Lyamin et al. Behav Brain Res. 2002 Feb 1;129(1-2):125-9

Maloney et al. Neuroscience. 1997 Jan;76(2):541-55.

Mednick et al. Nat Neurosci. 2002 Jul;5(7):677-81

Mednick et al. Nat Neurosci. 2003 Jul;6(7):697-8.

Mintz et al. Neurosci Lett. 1998 Dec 18;258(2):61-4.

Mukhametov et al. Zh Vyssh Nerv Deiat Im I P Pavlova. 1984 Mar-Apr;34(2):259-64.

Mukhametov. Neurosci Lett. 1987 Aug 18;79(1-2):128-32.

Nick & Konishi. Proc Natl Acad Sci U S A. 2001 Nov 20;98(24):14012-6.

Rattenborg et al. Behav Brain Res. 1999 Nov 15;105(2):163-72.

Rattenborg et al. PLoS Biol. 2004 Jul;2(7):E212.

Rowan & Tolusnky. "Primer of EEG". Butterworth Heinemann. Elsevier Science 2003

Siegel et al. Neuroscience. 1999;91(1):391-400.

Szymczak et al. Physiol Behav. 1993 Jun;53(6):1201-10.

Szymczak et al. Physiol Behav. 1996 Oct;60(4):1115-20.

Tchernichovski et al. Science. 2001 Mar 30;291(5513):2564-9.

Thomson, Proceedings of the IEEE, Vol. 70 (1982), pp. 1055-1096.

Wilson & McNaughton. Science. 1993 Aug 20;261(5124):1055-8.

Example 19- Exemplary Method for Determining Sleep States in a Subject over a Period of Time

FIG. 35 shows yet another exemplary method 3500 for determining sleep states in a subject over a period of time. The method 3500 incorportates a wide variety of techniques described herein.

Example 20 - Exemplary Transformation Techniques

There are a wide variety of data transformation methods used in signal processing to determine power for a variety of frequencies in time series data. As described herein, transformation methods can include multi-taper transform, Fourier transform, wavelet transform. Any other transformation method for measuring power for a variety of frequencies represented in a plurality of time series or epochs in a source signal can be used.

Example 21 - Exemplary Computational Methods for Differentiating Groups of Data

There are a wide variety of clustering and classification methods used in computational signal processing to differentiate data into distinct classes. As described herein, the clustering method used is k-means clustering but any computational signal processing method for differentiating groups of data could be used. Similarly, classification methods such as component analysis (e.g., principle and independent component analysis) are used as described herein.

An overview of computational methods is provided below.

Clustering (or cluster analysis) is unsupervised learning where the classes are unknown a priori and the goal is to discover these classes from data. For example, the identification of new tumor classes using gene expression profiles is a form of unsupervised learning.

Classification (or class prediction) is a supervised learning method where the classes are predefined and the goal is to understand the basis for the classification from a set of labeled objects and build a predictor for future unlabeled observations. For example, the classification of malignancies into known classes is a form of supervised learning.

CLUSTERING:

Clustering involves several distinct steps:

1. Defining a suitable distance between objects
2. Selecting a applying a clustering algorithm.

Clustering procedures commonly fall into two categories: hierarchical methods and partitioning methods. Hierarchical methods can be either divisive (top-down) or agglomerative (bottom-up). Hierarchical clustering methods produce a tree or dendrogram. Hierarchical methods provide a hierarchy of clusters, from the smallest, where all objects are in one cluster, through to the largest set, where each observation is in its own cluster

Partitioning methods usually require the specification of the number of clusters. Then, a mechanism for apportioning objects to clusters must be determined. These methods partition the data into a prespecified number k of mutually exclusive and exhaustive groups. The method iteratively reallocates the observations to clusters until some criterion is met (e.g. minimize within-cluster sums-of-squares). Examples of partitioning methods include k-means clustering, Partitioning around medoids (PAM), self organizing maps (SOM), and model-based clustering.

Most methods used in practice are agglomerative hierarchical methods, in a large part due to the availability of efficient exact algorithms. However both clustering methods have their advantages and disadvantages. Hierarchical advantages include fast computation, at least for agglomerative clustering, and disadvantages include that they are rigid and cannot be corrected later for erroneous decisions made earlier in the method. Partitioning advantages include that such methods can provide clusters that (approximately) satisfy an optimality criterion, and disadvantages include that one needs an initial k and the methods can take long computation time.

In summary, clustering is a more difficult problem than classifying for a variety of reasons including the following:

1. there is no learning set of labeled observations
2. the number of groups is usually unknown
3. implicitly, one must have already selected both the relevant features and distance measures used in clustering methods.

CLASSIFICATION:

Techniques involving statistics, machine learning, and psychometrics can be used. Examples of classifiers include logistic regression, discriminant analysis (linear and quadratic), principle component analysis (PCA), nearest neighbor classifiers (k-nearest neighbor), classification and regression trees (CART), prediction analysis for microarrays, neural networks and multinomial log-linear models, support vector machines, aggregated classifiers (bagging, boosting, forests), and evolutionary algorithms.

Logistic regression:

Logistic regression is a variation of linear regression which is used when the dependent (response) variable is a dichotomous variable (i.e., it takes only two values, which usually represent the occurrence or non-occurrence of some outcome event, usually coded as 0 or 1) and the independent (input) variables are continuous, categorical, or both. For example, in a medical study, the patient survives or dies, or a clinical sample is positive or negative for a certain viral antibody.

Unlike ordinary regression, logistic regression does not directly model a dependent variable as a linear combination of dependent variables, nor does it assume that the dependent variable is normally distributed. Logistic regression instead models a function of the probability of event occurrence as a linear combination of the explanatory variables. For logistic regression, the function relating the probabilities to the explanatory variables in this way is the logistic function, which has a sigmoid or S shape when plotted against the values of the linear combination of the explanatory variables.

Logistic regression is used in classification by fitting the logistic regression model to data and classifying the various explanatory variable patterns based on their fitted probabilities. Classifications of subsequent data are then based on their covariate patterns and estimated probabilities.

Discriminant analysis:

In summary discriminant analysis represents samples as points in space and then classifies the points. Linear discriminant analysis (LDA) finds an optimal plane surface that best separates points that belong to two classes. Quadratic discriminant analysis (QDA) finds an optimal curved (quadratic) surface instead. Both methods seek to minimize some form of classification error.

Fisher linear discriminant analysis (FLDA or LDA):

LDA finds linear combinations (discriminant variables) of data with large ratios of between-groups to within-groups sums of squares and predicts the class of an observation x by the class whose

mean vector is closest to x in terms of the discriminant variables. Advantages of LDA include that it is simple and intuitive where the predicted class of a test case is the class with the closest mean and it is easy to implement with a good performance in practice. Disadvantages of LDA include the following:

1. linear discriminant boundaries may not be flexible enough
2. features may have different distributions within classes
3. in the case of too many features, performance may degrade rapidly due to over parameterization and high variance of parameter estimates.

Nearest neighbor classifiers:

Nearest neighbor methods are based on a measure of distance between observations, such as the Euclidean distance or one minus the correlation between two data sets. K-nearest neighbor classifiers work by classifying an observation x as follows:

- find the k observations in the learning set that are closest to x
- predict the class of x by majority vote, i.e., choose the class that is most common among these k neighbors. Simple classifiers with k=1 can generally be quite successful. A large number of irrelevant or noise variables with little or no relevance can substantially degrade the performance of a nearest neighbor classifier.

Classification trees:

Classification trees can be used, for example, to split a sample into two sub-samples according to some rule (feature variable threshold). Each sub-sample can be further split, and so on. Binary tree structured classifiers are constructed by repeated splits of subsets (nodes) into two descendant subsets. Each terminal subset of the tree is assigned a class label and the resulting partition corresponds to the classifier. The three main aspects of tree construction include selection of splits (at each node, the split that maximize the decrease in impurity is chosen), decision to declare a node terminal or to continue splitting (to grow a large tree, the tree is selectively pruned upwards getting a decreasing sequence of subtrees), and assignment of each terminal node to a class (the class the minimizes the resubstitution estimate of the misclassification probability is chosen for each terminal node).

Prediction analysis for microarrays:

These methods utilize nearest shrunken centroid methodology. First, a standardized centroid for each class is computed. Then each class centroid is shrunk toward the overall centroid for all classes by the so-called threshold (chosen by the user). Shrinkage consists of moving the centroid towards zero by threshold, setting it equal to zero if it hits zero.

Artificial Neural Networks :

The key element of the artificial neural network (ANN) model is the novel structure of the information processing system. It is composed of many highly interconnected processing elements that are analogous to neurons and are tied together with weighted connections that are analogous to

synapses. As with all classification methods, once the ANN is trained on known samples, it will be able to predict samples automatically.

Support Vector Machines:

Support Vector Machines are learning machines that can perform binary classification (pattern recognition) and real valued function approximation (regression estimation) tasks. Support Vector Machines non-linearly map their n-dimensional input space into a higher dimensional feature space. In this high dimensional feature space a linear classifier is constructed.

Aggregating classifiers:

This method works by aggregating predictors built from perturbed versions of a learning set. In classification, the multiple versions of the predictor are aggregated by voting. Bootstrapping is the simplest form of bagging in which perturbed learning sets of the same size as the original learning set are non-parametric bootstrap replicates of the learning set, i.e., drawn at random with replacement from the learning set. Parametric bootstrapping involves perturbed learning sets that are generated according to a mixture of multivariate Gaussian distributions. Random Foresting is a combination of tree classifiers (or other), where each tree depends on the value of a random vector for all trees in the forest. In boosting, classifiers are constructed on weighted version the training set, which are dependent on previous classification results. Initially, all objects have equal weights, and the first classifier is constructed on this data set. Then, weights are changed according to the performance of the classifier. Erroneously classified objects get larger weights, and the next classifier is boosted on the reweighted training set. In this way, a sequence of training sets and classifiers is obtained, which is then combined by simple majority voting or by weighted majority voting in the final decision.

Example 22 - Exemplary Sleep Data Presenter

In any of the examples herein, an electronic or paper-based report based on sleep state data can be presented. Such reports can include customized sleep state information, sleep state statistics, pathological conditions, medication and/or chemical effects on sleep, and the like for a subject. Recommendations for screening tests, behavioral changes, and the like can also be presented. Although particular sleep data and low frequency information results are shown in some examples, other sleep data presenters and visualizations of data can be used.

Example 23 - Exemplary Sleep State Information for Subjects

Exemplary sleep state information can be obtained from a variety of subjects using any of the technologies described herein. FIG. 33 includes a screenshot 3300 of an exemplary visualization of classified anesthesized states of an anesthetized cat based on analyzed EEG spectrogram data. For example, in screenshot 3300, a SWS classification corresponds to a deep anesthesized state, a REM sleep classification corresponds to a light anesthesized state, and an INTER sleep classification corresponds to an intermediate anesthesized state. In such a manner, the technologies described herein can be utilized to determine anesthesized states in a human or other mammalian subject. FIGS.

34 includes a screenshot 3400 of an exemplary visualization of classified sleep states of a human subject based on analyzed EEG spectrogram data.

Example 24 - Exemplary Advantages and Applications of Technologies

The speed at which this data analysis can be performed, the customized and unsupervised nature of analysis, and the ability to extract previously disregarded or unanalyzed low power frequency information make this methodology particularly attractive to a variety of fields of study. The technology can be highly adaptable using a variable number of states, a variable number of identification rules, adaptable calibration, variable time resolution, and variable spectral resolution. Adjusting source data to generate adjusted source data can be especially applicable to analyzing animal signal data in testing for pathological conditions and medication and chemical effects. In any of the examples herein, low amplitude but highly variable frequency data can be extracted and analyzed (e.g., discovering temporal patterns in data). Applications can include diverse uses from analyzing stock market data (e.g., analyzing fluctuations in penny stocks to determine common variability otherwise disregarded due to small price changes) to accessing encoded data (e.g., Morse code data stored in low power, very high or very low frequencies within sound waves) to analyzing visual images with several spatial frequencies. Similarly, the technologies described herein can be used to determine customized sleep quality determinations for a subject via sleep state information generated.

In any of the examples herein, the methods can be applied to source data received from one channel or multiple channels. The methods can be applied independently to source data from multiple channels with comparison made between the channels. For example, unihemispheric sleep can be determined from independent EEG channel data received from each hemisphere of a brain. FIG. 40 shows a screen shot 4000 of unihemispheric sleep determined from independent EEG channel data received from each hemisphere of a bird's brain. Alternatively, the methods can be simultaneously applied to source data from multiple channels, thereby analyzing combined multiple channel source data. For example, EEG channel data and EMG channel data for a subject can be simultaneously analyzed to determine awake versus REM sleep states whereby a REM designated sleep state from analysis of EEG data can be reassigned as an awake sleep state if the EMG data falls into a high amplitude cluster.

Further, in any of the examples herein, methods such as denoising source separation (dss) and the like can be used in combination with the methods described herein to determine sleep states. For example, dss can use low frequency information to determine REM sleep.

While the techniques described herein can be particularily valuable for analyzing low power frequency information they can also be applied to clustering and determining sleep stages from any variety of signals including signals wherein the high and low frequencies have the same power distributions. Additionally, techniques pertaining to spectrogram analysis, stage classification and confidence measures can be used independently of one another.

Example 25 - Exemplary Visualizations of Data

In any of the techniques described herein, exemplary visualizations of data can utilize colors to depict different aspects of that data. For example, classified data (e.g., sleep state classifications such as REM, SWS, and INTER) can be color coded for each classification state for visualization of the classified data. Alternatively, greyscale can be used to code for each classification state for visualization of the classified data.

Example 26 - Exemplary Computer System for Conducting Analysis

FIG. 36 and the following discussion provide a brief, general description of a suitable computing environment for the software (for example, computer programs) described above. The methods described above can be implemented in computer-executable instructions (for example, organized in program modules). The program modules can include the routines, programs, objects, components, and data structures that perform the tasks and implement the data types for implementing the techniques described above.

While FIG. 36 shows a typical configuration of a desktop computer, the technologies may be implemented in other computer system configurations, including multiprocessor systems, microprocessor-based or programmable consumer electronics, minicomputers, mainframe computers, and the like. The technologies may also be used in distributed computing environments where tasks are performed in parallel by processing devices to enhance performance. For example, tasks can be performed simultaneously on multiple computers, multiple processors in a single computer, or both. In a distributed computing environment, program modules may be located in both local and remote memory storage devices. For example, code can be stored on a local machine/server for access through the Internet, whereby data from assays can be uploaded and processed by the local machine/server and the results provided for printing and/or downloading.

The computer system shown in FIG. 36 is suitable for implementing the technologies described herein and includes a computer 3620, with a processing unit 3621, a system memory 3622, and a system bus 3623 that interconnects various system components, including the system memory to the processing unit 3621. The system bus may comprise any of several types of bus structures including a memory bus or memory controller, a peripheral bus, and a local bus using a bus architecture. The system memory includes read only memory (ROM) 3624 and random access memory (RAM) 3625. A nonvolatile system (for example, BIOS) can be stored in ROM 3624 and contains the basic routines for transferring information between elements within the personal

computer 3620, such as during start-up. The personal computer 3620 can further include a hard disk drive 3627, a magnetic disk drive 3628, for example, to read from or write to a removable disk 3629, and an optical disk drive 3630, for example, for reading a CD-ROM disk 3631 or to read from or write to other optical media. The hard disk drive 3627, magnetic disk drive 3628, and optical disk 3630 are connected to the system bus 3623 by a hard disk drive interface 3632, a magnetic disk drive interface 3633, and an optical drive interface 3634, respectively. The drives and their associated computer-readable media provide nonvolatile storage of data, data structures, computer-executable instructions (including program code such as dynamic link libraries and executable files), and the like for the personal computer 3620. Although the description of computer-readable media above refers to a hard disk, a removable magnetic disk, and a CD, it can also include other types of media that are readable by a computer, such as magnetic cassettes, flash memory cards, DVDs, and the like.

A number of program modules may be stored in the drives and RAM 3625, including an operating system 3635, one or more application programs 3636, other program modules 3637, and program data 3638. A user may enter commands and information into the personal computer 3620 through a keyboard 3640 and pointing device, such as a mouse 3642. Other input devices (not shown) may include a microphone, joystick, game pad, satellite dish, scanner, or the like. These and other input devices are often connected to the processing unit 3621 through a serial port interface 3646 that is coupled to the system bus, but may be connected by other interfaces, such as a parallel port, game port, or a universal serial bus (USB). A monitor 3647 or other type of display device is also connected to the system bus 3623 via an interface, such as a display controller or video adapter 3648. In addition to the monitor, personal computers typically include other peripheral output devices (not shown), such as speakers and printers.

The above computer system is provided merely as an example. The technologies can be implemented in a wide variety of other configurations. Further, a wide variety of approaches for collecting and analyzing source data are possible. For example, the data can be collected and analyzed, and the results presented on different computer systems as appropriate. In addition, various software aspects can be implemented in hardware, and vice versa. Further, paper-based approaches to the technologies are possible, including, for example, purely paper-based approaches that utilize instructions for interpretation of algorithms, as well as partially paper-based approaches that utilize scanning technologies and data analysis software.

Example 27 - Exemplary Computer-Implemented Methods

Any of the computer-implemented methods described herein can be performed by software executed by software in an automated system (for example, a computer system). Fully-automatic (for example, without human intervention) or semi-automatic operation (for example, computer processing assisted by human intervention) can be supported. User intervention may be desired in some cases, such as to adjust parameters or consider results.

Such software can be stored on one or more computer-readable media comprising computer-executable instructions for performing the described actions. Such media can be tangible (e.g., physical) media.

Alternatives

Having illustrated and described the principles of the invention in exemplary embodiments, it should be apparent to those skilled in the art that the described examples are illustrative embodiments and can be modified in arrangement and detail without departing from such principles. Techniques from any of the examples can be incorporated into one or more of any of the other examples.

In view of the many possible embodiments to which the principles of the invention may be applied, it should be understood that the illustrative embodiments are intended to teach these principles and are not intended to be a limitation on the scope of the invention. We therefore claim as our invention all that comes within the scope and spirit of the following claims and their equivalents.

CLAIMS

We claim:

1. A method of analyzing source data comprising:

receiving the source data, wherein the source data exhibits lower dynamic range for power in at least one low power first frequency range in a frequency spectrum as compared to a second frequency range in the frequency spectrum;

applying an adjustment technique to the source data thereby generating adjusted source data; and

wherein the adjustment technique comprises increasing the dynamic range for power within the low power frequency range of the frequency spectrum as compared to the second frequency range.

2. The method of claim 1 further comprising removing artifacts from the source data.

3. The method of claim 1 further comprising presenting a visualization of the adjusted source data.

4. The method of claim 1 further comprising:

prior to applying the adjustment technique, segmenting the source data in a plurality of time segments.

5. The method of claim 4 wherein segmenting the source data comprises:

direct current filtering; and

separating the source data into one or more epochs of similar length.

6. The method of claim 5 wherein the separating comprises determining a scanning window and a sliding window.

7. The method of claim 6 wherein the separating comprises determining at least one time series increment selected from the group consisting of:

whole time series;

overlapping time series; and

non-overlapping series.

8. The method of claim 5 wherein power content of one or more frequencies within the one or more epoch is determined via at least one transformation method selected from the group consisting of:

multi-taper transform;

Fourier transform; and

wavelet transform.

9. The method of claim 8 wherein the adjustment technique comprises weighting frequency power of the one or more frequencies of the one or more epochs across time.

10. The method of claim 9 wherein the source data comprises at least one type of data selected from the group consisting of:

electromyography data;

electrocardiography data;

electrooculography data; and

wave data.

11. The method of claim 9 wherein the source data comprises electroencephalography data for a subject.

12. The method of claim 11 wherein the electroencephalography data is received via a single channel.

13. The method of claim 11 further comprising classifying at least one state in the subject from the electroencephalography data for the subject selected from the group consisting of:

sleep states;

anesthesia states; and

vigilance states.

14. A method of accessing encoded data stored at low power frequency within source data comprising the method of claim 1.

15. One or more computer-readable media having instructions stored thereon for causing a computer system to perform the method of claim 1.

16. A method for determining sleep states in a subject over a period of time comprising:

receiving electroencephalography data for the subject over the period of time, wherein the electroencephalography data exhibits lower dynamic range for power in at least one low power first frequency range in a frequency spectrum as compared to a second frequency range in the frequency spectrum;

segmenting the electroencephalography data into one or more epochs;

weighting frequency power of the one or more epochs across time, wherein the weighting comprises increasing the dynamic range for power within the low power frequency range of the frequency spectrum as compared to the second frequency range, thereby generating one or more frequency weighted epochs; and

classifying sleep states in the subject based on the one or more frequency weighted epochs.

17. The method for claim 16 wherein classifying sleep states in the subject comprises:

clustering the one or more frequency weighted epochs; and

assigning sleep state designations to the one or more frequency weighted epochs according to the clustering; and

presenting the sleep state designations as indicative of sleep states in the subject for the period of time represented by the one or more frequency weighted epochs.

18. The method of claim 17 wherein clustering the one or more frequency weighted epochs comprises k-means clustering.

19. The method of claim 17 further comprising pretreating the electroencephalography data with component analysis.

20. The method of claim 16 wherein classifying sleep states in the subject comprises applying independent component analysis to the one or more frequency weighted epochs.

21. The method of claim 16 wherein classifying sleep states further comprises incorporating manually determined sleep states.

22. The method of claim 16 wherein classifying sleep states further comprises incorporating artifact information.

23. The method of claim 17 wherein assigning sleep state designations to the one or more frequency weighted epochs comprises:

determining a slow wave sleep designation from a non-slow wave sleep designation based at least on low frequency information; and

determining a rapid eye movement sleep designation from a non-rapid eye movement sleep designation based at least on high frequency information.

24. The method of claim 23 wherein an epoch with significant weighted power at low frequency is assigned a slow wave sleep designation.

25. The method of claim 23 wherein an epoch with significant weighted power at high frequency is assigned a rapid eye movement sleep designation.

26. The method of claim 23 wherein assigning sleep state designations to the one or more frequency weighted epochs further comprises determining at least one sleep state designation based on both low frequency and high frequency information, the sleep state designation comprising at least one sleep state designation selected from the group consisting of:

intermediate stage I sleep designation;

intermediate stage II sleep designation; and

outlier sleep designation.

27. The method of claim 26 wherein an epoch with insignificant weighted power at both high and low frequencies is assigned an intermediate or an intermediate stage I sleep designation.

28. The method of claim 26 wherein an epoch with significant weighted power at both high and low frequencies is assigned an outlier or intermediate stage II sleep designation.

29. The method of claim 17 wherein assigning sleep state designations to the one or more frequency weighted epochs further comprises applying a smoothing window to the one or more weighted epochs, wherein the smoothing window comprises averaging sleep state designations across the one or more weighted epochs.

30. The method of claim 17 further comprising presenting one or more frequency weighted epochs as canonical spectra representative of the sleep state in the subject for the period of time represented by the one or more epochs having similar sleep state designations

31. The method of claim 30 further comprising analyzing the canonical spectra with independent component analysis to establish sleep state classification confidence.

32. The method of claim 17 further comprising presenting sleep statistics for the subject according to the sleep state designations of the one or more frequency weighted epochs.

33. The method of claim 32 wherein sleep statistics comprise at least one sleep statistical measurement selected from the group consisting of:

sleep stage densities;

number of sleep stage episodes;

sleep stage average duration;

cycle time;

interval time between sleep stages;

sleep stage separation statistics;

onset of sleep;

rapid eye movement sleep latency;

regression coefficients of trends; and

measures of statistical significance of trends.

34. A method of assessing sleep quality in a subject comprising determining sleep states over a period of time according to claim 16.

35. A method of determining the effect of medication on sleep states of a subject comprising determining the sleep states prior and subsequent to the administration of medication according to claim 16.

36. The method of claim 35 wherein the medication comprises at least one medication selected from the group consisting of:

anesthetics; and

anti-depressants.

37. One or more computer-readable media having instructions stored thereon for causing a computer system programmed thereby to perform the method of claim 16.

38. A computer implemented method for detecting a pathological condition in a subject, the method comprising:

receiving electroencephalography channel data for the subject;

analyzing the data with frequency analysis, the frequency analysis comprising normalizing the data;

assigning sleep states in the subject according to the analyzing; and

detecting the pathological condition for the subject according to the sleep states.

39. The computer implemented method of claim 38 wherein the pathological condition is depression.

40. The computer implemented method of claim 38 wherein the pathological condition is brain trauma.

41. The computer implemented method of claim 38 wherein the pathological condition is Alzheimer's disease.

42. A system for dynamic customized sleep scoring for a subject, the system comprising:

a sleep data collector for obtaining electroencephalography data for a subject from a period of sleep;

a sleep data normalizer for assessing the electroencephalography data to determine low power frequency information; and

a sleep data presenter for presenting sleep states for the subject based at least on the low power frequency information.

43. A system for dynamic customized sleep scoring for a subject, the system comprising:

means for obtaining electroencephalography data for a subject from a period of sleep;

means for assessing the electroencephalography data to determine low power frequency information; and

means for presenting sleep states for the subject based at least on the low power frequency information.

FIG. 1

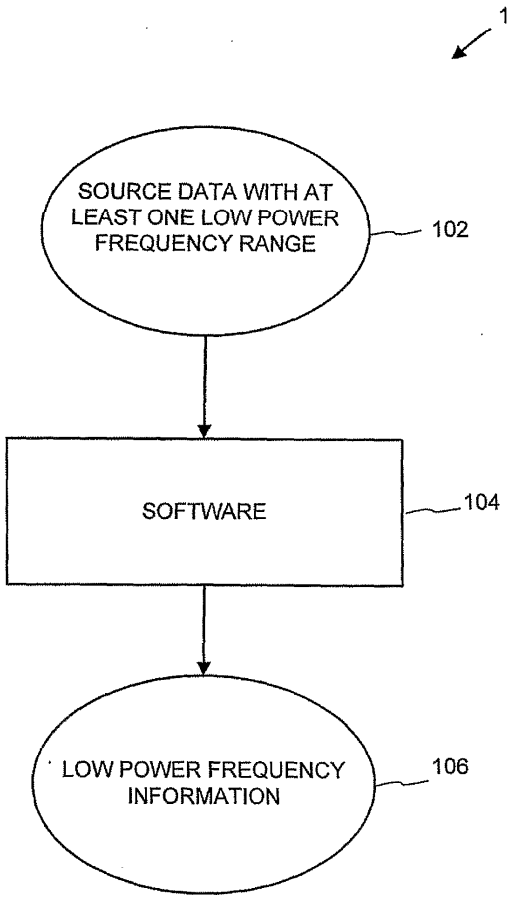
100
SOURCE DATA WITH AT LEAST ONE LOW POWER FREQUENCY RANGE
102
SOFTWARE
104
LOW POWER FREQUENCY INFORMATION
106

FIG. 2

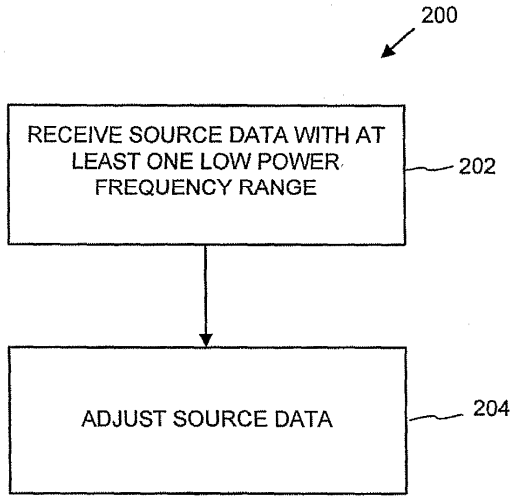
200
RECEIVE SOURCE DATA WITH AT LEAST ONE LOW POWER FREQUENCY RANGE
202
ADJUST SOURCE DATA
204

FIG. 3

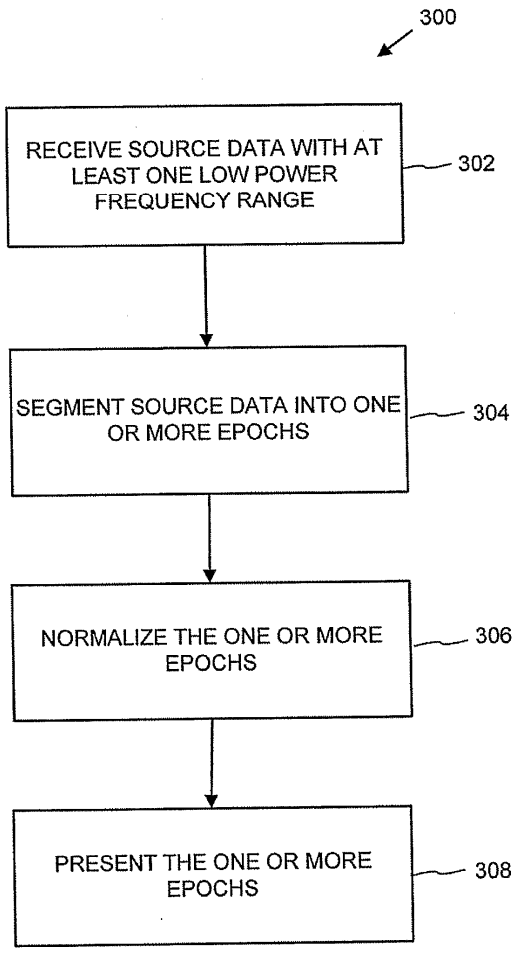
300
RECEIVE SOURCE DATA WITH AT LEAST ONE LOW POWER FREQUENCY RANGE
302
SEGMENT SOURCE DATA INTO ONE OR MORE EPOCHS
304
NORMALIZE THE ONE OR MORE EPOCHS
306
PRESENT THE ONE OR MORE EPOCHS
308

FIG. 4

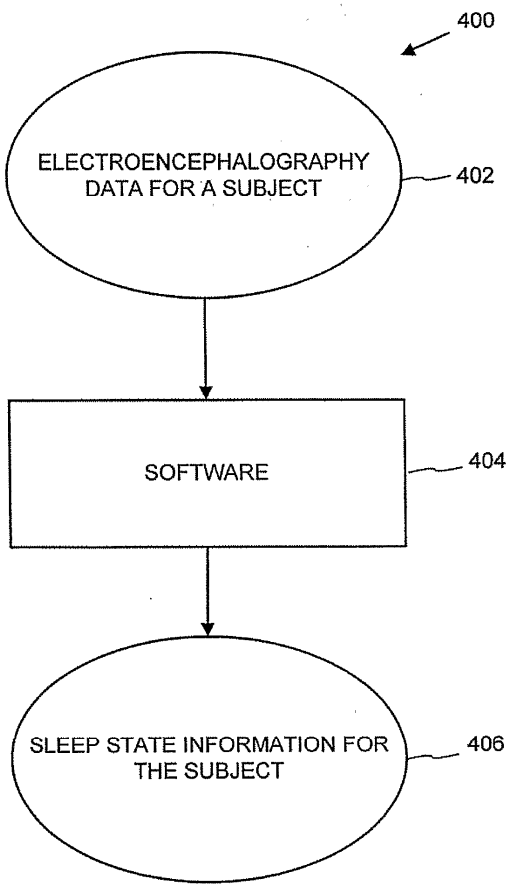
400
ELECTROENCEPHALOGRAPHY DATA FOR A SUBJECT
402
SOFTWARE
404
SLEEP STATE INFORMATION FOR THE SUBJECT
406

FIG. 5

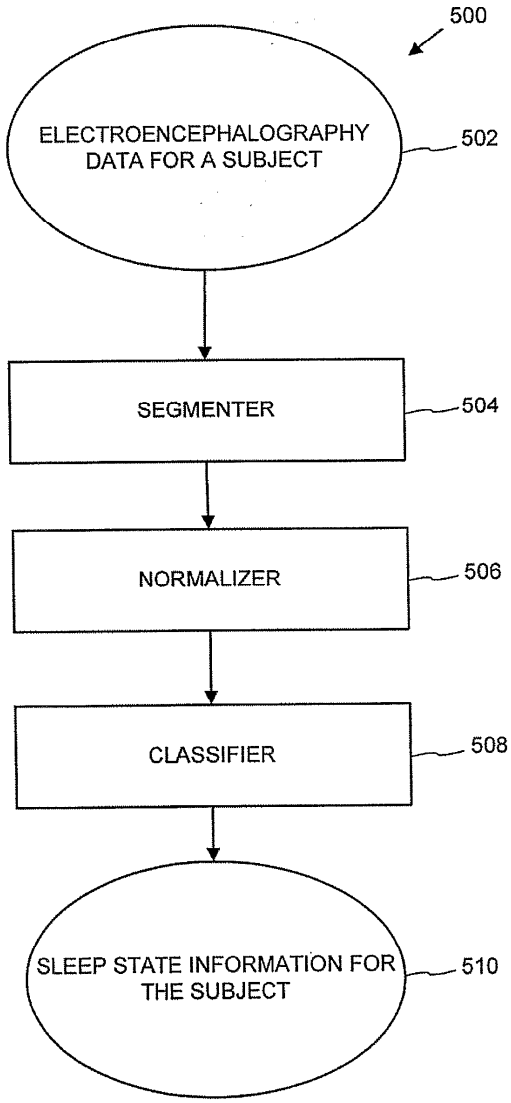
500
ELECTROENCEPHALOGRAPHY DATA FOR A SUBJECT
502
SEGMENTER
504
NORMALIZER
506
CLASSIFIER
508
SLEEP STATE INFORMATION FOR THE SUBJECT
510

FIG. 6

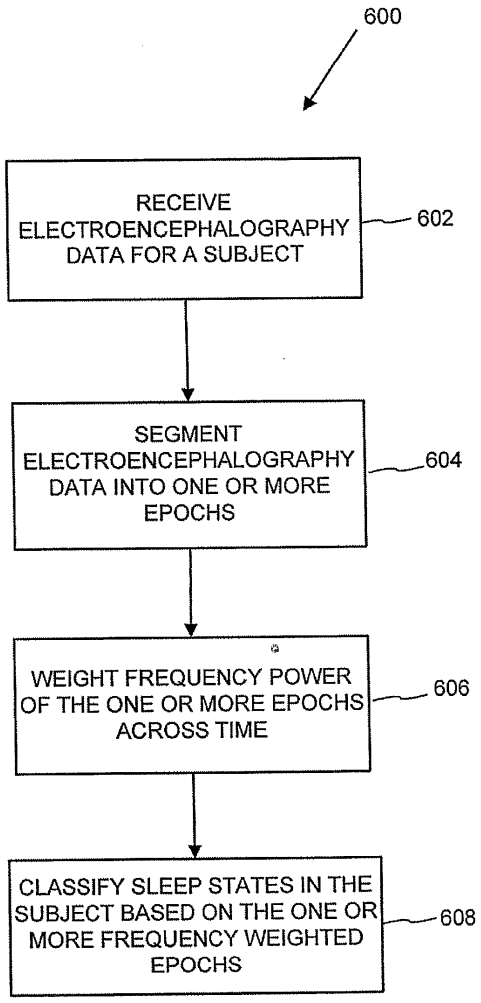
600
RECEIVE ELECTROENCEPHALOGRAPHY DATA FOR A SUBJECT
602
SEGMENT ELECTROENCEPHALOGRAPHY DATA INTO ONE OR MORE EPOCHS
604
WEIGHT FREQUENCY POWER OF THE ONE OR MORE EPOCHS ACROSS TIME
606
CLASSIFY SLEEP STATES IN THE SUBJECT BASED ON THE ONE OR MORE FREQUENCY WEIGHTED EPOCHS
608

FIG. 7

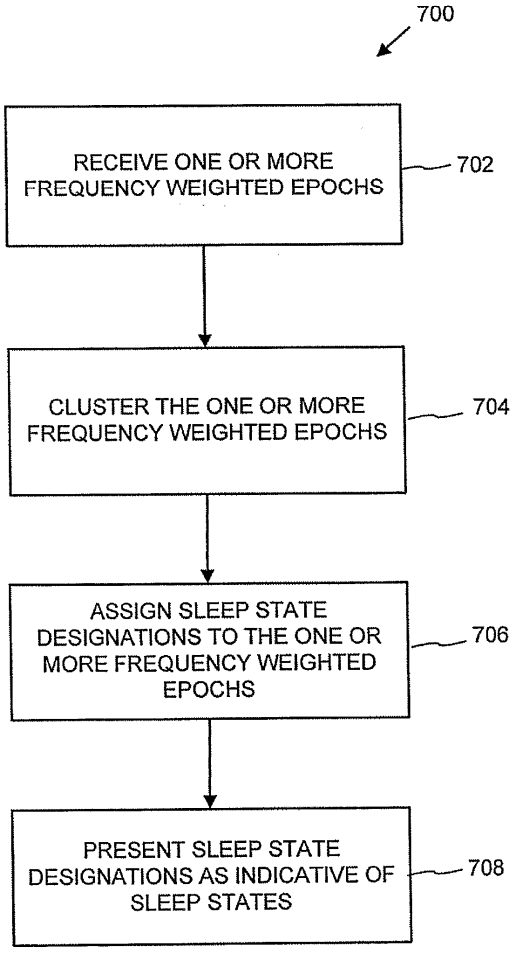
700
RECEIVE ONE OR MORE FREQUENCY WEIGHTED EPOCHS
702
CLUSTER THE ONE OR MORE FREQUENCY WEIGHTED EPOCHS
704
ASSIGN SLEEP STATE DESIGNATIONS TO THE ONE OR MORE FREQUENCY WEIGHTED EPOCHS
706
PRESENT SLEEP STATE DESIGNATIONS AS INDICATIVE OF SLEEP STATES
708

FIG. 8

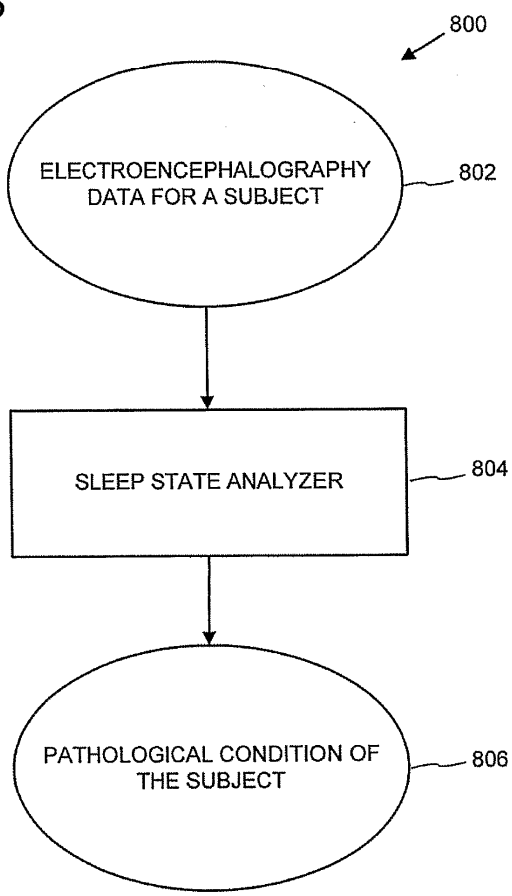
800
ELECTROENCEPHALOGRAPHY DATA FOR A SUBJECT
802
SLEEP STATE ANALYZER
804
PATHOLOGICAL CONDITION OF THE SUBJECT
806

FIG. 9

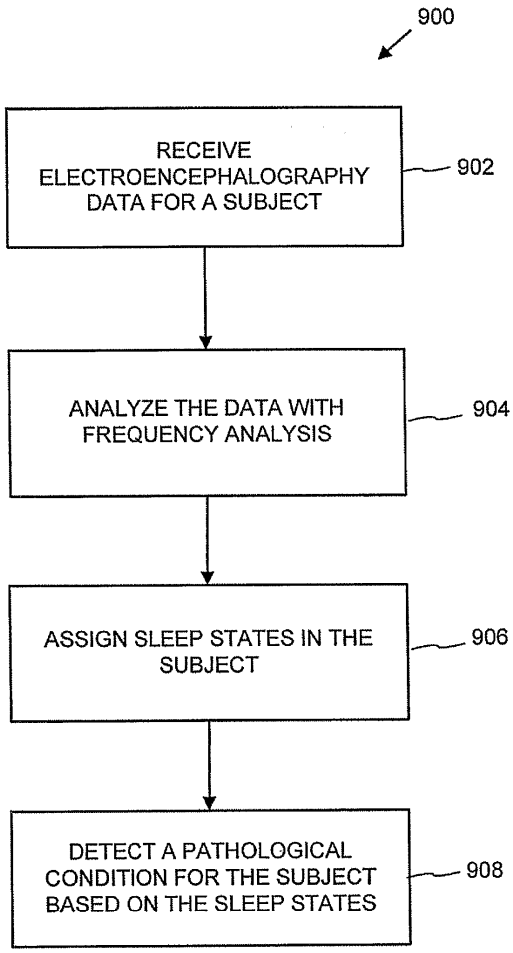
900
RECEIVE ELECTROENCEPHALOGRAPHY DATA FOR A SUBJECT
902
ANALYZE THE DATA WITH FREQUENCY ANALYSIS
904
ASSIGN SLEEP STATES IN THE SUBJECT
906
DETECT A PATHOLOGICAL CONDITION FOR THE SUBJECT BASED ON THE SLEEP STATES
908

FIG. 10

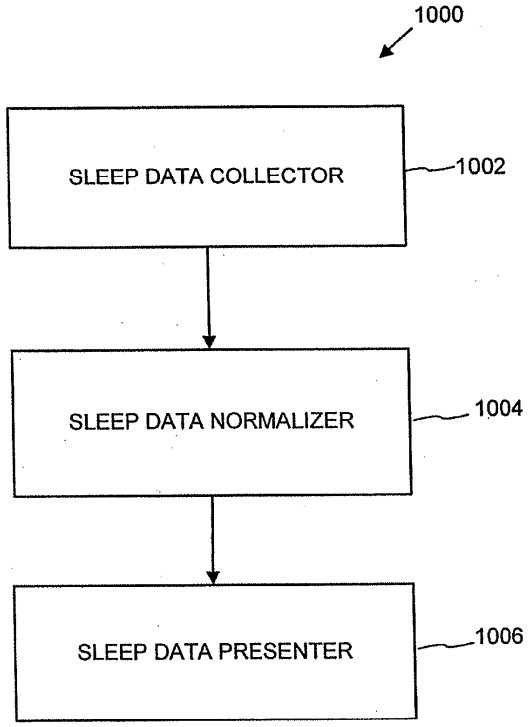
1000
SLEEP DATA COLLECTOR
1002
SLEEP DATA NORMALIZER
1004
SLEEP DATA PRESENTER
1006

FIG. 11

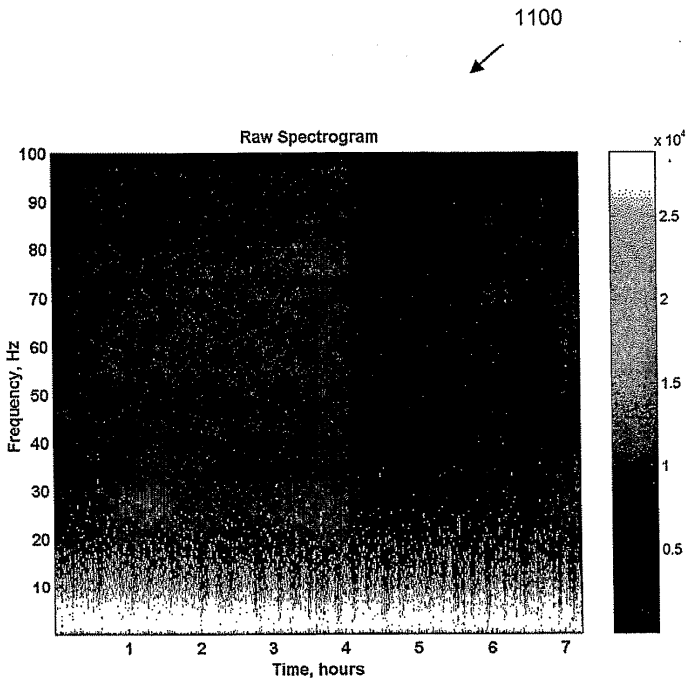
1100
Raw Spectrogram
x 10^4
2.5
2
1.5
1
0.5
Frequency, Hz
100
90
80
70
60
50
40
30
20
10
1
2
3
4
5
6
7
Time, hours

FIG. 12

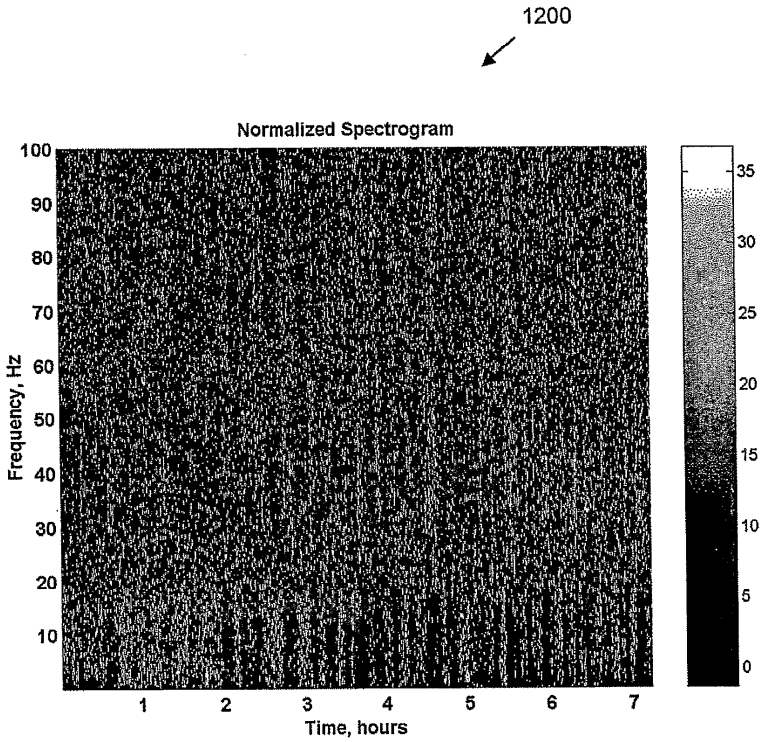
1200
Normalized Spectrogram
Frequency, Hz
100
90
80
70
60
50
40
30
20
10
1
2
3
4
5
6
7
Time, hours
35
30
25
20
15
10
5
0

FIG. 13

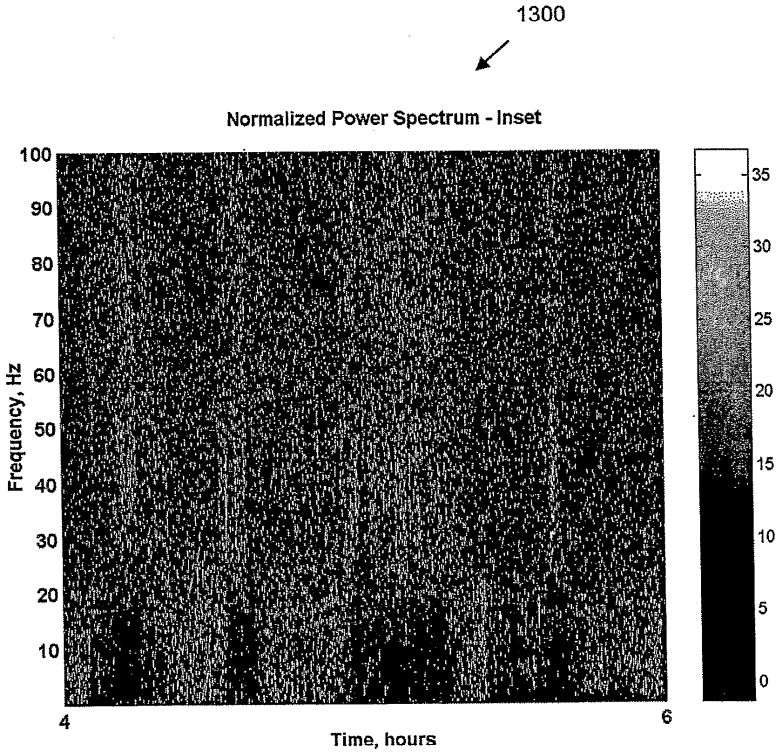
1300
Normalized Power Spectrum - Inset
Frequency, Hz
100
90
80
70
60
50
40
30
20
10
4
6
Time, hours
35
30
25
20
15
10
5
0

FIG. 14

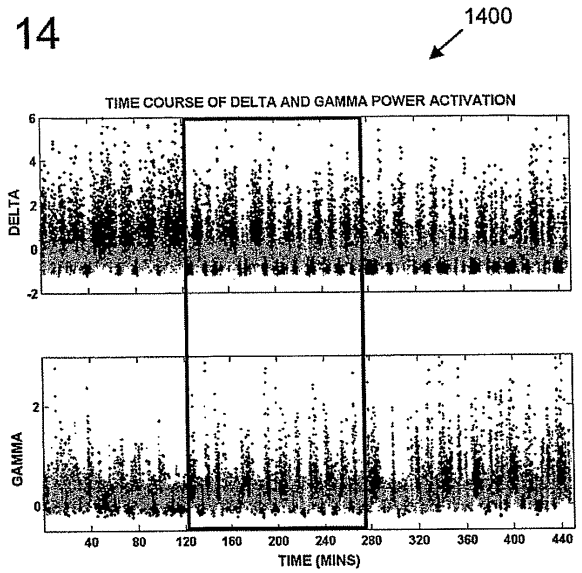
1400
TIME COURSE OF DELTA AND GAMMA POWER ACTIVATION
DELTA
GAMMA
TIME (MINS)

FIG. 15

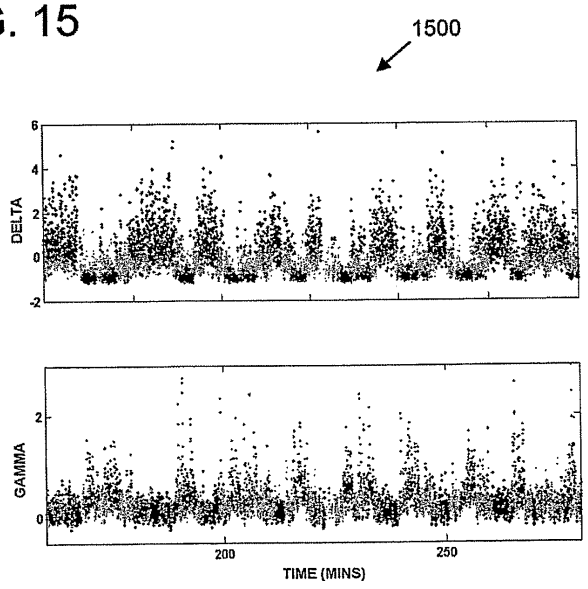
1500
DELTA
GAMMA
TIME (MINS)

FIG. 16

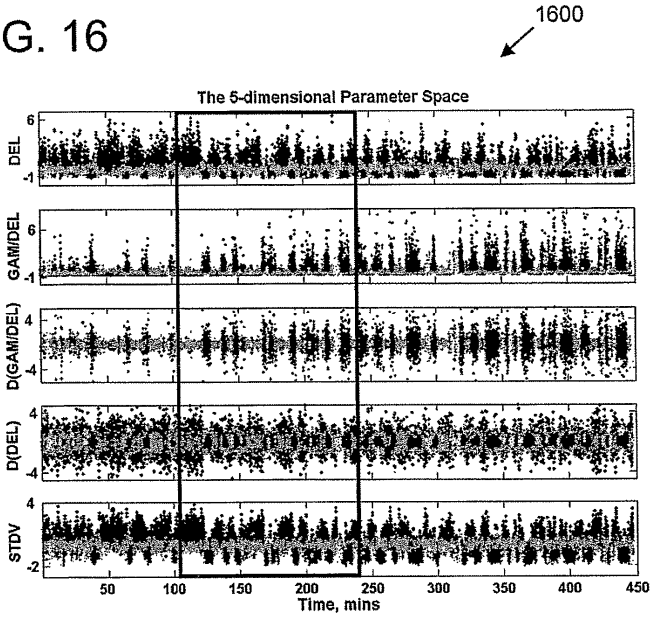
1600
The 5-dimensional Parameter Space
DEL
GAM/DEL
D(GAM/DEL)
D(DEL)
STDV
Time, mins

FIG. 17

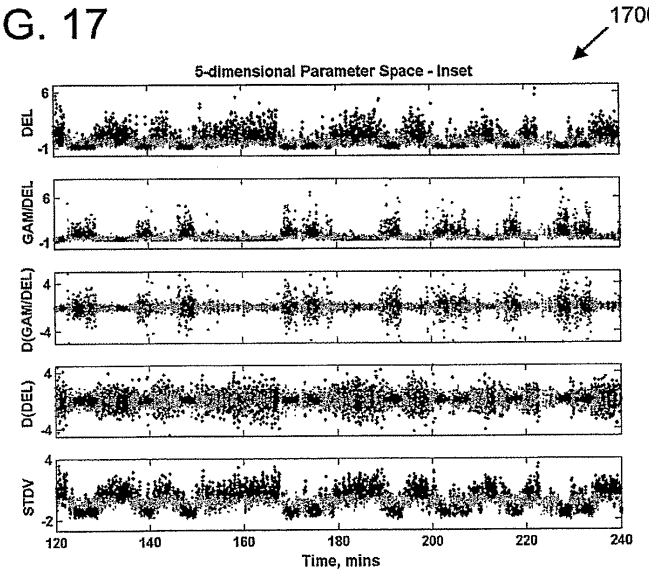
1700
5-dimensional Parameter Space - Inset
DEL
GAM/DEL
D(GAM/DEL)
D(DEL)
STDV
Time, mins

FIG. 18

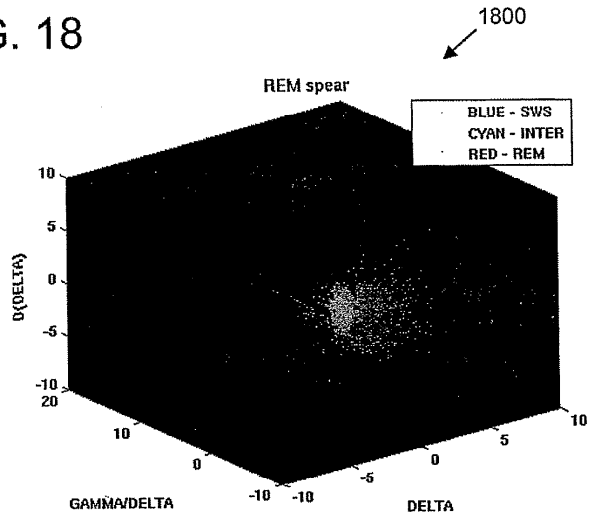
1800
REM spear
BLUE - SWS
CYAN - INTER
RED - REM
D(DELTA)
10
5
0
-5
-10
20
10
0
-10
GAMMA/DELTA
-10
-5
0
5
10
DELTA

FIG. 19

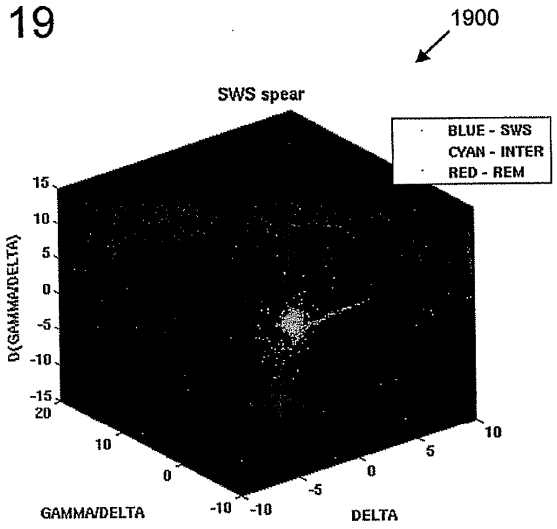
1900
SWS spear
BLUE - SWS
CYAN - INTER
RED - REM
D(GAMMA/DELTA)
15
10
5
0
-5
-10
-15
20
10
0
-10
GAMMA/DELTA
-10
-5
0
5
10
DELTA

FIG. 20

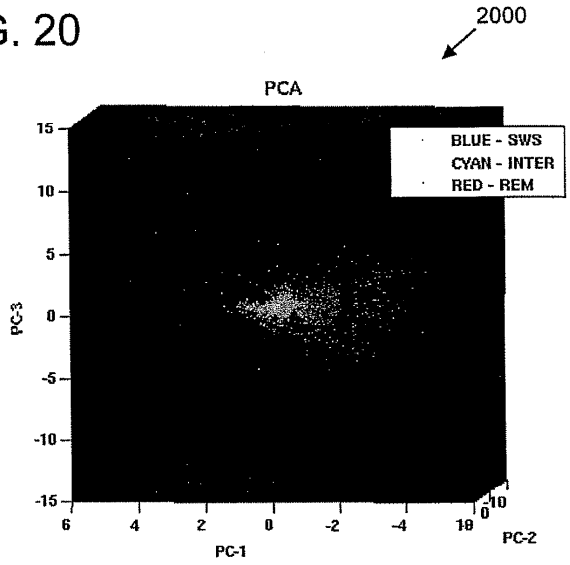
2000
PCA
BLUE - SWS
CYAN - INTER
RED - REM
PC-3
PC-1
PC-2

FIG. 21

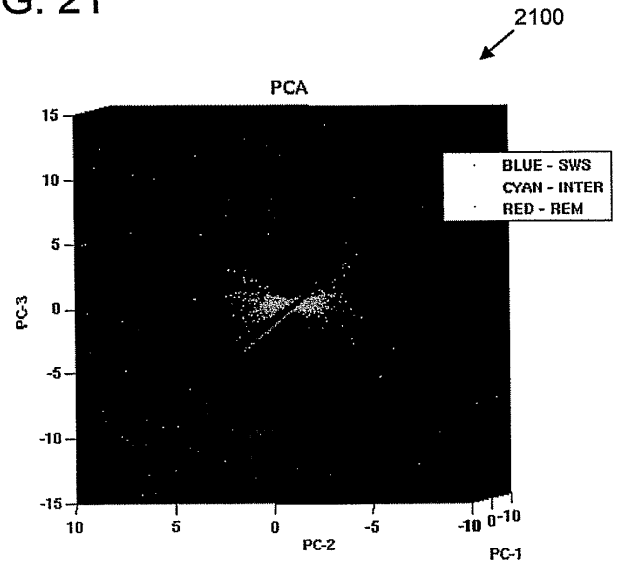
2100
PCA
BLUE - SWS
CYAN - INTER
RED - REM
PC-3
PC-2
PC-1

FIG. 22

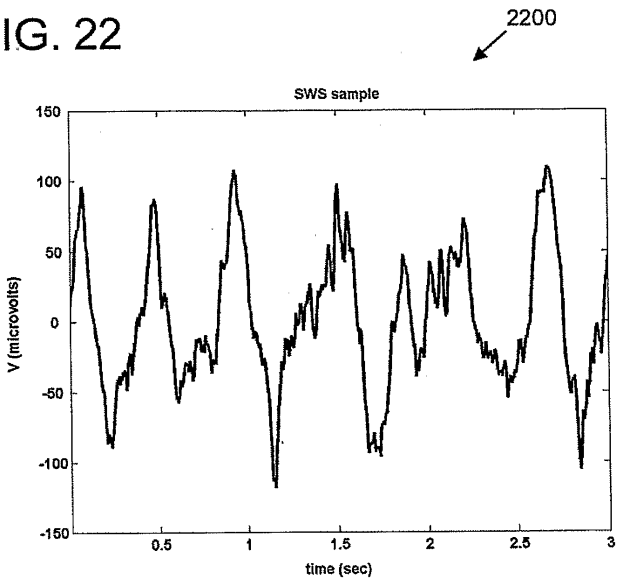
2200
SWS sample
150
100
50
0
-50
-100
-150
V (microvolts)
0.5
1
1.5
2
2.5
3
time (sec)

FIG. 23

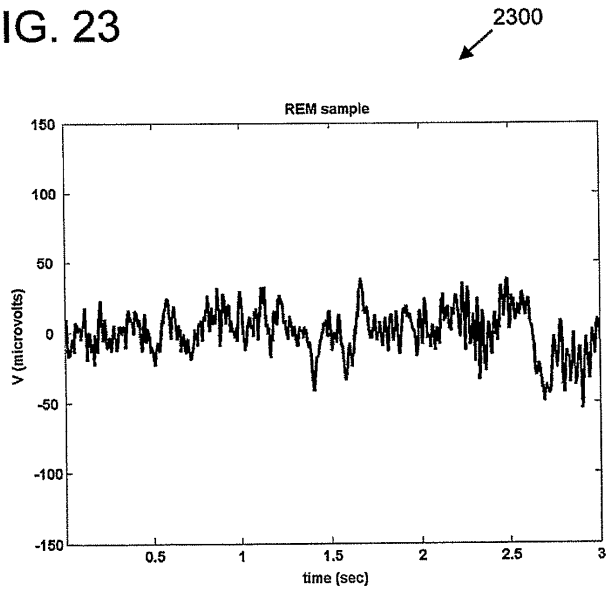
2300
REM sample
150
100
50
0
-50
-100
-150
V (microvolts)
0.5
1
1.5
2
2.5
3
time (sec)

FIG. 24

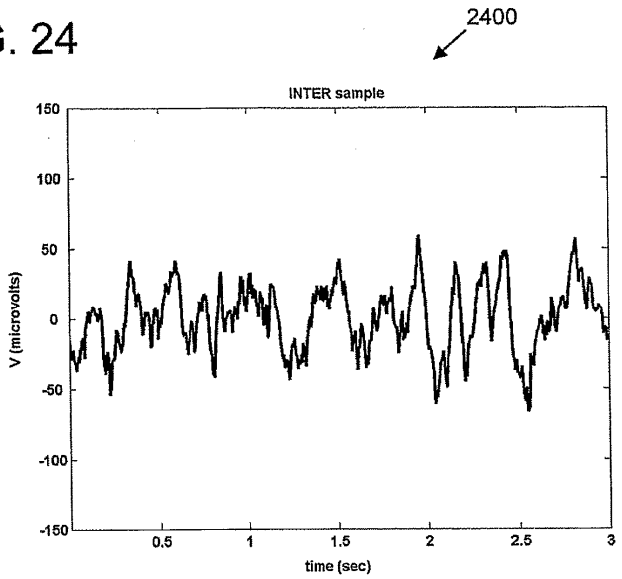
2400
INTER sample
150
100
50
0
-50
-100
-150
V (microvolts)
0.5
1
1.5
2
2.5
3
time (sec)

FIG. 25

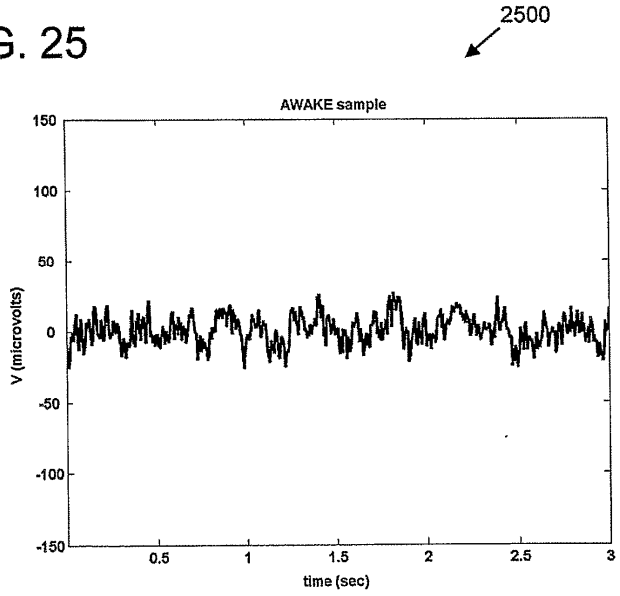
2500
AWAKE sample
150
100
50
0
-50
-100
-150
V (microvolts)
0.5
1
1.5
2
2.5
3
time (sec)

FIG. 26

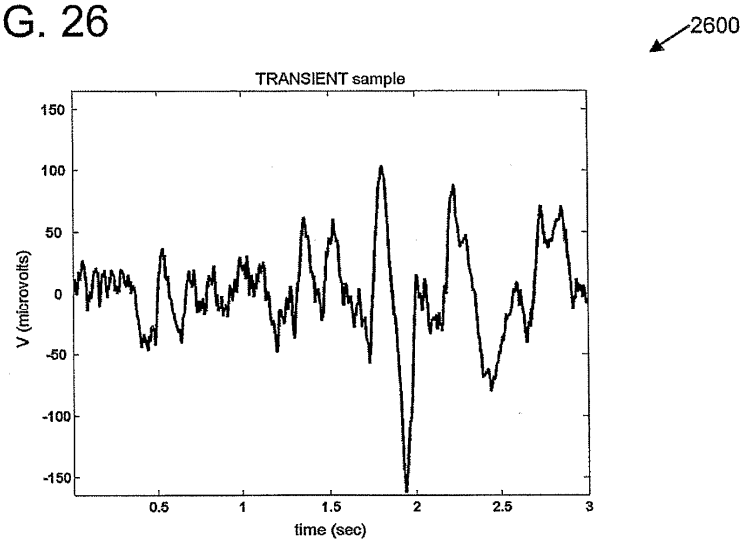
2600
TRANSIENT sample
150
100
50
0
-50
-100
-150
V (microvolts)
0.5
1
1.5
2
2.5
3
time (sec)

FIG. 27

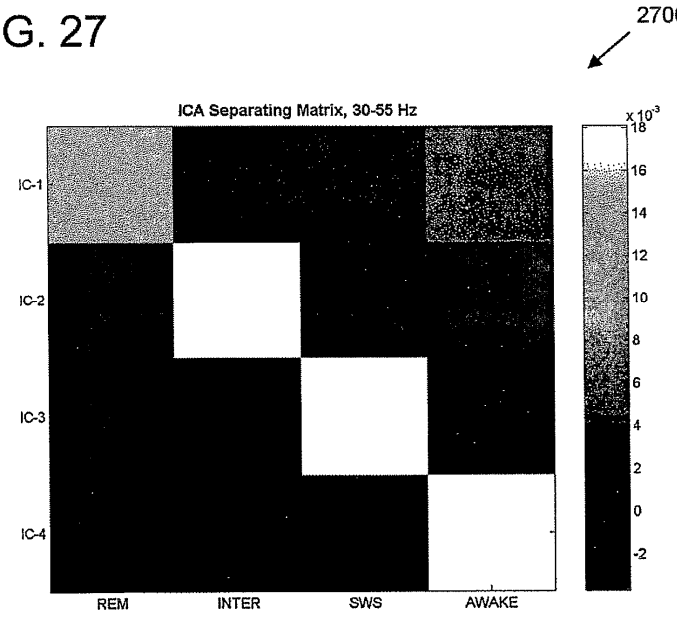
2700
ICA Separating Matrix, 30-55 Hz
x 10^-3
18
16
14
12
10
8
6
4
2
0
-2
IC-1
IC-2
IC-3
IC-4
REM
INTER
SWS
AWAKE

FIG. 28

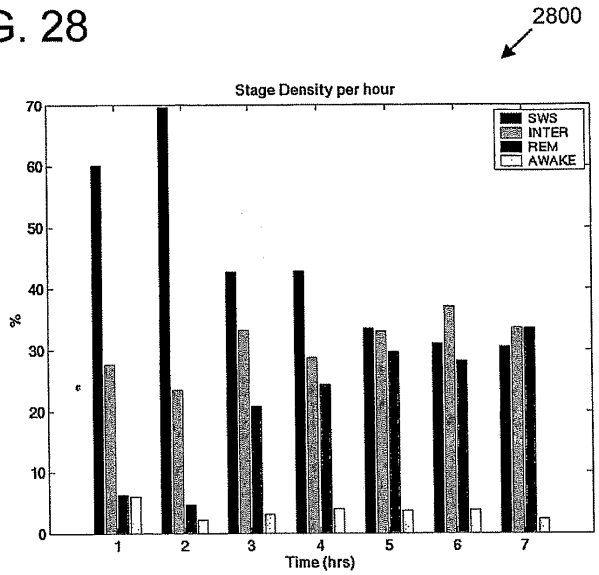
2800
Stage Density per hour
SWS
INTER
REM
AWAKE
%
Time (hrs)

FIG. 29

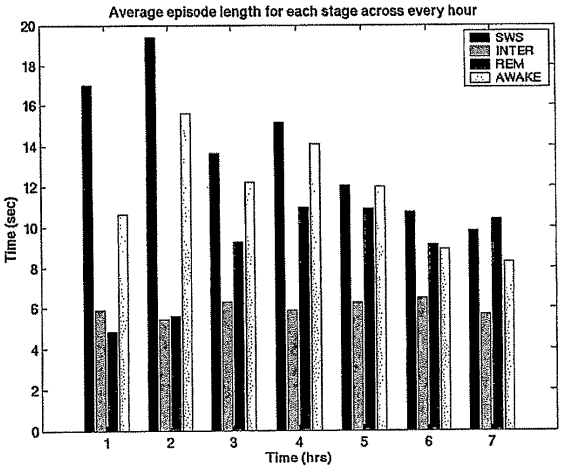
2900
Average episode length for each stage across every hour
SWS
INTER
REM
AWAKE
Time (sec)
Time (hrs)

FIG. 30

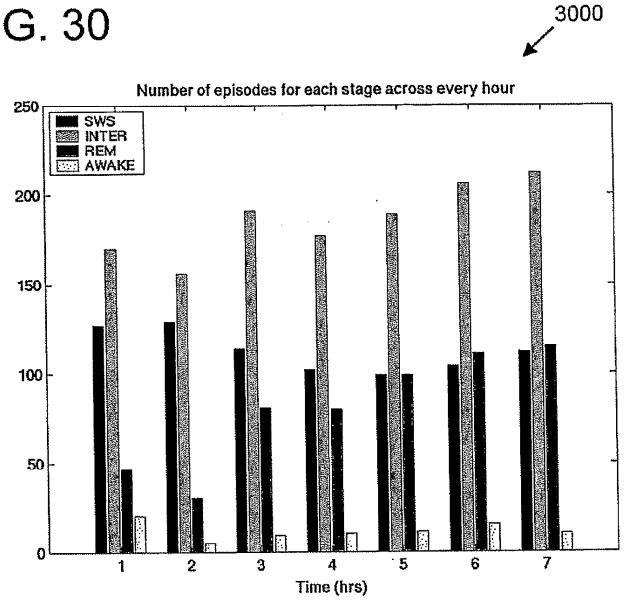
3000
Number of episodes for each stage across every hour
SWS
INTER
REM
AWAKE
250
200
150
100
50
0
1
2
3
4
5
6
7
Time (hrs)

FIG. 31

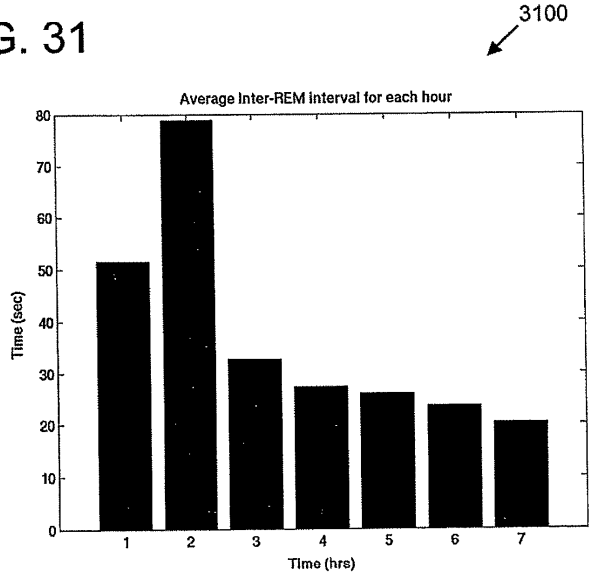
3100
Average Inter-REM interval for each hour
80
70
60
50
40
30
20
10
0
Time (sec)
1
2
3
4
5
6
7
Time (hrs)

3200

FIG. 32

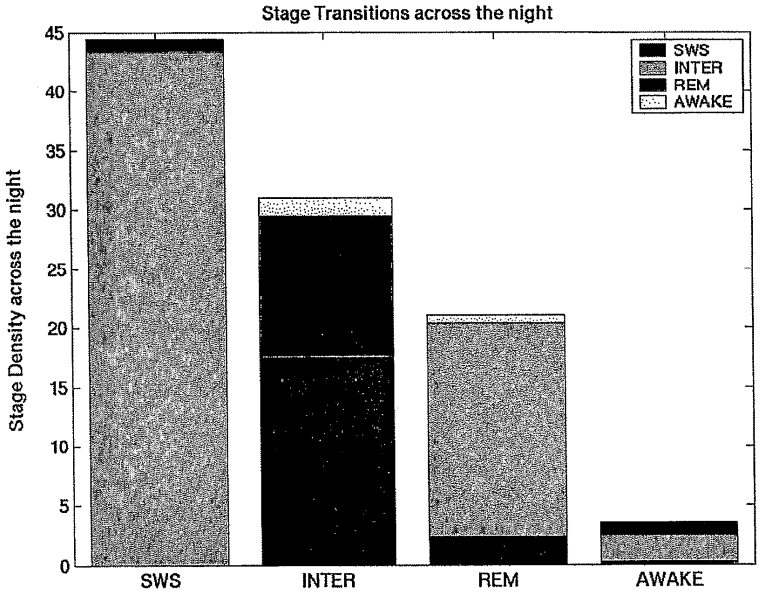
Stage Transitions across the night
Stage Density across the night
45
40
35
30
25
20
15
10
5
0
SWS
INTER
REM
AWAKE
SWS
INTER
REM
AWAKE

FIG. 33

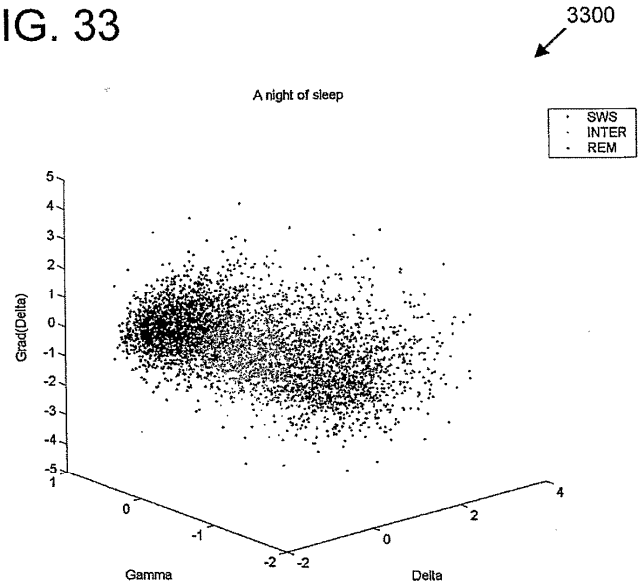
3300
A night of sleep
SWS
INTER
REM
Grad(Delta)
Gamma
Delta

FIG. 34

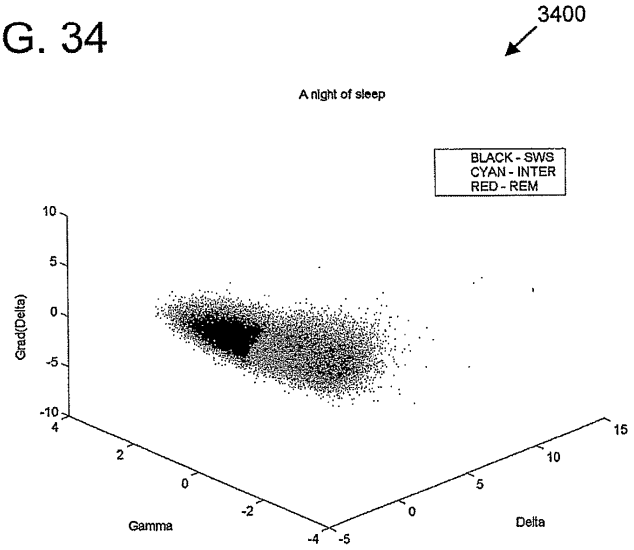
3400
A night of sleep
BLACK - SWS
CYAN - INTER
RED - REM
Grad(Delta)
Gamma
Delta

FIG. 35

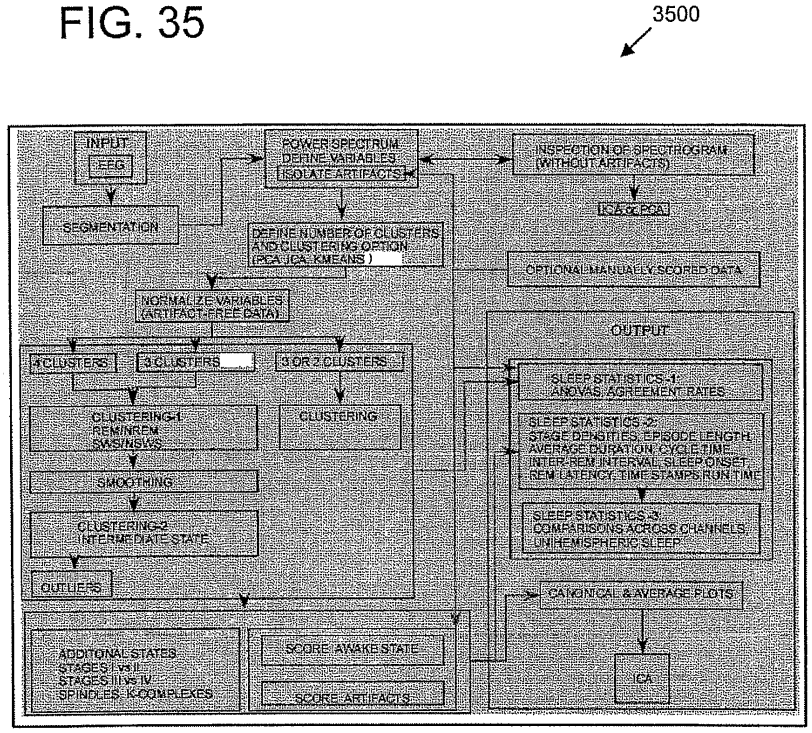
3500
INPUT
EEG
SEGMENTATION
POWER SPECTRUM
DEFINE VARIABLES
ISOLATE ARTIFACTS
DEFINE NUMBER OF CLUSTERS AND CLUSTERING OPTION (PCA/ICA, KMEANS)
NORMALIZE VARIABLES (ARTIFACT-FREE DATA)
4 CLUSTERS
3 CLUSTERS
3 OR 2 CLUSTERS
CLUSTERING-1 REM/NREM SWS/NSWS
CLUSTERING
SMOOTHING
CLUSTERING-2 INTERMEDIATE STATE
OUTLIERS
ADDITIONAL STATES STAGES I vs II STAGES III vs IV SPINDLES, K-COMPLEXES
SCORE AWAKE STATE
SCORE ARTIFACTS
INSPECTION OF SPECTROGRAM (WITHOUT ARTIFACTS)
ICA or PCA
OPTIONAL MANUALLY SCORED DATA
OUTPUT
SLEEP STATISTICS -1: ANOVAS, AGREEMENT RATES
SLEEP STATISTICS -2: STAGE DENSITIES, EPISODE LENGTH, AVERAGE DURATION, CYCLE TIME, INTER-REM INTERVAL, SLEEP ONSET, REM LATENCY, TIME STAMPS, RUN TIME
SLEEP STATISTICS -3: COMPARISONS ACROSS CHANNELS UNI HEMISPHERIC SLEEP
CATEGORICAL & AVERAGE PLOTS
ICA

FIG. 36

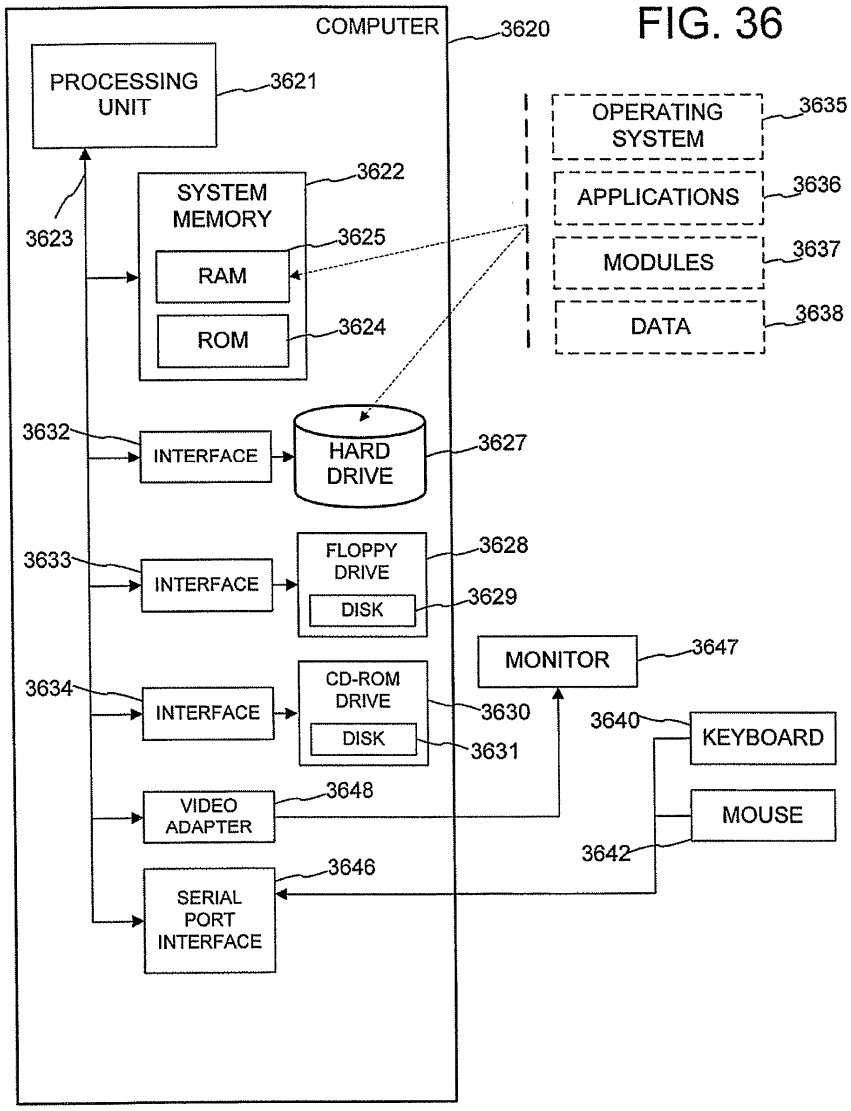
COMPUTER
3620
PROCESSING UNIT
3621
SYSTEM MEMORY
3622
3623
RAM
3625
ROM
3624
OPERATING SYSTEM
3635
APPLICATIONS
3636
MODULES
3637
DATA
3638
3632
INTERFACE
HARD DRIVE
3627
3633
INTERFACE
FLOPPY DRIVE
3628
DISK
3629
3634
INTERFACE
CD-ROM DRIVE
3630
DISK
3631
MONITOR
3647
3640
KEYBOARD
MOUSE
3642
VIDEO ADAPTER
3648
SERIAL PORT INTERFACE
3646

FIG. 37

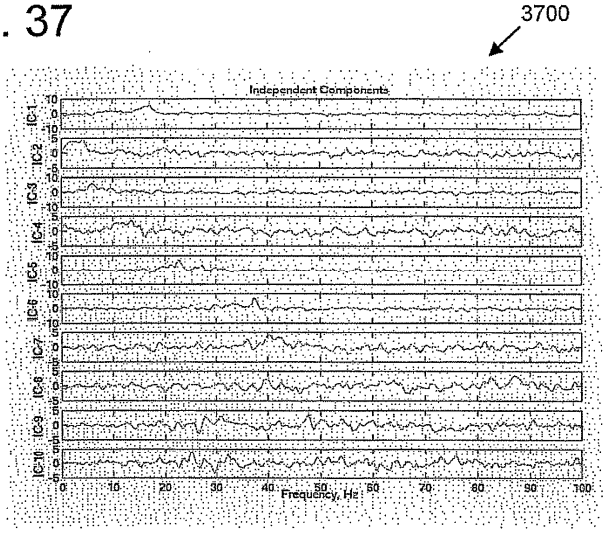
3700
Independent Components
IC-1
IC-2
IC-3
IC-4
IC-5
IC-6
IC-7
IC-8
IC-9
IC-10
Frequency, Hz

FIG. 38

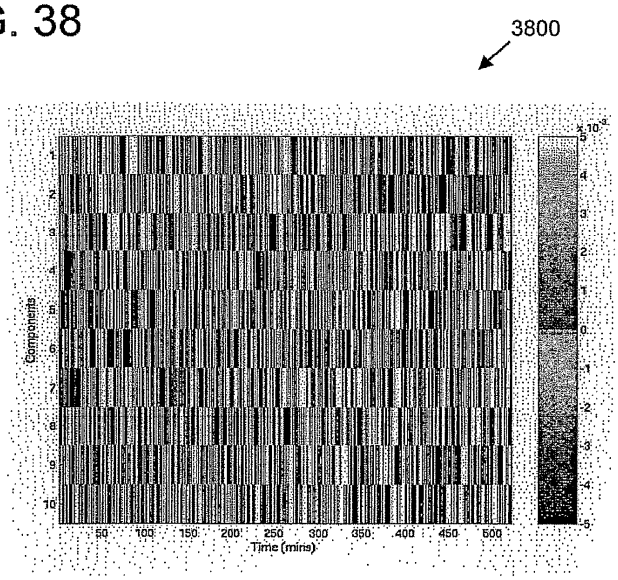
3800
Components
Time (mins)

FIG. 39

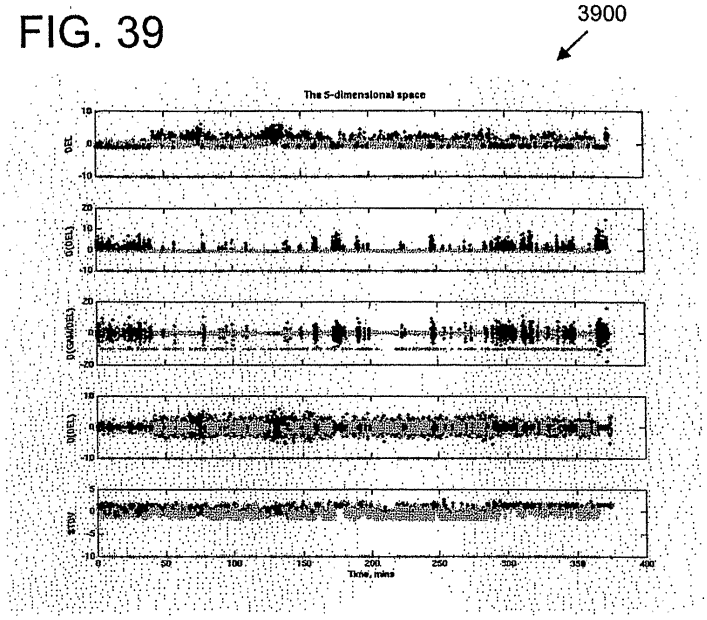
3900
The 5-dimensional space
Time, mins

FIG. 40

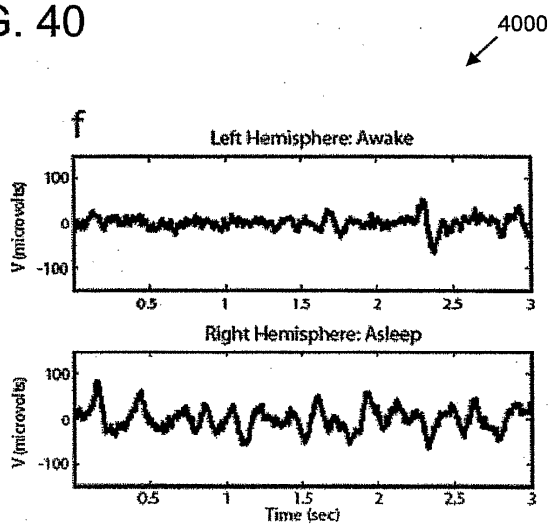
4000
f
Left Hemisphere: Awake
V (microvolts)
Right Hemisphere: Asleep
V (microvolts)
Time (sec)

INTERNATIONAL SEARCH REPORT

International application No.
PCT/US05/27562

A. CLASSIFICATION OF SUBJECT MATTER
IPC: **G06F 7/06**(2006.01)

USPC: 702/189;600/544;395/51
According to International Patent Classification (IPC) or to both national classification and IPC

B. FIELDS SEARCHED

Minimum documentation searched (classification system followed by classification symbols)
U.S. : 702/189; 600/544; 395/51

Documentation searched other than minimum documentation to the extent that such documents are included in the fields searched
NONE

Electronic data base consulted during the international search (name of data base and, where practicable, search terms used)
NONE

C. DOCUMENTS CONSIDERED TO BE RELEVANT

Category *	Citation of document, with indication, where appropriate, of the relevant passages	Relevant to claim No.
X	US 6,549,804 B1 (OSORIO et al.) 15 April 2003 (15.04.2003), columns 8-22.	1-16, 20-22,34
A	US 5,813,993 A (KAPLAN et al.) 29 September 1998 (29.09.1998), columns 11-12.	1
A	US 5,819,007 A (ELGHAZZAWI) 06 October 1998 (06.10.1998), columns 4-5.	1

☐ Further documents are listed in the continuation of Box C. ☐ See patent family annex.

* Special categories of cited documents:

"A" document defining the general state of the art which is not considered to be of particular relevance

"E" earlier application or patent published on or after the international filing date

"L" document which may throw doubts on priority claim(s) or which is cited to establish the publication date of another citation or other special reason (as specified)

"O" document referring to an oral disclosure, use, exhibition or other means

"P" document published prior to the international filing date but later than the priority date claimed

"T" later document published after the international filing date or priority date and not in conflict with the application but cited to understand the principle or theory underlying the invention

"X" document of particular relevance; the claimed invention cannot be considered novel or cannot be considered to involve an inventive step when the document is taken alone

"Y" document of particular relevance; the claimed invention cannot be considered to involve an inventive step when the document is combined with one or more other such documents, such combination being obvious to a person skilled in the art

"&" document member of the same patent family

Date of the actual completion of the international search
01 May 2006 (01.05.2006)

Date of mailing of the international search report
23 JUN 2006

Name and mailing address of the ISA/US
Mail Stop PCT, Attn: ISA/US
Commissioner of Patents
P.O. Box 1450
Alexandria, Virginia 22313-1450
Facsimile No. (571) 273-3201

Authorized officer
Marc Hoff

Telephone No. (703) 308 1782

Form PCT/ISA/210 (second sheet) (July 1998)

B. PCT Patent Application Serial No. US2006/018120 filed May 9, 2006, entitled "Automated Detection of Sleep and Waking States"

Inventors: Philip Low and Terrence Sejnowski

(12) INTERNATIONAL APPLICATION PUBLISHED UNDER THE PATENT COOPERATION TREATY (PCT)

(19) World Intellectual Property Organization
International Bureau

(43) International Publication Date
16 November 2006 (16.11.2006)

PCT

(10) International Publication Number
WO 2006/122201 A2

(51) International Patent Classification:
A61B 5/04 (2006.01)

(21) International Application Number:
PCT/US2006/018120

(22) International Filing Date: 9 May 2006 (09.05.2006)

(25) Filing Language: English

(26) Publication Language: English

(30) Priority Data:
60/679,951 10 May 2005 (10.05.2005) US

(71) Applicant *(for all designated States except US)*: **THE SALK INSTITUTE FOR BIOLOGICAL STUDIES** [US/US]; Intellectual Property and Technology Transfer, P.O. Box 85800, San Diego, California 92186-5800 (US).

(72) Inventors; and

(75) Inventors/Applicants *(for US only)*: **LOW, Philip, S.** [US/US]; 8870 Villa La Jolla Dr., Apt. 214, La Jolla, California 92037 (US). **SEJNOWSKI, Terrence, J.** [US/US]; 672 San Mario Drive, Solana Beach, California 92075 (US).

(74) Agent: **HARRIS, Scott, C.**; FISH & RICHARDSON P.C., P.O. Box 1022, Minneapolis, Minnesota 55440-1022 (US).

(81) Designated States *(unless otherwise indicated, for every kind of national protection available)*: AE, AG, AL, AM, AT, AU, AZ, BA, BB, BG, BR, BW, BY, BZ, CA, CH, CN, CO, CR, CU, CZ, DE, DK, DM, DZ, EC, EE, EG, ES, FI, GB, GD, GE, GH, GM, HR, HU, ID, IL, IN, IS, JP, KE, KG, KM, KN, KP, KR, KZ, LC, LK, LR, LS, LT, LU, LV, LY, MA, MD, MG, MK, MN, MW, MX, MZ, NA, NG, NI, NO, NZ, OM, PG, PH, PL, PT, RO, RU, SC, SD, SE, SG, SK, SL, SM, SY, TJ, TM, TN, TR, TT, TZ, UA, UG, US, UZ, VC, VN, YU, ZA, ZM, ZW.

(84) Designated States *(unless otherwise indicated, for every kind of regional protection available)*: ARIPO (BW, GH, GM, KE, LS, MW, MZ, NA, SD, SL, SZ, TZ, UG, ZM, ZW), Eurasian (AM, AZ, BY, KG, KZ, MD, RU, TJ, TM), European (AT, BE, BG, CH, CY, CZ, DE, DK, EE, ES, FI, FR, GB, GR, HU, IE, IS, IT, LT, LU, LV, MC, NL, PL, PT, RO, SE, SI, SK, TR), OAPI (BF, BJ, CF, CG, CI, CM, GA, GN, GQ, GW, ML, MR, NE, SN, TD, TG).

[Continued on next page]

(54) Title: AUTOMATED DETECTION OF SLEEP AND WAKING STATES

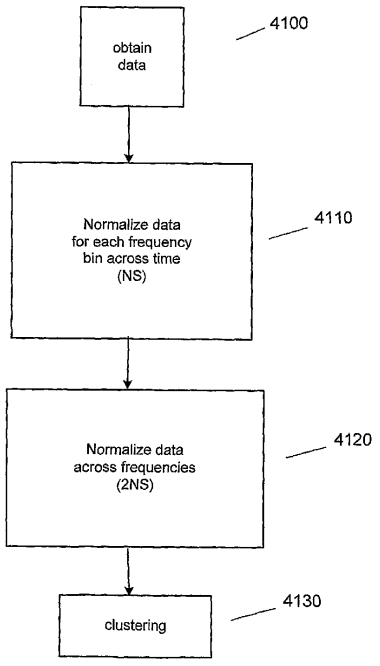

(57) Abstract: Determining low power frequency range information from spectral data. Raw signal data can be adjusted to increase dynamic range for power within low power frequency ranges as compared to higher-power frequency ranges to determine adjusted source data valuable for acquiring low power frequency range information. Low power frequency range information can be used in the analysis of a variety of raw signal data. For example, low power frequency range information within electroencephalography data for a subject from a period of sleep can be used to determine sleep states. Similarly, automated full-frequency spectral electroencephalography signal analysis can be useful for customized analysis including assessing sleep quality, detecting pathological conditions, and determining the effect of medication on sleep states.

WO 2006/122201 A2

WO 2006/122201 A2

Published:
— *without international search report and to be republished upon receipt of that report*

For two-letter codes and other abbreviations, refer to the "Guidance Notes on Codes and Abbreviations" appearing at the beginning of each regular issue of the PCT Gazette.

AUTOMATED DETECTION OF SLEEP AND WAKING STATES

Cross-Reference to Related Applications

[0001] This application claims priority to U.S. Provisional Application Serial No. 60/679,951, filed on May 10, 2005. The disclosure of the prior application is considered part of (and is incorporated by reference in) the disclosure of this application.

Background

[0002] Sleep states and other brain activity have been commonly analyzed via electroencephalography or EEG signals. As a person falls asleep, the brain activity is modulated, representing different depths and phases of sleep. In a typical person, the sleep states transition over time, starting at a first sleep state known as slow wave sleep or SWS. SWS has low frequency high power EEG activity. The sleep may lighten into so-called intermediate sleep states. Other sleep states known as rapid eye movement sleep is characterized by a lower power EEG activity.

[0003] EEG signals follow a distribution where higher frequency signals have lower amplitudes and therefore lower power. This so-called 1/f distribution means that the highest amplitudes are present at the lowest frequencies.

[0004] EEG signals for sleep stage determination are conventionally analyzed using the Rechtschaffen-Kales method. This method can rely on manually scoring sleep EEG signals due to the low power frequency limitations of automated signal analysis techniques. The Rechtschaffen-Kales method can be both highly unreliable and time consuming because statistically significant shifts at high frequencies are usually not detectable by a human scorer due to the very low amplitudes. Further, the Rechtschaffen-Kales method tends to have poor temporal and spatial resolution, does not make all of its variables known, and commonly leads to low inter-user agreement rates across both manual as well as automated scorers. Unfortunately, alternative sleep state determination methods, including artificial neural network classifiers, usually rely on multiple channels and tend to emulate human performance, thereby improving the time of determination without drastically improving quality.

Summary

[0005] The present application describes normalizing data indicative of brainwave activity to increase the dynamic range of information within the data.

[0006] The embodiments explain using this information to determine sleep states automatically. Other applications are described which automatically assess sleep quality, pathological conditions, and medication effects.

Brief description of the drawings

[0007] Figure 1 is a block diagram of an exemplary system for determining low power frequency information from source data with at least one low power frequency range;

[0008] Figure 2 is a flowchart showing an exemplary method for adjusting source data;

[0009] Figure 3 is a flowchart showing an exemplary method for adjusting source data to account for differences in power over a spectrum of frequencies over time;

[0010] Figure 4 is a block diagram of an exemplary system for determining sleep state information for a subject;

[0011] Figure 5 is a block diagram of another exemplary system for determining sleep state information for a subject;

[0012] Figure 6 is a flowchart showing an exemplary method for determining sleep states in a subject;

[0013] Figure 7 is a flowchart showing an exemplary method for classifying sleep states in a subject;

[0014] Figure 8 is a block diagram of an exemplary system for determining a pathological condition of a subject from sleep states;

[0015] Figure 9 is a flowchart showing an exemplary computer-implemented method for determining a pathological condition for a subject based on sleep states;

[0016] Figure 10 is a block diagram of an exemplary system for dynamically determining customized sleep scores for a subject;

[0017] Figure 11 is a screen shot of an exemplary whole night EEG source data frequency power spectrogram;

[0018] Figure 12 is a screen shot of the exemplary whole night EEG source data shown in Figure 11 after an exemplary adjustment technique has been applied;

[0019] Figure 13 is a screen shot of a two hour time frame of the exemplary adjusted whole night EEG source data shown in Figure 12;

[0020] Figure 14 is a screen shot of an exemplary visualization of high and low power frequency bands within the whole night EEG spectrogram shown in Figure 12;

[0021] Figure 15 is a screen shot of a two hour and forty minutes time frame of the exemplary visualization of high and low power frequency bands within the whole night spectrogram shown in Figure 14.

[0022] Figure 16 is a screen shot of an exemplary five-dimensional parameter space visualization of the whole night EEG spectrogram of Figure 12;

[0023] Figure 17 is a screen shot of a two hour time frame of the exemplary five-dimensional parameter space visualization of the whole night EEG visualization shown in Figure 16;

[0024] Figure 18 is a screen shot of an exemplary visualization of classified sleep states based on EEG spectrogram data;

[0025] Figure 19 is a screen shot of another exemplary visualization of classified sleep states based on EEG spectrogram data;

[0026] Figure 20 is a screen shot of yet another exemplary visualization of classified sleep states based on EEG spectrogram data;

[0027] Figure 21 is a screen shot from another vantage point of the exemplary visualization of classified sleep states based on EEG spectrogram data of Figure 20;

[0028] Figures 22, 23, 24 and 25 are screen shots of canonical spectra representative of frequency weighted epochs designated as distinct sleep states in a subject for a period of time;

[0029] Figure 26 is a screen shot of a canonical spectra representative of a frequency weighted epoch that displays a transient sleep state having characteristics of more than one sleep state;

[0030] Figure 27 is a screen shot of an exemplary visualization of the degree of sleep stager separation that distinguishes representative canonical spectra of distinct sleep state;

[0031] Figures 28, 29, 30, 31 and 32 are screen shots of exemplary visualization of sleep state statistics for a subject according to sleep state designations of one or more epochs;

[0032] Figures 33 is a screen shot of an exemplary visualization of classified anesthesia states of an anesthetized cat based on EEG spectrogram data;

[0033] Figure 34 is a screen shot of an exemplary visualization of classified sleep states of a human subject based on EEG spectrogram data;

[0034] Figure 35 is a flowchart showing yet another exemplary method for classifying sleep states in a subject that can be implemented with the described technologies;

[0035] Figure 36 is an exemplary computer system that can be implemented with the described technologies;

[0036] Figure 37 is a screen shot of an exemplary visualization of independent component analysis applied on a normalized spectrogram to further determine appropriate frequency windows for extracting information;

[0037] Figure 38 is a screen shot of an exemplary visualization of independent components of Figure 37 throughout time;

[0038] Figure 39 is a screen shot of a six and a half hour time frame of an exemplary five-dimensional parameter space visualization of frequency bands of the whole night EEG visualization from a human subject with Alzheimer's;

[0039] Figure 40 is a screen shot of an exemplary visualization of classified unihemispheric sleep from a bird;

[0040] Figure 41 illustrates a flowchart of operation of another embodiment which uses a double normalization;

[0041] Figures 42a-42c show the raw spectrogram, single normalized spectrogram, and double normalized spectrogram respectively;

[0042] Figure 43 shows the preferred frequency over time;

[0043] Figure 44 shows a diagram of these frequencies;

[0044] Figure 45 shows a three-dimensional view of the data; and

[0045] Figure 46 shows a graph of spectral fragmentation for the frequencies.

Detailed description

[0046] One important recognition of the present system is that the low frequency ranges in EEG signals often have the most energy, and hence have mistakenly led many researchers to overanalyze that low frequency range. However, one reason found for the increased power in those lower frequencies, was found by the inventors to be the low-pass characteristic of the skull. Other reasons may also contribute to the increased power in lower frequencies.

[0047] Obtained EEG signals are low-power frequency signals and follow a 1/f distribution, whereby the power in the signal is inversely related, e.g., inversely proportional, to the frequency.

[0048] EEG signals have typically been examined in time in series increments called epochs. For example, when the EEG signal is used for analyzing sleep, sleep may be segmented into one or more epochs to use for analysis. The epochs can be segmented into different sections using a scanning window, where the scanning window defines different sections of the time series increment. The scanning window can move via a sliding window, where sections of the sliding window have overlapping time series sequences. An epoch can alternatively span an entire time series, for example.

[0049] According to the present application, different forms of sleep state may be monitored. A sleep state is described as any distinguishable sleep or wakefulness that is representative of behavioral, physical or signal characteristics. Sleep states which are referred to in this application include slow wave sleep or SWS, rapid eye movement sleep or REM, intermediate sleep states also called inter or IS states, and awake states. Awake states may actually be part of the sleep state, and the awake states can be characterized by vigilance into attentiveness or levels of alertness. The intermediate sleep can also be characterized as intermediate-1 sleep and intermediate-2 sleep.

[0050] An artifact may also be obtained during acquisition of an EEG. An artifact is data that misrepresents the EEG. For example, movement within a user that registers on the EEG may be an artifact. Example artifacts include muscle twitches and the like.

[0051] *Example 1 - Exemplary Source Data*

[0052] In any of the embodiments described herein, a variety of source data can be analyzed including electroencephalography (EEG) data, electrocardiography data (EKG), electrooculography data (EOG), electromyography data (EMG), local field potential (LFP) data, spike train data, wave data including sound and pressure waves, and any data exhibiting where there are differences in dynamic range of power for various frequencies across a frequency spectrum of

the data e.g., a 1/f distribution. Source data can include encoded data stored at low power frequency within source data.

[0053] *Example 2 - Exemplary System for Determining Low Power Frequency Information from Source Data with at Least One Low Power Frequency Range*

[0054] FIG. 1 shows an exemplary system 100 for determining low power frequency information from source data with at least one low power frequency range.

[0055] Source data with at least one low power frequency range 102 is obtained and input into software 104 to determine low power frequency information 106.

[0056] The software 104 can employ any combination of technologies, such as those described herein, to determine low power frequency information 106 for the source data.

[0057] Methods for determining low power frequency information from source data with at least one low power frequency range are described in detail below.

[0058] *Example 3 - Exemplary Method for Adjusting Source Data*

[0059] FIG. 2 shows an exemplary method 200 for adjusting source data. For example, the method 200 can be implemented within system 100 of FIG. 1.

[0060] At 202, source data with at least one low power frequency range is received. For example, electroencephalography source data for a subject can be received. Source data can be received via a single channel or multiple channels.

[0061] At 204, source data is adjusted to increase the dynamic range for power within at least one low power frequency range of the frequency spectrum of the source data as compared to a second higher power frequency range. A number of adjustment techniques described herein, including normalization and frequency weighting can be used. In an embodiment, electroencephalography source data is normalized to increase the low power, higher frequency range data relative to the higher power, lower frequency range data or, more generally, to normalize the powers of the different signal parts.

[0062] After the source data is adjusted, various other processing can be done. For example, a visualization of the adjusted source data can be presented. Further, low power frequency information can be extracted from the adjusted source data. For example, low power frequency information can be extracted from adjusted electroencephalography source data. Higher power frequency information can also be extracted from the adjusted source data.

[0063] The method described in this or any of the other examples can be a computer-implemented method performed via computer-executable instructions in one or more computer-readable media. Any of the actions shown can be performed by software incorporated within a signal processing system or any other signal data analyzer system.

[0064] *Example 4 -Exemplary Method for Adjusting Source Data to Account for Differences in Power over a Spectrum of Frequencies over Time*

[0065] FIG. 3 shows an exemplary method 300 for adjusting source data to account for differences in power over a spectrum of frequencies over time. For example, the method 300 can be implemented within system 100 of FIG. 1.

[0066] At 302, source data with at least on low power frequency range is received. For example, electroencephalography data with at least one low power frequency range can be received. Artifacts in the data can be removed from the source data. For example, artifact data can be manually removed from the source data or automatically filtered out of source data via a filtering (e.g., DC filtering) or data smoothing technique. The source data can also be pretreated with component analysis.

[0067] At 304, the source data is segmented into one or more epochs; where each epoch is a portion of data from the series. For example, the source data can be segmented into a plurality of time segments via a variety of separating

techniques. Scanning windows and sliding windows can be used to separate the source data into time series increments.

[0068] At 306, the one or more epochs are normalized for differences in power of the one or more epochs across time. For example, the power of each epoch at one or more frequencies can be normalized across time to determine appropriate frequency windows for extracting information. Such normalization can reveal low power, statistically significant shifts in power at one or more frequencies (e.g., Delta, Gamma, and the like). Any frequency range can be revealed and utilized for analysis. Information can be calculated for each of the one or more epochs after appropriate frequency windows have been established. Such information can include low frequency power (e.g., Delta power), high frequency power (e.g., Gamma power), standard deviation, maximum amplitude (e.g., maximum of the absolute value of peaks) and the sort. Further calculations can be done on the information calculated for each of the one or more epochs creating information such as Gamma power/Delta power, time derivative of Delta, time derivative of Gamma power/Delta power and the like. Time derivatives can be computed over preceding and successive epochs. After calculating the information, that information can then be normalized across the one or more epochs. A variety of data normalization techniques can be conducted including z-scoring and other similar techniques.

[0069] At 308, results of the adjustment of source data to account for differences in power over a spectrum of frequencies over time can be presented as one or more epochs of data. For example, frequency weighted epochs can be presented as adjusted source data.

[0070] *Example 5 - Exemplary System for Determining Sleep State*

[0071] Information for a Subject

[0072] FIG. 4 shows an exemplary system 400 for determining sleep state information for a subject. Electroencephalography data for a subject 402 is obtained and input into software 404 to determine sleep state information for the subject 406.

[0073] The software 404 can employ any combination of technologies, such as those described herein, to determine sleep state information for the subject 406.

[0074] Methods for determining sleep state information for a subject are described in detail below.

[0075] *Example 6 - Another Exemplary System for Determining Sleep State Information for a Subject*

[0076] FIG. 5 shows an exemplary system 500 for determining sleep state information for a subject.

[0077] Electroencephalography data for a subject 502 is obtained and input into segmenter 504 to segment the data into one or more epochs. In practice, epochs are of similar (e.g., the same) length. Epoch length can be adjusted via a configurable parameter. The one or more epochs, in turn, are

input into normalizer 506 to normalize frequency data in the one or more epochs across time, thereby frequency weighting the one or more epochs of electroencephalography data. The one or more frequency weighted epochs are then input into classifier 508 to classify the data into sleep states, thereby generating sleep state information for the subject 510.

[0078] Methods for determining sleep state information for a subject are described in detail below.

[0079] *Example 7 - Exemplary Method for Determining Sleep States in a Subject*

[0080] FIG. 6 shows an exemplary method 600 for determining sleep states in a subject. For example, the method 600 can be implemented within system 500 of FIG. 5 or system 400 of FIG. 4.

[0081] At 602, electroencephalography (EEG) data for a subject is received. For example, electroencephalography data, which exhibits lower dynamic range for power in at least one low power first frequency range in a frequency spectrum as compared to a second frequency range in the frequency spectrum, can be received.

[0082] At 604, the electroencephalography data for the subject is segmented into one or more epochs. For example, the EEG data can be segmented into one or more epochs via a variety of separating techniques. Scanning windows and sliding windows can be used to separate the EEG data into one or more epochs. The source data can also be filtered via direct

current filtering during, prior to, or after segmenting. The source data can also be pretreated with component analysis (e.g., principle or independent component analysis).

[0083] FIG. 11 is a screen shot of an exemplary whole night EEG source data frequency power spectrogram for a subject that has been segmented over three second epochs spaced in 1 second increments. Power range is indicated in the shading, where white shaded regions are higher in power than dark shaded regions. The higher frequencies (e.g., Gamma) therefore exhibit lower power than the lower frequencies (e.g., Delta, Theta and the like) in the whole night EEG data.

[0084] At 606, frequency power of the one or more epochs is weighted across time. For example, the power of each epoch at one or more frequencies can be normalized across time to determine appropriate frequency windows for extracting information. Such normalization can reveal low power, statistically significant shifts in power at one or more frequencies (e.g., Delta, Gamma, and the like). Additionally, each epoch can be represented by the frequency with the highest relative power over time to determine appropriate frequency windows for extracting information. Alternatively, component analysis (e.g., principle component analysis (PCA) or independent component analysis (ICA)) can be utilized after normalization to further determine appropriate frequency windows for extracting information. For example, FIGS. 37 and 38 are screen shots of component analysis utilized after

normalization to suggest filters (e.g., screen shot 3700) and express independent components throughout time (e.g., screen shot 3800). Any frequency range can be revealed and utilized for analysis.

[0085] Information can be calculated for each of the one or more epochs after appropriate frequency windows have been established (e.g., after weighting frequency). Such information can include low frequency power (e.g., Delta power), high frequency power (e.g., Gamma power), standard deviation, maximum amplitude (e.g., maximum of the absolute value of peaks) and the sort. Further calculations can be done on the information calculated for each of the one or more epochs creating information such as Gamma power/Delta power, time derivative of Delta, time derivative of Gamma power/Delta power and the like. Time derivatives can be computed over preceding and successive epochs. After calculating the information, it can then be normalized across the one or more epochs. A variety of data normalization techniques can be conducted including z-scoring and the like.

[0086] FIG. 12 is a screen shot of the exemplary whole night EEG source data shown in FIG.11 after an exemplary frequency power of the one or more epochs has been weighted across time. The higher frequency data is now more clearly visible. FIG. 13 is a screen shot of a two hour time frame of the exemplary adjusted whole night EEG source data shown in FIG.12. FIG. 14 is a screen shot of an exemplary visualization

of high (e.g., Gamma) and low (e.g., Delta) power frequency bands within the whole night EEG spectrogram shown in FIG. 12. FIG. 15 is a screen shot of a two hour and forty minutes time frame of the exemplary visualization of high and low power frequency bands shown in FIG. 14.

[0087] FIG. 16 is a screen shot of an exemplary five-dimensional parameter space visualization of the whole night EEG spectrogram of FIG. 12. The five parameters (e.g., variables) are information calculated for each of the one or more epochs after weighting frequency. FIG. 17 is a screen shot of a two hour time frame of the exemplary five-dimensional parameter space visualization of the whole night EEG visualization shown in FIG.16.

[0088] At 608, sleep states in the subject are classified based on the one or more frequency weighted epochs. For example, the one or more frequency weighted epochs can be clustered by any variety of clustering techniques including k-means clustering. The clustering can be done on information calculated from the epochs (e.g., Delta power, Gamma power, standard deviation, maximum amplitude (Gamma/Delta), time derivative of Delta, time derivative of (Gamma /Delta, and the sort). Component analysis (e.g., PCA or ICA) can be used to determine the parameter space (e.g., types of information used) in the clustering.

[0089] Subsequent to clustering, sleep state designations can be assigned to the epochs. Sleep state designated epochs can then be presented as representations of sleep states in the subject for the period of time represented by the epoch. Classification can also incorporate manually determined sleep states (e.g., manually determined "awake" versus "sleeping" sleep states). Additionally, artifact information (e.g. movement data, poor signal data, or the like) can be utilized in the classification.

[0090] *Example 8 - Exemplary Sleep State Classification Techniques*

[0091] Epochs can be classified according to the sleep states they represent. An epoch can be classified according to normalized variables (e.g., information calculated for an epoch) based on high frequency information, low frequency information, or both high and low frequency information. For example, REM sleep state epochs can have higher relative power than SWS at higher frequencies and lower relative power than SWS at lower frequencies. Similarly, SWS sleep state epochs can have lower relative power than REM at higher frequencies and higher relative power than REM at lower frequencies. Additionally, epochs initially classified as both NREM and NSWS sleep (e.g., epochs having low relative power at both higher and lower frequencies) can be classified as intermediate sleep and epochs classified as both REM and SWS sleep (e.g., epochs having high relative power at both higher

and lower frequencies) can be classified as outliers. Further, epochs initially classified as both NREM and NSWS sleep can be classified as intermediate stage I sleep and epochs initially classified as both REM and SWS sleep can be classified as intermediate stage II sleep. Additionally, sleep states can be split in the classifying to look for spindles, k-complexes, and other parts. Any group of epochs initially classified as one sleep state can be split into multiple sub-classified sleep states according to increasing levels of classification detail. For example, a group of epochs classified as SWS can be reclassified as two distinct types of SWS.

[0092] *Example 9 - Exemplary Artifact Classification Techniques*

[0093] Artifact data (e.g. movement data, poor signal data, and the like) can also be used in sleep state classification. For example, artifacts can be used to analyze whether epochs initially assigned a sleep state designation should be reassigned a new sleep state designation due to neighboring artifact data. For example, an epoch assigned a sleep state designation of REM that has a preceding movement artifact or awake epoch can be reassigned a sleep state designation of awake. Further, for example, an artifact epoch that has a succeeding SWS epoch can be reassigned a sleep state designation of SWS because there is a high likelihood that the epoch represents a large SWS sleep epoch rather than a large movement artifact which is more common during wakefulness. In

such ways, for example, artifact data can be utilized in a data smoothing technique.

[0094] *Example 10 - Exemplary Smoothing Techniques*

[0095] Any variety of data smoothing techniques can be used during the assigning of sleep states. For example, numbers (e.g., 0 and 1) can be used to represent designated sleep states. Neighboring epochs' sleep state designation numbers can then be averaged to determine if one of the epochs is inaccurately assigned a sleep state designation. For example, abrupt jumps from SWS-NSWS-SWS (and REM-NREM-REM) are rare in sleep data. Therefore, should a group of epochs be assigned sleep state designations representing abrupt jumps in sleep states, smoothing techniques can be applied to improve the accuracy of the assigning.

[0096] For example, in a scenario in which 0 represents SWS, 1 represents NSWS and the following sleep state designations existed for five neighboring epochs, 00100, then an average of the five sleep states would be 0.2. In such an instance, the middle epoch initially assigned a sleep designation of 1 (SWS) would be reassigned a sleep state designation of 0 (NSWS). The same technique could be used for REM versus NREM where a second set of sleep designations for the same five neighboring epochs is determined. For example, 1 can represent REM, 0 can represent NREM, and the following designations can exit for the five neighboring epochs, 00100. Again, the average of the five sleep states would be 0.2.

Again, the middle epoch initially assigned a designation of 1 (REM) would be reassigned a sleep state designation of 0 (NREM). Such smoothing techniques can improve the accuracy of assigning sleep state designations.

[0097] *Example 11 - Exemplary Method for Classifying Sleep States in a Subject*

[0098] FIG. 7 shows in a flowchart an exemplary method 700 for classifying sleep states in a subject. For example, the method 700 can be implemented within system 500 of FIG. 5, system 400 of FIG. 4 or within the classifying 608 of method 600.

[0099] At 702, one or more frequency weighted epochs are received. For example, frequency weighted epochs determined from the weighting 606 of method 600 can be received.

[00100] At 704, the one or more frequency weighted epochs are clustered. For example, the one or more frequency weighted epochs can be clustered by any variety of clustering techniques including k-means clustering. The clustering can be done on information calculated from the epochs (e.g., Delta power, Gamma power, standard deviation, maximum amplitude (Gamma/Delta), time derivative of Delta, time derivative of Gamma /Delta, and the sort). Exemplary visualizations of clustered sleep states are shown in FIGS. 18 and 19. FIG. 18 shows epochs clustered via Delta, Gamma/Delta, and the time derivative of Delta. In such a manner, REM-like epochs form a visual spear point shape. FIG. 19 shows epochs clustered via

Delta, Gamma/Delta, and the time derivative of (Gamma/Delta). In such a manner, SWS-like epochs form a visual spear point shape. Additional exemplary visualizations of clustered sleep states are shown in FIGS. 20 and 21, in which clustering was done using parameters (e.g., variables) derived via principle component analysis.

[00101] At 706, the one or more clustered, frequency weighted epochs are assigned sleep state designations. For example, an epoch with significant relative power at low frequency can be assigned a slow wave sleep designation and an epoch with significant relative power at high frequency can be assigned a rapid eye movement sleep designation. For example, REM sleep can have higher Gamma/Delta and a higher absolute value of the time derivative of (Gamma/Delta) compared to SWS, whereas SWS can have higher delta and a higher absolute value of the time derivative of delta than REM sleep. Further, for example, standard deviation can be used in assigning sleep state designations. It is possible for the same epoch to be assigned both a slow wave sleep designation and a rapid eye movement sleep designation. In such cases, the epoch can be reassigned a new sleep state designation of outlier or intermediate stage II sleep. Alternatively, an epoch can be assigned both a non-slow wave sleep designation and a non-rapid eye movement sleep designation. In such cases, the epoch can be reassigned a new sleep state designation of intermediate sleep or intermediate stage I sleep. For example,

when high frequency is expressed by dividing it by Delta and the parameter space Delta, Gamma/Delta, abs(derivative(Delta)), abs(derivative(Gamma/Delta)), and, optionally, standard deviation, then intermediate sleep designation can be the intersection between NREM and NSWS while outlier designation can be the intersection between REM and SWS. Alternatively, for example, if Delta alone or with standard deviation is used to determine SWS from NSWS and gamma alone or with abs(derivative(Delta)) alone or with standard deviation is used to determine REM from NREM, then intermediate stage I sleep designation can be the intersection between NREM and NSWS while intermediate stage II sleep designation can be the intersection between REM and SWS. Any variety of data smoothing techniques can be used during the assigning of sleep states. Artifact data can also be used during the assigning of sleep states.

[00102] At 708, sleep state designations are presented as indicative of sleep states for the period of time represented by the one or more epochs. The sleep states can be presented in the form of sleep statistics across time. For example, FIGS. 28, 29, 30, 31, and 32 depict presentations of sleep statistics for sleep state designated epochs as a function of time. For example in FIG. 28, a screen shot 2800 depicts sleep state density as a percentage for each sleep state type per hour during a night of electroencephalography data for a subject. In FIG. 29, a screen shot 2900 depicts average

episode length for each sleep stage across every hour. In FIG. 30, a screen shot 3000 depicts number of episodes for each sleep stage across every hour. In FIG. 31, a screen shot 3100 depicts average time intervals between successive REM sleep state intervals for each hour. In FIG. 32, a screen shot 3200 depicts stage transitions across the night.

[00103] Additionally, one or more frequency weighted epochs can be presented as canonical spectra representative of the sleep state in the subject for the period of time represented by the one or more epochs having similar sleep state designations. For example, an epoch within the middle of a group of epochs designated as having the same sleep state designations can be selected and its spectra presented as canonical spectra representative of the sleep state. Alternatively, an epoch having a weighted power closest to the average weighted power of one or more epochs having similar sleep state designations can be selected and its spectra presented as canonical spectra representative of the sleep state. For example, FIGS. 22, 23, 24, 25, and 26 are screen shots of exemplary visualizations of epochs for various sleep states in a subject (e.g., screen shot 2200 is SWS, screen shot 2300 is REM sleep, screen shot 2400 is Intermediate sleep, screen shot 2500 is awake, and screen shot 2600 is transient) based on EEG spectrogram data analysis.

[00104] Additionally, sleep state designations can be presented as a function of success versus manual scoring and quality measures can be presented (e.g., sleep state designation separation statistics including single variable and multivariable one-way ANOVAs, regression coefficients calculated for each stage for sleep densities, number of episodes, average episode length, cycle time, and the like). An exemplary visualization of presenting quality measures is shown in FIG. 27. A screen shot 2700 depicts an exemplary visualization of the degree of sleep stage separation that distinguishes representative canonical spectra of distinct sleep states. For example, independent component analysis (ICA) can be used to establish the quality of sleep stage separation in the presented sleep states by applying ICA to canonical spectra or average spectra for each sleep state presented. Any variety of classifying techniques can be used to determine the quality of initially sleep stage classification.

[00105] *Example 12 - Exemplary System for Determining a Pathological Condition of a Subject from Sleep States*

[00106] FIG. 8 shows an exemplary system 800 for determining a pathological condition of a subject from sleep states.

[00107] Electroencephalography data for a subject 802 is obtained and input into sleep state analyzer 804 to determine a pathological condition of the subject 806.

[00108] Methods for determining a pathological condition of a subject from sleep states exhibited by a subject, as determined from analyzing electroencephalography data, are described in detail below.

[00109] *Example 13 - Exemplary Computer-Implemented Method for Determining a Pathological Condition for a Subject from Sleep States*

[00110] FIG. 9 shows an exemplary computer-implemented method 900 for determining a pathological condition for a subject from sleep states. The computer-implemented method 900 can be utilized in system 800 of FIG. 8.

[00111] At 902, electroencephalography data for a subject is received. For example, electroencephalography data which exhibits lower dynamic range for power in at least one low power first frequency range in a frequency spectrum as compared to a second frequency range in the frequency spectrum can be received.

[00112] At 904, the electroencephalography data is analyzed with frequency analysis. For example, frequency analysis can be the adjusting 204 of method 200.

[00113] At 906, sleep states in the subject are assigned based on the frequency analysis. For example, method 700 for classifying sleep states of FIG. 7 can be used to assign sleep states in the subject.

[00114] At 908, a pathological condition can be detected in a subject based on the sleep states. For example, sleep states can be acquired for an individual and analyzed to determine whether the sleep states represent normal sleep or abnormal sleep. Abnormal sleep could indicate a pathological condition. For example, sleep states can be acquired from individuals with pathological conditions and analyzed for common attributes to generate an exemplary distinctive "pathological condition" sleep state profile and/or sleep state statistics representative of having the pathological condition. Such a profile or statistics can be compared to sleep states determined for a subject in order to detect whether the subject has the pathological condition or any early indicators of the pathological condition. Any variety of pathological conditions can be detected and/or analyzed. For example, sleep related pathological conditions can include epilepsy, Alzheimer's disease, depression, brain trauma, insomnia, restless leg syndrome, and sleep apnea. For example, polysomnographically, subjects with Alzheimer's can show decreased rapid eye movement sleep in proportion to the extent of their dementia.

[00115] *Example 14 - Exemplary System for Dynamically Determining Customized Sleep Scores for a Subject*

[00116] FIG. 10 shows an exemplary system for dynamically determining customized sleep scores for a subject.

[00117] A data collector 1002 can obtain electroencephalography data for a subject from a period of sleep.

[00118] A data normalizer 1004 can assess the electroencephalography data to determine low power frequency information.

[00119] A data presenter 1006 can present sleep states for the subject based at least on the low power frequency information.

[00120] Methods for dynamically determining customized sleep scores for a subject are described herein, including method 500 of FIG. 5, method 600 of FIG. 6, and method 700 of FIG. 7.

[00121] *Example 15 - Exemplary Pathological Conditions*

[00122] In any of the technologies described herein, a variety of pathological conditions can be determined from source data obtained for a subject. For example, depression, brain trauma, epilepsy, and Alzheimer's disease can be pathological conditions determined from sleep states determined from source data obtained for a subject. For example, FIG. 39 is a screenshot 3900 of an application of the technologies described herein to determine sleep states indicative of characterizations of Alzheimer's disease from a whole night EEG from a human subject with Alzheimer's.

[00123] *Example 16 - Exemplary Medications and Chemicals that can Affect Sleep*

[00124] In any of the technologies described herein, the effect of medications and chemicals on sleep states of a subject can be determined via analyzing source data obtained for a subject. For example, sleep states can be modified by alcohol, nicotine, and cocaine use. Exemplary medications that affect sleep include steroids, theophylline, decongestants, benzodiazepines, antidepressants, monoamine oxidase inhibitors (e.g., Pheneizine and Moclobemide), selective serotonin reuptake inhibitors (e.g., Fluoxetine (distributed under the Prozac® name) and Sertralie (distributed under the Zoloft® name), thyroxine, oral contraceptive pills, antihypertensives, antihistamines, neuroleptics, amphetamines, barbiturates, anesthetics, and the like.

[00125] *Example 17 - Exemplary Sleep Statistics*

[00126] In any of the technologies described herein, any variety of statistics can be generated from adjusted source data. For example, sleep statistics can be generated from adjusted source EEG data that has been classified into sleep states. Exemplary sleep statistics can include information including sleep stage densities, number of sleep stage episodes, sleep stage average duration, cycle time, interval time between sleep stages, sleep stage separation statistics, onset of sleep, rapid eye movement sleep latency, regression

coefficients of trends, measures of statistical significance of trends, and the like.

[00127] *Example 18 - Exemplary Implementation of a Method of Determining Sleep States in a Subject over a Period of Time*

[00128] Sleep is common and may be ubiquitous in all major taxa of the animal kingdom, but it is poorly understood. There is growing evidence from human studies from a variety of low-level psychophysical perceptual and motor tasks that sleep helps to remediate performance loss that is otherwise observed following task learning (Karni et al. 1994; Mednick et al. 2002; Mednick et at. 2003; Fenn et al. 2003). Animal studies have provided evidence of 'replay' during sleep, which may be a central component of the sleep process involved in consolidation of performance.

[00129] Recently, it has been shown that during sleep, robustus archistriatalis (RA) neurons of the zebra finch, Taeniopygia guttata, song system rehearse song patterns spontaneously and respond to playback of the bird's own song (Dave & Margoliash, 2000). During song development in zebra finches, juvenile birds start changing singing patterns the day following exposure to new vocal material from tutors (Tchernichovski et al. 2001). There is no conclusive evidence though that song learning in juveniles or song maintenance in adult birds requires or benefits from sleep.

[00130] Investigation of the possible role of sleep in song learning or maintenance is hampered by the limited knowledge of sleep states in passerine birds. Previous studies have not reported different phases of sleep in the zebra finch (Nick & Konishi, 2002; Hahnloser et al., 2002). In contrast, studies in other birds, including passerine birds (Ayala-Guerrero et al., 1988; Szymczak et al., 1993; Rattenborg et al., 2004), have reported REM sleep in this phylum. Moreover, in rat hippocampus different patterns of neuronal replay are known to take place during different phases of sleep (Buzsaki, 1989; Wilson & McNaughton, 1994; Louie & Wilson, 2001). Therefore, staging of sleep in zebra finches was investigated.

[00131] In order to determine the type, arrangement and location of electrodes, a series of acute experiments with birds anesthetized with urethane (20%, circa 90 1.11 over I hr) was first conducted. Optimal EEG recordings, as judged by amplitude and reliability of signals, were obtained using differentially paired thick platinum electrodes (A-M systems, WA) touching the dura mater, with an additional ground over the cerebellum. The stereotaxic coordinates for the recording and ground electrodes were respectively: (1.5R, 3L), (3R, 2L) and (0.5C, OL).

[00132] Five birds were then anesthetized and implanted with 3 mm long L-shaped platinum electrodes at the aforementioned locations with the last 2 mm of the electrodes tangential to the dura mater along the medial-lateral axis. The electrode impedance was 0.15 Ohms. In order to assess unihemispheric sleep, three birds were implanted with bilateral EEG electrodes. Electrodes were secured at their base with dental acrylic and attached with fine copper wire (A-M systems, WA) to a head connector. Birds were given 3 days to recover from the surgery and to habituate to the recording environment.

[00133] During recordings, a light cable was attached linking the bird's head to an overhead mercury commutator (Drangonfly Inc, WV). This setup allowed the bird relative freedom of movement within the cage and is preferable to restraining the animal since restraint-induced stress is known to modify sleep architecture (Altman et al., 1972). During the dark phase of the 16:8 light/dark cycle, electrophysiological recordings with direct observation of sleeping birds were combined. Birds were bathed in infrared (IR) light and monitored with an IR camera (Ikegama, Japan). Strategically placed mirrors facilitated detection of eye, head, and body movements. EEGs were amplified by 1K, sampled at 1 kHz and filtered at 1-100 Hz. In one bird, which exhibited low frequency artifacts, the data was filtered at 2-100 Hz. A 60Hz notch filter was also used to improve the signal-to-noise ratio.

[00134] In order to establish high confidence in the data analysis, the data was scored both manually as well as automatically. Manual scoring relied on visual inspection of 3 seconds EEG epochs in parallel with scoring of overt behaviors such as eye, head and body movements. Manual scoring classified each epoch as either REM, NREM (non-REM) or awake, including the artifacts. Automated scoring was restricted to the sleep data. The Sleep Parametric EEG Automated Recognition System (SPEARS) for stage separation and quantification of single channel EEG data was used. EEGs were downsampled to 200 Hz, DC filtered, and analyzed over 3 seconds epochs using a 1 second sliding window to combine high spectral, temporal and statistical resolutions. In order to minimize spectral leakage and to increase statistical resolution in the frequency domain, EEG power spectra were computed over 2 orthogonal tapers following a standard multi-taper estimation technique (Thomson, 1982).

[00135] The 1-4 Hz (Delta) and 30-55 Hz (Gamma) frequency bands were selected for the stage classification. Delta and Gamma/Delta were respectively used to separate SWS from NSWS (Non-SWS) and REM from NREM. The separation was done with a k-means clustering algorithm and refined by the inclusion of additional variables: the standard deviation and the absolute values of the time derivative of Delta and of (Gamma/Delta). For each epoch, the time derivative was computed over the preceding and successive epochs, using the Matlab "gradient"

function. The initial separation was done over the artifact free sleep data. Thereafter, sleep artifacts were attributed the same score as the first non-artifact epoch immediately following it, unless it was an awake epoch in which case the sleep artifact was given the score of the first preceding artifact free epoch (which could not be an awake epoch for otherwise the artifact would have been labeled as an awake artifact by manual scoring). This convention did not significantly reduce the agreement rate with manual scoring (TABLE 1). It was important to include the sleep artifacts since removing or not scoring them would respectively shrink or puncture sleep episodes and thereby change the calculated density, average number of epochs and length for each stage.

[00136] Following initial separation, the score of each epoch was smoothed using a 5 second window in order to minimize the score contamination by brief artifacts which might not have been isolated by manual scoring. Epochs that were scored neither as REM nor as SWS were labeled as intermediate (INTER). Conversely, any epoch that had been labeled as belonging to both REM and SWS was relabeled as an outlier. There were very few outliers in the data (TABLE 1).

[00137] The REM, SWS and intermediate epochs can be visualized in a 3-dimensional space (FIGS. 20-21) defined by the principal components of the 5 dimensional space defined by Delta, Gamma/Delta, the standard deviation and the derivatives of Delta and (Gamma/Delta) (FIGS. 16-17). In each bird, a

multivariate ANOVA on the 5-dimensional clustering space yielded a $P < 0.001$ for the separation of REM, SWS and the intermediate stage.

[00138] Using the MATLAB "silhouette" function, the most representative examples for the SWS, REM, intermediate and awake epochs were automatically generated (FIGS. 22, 23, 24, 25, and 26).

[00139] The agreement between manual and automated scoring was calculated by classifying each epoch scored as REM by only the manual or the automated scoring as an error. The general agreement rate was remarkably high given the high temporal resolution of the manual and automated scoring (TABLE 1).

[00140] Based on the automated analysis, the stage density (FIG. 28), average episode number (FIG. 30) and duration (FIG. 29), inter REM interval (FIG. 31) and stage transitions (FIG. 32) were computed (TABLE 1). All analyses were conducted in Matlab (MathWorks Inc, MA).

[00141] Table 1. Stage statistics for 5 nights of sleep in 5 birds.

[00142] Stage density, average episode duration and number and stage transitions were determined. The percentage of transitions out of each stage towards the intermediate stage and the percentage of transitions out of the intermediate stage towards the other stages are shown. For the bihemispherically implanted birds (Animals 1-3), unihemispheric sleep is reported and the other statistics were

computed over the hemisphere with the most reliable data as determined by visual inspection of the EEG and video and the absence of outliers. The coefficient of regression was computed over the stage densities and inter-REM intervals for each hour and reflect the circadian distribution of SWS and REM (* = [r^2> 0.5 and p < 0.05], § = [r^2 > 0.5 and p = 0.05), £ for values calculated for hours 2-8, ε for values calculated for hours 1-7). The agreement rate between automated and manual scoring was determined with and without artifact rejection.

TABLE 1	Animal 1	Animal 2	Animal 3	Animal 4	Animal 5
Stage Density (%)					
SWS	44.44	30.14	41.03	25.71	36.59
INTER	30.96	30.34	37.46	31.70	37.49
REM	21.06	30.51	15.79	30.77	15.12
AWAKE	3.54	8.94	5.73	11.83	10.80
UNIHEM	0.09	0.59	0.65	N/A	N/A
OUTLIER	0.00	0.08	0.00	0.00	0.00
Average Episode Duration (sec)					
SWS	14.11	12.54	10.84	10.90	9.11
INTER	5.95	6.05	6.67	8.07	6.62
REM	9.84	10.11	8.53	16.98	9.21
AWAKE	11.37	12.10	9.30	16.11	12.02
UNIHEM	3.38	3.84	3.19	N/A	N/A
OUTLIER	N/A	2.22	N/A	N/A	N/A
Number of Episodes					
SWS	835	704	1092	629	1073
INTER	1378	1482	1623	1137	1601
REM	599	853	541	572	557
AWAKE	85	113	159	65	100
UNIHEM	8	44	59	N/A	N/A
OUTLIER	0	9	0	0	0
Transitions					
SWS-INTER (% SWS)	97.57	88.54	95.21	93.93	97.05
REM-INTER (% REM)	85.49	90.34	86.06	92.64	83.75
AWAKE-INTER (% AWAKE)	60.49	71.94	72.15	27.79	64.16
OUT-INTER (% OUT)	N/A	25.00	N/A	N/A	N/A
INTER-SWS (% INTER)	56.57	43.06	63.23	51.31	66.49
INTER-REM (% INTER)	38.55	49.33	29.52	43.72	26.78
INTER-AWAKE (% INTER)	4.88	7.61	7.25	4.97	6.73
INTER-OUT (% INTER)	N/A	0.00	N/A	N/A	N/A
Regression coefficients					
Stage Density per hour					
SWS	-6.20	-1.11	0.10	-5.46	-2.94
INTER	1.57	1.93	-0.29	4.21	4.09
REM	4.89	3.16	2.44	8.08	4.77
AWAKE	-0.25	-3.99	-2.25	-6.83	-5.92
OUTLIER	N/A	0.01	N/A	N/A	N/A
Average Episode Duration per hour					
SWS	-1.44	-0.37	0.59	-6.08	-1.11
INTER	0.05	0.24	0.21	1.37	0.31
REM	0.90	0.80	1.06	2.77	0.53
AWAKE	-0.74	-0.89	-0.21	-6.34	-0.92
OUTLIER	N/A	N/A	N/A	N/A	N/A
Number of Episodes per hour					
SWS	-3.93	-1.07	-6.13	-3.61	0.82
INTER	8.00	5.29	-8.11	2.93	14.46
REM	13.82	5.68	2.01	6.93	16.21
AWAKE	-0.29	-1.54	-6.05	0.18	-1.61
OUTLIER	N/A	-0.04	N/A	N/A	N/A
Inter-REM-interval per hour	-7.56	-2.66	-2.27	-0.75	-13.10
Cycle Time per hour	10.45	21.50	4.88	93.51	1.45
Agreement Rate (%)	89.94	76.75	90.52	73.23	88.44
Agreement Rate - No artifacts (%)	90.08	76.93	91.52	73.91	88.28

[00143] The analysis of the recordings indicate that zebra finches exhibit at least three distinct phases of sleep: SWS, REM and intermediate sleep. SWS had a high amplitude EEG signal with significant power in the Delta range (FIGS.14-17). REM was characterized by a very low amplitude "awake-like" EEG signal (FIG. 23), typically about ±30 μV with higher power in Gamma (FIGS. 14 and 15) than NREM, a feature that up to now had only been detected in mammals (Maloney et al., 1997; Cantero et al., 2004). The intermediate epochs had highly variable amplitudes, centered around ±50 μV and did not have significant power in either the Delta or Gamma ranges (FIGS. 14, 15 and 24). The intermediate stage has previously only been observed in mammals (Gottesmann et al., 1984; Glin et al., 1991; Kirov & Moyanova, 2002). Both birds on normal circadian patterns and shifted circadian schedules displayed these three sleep stages.

[00144] SWS epochs were longer than REM and intermediate episodes early in the night and would, following a mammalian-like distribution, decrease in duration (FIG. 29) throughout the night, leading to an overall decrease in stage density (FIG. 28) (TABLE 1).

[00145] During NREM birds breathe slowly and regularly; eye and head movements do not follow a stereotypical pattern and are quite distinct from those in REM. We observed several instances when one eye was open and the other was closed. The hemisphere contralateral to the open eye displayed a low

amplitude and high frequency EEG while the hemisphere contralateral to the closed eye displayed SWS oscillations. These instances of unihemispheric sleep would usually account for less than 5% of the dark cycle (TABLE 1) and were more frequent in the light cycle. Such patterns of unihemispheric sleep have been previously detected in other species of birds, cetaceans and other marine mammals (Mukhametov et al., 1984; Mukhametov, 1987; Szymczak et al., 1996; Rattenborg et al., 1999; Lyamin et al., 2002).

[00146] REM episodes were typically brief early in the night and would become longer throughout the night (FIG. 29) as the number of episodes would increase as well (FIG. 30), leading the Inter-REM intervals to exhibit a downward "mammalian-like" trend throughout the night (FIG. 31) (TABLE 1). REM occurred reliably in conjunction with eye and subtle twitching head movements, as seen in other species (Siegel et al., 1999). The eye movements were on the order of one saccade per second. The head movements were not as reliable, but tended to follow the directional movement of the eyes when present. Head movements were not the result of displacement of the head by the weight of the attached cable during REM neck muscle atonia because the head movements were observed in conjunction with eye movements in intact, un-tethered animals.

[00147] The intermediate epochs were brief and numerous. The intermediate state was usually more stable throughout the night, in term of density (FIG. 28), average epoch duration (FIG. 29) and average number of episodes per hour (FIG.30) than REM and SWS. As is the case in mammals, the intermediate stage consistently acted as -but was not limited to- a transition phase between SWS and REM (FIG. 32) (TABLE 1).

[00148] In all birds, large peak-to-peak EEG transients lasting approximately 500 milliseconds were detected in NREM (FIG. 26). These signals are reminiscent of the description of mammalian K-complexes (Rowan & Tolunsky, 2003). K-complexes have likely never been previously observed in a non-mammalian species.

[00149] In previous studies of zebra finch sleep EEG, only SWS has been reported. In addition to finding a suitable location over which to implant EEG electrodes, this study was successful in detecting NSWS (REM and the intermediate stage) presumably because the nature of the chronic recording setup did not restrain the animals and obviated the need of pharmacological agents such as melatonin to induce sleep. In one study (Mintz et al., 1998), infusion of melatonin was shown to induce SWS in pigeons. It is possible that melatonin might have a similar effect in zebra finches, thus reducing the amount of observable NSWS at night (Hahnloser et al. 2002).

[00150] The data analysis technique enabled resolving changes in power at the lower power, high frequencies, which was a key differentiating factor for REM sleep detection. Moreover, the automated analysis restricted manual scoring to the awake state and artifacts, which are easily detectable to a human scorer. Additionally, automated EEG scoring relied on whole night statistics (Gervasoni et al.) rather than on arbitrarily defined threshold, maximum likelihood methods or supervised nonlinear classifiers all of which tend to reflect and impose a human bias on the data analysis.

[00151] The results imply that mammalian-like sleep features have evolved in parallel in both mammals and birds. The basic pattern of interdigitation between Delta and Gamma power activation described herein (FIGS. 14 and 15) is highly similar to the one observed in the mammalian cortex during sleep (Destexhe, Contreras & Steriade, 1999). Furthermore, some of the signals we have observed have been specifically attributed to the mammalian cortex (Amzica & Steriade, 1998). Birds are however devoid of a large laminar cortex, raising the possibility that the cortex might be at best sufficient but not necessary for the development of mammalian-like sleep features. Conversely, it is conceivable that birds do indeed possess a mammalian cortex homolog in a non-laminar form (Karten, 1997). Future work at the cellular and molecular levels will be needed to assess which of these highly intriguing possibilities proves to be correct.

[00152] References cited:

[00153] Altman et al. Psychon. Sci. 26 (1972), pp. 152-154. Amzica & Steriade. Neuroscience. 1998 Feb;82(3):671-86. Ayala-Guerrero et al. Physiol Behav. 1988;43(5):585-9. Buzsaki. Neuroscience. 1989;31(3):551-70.

[00154] Cantero et al. Neuroimage. 2004 Jul;22(3):1271-80.

[00155] Dave & Margoliash. Science. 2000 Oct 27;290(5492):812-6. Destexhe, Contreras & Steriade. 1999 Jun 1;19(11):4595-608. Fenn et al. Nature. 2003 Oct 9;425(6958):614-6. Gervasoni et al. J Neurosci. 2004 Dec 8;24(49):11137-47. Glin et al. Physiol Behav. 1991 Nov;50(5):951-3. Gottesmann et al. J Physiol (Paris). 1984;79(5):365-72.

[00156] Hahnloser et al. Nature. 2002 Scp 5;419(6902):65-70. Karni et al. Science. 1994 Jul 29; 265(5172):679-682

[00157] Karten. Proc Natl Acad Sci U S A. 1997 Apr 1;94(7):2800-4. Khazipov et al. Society for Neuroscience Abstracts 2004. Kirov & Moyanova. Neurosci Lett. 2002 Apr 5;322(2):134-6. Louie & Wilson. Neuron. 2001 Jan;29(1):145-56. Lyamin et al. Behav Brain Res. 2002 Feb 1;129(1-2):125-9 Maloney et al. Neuroscience. 1997 Jan;76(2):541-55. Mednick et al. Nat Neurosci. 2002 Jul;5(7):677-81 Mednick et al. Nat Neurosci. 2003 Jul;6(7):697-8. Mintz et al. Neurosci Lett. 1998 Dec 18;258(2):61-4.

[00158] Mukhametov et al. Zh Vyssh New Deiat Im I P Pavlova. 1984 Mar-Apr;34(2):259-64.

[00159] Mukhametov. Neurosci Lett. 1987 Aug 18;79(1-2):128-32.

[00160] Nick & Konishi. Proc Natl Acad Sci U S A. 2001 Nov 20;98(24):14012-6.

[00161] Rattenborg et al. Behav Brain Res. 1999 Nov 15;105(2):163-72. Rattenborg et al. PLoS Biol. 2004 Jul;2(7):E212.

[00162] Rowan & Tolusnky. "Primer of EEG". Butterworth Heinemann. Elsevier Science 2003

[00163] Siegel et al. Neuroscience. 1999;91(1):391-400.

[00164] Szymczak et al. Physiol Behav. 1993 Jun;53(6):1201-10. Szymczak et al. Physiol Behav. 1996 Oct;60(4):1115-20. Tchernichovski et al. Science. 2001 Mar 30;291(5513):2564-9. Thomson, Proceedings of the IEEE, Vol. 70 (1982), pp. 1055-1096. Wilson & McNaughton. Science. 1993 Aug 20;261(5124):1055-8

[00165]

[00166] *Example 19- Exemplary Method for Determining Sleep States in a Subject over a Period of Time*

[00167] FIG. 35 shows yet another exemplary method 3500 for determining sleep states in a subject over a period of time. The method 3500 incorporates a wide variety of techniques described herein.

[00168] *Example 20 - Exemplary Transformation Techniques*

[00169] There are a wide variety of data transformation methods used in signal processing to determine power for a variety of frequencies in time series data. As described herein, transformation methods can include multi-taper transform, Fourier transform, wavelet transform. Any other transformation method for measuring power for a variety of frequencies represented in a plurality of time series or epochs in a source signal can be used.

[00170] *Example 21 - Exemplary Computational Methods for Differentiating Groups of Data*

[00171] There are a wide variety of clustering and classification methods used in computational signal processing to differentiate data into distinct classes. As described herein, the clustering method used is k-means clustering but any computational signal processing method for differentiating groups of data could be used. Similarly, classification methods such as component analysis (e.g., principle and independent component analysis) are used as described herein.

[00172] An overview of computational methods is provided below.

[00173] Clustering (or cluster analysis) is unsupervised learning where the classes are unknown a priori and the goal is to discover these classes from data. For example, the identification of new tumor classes using gene expression profiles is a form of unsupervised learning.

[00174] Classification (or class prediction) is a supervised learning method where the classes are predefined and the goal is to understand the basis for the classification from a set of labeled objects and build a predictor for future unlabeled observations. For example, the classification of malignancies into known classes is a form of supervised learning.

[00175] CLUSTERING:

[00176] Clustering involves several distinct steps:

[00177] Defusing a suitable distance between objects

[00178] Selecting a applying a clustering algorithm.

[00179] Clustering procedures commonly fall into two categories: hierarchical methods and partitioning methods. Hierarchical methods can be either divisive (top-down) or agglomerative (bottom-up). Hierarchical clustering methods produce a tree or dendrogram. Hierarchical methods provide a hierarchy of clusters, from the smallest, where all objects are in one cluster, through to the largest set, where each observation is in its own cluster

[00180] Partitioning methods usually require the specification of the number of clusters. Then, a mechanism for apportioning objects to clusters must be determined. These methods partition the data into a prespecified number k of mutually exclusive and exhaustive groups. The method iteratively reallocates the observations to clusters until some criterion is met (e.g. minimize within-cluster sumsof-squares). Examples of partitioning methods include k-means clustering, Partitioning around medoids (PAM), self organizing maps (SOM), and model-based clustering.

[00181] Most methods used in practice are agglomerative hierarchical methods, in a large part due to the availability of efficient exact algorithms. However both clustering methods have their advantages and disadvantages. Hierarchical advantages include fast computation, at least for agglomerative clustering, and disadvantages include that they are rigid and cannot be corrected later for erroneous

decisions made earlier in the method. Partitioning advantages include that such methods can provide clusters that (approximately) satisfy an optimality criterion, and disadvantages include that one needs an initial k and the methods can take long computation time.

[00182] In summary, clustering is a more difficult problem than classifying for a variety of reasons including the following:

[00183] there is no learning set of labeled observations

[00184] the number of groups is usually unknown

[00185] implicitly, one must have already selected both the relevant features and distance measures used in clustering methods.

[00186] CLASSIFICATION:

[00187] Techniques involving statistics, machine learning, and psychometrics can be used. Examples of classifiers include logistic regression, discriminant analysis (linear and quadratic), principle component analysis (PCA), nearest neighbor classifiers (k-nearest neighbor), classification and regression trees (CART), prediction analysis for microarrays, neural networks and multinomial log-linear models, support vector machines, aggregated classifiers (bagging, boosting, forests), and evolutionary algorithms.

[00188] Logistic regression:

[00189] Logistic regression is a variation of linear regression which is used when the dependent (response)

variable is a dichotomous variable (i.e., it takes only two values, which usually represent the occurrence or non-occurrence of some outcome event, usually coded as 0 or 1) and the independent (input) variables are continuous, categorical, or both. For example, in a medical study, the patient survives or dies, or a clinical sample is positive or negative for a certain viral antibody.

[00190] Unlike ordinary regression, logistic regression does not directly model a dependent variable as a linear combination of dependent variables, nor does it assume that the dependent variable is normally distributed. Logistic regression instead models a function of the probability of event occurrence as a linear combination of the explanatory variables. For logistic regression, the function relating the probabilities to the explanatory variables in this way is the logistic function, which has a sigmoid or S shape when plotted against the values of the linear combination of the explanatory variables.

[00191] Logistic regression is used in classification by fitting the logistic regression model to data and classifying the various explanatory variable patterns based on their fitted probabilities. Classifications of subsequent data are then based on their covariate patterns and estimated probabilities.

[00192] Discriminant analysis:

[00193] In summary discriminant analysis represents samples as points in space and then classifies the points. Linear discriminant analysis (LDA) fmds an optimal plane surface that best separates points that belong to two classes. Quadratic discriminant analysis (QDA) fmds an optimal curved (quadratic) surface instead. Both methods seek to minimize some form of classification error.

[00194] Fisher linear discriminant analysis (FLDA or LDA):

[00195] LDA fmds linear combinations (discriminant variables) of data with large ratios of between-groups to within-groups sums of squares and predicts the class of an observation x by the class whose mean vector is closest to x in terms of the discriminant variables. Advantages of LDA include that it is simple and intuitive where the predicted class of a test case is the class with the closest mean and it is easy to implement with a good performance in practice. Disadvantages of LDA include the following:

[00196] linear discriminant boundaries may not be flexible enough

[00197] features may have different distributions within classes

[00198] in the case of too many features, performance may degrade rapidly due to over parameterization and high variance of parameter estimates.

[00199] Nearest neighbor classifiers:

[00200] Nearest neighbor methods are based on a measure of distance between observations, such as the Euclidean distance or one minus the correlation between two data sets. K-nearest neighbor classifiers work by classifying an observation x as follows:

[00201] - find the k observations in the learning set that are closest to x.

[00202] - predict the class of x by majority vote, i.e., choose the class that is most common among these k neighbors. Simple classifiers with k=1 can generally be quite successful. A large number of irrelevant or noise variables with little or no relevance can substantially degrade the performance of a nearest neighbor classifier.

[00203] Classification trees:

[00204] Classification trees can be used, fir example, to split a sample into two sub-samples according to some rule (feature variable threshold). Each sub-sample can be further split, and so on. Binary tree structured classifiers are constructed by repeated splits of subsets (nodes) into two descendant subsets. Each terminal subset of the tree is assigned a class label and the resulting partition corresponds to the classifier. The three main aspects of tree construction include selection of splits (at each node, the split that maximize the decrease in impurity is chosen), decision to declare a node terminal or to continue splitting (to grow a

large tree, the tree is selectively pruned upwards getting a decreasing sequence of subtrees), and assignment of each terminal node to a class (the class the minimizes the resubstitution estimate of the misclassification probability is chosen for each terminal node).

[00205] Prediction analysis for microarrays:

[00206] These methods utilize nearest shrunken centroid methodology. First, a standardized centroid for each class is computed. Then each class centroid is shrunk toward the overall centroid for all classes by the so-called threshold (chosen by the user). Shrinkage consists of moving the centroid towards zero by threshold, setting it equal to zero if it hits zero.

[00207] Artificial Neural Networks :

[00208] The key element of the artificial neural network (ANN) model is the novel structure of the information processing system. It is composed of many highly interconnected processing elements that are analogous to neurons and are tied together with weighted connections that are analogous to synapses. As with all classification methods, once the ANN is trained on known samples, it will be able to predict samples automatically.

[00209] Support Vector Machines:

[00210] Support Vector Machines are learning machines that can perform binary classification (pattern recognition) and real valued function approximation (regression estimation)

tasks. Support Vector Machines non-linearly map their n-dimensional input space into a higher dimensional feature space. In this high dimensional feature space a linear classifier is constructed.

[00211] Aggregating classifiers:

[00212] This method works by aggregating predictors built from perturbed versions of a learning set. In classification, the multiple versions of the predictor are aggregated by voting. Bootstrapping is the simplest form of bagging in which perturbed learning sets of the same size as the original learning set are non-parametric bootstrap replicates of the learning set, i.e., drawn at random with replacement from the learning set. Parametric bootstrapping involves perturbed learning sets that are generated according to a mixture of multivariate Gaussian distributions. Random Foresting is a combination of tree classifiers (or other), where each tree depends on the value of a random vector for all trees in the forest. In boosting, classifiers are constructed on weighted version the training set, which are dependent on previous classification results. Initially, all objects have equal weights, and the first classifier is constructed on this data set. Then, weights are changed according to the performance of the classifier. Erroneously classified objects get larger weights, and the next classifier is boosted on the reweighted training set. In this way, a sequence of training sets and classifiers is obtained, which is then combined by simple

majority voting or by weighted majority voting in the decision.

[00213] *Example 22 - Exemplary Sleep Data Presenter*

[00214] In any of the examples herein, an electronic or paper-based report based on sleep state data can be presented. Such reports can include customized sleep state information, sleep state statistics, pathological conditions, medication and/or chemical effects on sleep, and the like for a subject. Recommendations for screening tests, behavioral changes, and the like can also be presented. Although particular sleep data and low frequency information results are shown in some examples, other sleep data presenters and visualizations of data can be used.

[00215] *Example 23 - Exemplary Sleep State Information for Subjects*

[00216] Exemplary sleep state information can be obtained from a variety of subjects using any of the technologies described herein. FIG. 33 includes a screenshot 3300 of an exemplary visualization of classified anesthesized states of an anesthetized cat based on analyzed EEG spectrogram data. For example, in screenshot 3300, a SWS classification corresponds to a deep anesthesized state, a REM sleep classification corresponds to a light a:nesthesized state, and an INTER sleep classification corresponds to an intermediate anesthesized state. In such a manner, the technologies described herein can be utilized to determine anesthesized

states in a human or other mammalian subject. FIG. 34 includes a screenshot 3400 of an exemplary visualization of classified sleep states of a human subject based on analyzed EEG spectrogram data.

[00217] *Example 24 - Exemplary Advantages and Applications of Technologies*

[00218] The speed at which this data analysis can be performed, the customized and unsupervised nature of analysis, and the ability to extract previously disregarded or unanalyzed low power frequency information make this methodology particularly attractive to a variety of fields of study. The technology can be highly adaptable using a variable number of states, a variable number of identification rules, adaptable calibration, variable time resolution, and variable spectral resolution. Adjusting source data to generate adjusted source data can be especially applicable to analyzing animal signal data in testing for pathological conditions and medication and chemical effects. In any of the examples herein, low amplitude but highly variable frequency data can be extracted and analyzed (e.g., discovering temporal patterns in data). Applications can include diverse uses from analyzing stock market data (e.g., analyzing fluctuations in penny stocks to determine common variability otherwise disregarded due to small price changes) to accessing encoded data (e.g., Morse code data stored in low power, very high or very low frequencies within sound waves) to analyzing visual images

with several spatial frequencies. Similarly, the technologies described herein can be used to determine customized sleep quality determinations for a subject via sleep state information generated.

[00219] In any of the examples herein, the methods can be applied to source data received from one channel or multiple channels. The methods can be applied independently to source data from multiple channels with comparison made between the channels. For example, unihemispheric sleep can be determined from independent EEG channel data received from each hemisphere of a brain. FIG. 40 shows a screen shot 4000 of unihernispheric sleep determined from independent EEG channel data received from each hemisphere of a bird's brain. Alternatively, the methods can be simultaneously applied to source data from multiple channels, thereby analyzing combined multiple channel source data. For example, EEG channel data and EMG channel data for a subject can be simultaneously analyzed to determine awake versus REM sleep states whereby a REM designated sleep state from analysis of EEG data can be reassigned as an awake sleep state if the EMG data falls into a high amplitude cluster.

[00220] Further, in any of the examples herein, methods such as denoising source separation (dss) and the like can be used in combination with the methods described herein to determine sleep states. For example, dss can use low frequency information to determine REM sleep.

[00221] While the techniques described herein can be particularily valuable for analyzing low power frequency information they can also be applied to clustering and determining sleep stages from any variety of signals including signals wherein the high and low frequencies have the same power distributions. Additionally, techniques pertaining to spectrogram analysis, stage classification and confidence measures can be used independently of one another.

[00222] *Example 25 - Exemplary Visualizations of Data*

[00223] In any of the techniques described herein, exemplary visualizations of data can utilize colors to depict different aspects of that data. For example, classified data (e.g., sleep state classifications such as REM, SWS, and INTER) can be color coded for each classification state for visualization of the classified data. Alternatively, greyscale can be used to code for each classification state for visualization of the classified data.

[00224] *Example 26 - Exemplary Computer System for Conducting Analysis*

[00225] FIG. 36 and the following discussion provide a brief, general description of a suitable computing environment for the software (for example, computer programs) described above. The methods described above can be implemented in computer-executable instructions (for example, organized in program modules). The program modules can include the routines, programs, objects, components, and data structures

that perform the tasks and implement the data types for implementing the techniques described above.

[00226] While FIG. 36 shows a typical configuration of a desktop computer, the technologies may be implemented in other computer system configurations, including multiprocessor systems, microprocessor-based or programmable consumer electronics, minicomputers, mainframe computers, and the like. The technologies may also be used in distributed computing environments where tasks are performed in parallel by processing devices to enhance performance. For example, tasks can be performed simultaneously on multiple computers, multiple processors in a single computer, or both. In a distributed computing environment, program modules may be located in both local and remote memory storage devices. For example, code can be stored on a local machine/server for access through the Internet, whereby data from assays can be uploaded and processed by the local machine/server and the results provided for printing and/or downloading.

[00227] The computer system shown in FIG. 36 is suitable for implementing the technologies described herein and includes a computer 3620, with a processing unit 3621, a system memory 3622, and a system bus 3623 that interconnects various system components, including the system memory to the processing unit 3621. The system bus may comprise any of several types of bus structures including a memory bus or memory controller, a peripheral bus, and a local bus using a bus architecture. The

system memory includes read only memory (ROM) 3624 and random access memory (RAM) 3625. A nonvolatile system (for example, BIOS) can be stored in ROM 3624 and contains the basic routines for transferring information between elements within the personal computer 3620, such as during start-up. The personal computer 3620 can further include a hard disk drive 3627, a magnetic disk drive 3628, for example, to read from or write to a removable disk 3629, and an optical disk drive 3630, for example, for reading a CD-ROM disk 3631 or to read from or write to other optical media. The hard disk drive 3627, magnetic disk drive 3628, and optical disk 3630 are connected to the system bus 3623 by a hard disk drive interface 3632, a magnetic disk drive interface 3633, and an optical drive interface 3634, respectively. The drives and their associated computer-readable media provide nonvolatile storage of data, data structures, computer-executable instructions (including program code such as dynamic link libraries and executable files), and the like for the personal computer 3620. Although the description of computer-readable media above refers to a hard disk, a removable magnetic disk, and a CD, it can also include other types of media that are readable by a computer, such as magnetic cassettes, flash memory cards, DVDs, and the like.

[00228] A number of program modules may be stored in the drives and RAM 3625, including an operating system 3635, one or more application programs 3636, other program modules 3637, and program data 3638. A user may enter commands and information into the personal computer 3620 through a keyboard 3640 and pointing device, such as a mouse 3642. Other input devices (not shown) may include a microphone, joystick, game pad, satellite dish, scanner, or the like. These and other input devices are often connected to the processing unit 3621 through a serial port interface 3646 that is coupled to the system bus, but may be connected by other interfaces, such as a parallel port, game port, or a universal serial bus (USB). A monitor 3647 or other type of display device is also connected to the system bus 3623 via an interface, such as a display controller or video adapter 3648. In addition to the monitor, personal computers typically include other peripheral output devices (not shown), such as speakers and printers.

[00229] The above computer system is provided merely as an example. The technologies can be implemented in a wide variety of other configurations. Further, a wide variety of approaches for collecting and analyzing source data are possible. For example, the data can be collected and analyzed, and the results presented on different computer systems as appropriate. In addition, various software aspects can be implemented in hardware, and vice versa. Further, paper-based approaches to the technologies are possible, including, for

example, purely paper-based approaches that utilize instructions for interpretation of algorithms, as well as partially paper-based approaches that utilize scanning technologies and data analysis software.

[00230] *Example 27 - Exemplary Computer-Implemented Methods*

[00231] Any of the computer-implemented methods described herein can be performed by software executed by software in an automated system (for example, a computer system). Fully-automatic (for example, without human intervention) or semi-automatic operation (for example, computer processing assisted by human intervention) can be supported. User intervention may be desired in some cases, such as to adjust parameters or consider results.

[00232] Such software can be stored on one or more computer-readable media comprising computer-executable instructions for performing the described actions. Such media can be tangible (e.g., physical) media.

[00233] Having illustrated and described the principles of the invention in exemplary embodiments, it should be apparent to those skilled in the art that the described examples are illustrative embodiments and can be modified in arrangement and detail without departing from such principles. Techniques from any of the examples can be incorporated into one or more of any of the other examples.

[00234] Another embodiment uses a dual normalization for even further dynamic range increase. This embodiment explains, and relies on, data from human sleep subjects, rather than birds as in some of the previous embodiments. Moreover, any of the applications described above for the previous embodiments are equally applicable for this embodiment, as are the techniques of normalization and clustering.

[00235] This embodiment uses many of the characteristics of the previous embodiments and also adds some refinements. The embodiment operates to analyze brain wave activities. The signals from a brainwave, e.g., an EEG, typically follows the characteristic where the amount of power in the brain wave is related to, e.g., proportional to 1/f, where f is the frequency of the brain wave: The amount of power is inversely proportional to the frequency. As explained with reference to previous embodiments, this 1/f spectral distribution has tended to obscure the higher frequency portions of the signal, since those higher frequency portions of the signals had smaller voltage amplitudes.

[00236] Human observers who observed the waves representing the EEGs have historically been unable to ascertain any substantial information relative to the higher frequency. Many reasons for this have been postulated by the inventors. One reason is that higher frequencies of brainwave activities have been more filtered from the skull, because the physical structure of the skull acts as a low pass filter.

[00237] Previous embodiments have shown how normalization, for example using Z scoring, allowed analysis of more information from the brainwave signal. The analysis which was previously carried out normalized power information across frequencies. The normalization preferably used Z scoring, but any other kind of data normalization can be used. The normalization which is used is preferably unitless, like Z scoring. As well-known in the art, z scoring can be used to normalize a distribution without changing a shape of the envelope of the distribution. The z scores are essentially changed to units of standard deviation. Each z score normalized unit reflects the amount of power in the signal, relative to the average of the signal. The scores are converted into mean deviation form, by subtracting the mean from each score. The scores are then normalized relative to standard deviation. All of the z scored normalized units have standard deviations that are equal to unity.

[00238] While the above describes normalization using Z scores, it should be understood that other normalizations can also be carried out, including T scoring, and others.

[00239] The above embodiments describe normalizing the power at every frequency within a specified range. The range may be from 0, to 100 hz, or to 128 hz, or to 500 hz. The range of frequencies is only restricted by the sampling rate. With an exemplary sampling rate of 30KHz, an analysis up to 15KHz can be done.

[00240] According to the present embodiment, an additional normalization is carried out which normalizes the power across time for each frequency. This results in information which has been normalized across frequencies and across time being used to create a doubly normalized spectrogram.

[00241] This embodiment can obtain additional information from brainwave data, and the embodiment describes automatically detecting different periods of sleep from the analyzed data. The periods of sleep that can be detected can include, but are not limited to, short wave sleep (SWS), rapid eye movement sleep (REM), intermediate sleep (IIS) and wakefulness. According to an important feature, a single channel of brainwave activity (that is obtained from a single location on the human skull) is used for the analysis.

[00242] The operation is carried out according to the flowchart of figure 41, which may be executed in any of the computer devices described herein, or may be executed across a network or in any other known way. At 4100, data is obtained. As described above, the obtained data can be one channel of EEG information from a human or other subject. The EEG data as obtained can be collected, for example, using a 256 Hz sampling rate, or can be sampled at a higher rate. The data is divided into epochs, for example 30 second epochs, and characterized according to frequency.

[00243] At 4110, a first frequency normalization is carried out. The power information is normalized using a z scoring technique on each frequency bin. In the embodiment, the bins may extend from one to 100 Hz and 30 bins per hertz. The normalization occurs across time. This creates a normalized spectrogram or NS, in which each frequency band from the signal has substantially the same weight. In the embodiment, each 30 second epoch is represented by a "preferred frequency" which is the frequency with the largest z score within that epoch.

[00244] This creates a special frequency space called the preferred frequency space. Figure 42A illustrates the raw spectrogram, and figure 42 B illustrates the normalized spectrum. Each epoch, e.g., a 30 second segment in figure 43, or or a 1 second sliding window epoch in Figure 44, is represented by the frequency with the largest z score. Figure 44 illustrates how this broadly separates into different patterns.

[00245] Analysis of how those patterns are formed and allow analysis of the characteristics of the patterns. For example, the W or wakefulness state has been found by analysis to be characterized by a band in the alpha band, or 7 to 12 Hz and sometimes by a band in the beta (15 to 25 Hz).

[00246] Intermediate states display Delta values in the 1 to 4 Hz range, and the spindle frequencies in 12 to 15 Hz. These also show activity of the higher frequencies and the gamma range 3- 90 Hz. Surprisingly, REM state defines compact bands at Delta and Theta frequencies, and short wave sleep was dominated by diffuse broad-spectrum activity.

[00247] Different sleep states, therefore, can be defined according to a discrimination function, where the discrimination function looks for certain activity in certain areas, and non-activity in other areas. The function may evaluate sleep states according to which of the frequency at areas have activity and which do not have activity.

[00248] More generally, however, any form of dynamic spectral scoring can be carried out on the compensated data. The discrimination function may require specific values, or may simply require a certain amount of activity to be present or not present, in each of a plurality of frequency ranges. The discrimination function may simply match envelopes of frequency response. The discrimination function may also look at spectral fragmentation and temporal fragmentation.

[00249] 4120 illustrates a second normalization which is carried out across frequencies. The second normalization at 4120 produces a doubly normalized spectrogram. This produces a new frequency space, in which the bands become even more apparent. The second normalization is shown as Figure 42C, where bands show as lighter values, representing the positive

values, while darker regions will tend to have negative values.

[00250] The doubly normalized spectrogram values can be used to form filters that maximally separate the values within the space. Figure 43 illustrates a graph of preferred frequency as a function of time, showing the different clusters of frequencies.

[00251] 4130 illustrates a clustering technique which is carried out on the doubly normalized frequency. For example, the clustering technique may be a K means technique as described in the previous embodiments. The clusters form groups, as shown in Figure 43. Figure 44 illustrates how the areas between different states, such as boundary 4400, form multiple different clusters. Each cluster can represent a sleep state.

[00252] The clusters are actually multi dimensional clusters, which can themselves be graphed to find additional information, as shown in Figure 45. The number of dimensions can depend on the number of clustering variables. This illustrates how the doubly normalized spectrogram also allows many more measurement characteristics. Figure 45 is actually a three-dimensional graph, of different characteristics, and can allow detection of the different states. The analysis, however, reveals that slow wave sleep is more unstable and time and frequency than rapid eye movement sleep or

wakefulness. Intermediate sleep often forms a bridge to and from the short wave sleep.

[00253] Measurement of the average spread in normalized power across frequency which illustrates the spectral fragmentation is also possible, as shown in Figure 46 illustrates the spectral fragmentation. Fragmentation values can alternatively be based on temporal fragmentation for the different states may also be used as part of the discrimination function.

[00254] For example:

[00255] Using Z and ZZ to correspond to the NS and 2NS values respectively:

[00256] w_filter=mean(ZZ(12-15 Hz))+mean(ZZ(1-4 Hz))+mean(ZZ(4-7 Hz)).

[00257] nrem_filter=mean(ZZ(60-100 Hz))+mean(ZZ(4-7 Hz))-[mean(ZZ(12-15 Hz))+mean(ZZ(25-60Hz))+mean(ZZ(15-25 Hz))]

[00258] sws_filter= mean(Z(4-7 Hz))+mean(Z(7-12 Hz))

[00259] The fragmentation values are as follows:

[00260] Spectral_frag= mean(abs(grad_f(ZZ(1-100 Hz))));

[00261] Spectral_temp= mean(abs(grad_t(ZZ(1-100 Hz))));

[00262] Where grad_f and grad_t correspond to the two-dimensional nearest neighbor gradients of ZZ.

[00263] These two functions are evaluated on the doubly normalized spectrum, relying on homogeneous increases in gain at all frequencies as caused movement artifacts in NREM sleep and W would lead to abnormally elevated fragmentation values in the singly normalized spectrum.

[00264] These fragmentation values may be used as part of the discrimination function. Importantly, and as described above, this discrimination function is typically not apparent from any previous analysis technique, including manual techniques.

[00265] The computation may be characterized by segmenting, or may use overlapping windows or a sliding window, to increase the temporal registration. This enables many techniques that have never been possible before. By characterizing on-the-fly, this enables distinguishing using the dynamic spectral scoring, between sleep states and awake states using the brainwave signature alone.

[00266] Another aspect includes a machine which automatically obtains EEG information, and includes a computer that analyzes the EEG information to determine information about the sleep state. For example, the information may include the actual sleep state, or other parts of the sleep state. The computer may also include nonvolatile memory therein to store the information indicative of the sleep state, and may include, for example, a wireless network connection to allow sending the information indicative of the

sleep state to a remote device. The user can wear the machine, or an electrode that is connected to the machine, in order to characterize his or her sleep.

[00267] The above has described how information can be used to determine sleep states. These techniques may also be used for other applications including characterizing sleep states, and other techniques. Applications may include determination of whether a patient has taken certain kinds of drugs based on their sleep state, and based on variables that were previously determined as changing in brain function based on those sleep states. Another application can analyze brain wave signals to determine alcohol consumption, e.g., forming a system that can be used as a "breathalyzer".

[00268] The general structure and techniques, and more specific embodiments which can be used to effect different ways of carrying out the more general goals are described herein.

[00269] Although only a few embodiments have been disclosed in detail above, other embodiments are possible and the inventors intend these to be encompassed within this specification. The specification describes specific examples to accomplish a more general goal that may be accomplished in another way. This disclosure is intended to be exemplary, and the claims are intended to cover any modification or alternative which might be predictable to a person having ordinary skill in the art. For example, other applications

are possible, and other forms of discrimination functions and characterization is possible. While the above extensively described characterizing the frequency in terms of its "preferred frequency", it should be understood that more rigorous characterization of the information may be possible. Also, while the above only refers to determining sleep states from the EEG data, and refers to only a few different kinds of determination of sleep states, it should be understood that other applications are contemplated.

[00270] Also, the inventors intend that only those claims which use the words "means for" are intended to be interpreted under 35 USC 112, sixth paragraph. Moreover, no limitations from the specification are intended to be read into any claims, unless those limitations are expressly included in the claims.

[00271] The computers described herein may be any kind of computer, either general purpose, or some specific purpose computer such as a workstation. The computer may be a Pentium class computer, running Windows XP or Linux, or may be a Macintosh computer. The computer may also be a handheld computer, such as a PDA, cell phone, or laptop.

[00272] The programs may be written in C, or Java, Brew or any other programming language. The programs may be resident on a storage medium, e.g., magnetic or optical, e.g. the computer hard drive, a removable disk or media such as a memory stick or SD media, or other removable medium. The

programs may also be run over a network, for example, with a server or other machine sending signals to the local machine, which allows the local machine to carry out the operations described herein.

What is claimed is

1. A method, comprising:

obtaining data indicative of brainwave activity;

normalizing at least one frequency range of said data to change a power level of the data in said at least one frequency range relative to data in another frequency range, to form normalized data indicative of brainwave activity; and

analyzing said normalized data indicative of brainwave activity to determine at least one parameter indicative of sleep state from said analyzing.

2. A method as in claim 1, wherein said analyzing comprises automatically clustering said normalized data into clusters, and using said clusters in said analyzing, to determine said parameter.

3. A method as in claim 1, wherein said normalizing comprises Z scoring the data.

4. A method as in claim 1, further comprising a second normalizing the data, to form double normalized data, prior to said analyzing.

5. A method as in claim 4, wherein said second normalizing comprises normalizing frequencies across time.

6. A method as in claim 5, wherein said first and second normalizing each use Z scoring for the normalizing.

7. A method as in claim 5, further comprising defining a discrimination function which represents characteristics of the said double normalized data for a plurality of different sleep states, and using said discrimination function to determine a sleep state from said double normalized data.

8. A method as in claim 7, wherein said discrimination function is a function that is in terms of frequencies which are present in specified ranges and not present in specified other ranges, to define a sleep state.

9. A method as in claim 4, further comprising characterizing a preferred frequency as a frequency which has the highest normalized value in any specified time, and analyzing the preferred frequency to determine said at least one parameter.

10. A method as in claim 9, further comprising defining a discrimination function as a function of preferred frequency, where a discrimination function defines a sleep state in terms of frequencies which are present, and frequencies which are not present.

11. A method as in claim 4, further comprising analyzing a fragmentation of the double normalized data, and using the fragmentation as to the part of said analyzing.

12. A method as in claim 1, wherein said parameter indicative of sleep state comprises a probable sleep state corresponding to the current time period.

13. A method as in claim 1, wherein said parameter indicative of sleep state comprises information indicative of likely drug consumption.

14. A method as in claim 1, wherein said normalizing is carried out using a computer to change the data.

15. The method of claim 1 further comprising removing artifacts from the source data.

16. The method of claim 1 further comprising: prior to said normalizing, segmenting the source data in a plurality of time segments.

17. The method of claim 16 wherein the separating comprises using one of a scanning window or a sliding window.

18. The method of claim 17 wherein the separating comprises determining at least one time series increment selected from the group consisting of:

whole time series;

overlapping time series; and

non-overlapping series.

19. A method for determining sleep states in a subject over a period of time comprising:

receiving brain wave data for the subject over the period of time, wherein the brain wave data exhibits lower dynamic range for power in at least one low power first frequency range in a frequency spectrum as compared to a second frequency range in the frequency spectrum;

segmenting the brain wave data into one or more epochs;

weighting frequency power of the one or more epochs across time, wherein the weighting comprises increasing the dynamic range for power within the low power frequency range of the frequency spectrum as compared to the second frequency range, thereby generating one or more frequency weighted epochs; and

classifying sleep states in the subject based on the one or more frequency weighted epochs.

20. The method as in claim 19 wherein classifying sleep states in the subject comprises:

clustering the one or more frequency weighted epochs; and

assigning sleep state designations to the one or more frequency weighted epochs according to the clustering; and

presenting the sleep state designations as indicative of sleep states in the subject for the period of time represented by the one or more frequency weighted epochs.

21. The method of claim 19 wherein clustering the one or more frequency weighted epochs comprises k-means clustering.

22. The method of claim 19 further comprising pretreating the electroencephalography data with component analysis.

23. The method of claim 19 wherein classifying sleep states in the subject comprises applying independent component analysis to the one or more frequency weighted epochs.

24. The method of claim 19 wherein classifying sleep states further comprises incorporating manually determined sleep states.

25. The method of claim 19 wherein assigning sleep state designations to the one or more frequency weighted epochs comprises:

determining a slow wave sleep designation from a non-slow wave sleep designation based at least on low frequency information; and

determining a rapid eye movement sleep designation from a non-rapid eye movement sleep designation based at least on high frequency information.

26. The method of claim 25 further comprising assigning a slow wave sleep designation to an epoch that has significant weighted power at low frequencies.

27. The method of claim 25 further comprising assigning a rapid eye movement sleep designation to an epoch with significant weighted power at high frequency.

28. The method of claim 19 wherein assigning sleep state designations to the one or more frequency weighted epochs further comprises applying a smoothing window to the one or more weighted epochs, wherein the smoothing can comprise averaging sleep state designations across the one or more weighted epochs.

29. The method of claim 19 further comprising presenting one or more frequency weighted epochs as canonical spectra representative of the sleep state in the subject for the period of time represented by the one or more epochs having similar sleep state designations.

30. The method of claim 29 further comprising analyzing the canonical spectra with independent component analysis to establish sleep state classification confidence.

31. The method of claim 19 further comprising presenting sleep statistics for the subject according to the sleep state designations of the one or more frequency weighted epochs.

32. The method as in claim 19, further comprising second weighting power to normalize the data according to a second dimension, prior to said classifying to form doubly normalized data.

33. The method as in claim 32, wherein said second weighting comprises normalizing at least one frequency across time.

34. A method as in claim 32,wherein said weighting and said second weighting each use Z scoring to carry out normalizing.

35. A method as in claim 32, further comprising defining a discrimination function which represents characteristics of the double normalized data for a plurality of different sleep states, and using said discrimination function to determine a sleep state from said double normalized data.

36. A method as in claim 35, wherein said discrimination function is a function that is in terms of frequencies which are present in specified ranges and not present in specified other ranges, to define a sleep state.

37. A method as in claim 32, further comprising characterizing a preferred frequency as a frequency which has the highest normalized value in any specified time, and analyzing the preferred frequency to determine said at least one parameter.

38. A method as in claim 37, further comprising defining a discrimination function as a function of said preferred frequency, where a discrimination function defines a sleep state in terms of frequencies which are present, and frequencies which are not present.

39. A method as in claim 32, further comprising analyzing a spectral fragmentation of the double normalized data, and using the spectral fragmentation as part of said analyzing.

40. A method as in claim 32, further comprising analyzing a temporal fragmentation of the double normalized data, and using the temporal fragmentation as part of said analyzing.

41. An apparatus, comprising:

a computing device, receiving at least one signal indicative of brainwave activity, and normalizing at least one frequency range of said signal to change a power level of data in said at least one frequency range relative to data in another frequency range, to form normalized data indicative of brainwave activity and using said normalized data indicative of brainwave activity to determine at least one parameter indicative of sleep state.

42. An apparatus as in claim 41, wherein said computing device carries out said normalizing by Z scoring the data.

43. An apparatus as in claim 41, wherein said computer operates to carry out a second normalizing of the data, to form double normalized data, prior to using said data.

44. An apparatus as in claim 43, wherein said second normalizing carried out by said computer comprises normalizing frequencies across time.

45. An apparatus as in claim 42, wherein said computer operates based on a discrimination function which represents characteristics of said double normalized data for plurality of different sleep states, and uses said discrimination function to determine a sleep state from said normalized data.

46. An apparatus as in claim 46, wherein said discrimination function is a function that is in terms of frequencies which are present in specified ranges and not present in specified other ranges, to define a sleep state.

47. An apparatus as in claim 43, wherein said computer operates to determine a preferred frequency as a frequency which has a highest normalized value in any specified time, and analyzes the preferred frequency to determine said at least one parameter.

48. An apparatus as in claim 43, wherein said computer determines a fragmentation of the double normalized data as a part of said analyzing.

49. An apparatus as in claim 41, further comprising a brain wave electrode, connected to obtain said signal.

50. An apparatus, comprising:

a first receiving part, receiving information indicative of brainwave signals; and

a processing part, normalizing at least one frequency range of said brainwave signals, to form normalized data indicative of brainwave activity and using said normalized data indicative of brainwave activity to determine at least one parameter indicative of sleep state.

51. An apparatus as in claim 50, wherein said processing part carries out said normalizing by Z scoring the data.

52. An apparatus as in claim 50, wherein said processing part carries out two separate normalizing of the data, to form double normalized data, prior to using said data.

FIG. 1

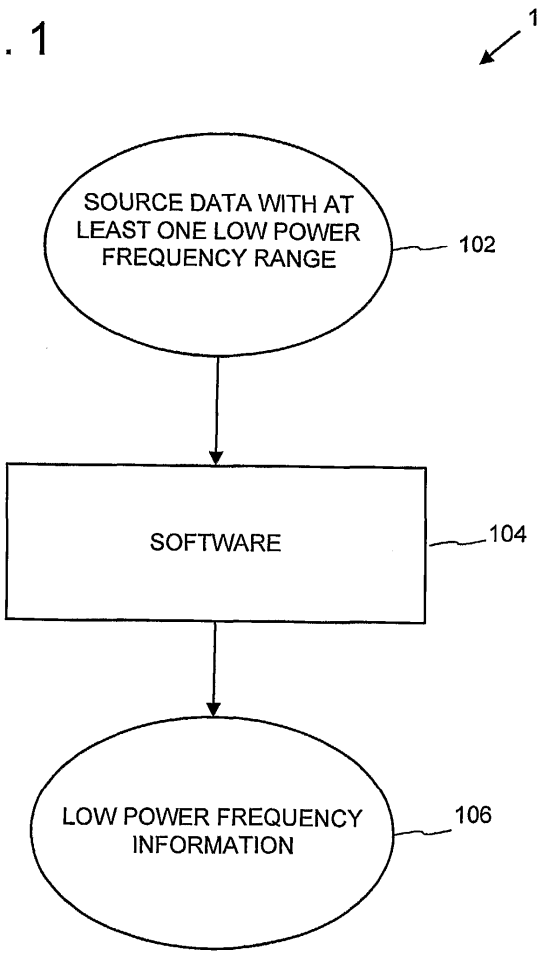
100
SOURCE DATA WITH AT LEAST ONE LOW POWER FREQUENCY RANGE
102
SOFTWARE
104
LOW POWER FREQUENCY INFORMATION
106

FIG. 2

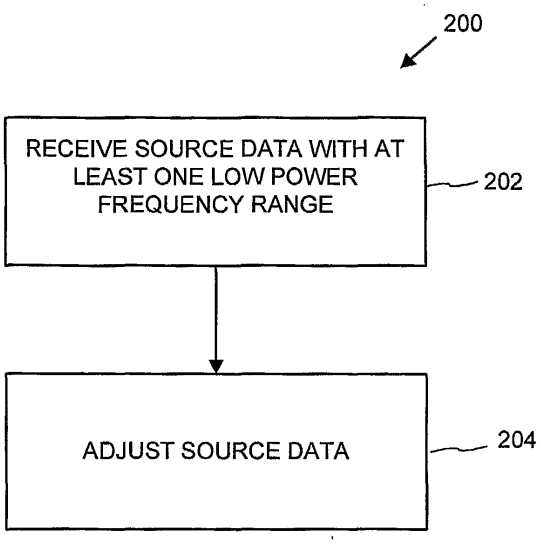
200
RECEIVE SOURCE DATA WITH AT LEAST ONE LOW POWER FREQUENCY RANGE
202
ADJUST SOURCE DATA
204

FIG. 3

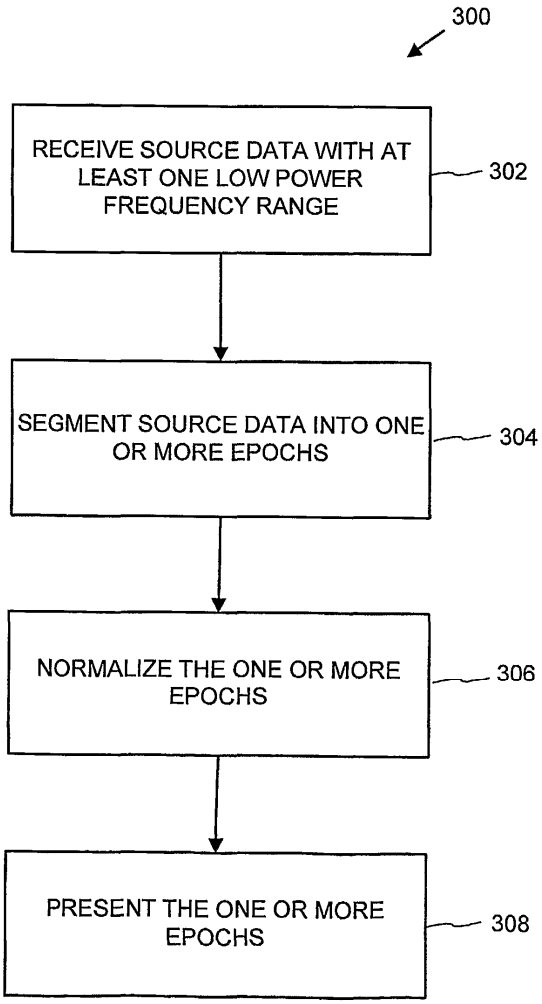
300
RECEIVE SOURCE DATA WITH AT LEAST ONE LOW POWER FREQUENCY RANGE
302
SEGMENT SOURCE DATA INTO ONE OR MORE EPOCHS
304
NORMALIZE THE ONE OR MORE EPOCHS
306
PRESENT THE ONE OR MORE EPOCHS
308

FIG. 4

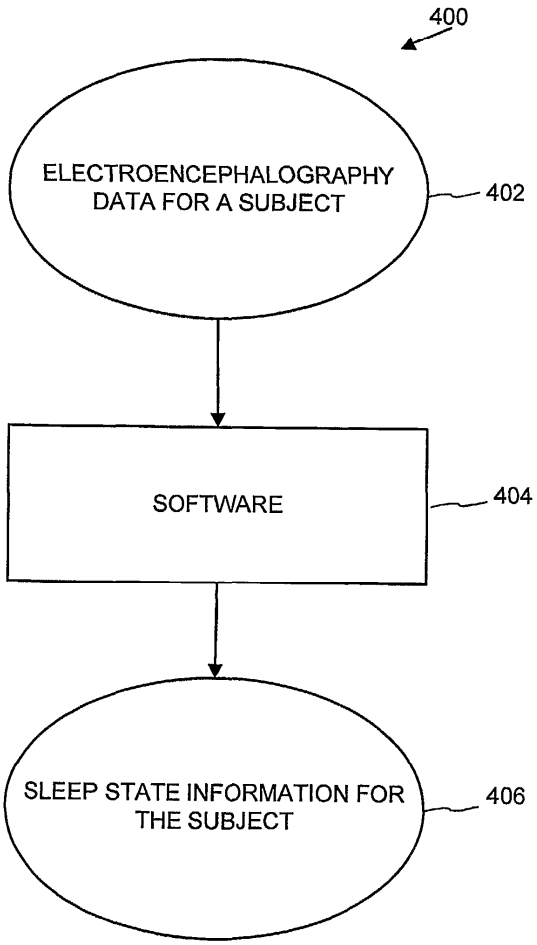
400
ELECTROENCEPHALOGRAPHY DATA FOR A SUBJECT
402
SOFTWARE
404
SLEEP STATE INFORMATION FOR THE SUBJECT
406

FIG. 5

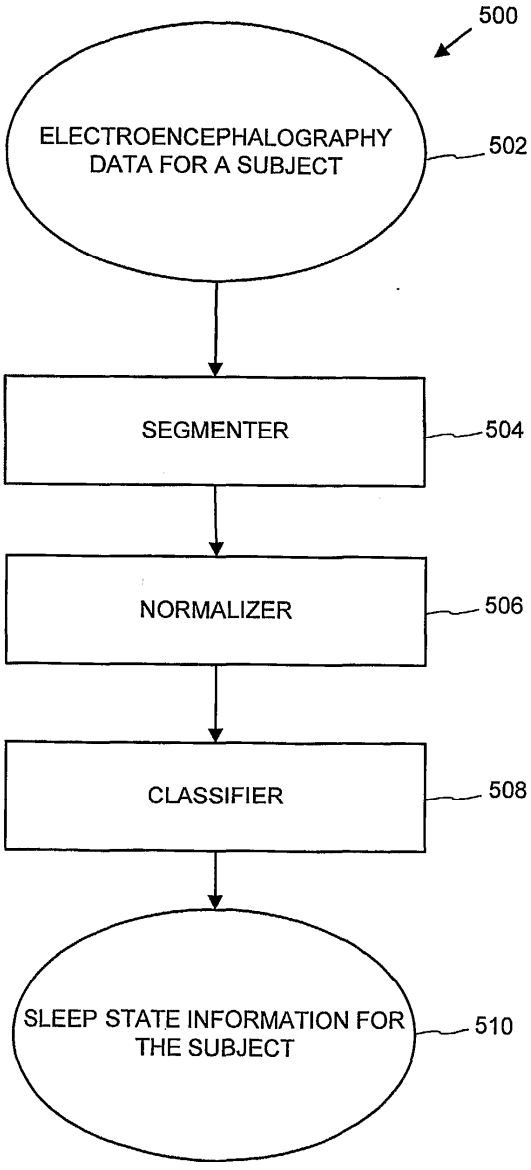
500
ELECTROENCEPHALOGRAPHY DATA FOR A SUBJECT
502
SEGMENTER
504
NORMALIZER
506
CLASSIFIER
508
SLEEP STATE INFORMATION FOR THE SUBJECT
510

FIG. 6

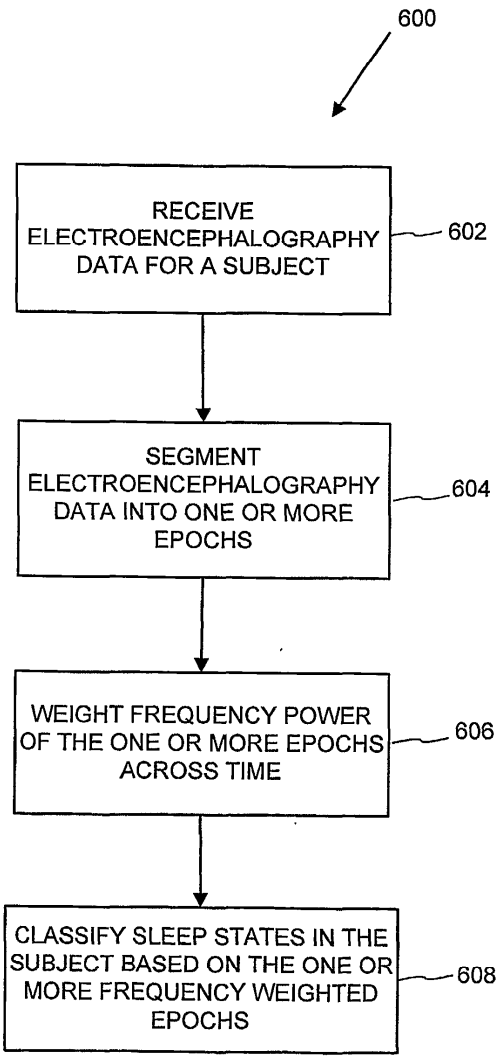
600
RECEIVE ELECTROENCEPHALOGRAPHY DATA FOR A SUBJECT
602
SEGMENT ELECTROENCEPHALOGRAPHY DATA INTO ONE OR MORE EPOCHS
604
WEIGHT FREQUENCY POWER OF THE ONE OR MORE EPOCHS ACROSS TIME
606
CLASSIFY SLEEP STATES IN THE SUBJECT BASED ON THE ONE OR MORE FREQUENCY WEIGHTED EPOCHS
608

FIG. 7

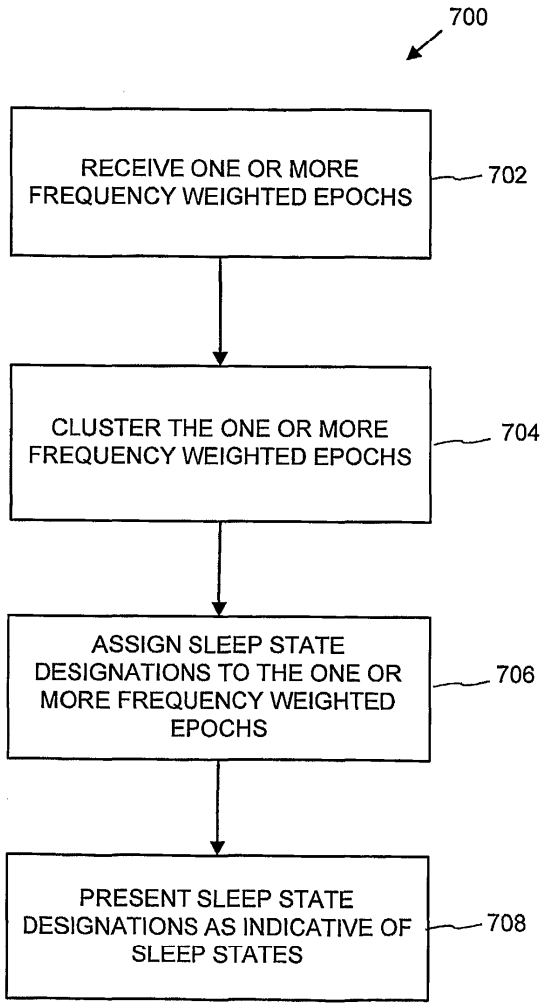
700
RECEIVE ONE OR MORE FREQUENCY WEIGHTED EPOCHS
702
CLUSTER THE ONE OR MORE FREQUENCY WEIGHTED EPOCHS
704
ASSIGN SLEEP STATE DESIGNATIONS TO THE ONE OR MORE FREQUENCY WEIGHTED EPOCHS
706
PRESENT SLEEP STATE DESIGNATIONS AS INDICATIVE OF SLEEP STATES
708

FIG. 8

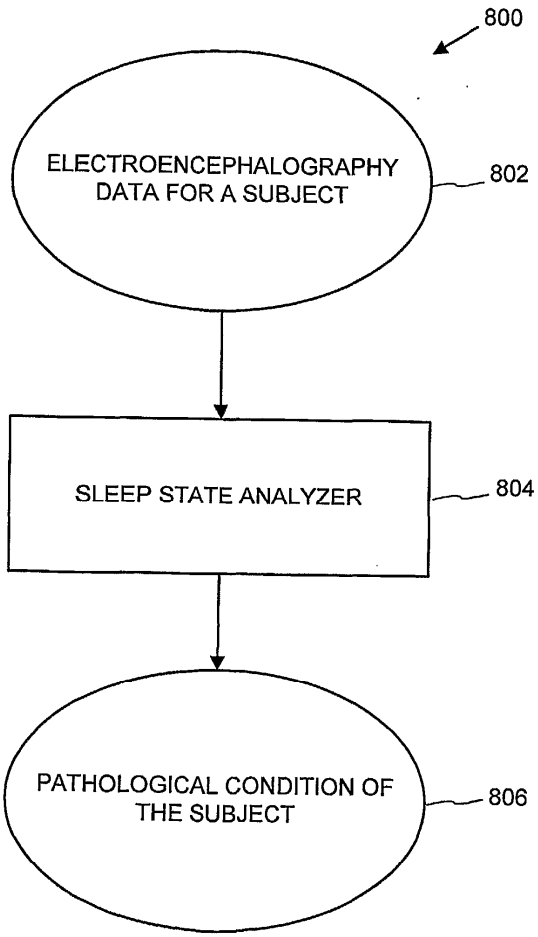
800
ELECTROENCEPHALOGRAPHY DATA FOR A SUBJECT
802
SLEEP STATE ANALYZER
804
PATHOLOGICAL CONDITION OF THE SUBJECT
806

FIG. 9

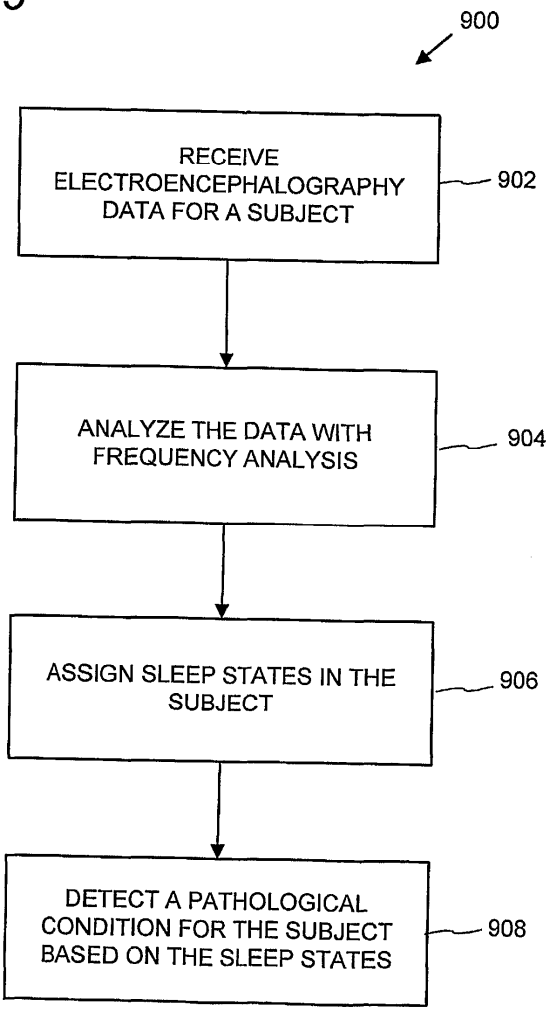
900
RECEIVE ELECTROENCEPHALOGRAPHY DATA FOR A SUBJECT
902
ANALYZE THE DATA WITH FREQUENCY ANALYSIS
904
ASSIGN SLEEP STATES IN THE SUBJECT
906
DETECT A PATHOLOGICAL CONDITION FOR THE SUBJECT BASED ON THE SLEEP STATES
908

FIG. 10

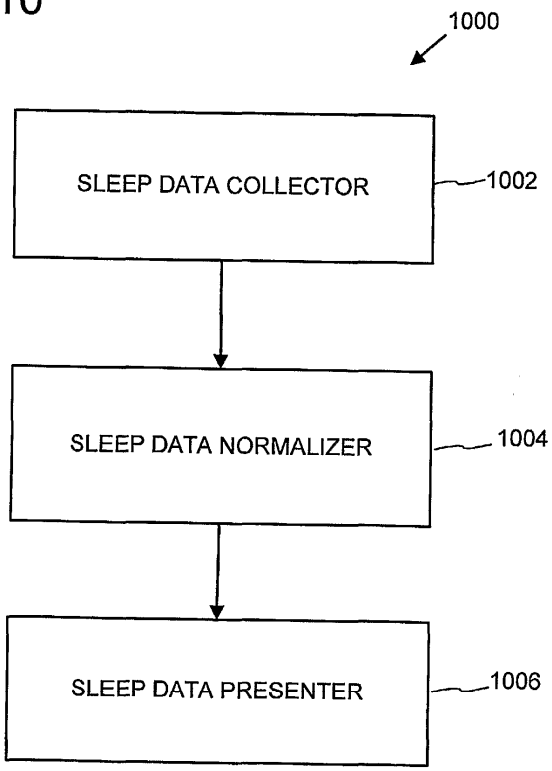
1000
SLEEP DATA COLLECTOR
1002
SLEEP DATA NORMALIZER
1004
SLEEP DATA PRESENTER
1006

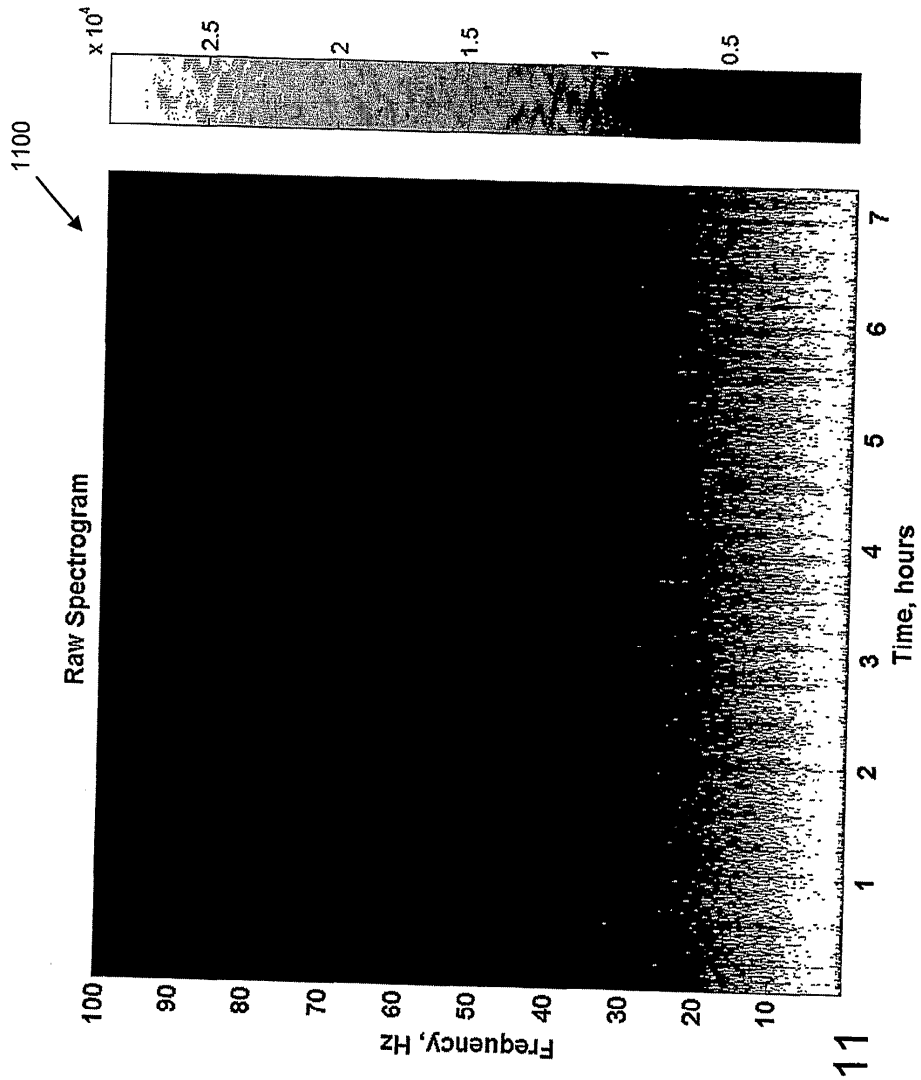
1100
x 10^4
2.5
2
1.5
1
0.5
Raw Spectrogram
Frequency, Hz
100
90
80
70
60
50
40
30
20
10
1
2
3
4
5
6
7
Time, hours

FIG. 11

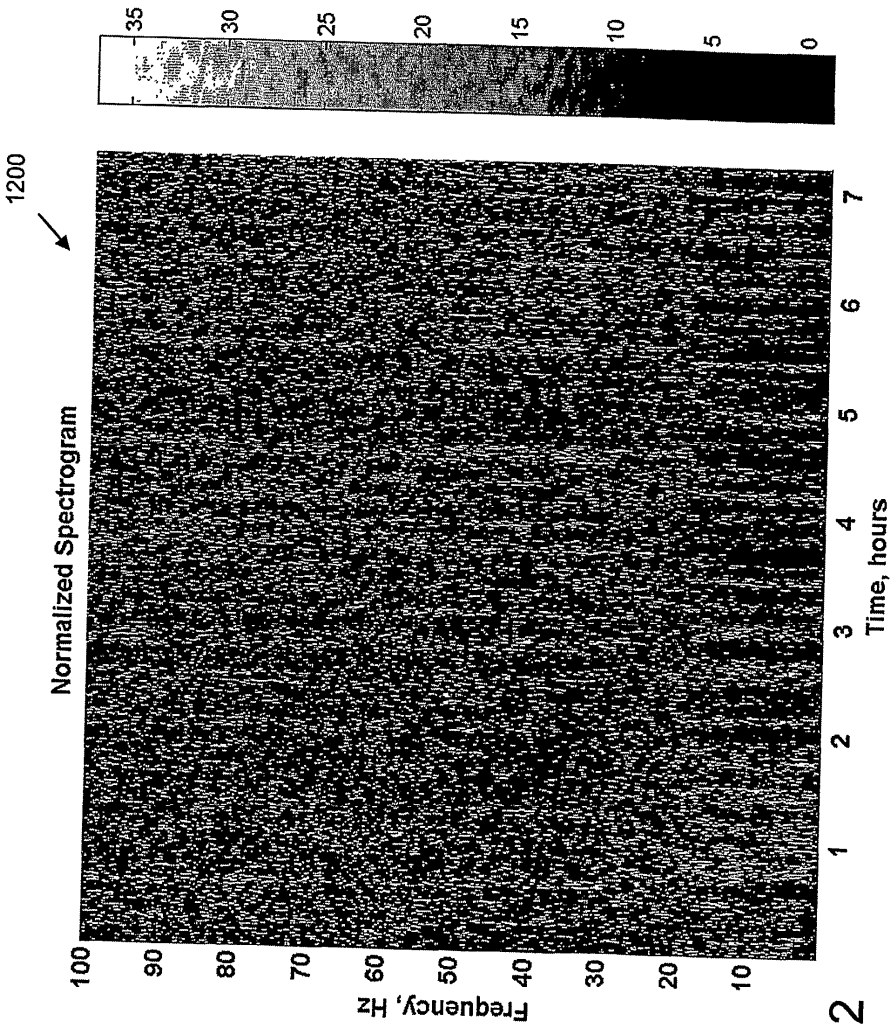
1200
Normalized Spectrogram
35
30
25
20
15
10
5
0
100
90
80
70
60
50
40
30
20
10
Frequency, Hz
1
2
3
4
5
6
7
Time, hours

FIG. 12

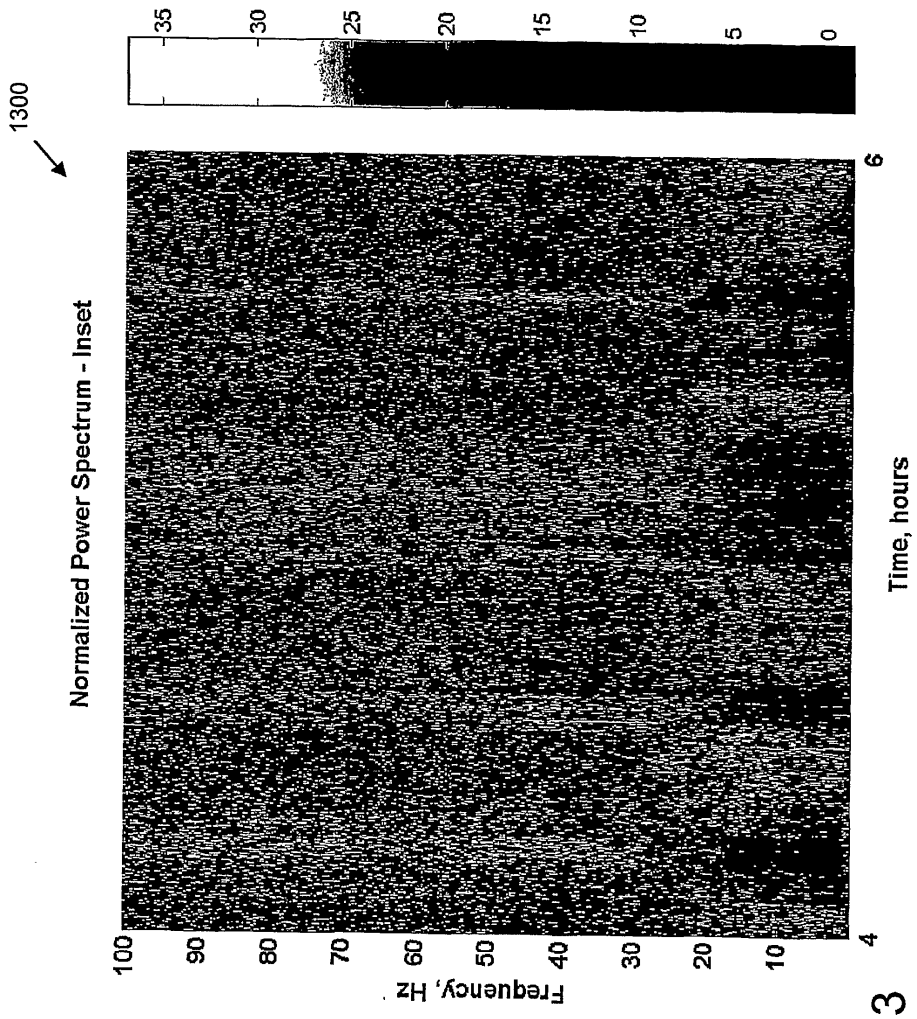
1300
35
30
25
20
15
10
5
0
Normalized Power Spectrum - Inset
Frequency, Hz
100
90
80
70
60
50
40
30
20
10
4
6
Time, hours

FIG. 13

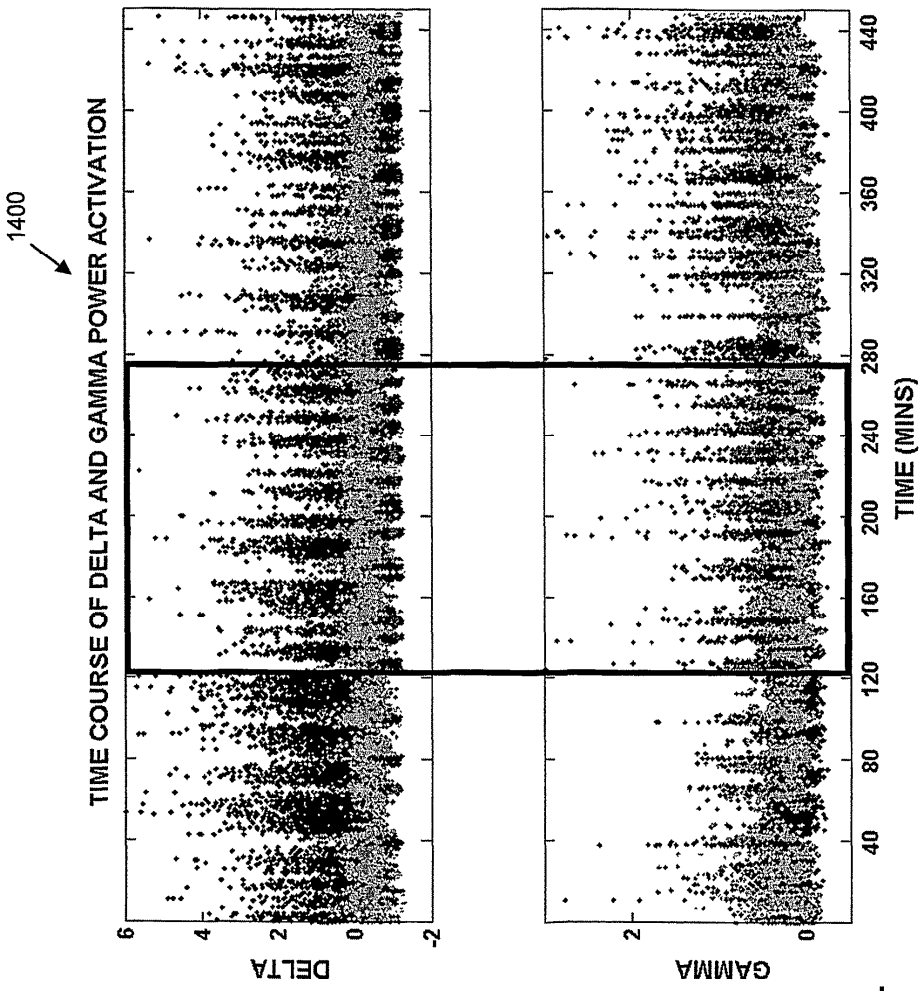
1400
TIME COURSE OF DELTA AND GAMMA POWER ACTIVATION
DELTA
6
4
2
0
-2
GAMMA
2
0
40
80
120
160
200
240
280
320
360
400
440
TIME (MINS)

FIG. 14

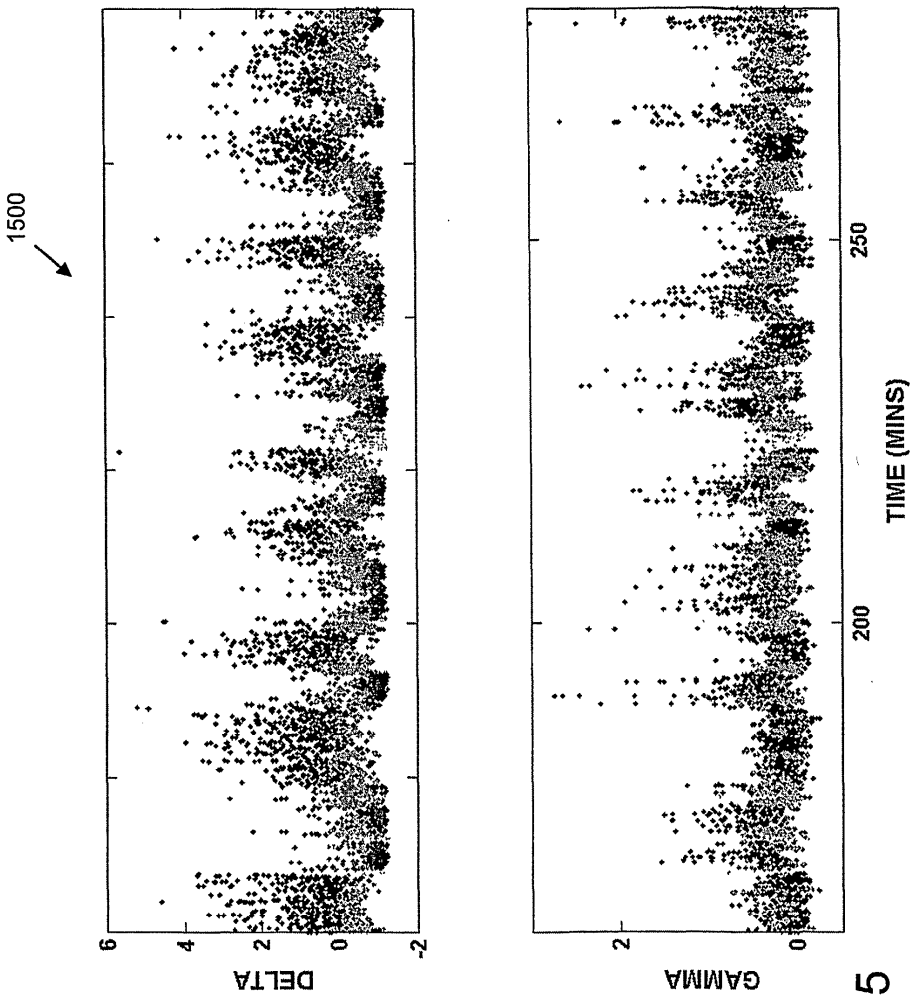

FIG. 15

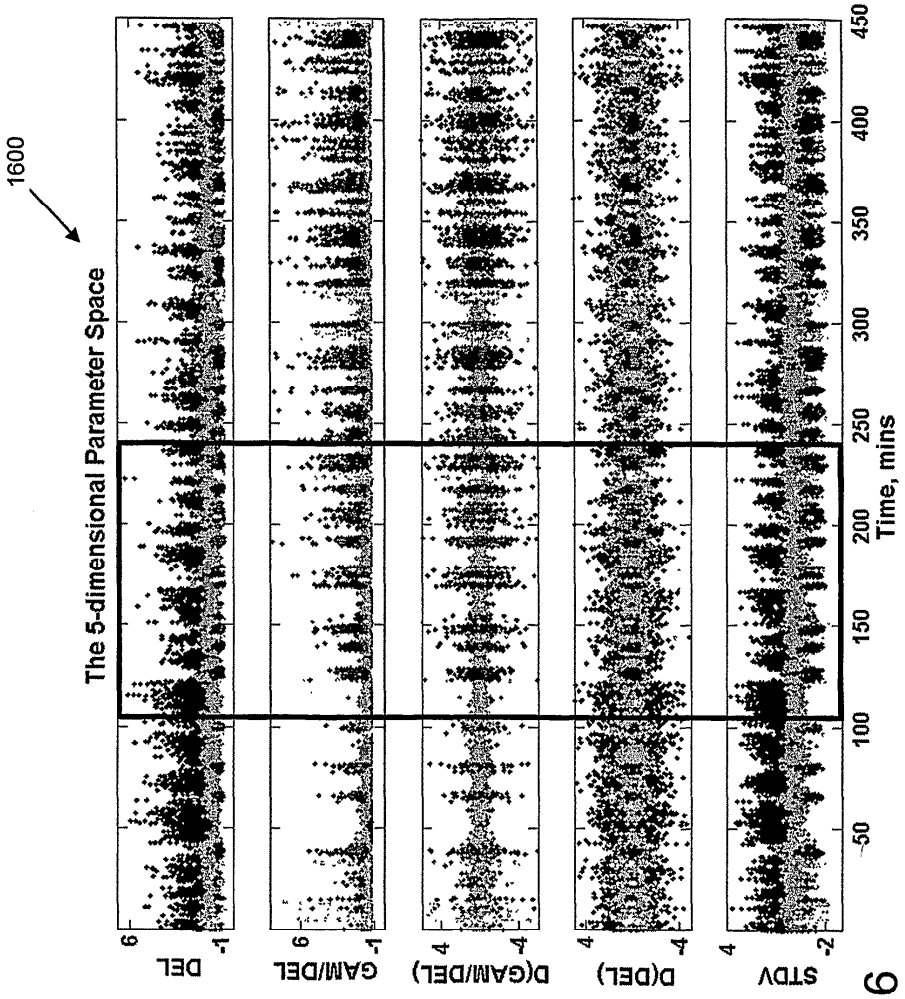
1600
The 5-dimensional Parameter Space
DEL
GAM/DEL
D(GAM/DEL)
D(DEL)
STDV
Time, mins
50
100
150
200
250
300
350
400
450

FIG. 16

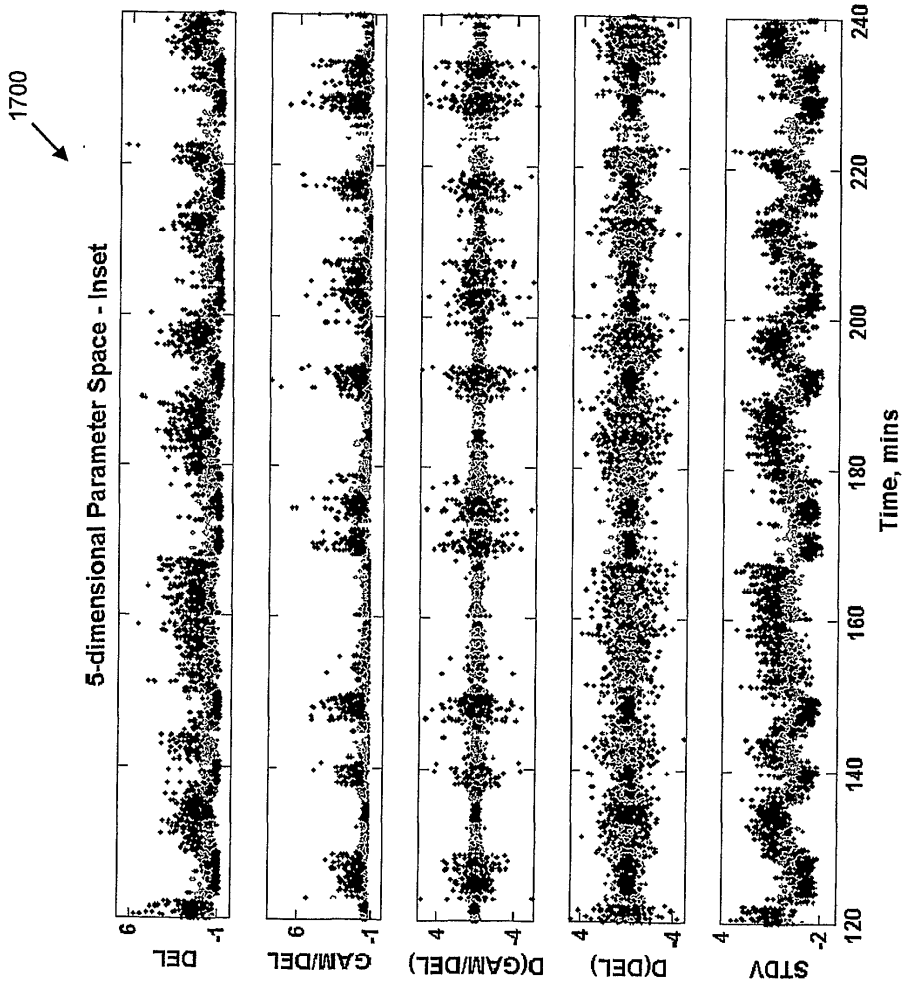
1700
5-dimensional Parameter Space - Inset
DEL
GAM/DEL
D(GAM/DEL)
D(DEL)
STDV
Time, mins
120
140
160
180
200
220
240

FIG. 17

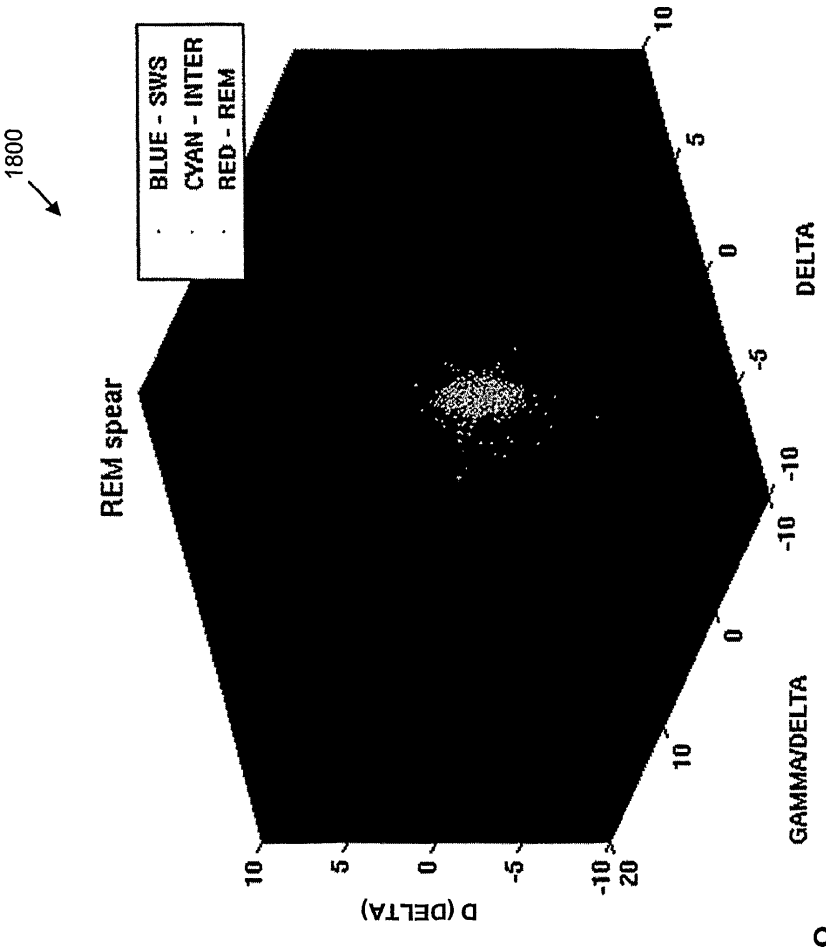
1800
BLUE - SWS
CYAN - INTER
RED - REM
REM spear
D (DELTA)
GAMMA/DELTA
DELTA
10
5
0
-5
-10
20

FIG. 18

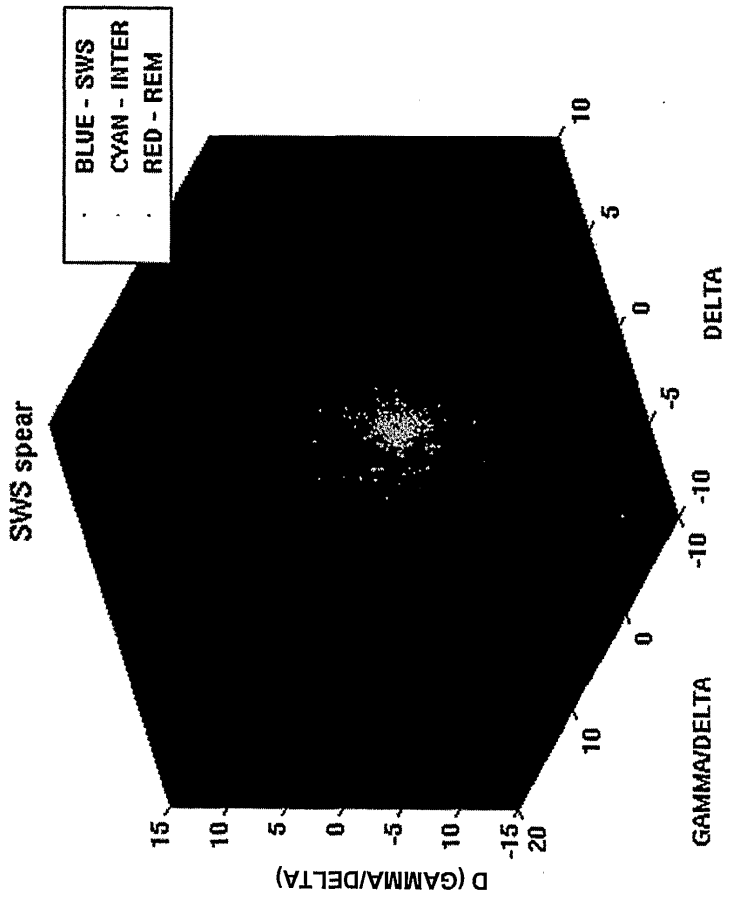
1900
BLUE - SWS
CYAN - INTER
RED - REM
SWS spear
D (GAMMA/DELTA)
15
10
5
0
-5
10
-15
20
GAMMA/DELTA
10
0
-10
-10
DELTA
10
5
0
-5

FIG. 19

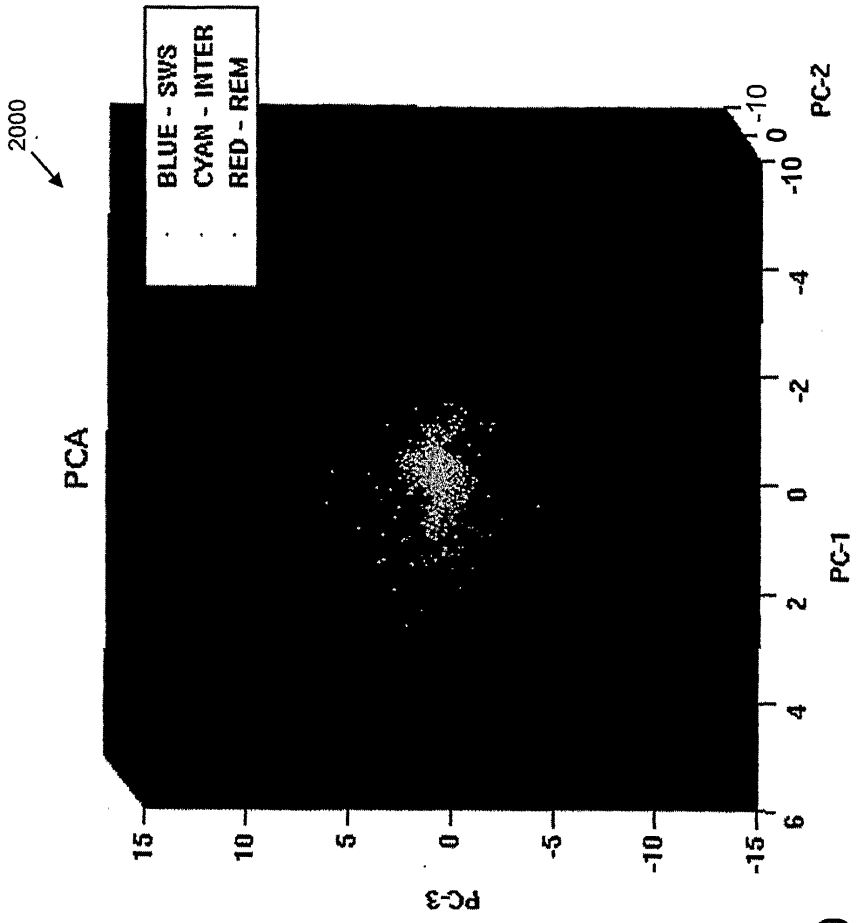
2000
PCA
BLUE - SWS
CYAN - INTER
RED - REM
PC-3
15
10
5
0
-5
-10
-15
PC-1
6
4
2
0
-2
-4
PC-2
-10
0
-10

FIG. 20

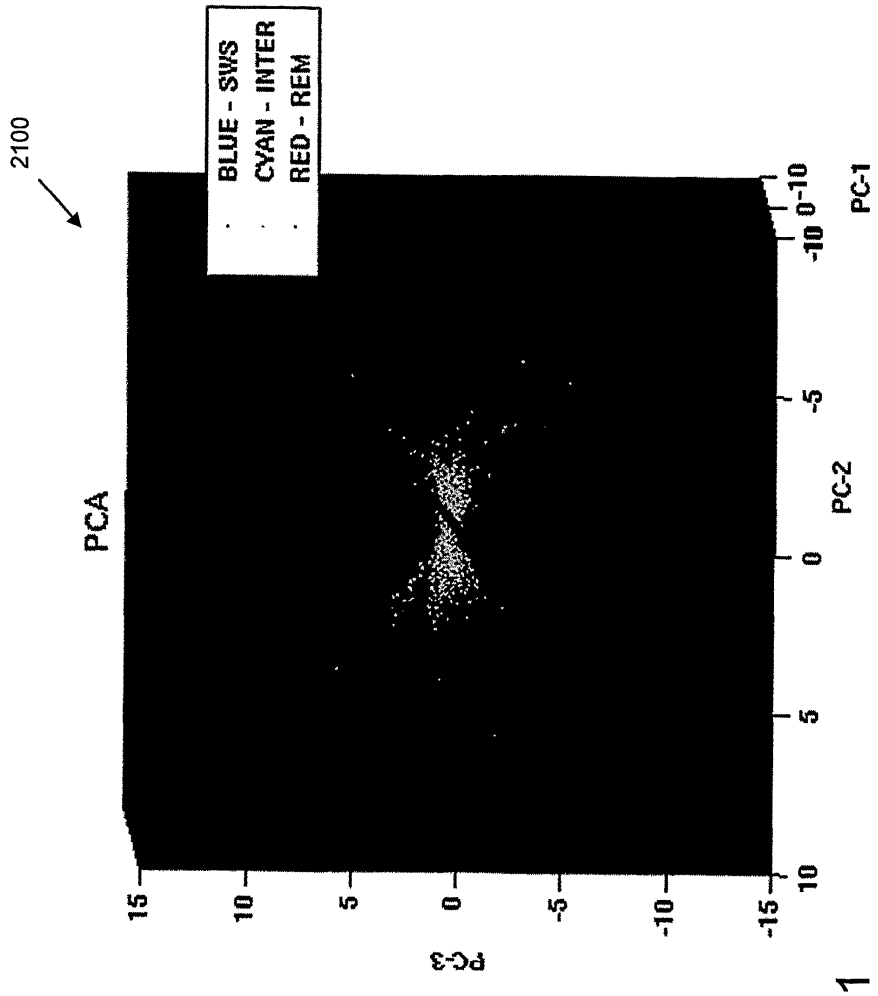
2100
BLUE - SWS
CYAN - INTER
RED - REM
PCA
PC-3
15
10
5
0
-5
-10
-15
PC-2
10
5
0
-5
-10
PC-1
10
0
-10

FIG. 21

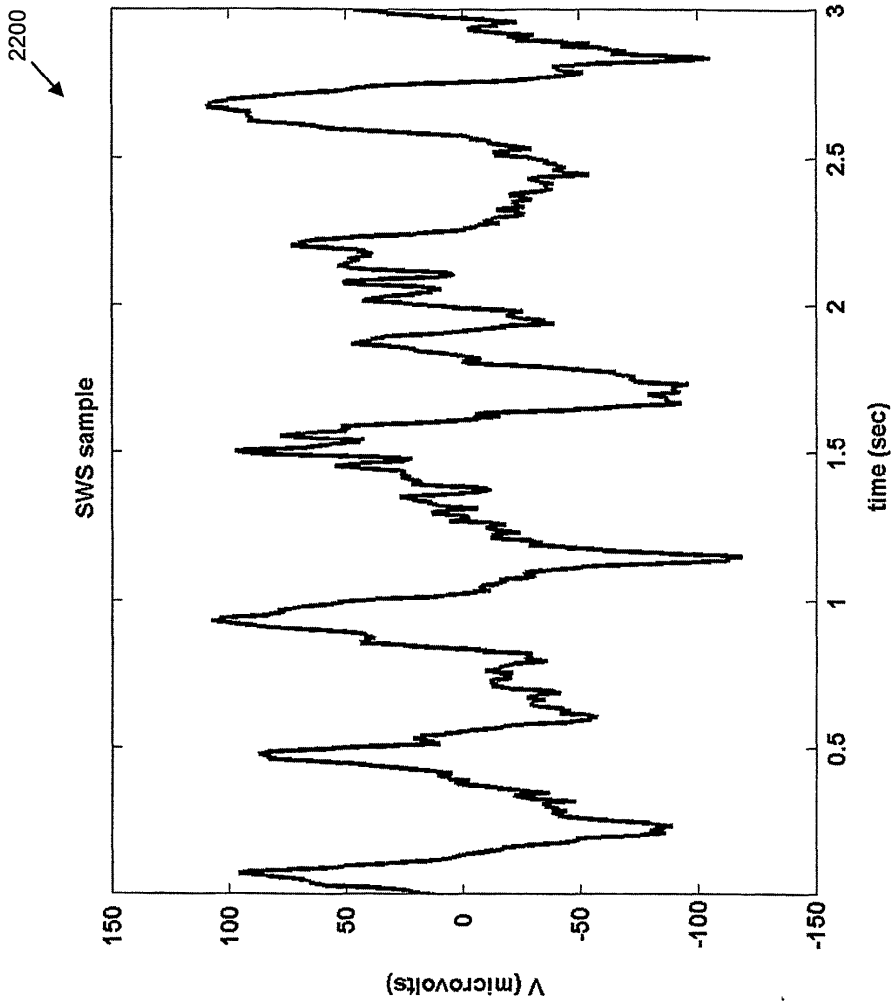
2200
SWS sample
V (microvolts)
150
100
50
0
-50
-100
-150
0.5
1
1.5
2
2.5
3
time (sec)

FIG. 22

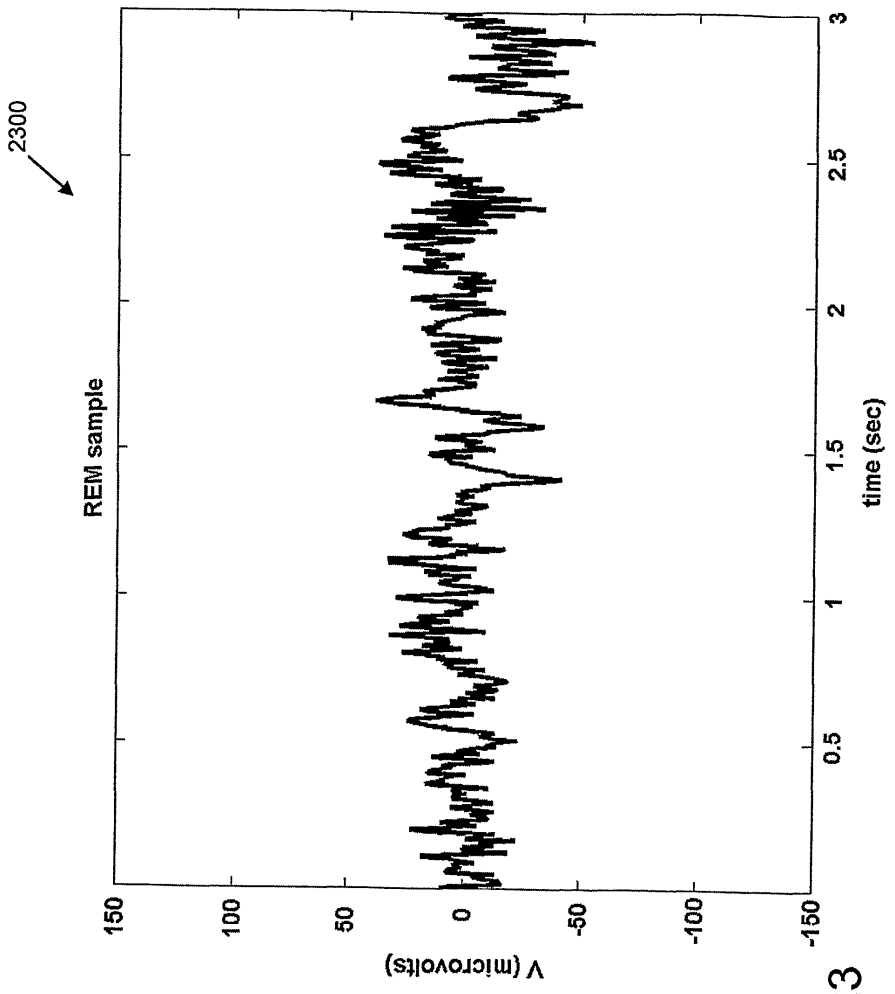
2300
REM sample
V (microvolts)
150
100
50
0
-50
-100
-150
0.5
1
1.5
2
2.5
3
time (sec)

FIG. 23

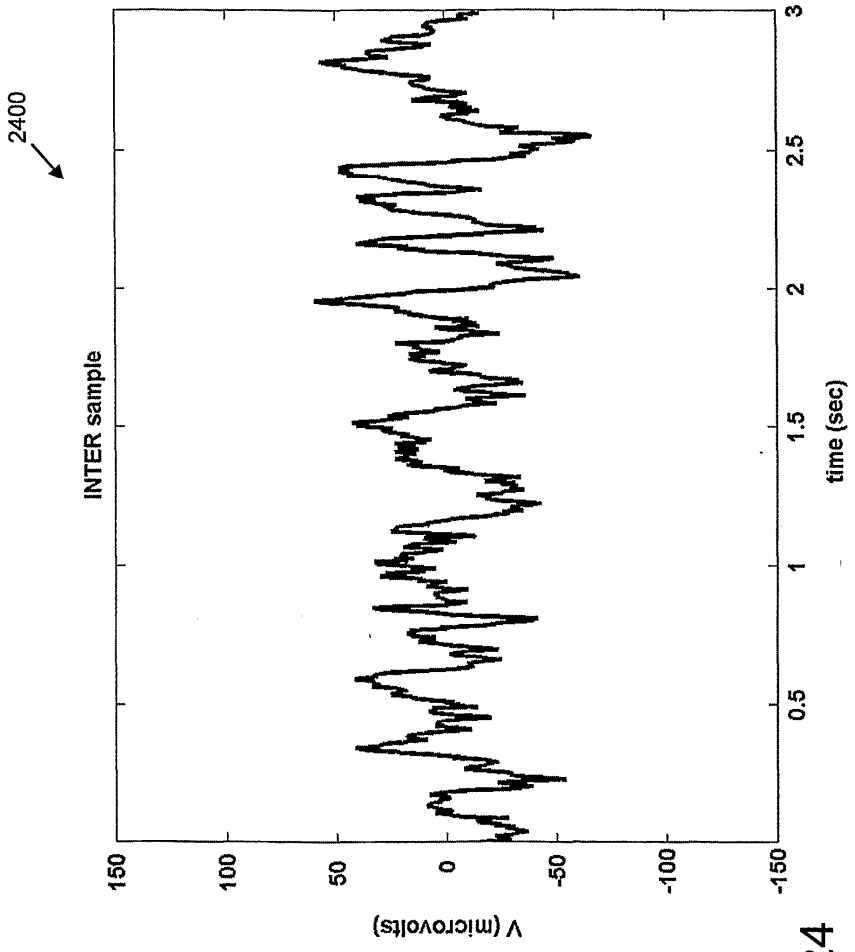
2400
INTER sample
V (microvolts)
150
100
50
0
-50
-100
-150
0.5
1
1.5
2
2.5
3
time (sec)

FIG. 24

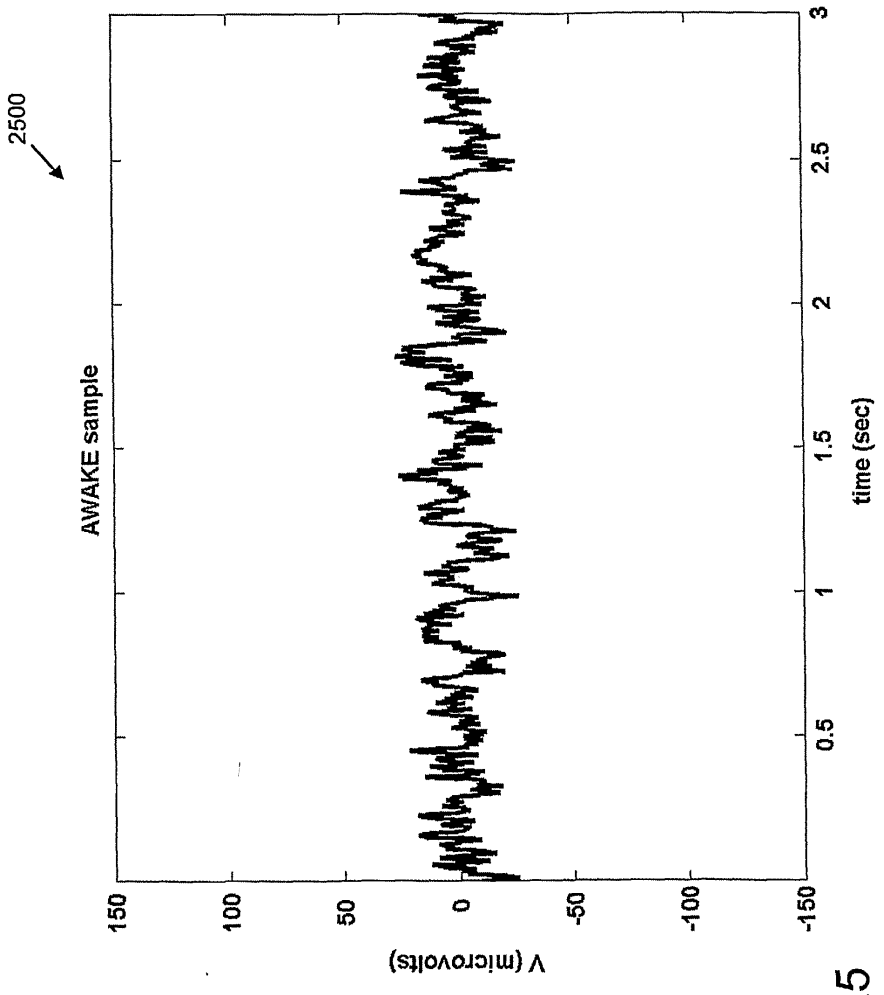
2500
AWAKE sample
V (microvolts)
150
100
50
0
-50
-100
-150
0.5
1
1.5
2
2.5
3
time (sec)

FIG. 25

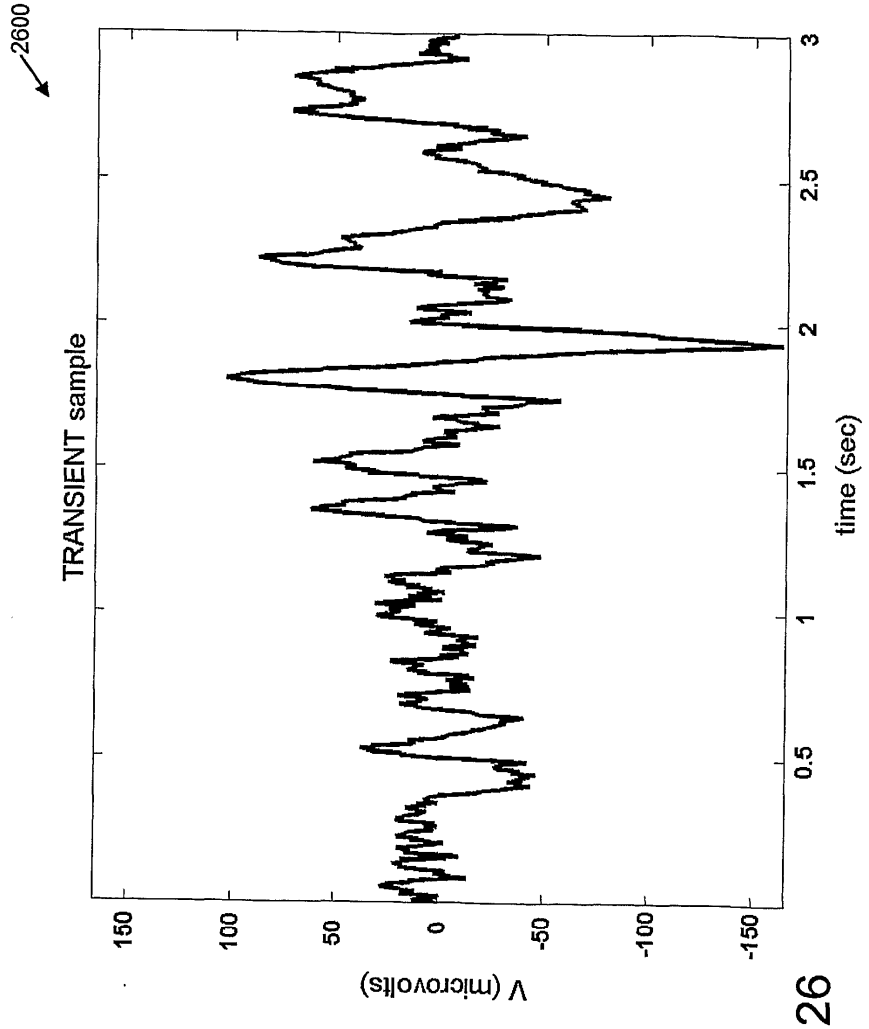
2600
TRANSIENT sample
V (microvolts)
150
100
50
0
-50
-100
-150
0.5
1
1.5
2
2.5
3
time (sec)

FIG. 26

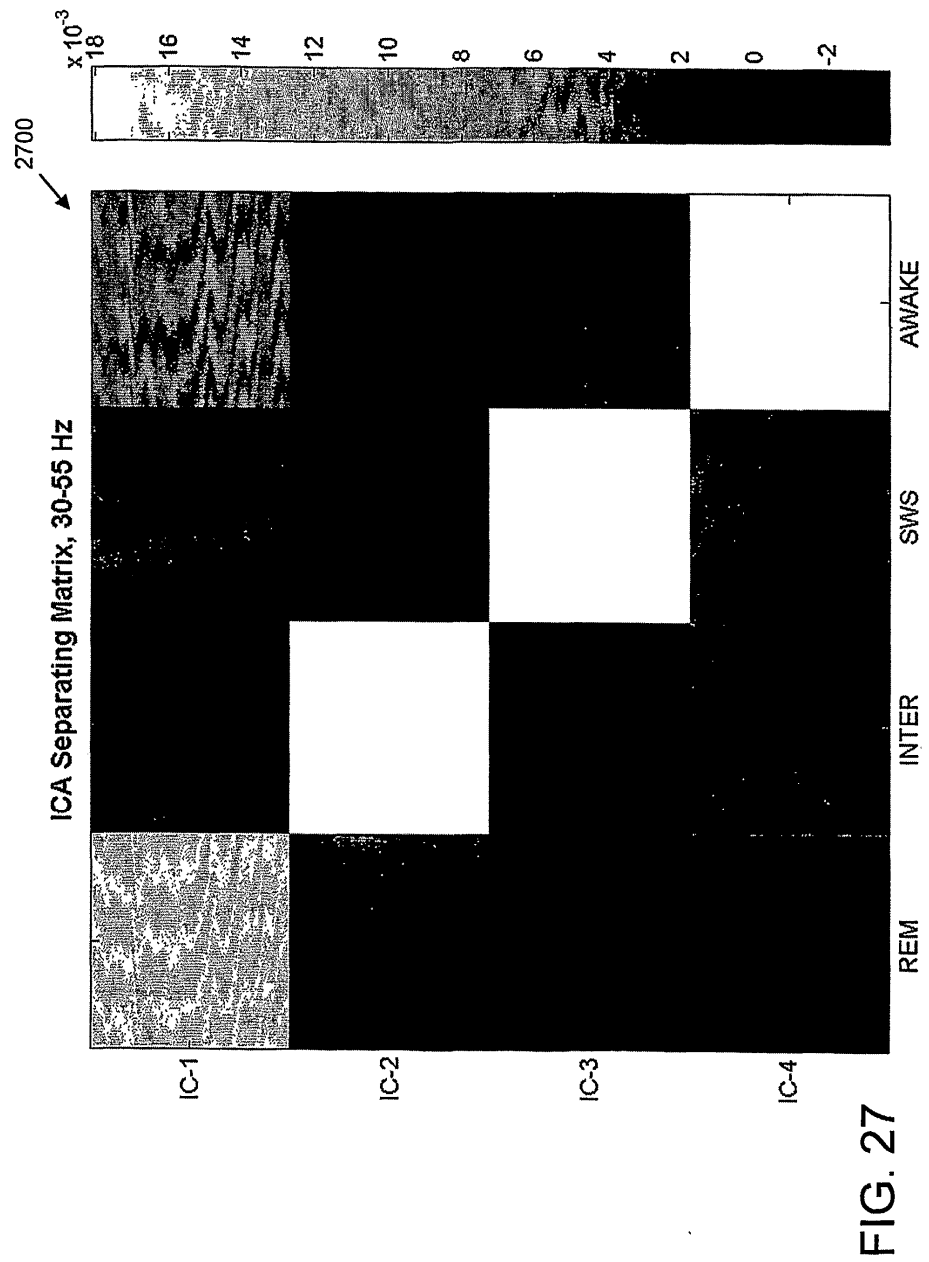
x 10^-3
18
16
14
12
10
8
6
4
2
0
-2
2700
ICA Separating Matrix, 30-55 Hz
AWAKE
SWS
INTER
REM
IC-1
IC-2
IC-3
IC-4

FIG. 27

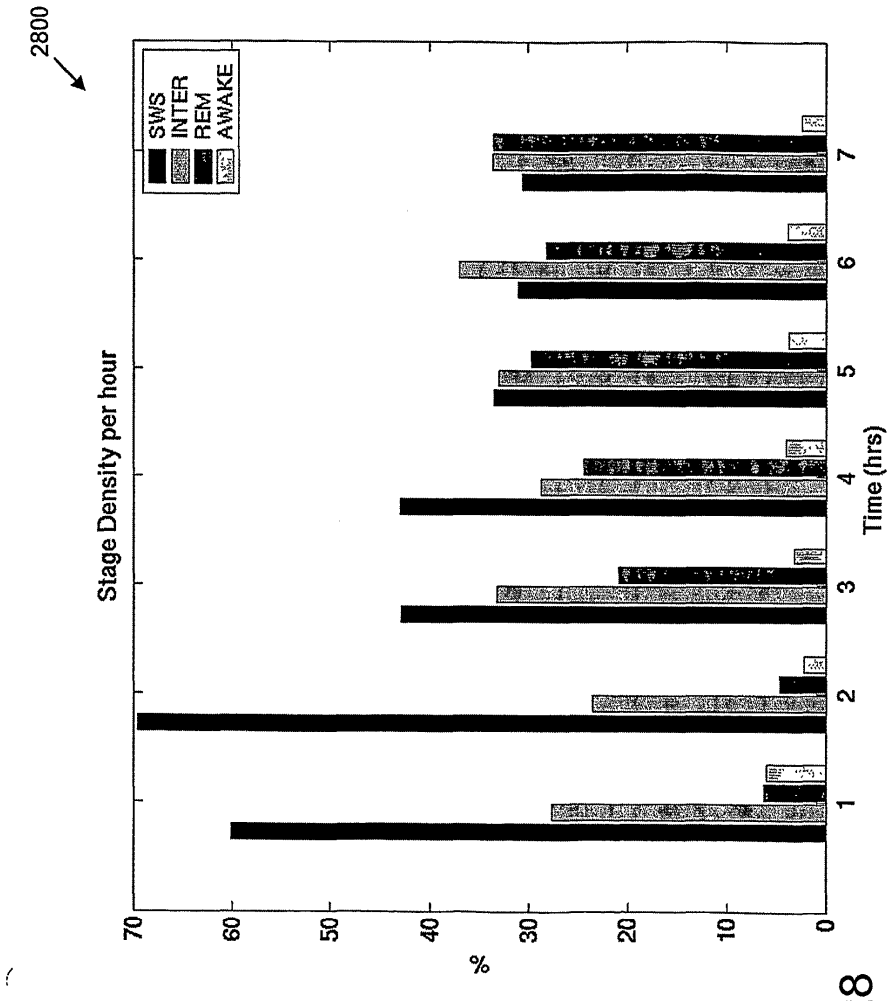
2800
SWS
INTER
REM
AWAKE
Stage Density per hour
%
0
10
20
30
40
50
60
70
1
2
3
4
5
6
7
Time (hrs)

FIG. 28

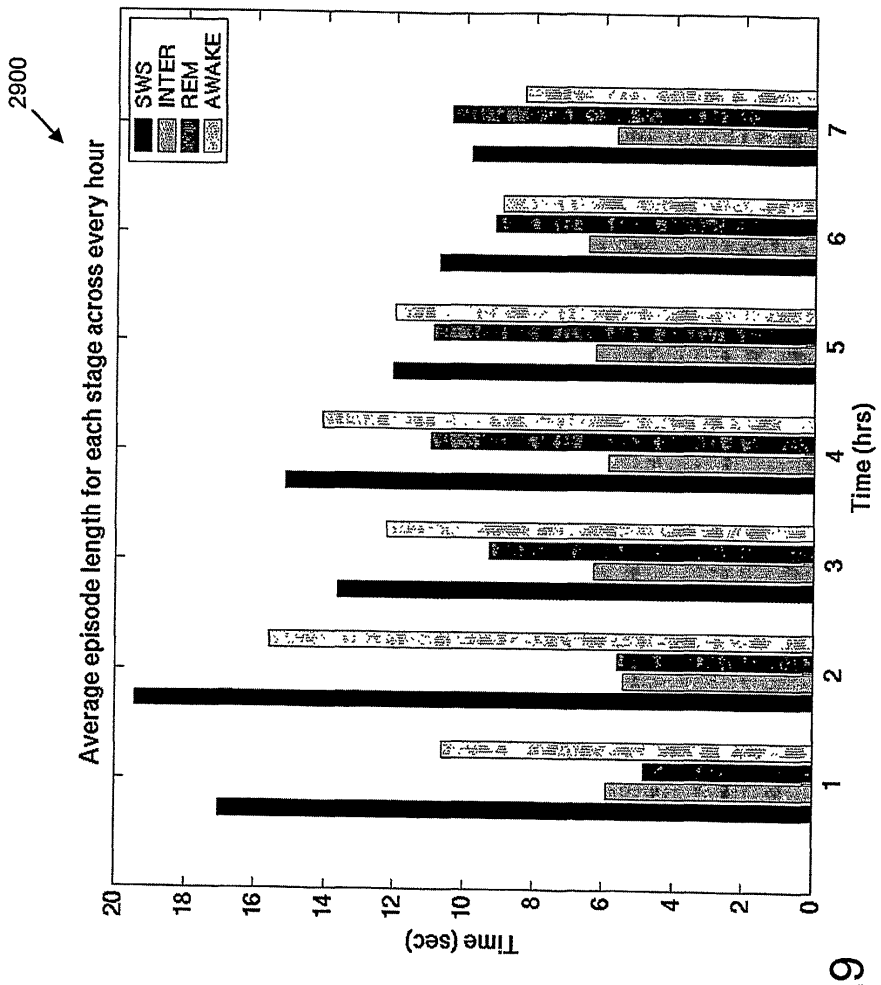
2900
Average episode length for each stage across every hour
SWS
INTER
REM
AWAKE
Time (sec)
0
2
4
6
8
10
12
14
16
18
20
1
2
3
4
5
6
7
Time (hrs)

FIG. 29

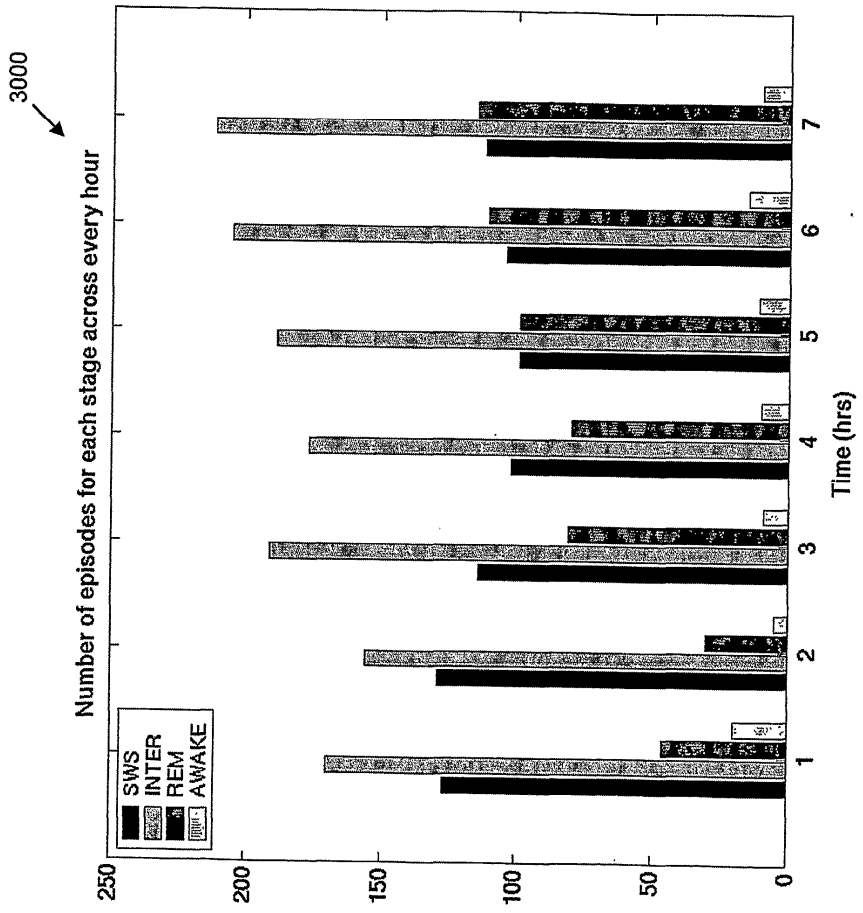
3000
Number of episodes for each stage across every hour
SWS
INTER
REM
AWAKE
250
200
150
100
50
0
1
2
3
4
5
6
7
Time (hrs)

FIG. 30

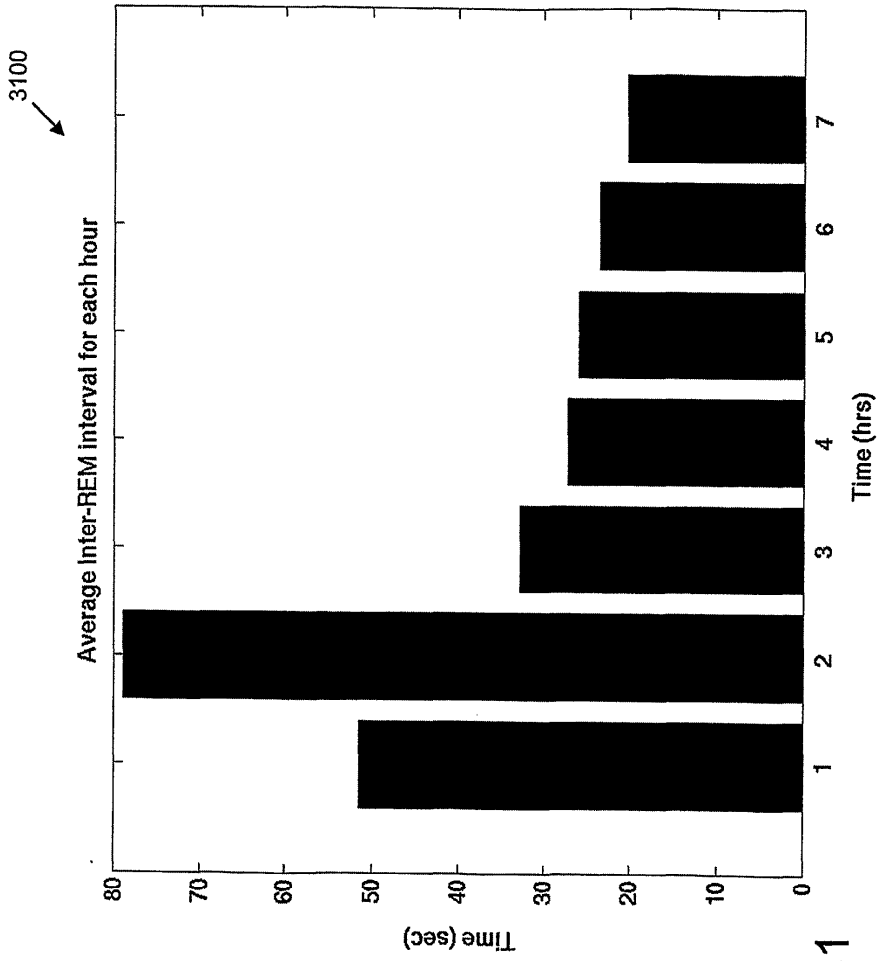
3100
Average Inter-REM interval for each hour
Time (sec)
0
10
20
30
40
50
60
70
80
1
2
3
4
5
6
7
Time (hrs)

FIG. 31

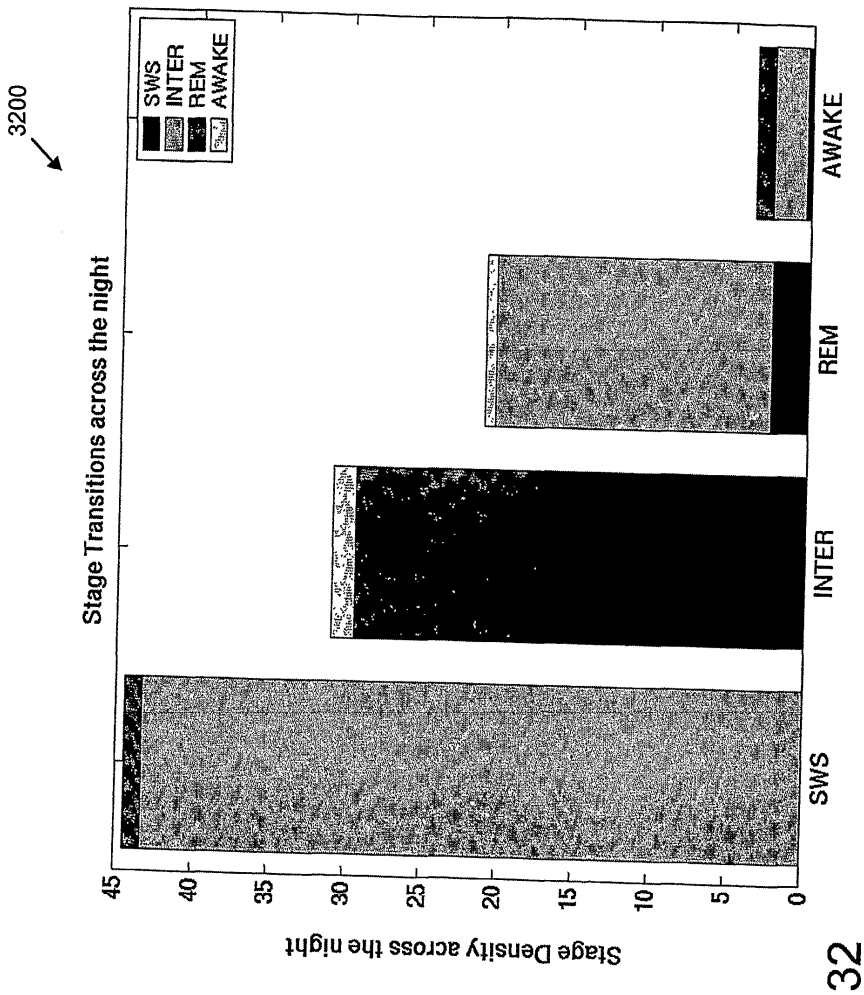
3200
SWS
INTER
REM
AWAKE
Stage Transitions across the night
Stage Density across the night
0
5
10
15
20
25
30
35
40
45
SWS
INTER
REM
AWAKE

FIG. 32

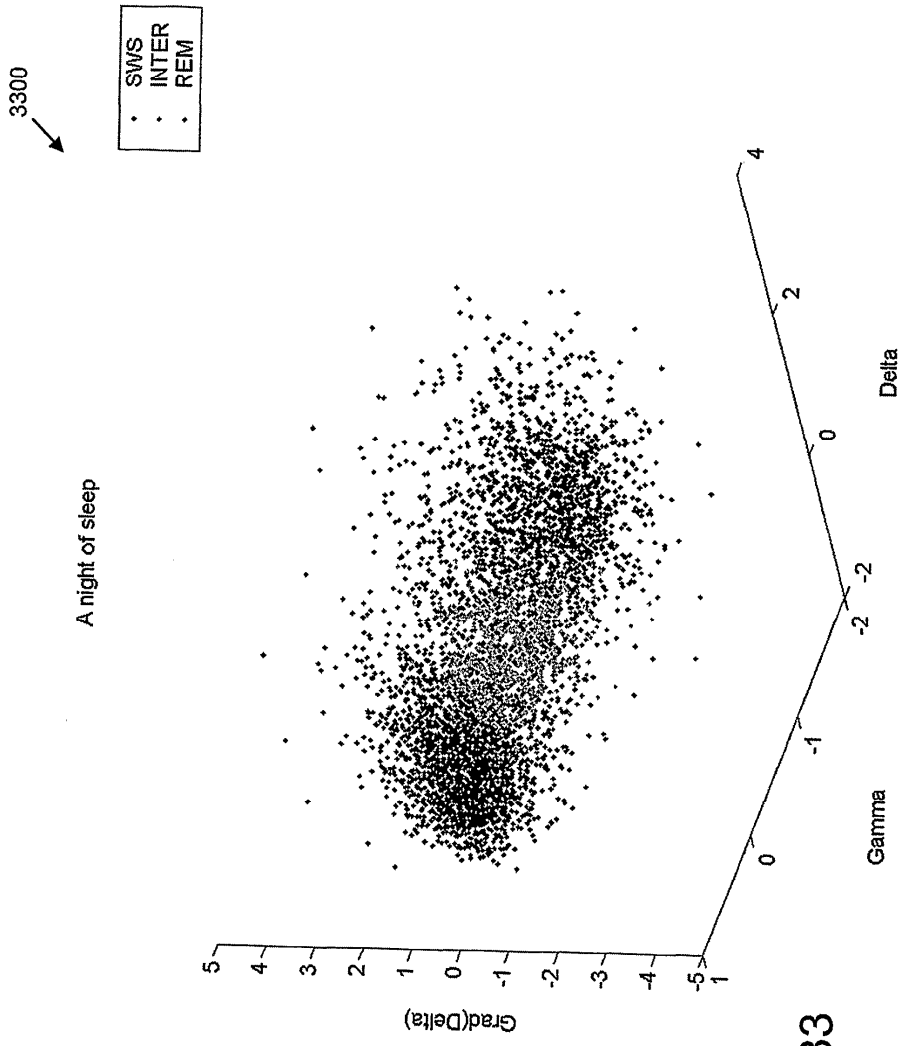

FIG. 33

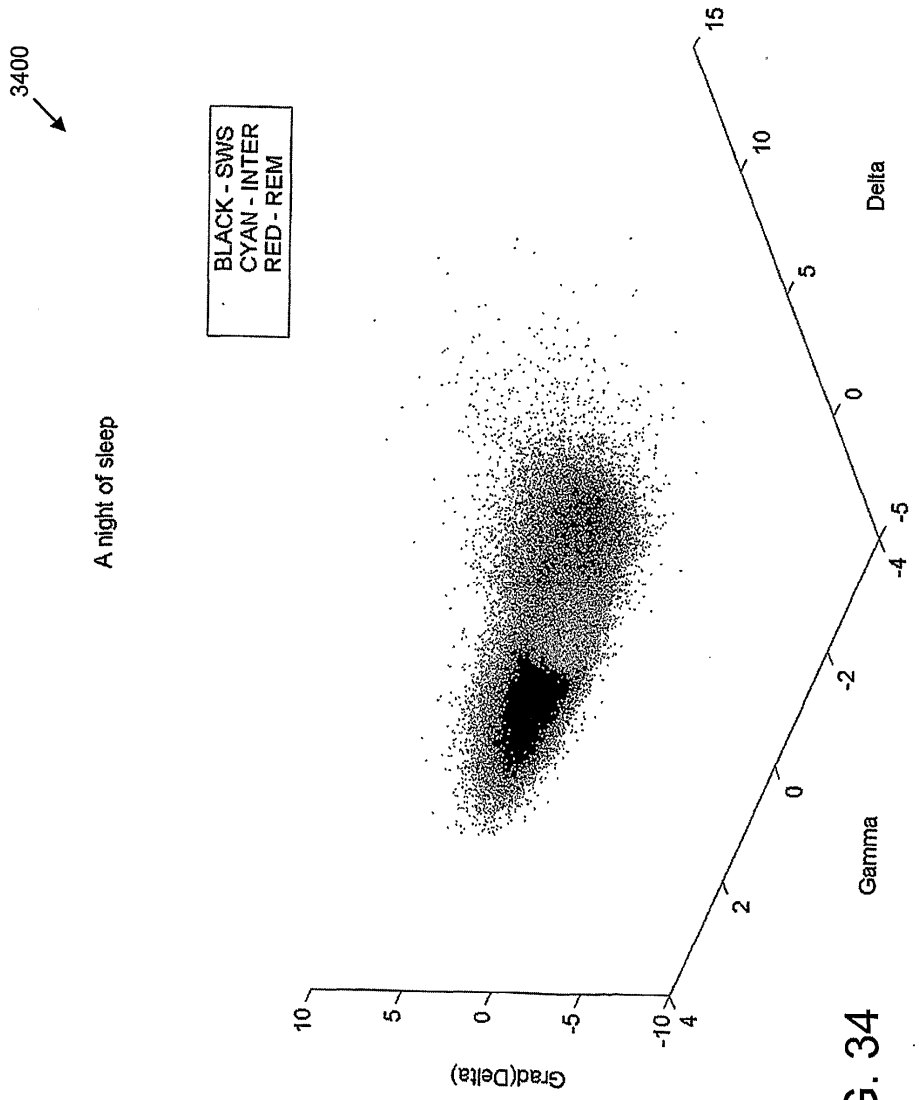
3400
A night of sleep
BLACK - SWS
CYAN - INTER
RED - REM
Grad(Delta)
10
5
0
-5
-10
4
2
0
-2
-4
-5
0
5
10
15
Gamma
Delta

FIG. 34

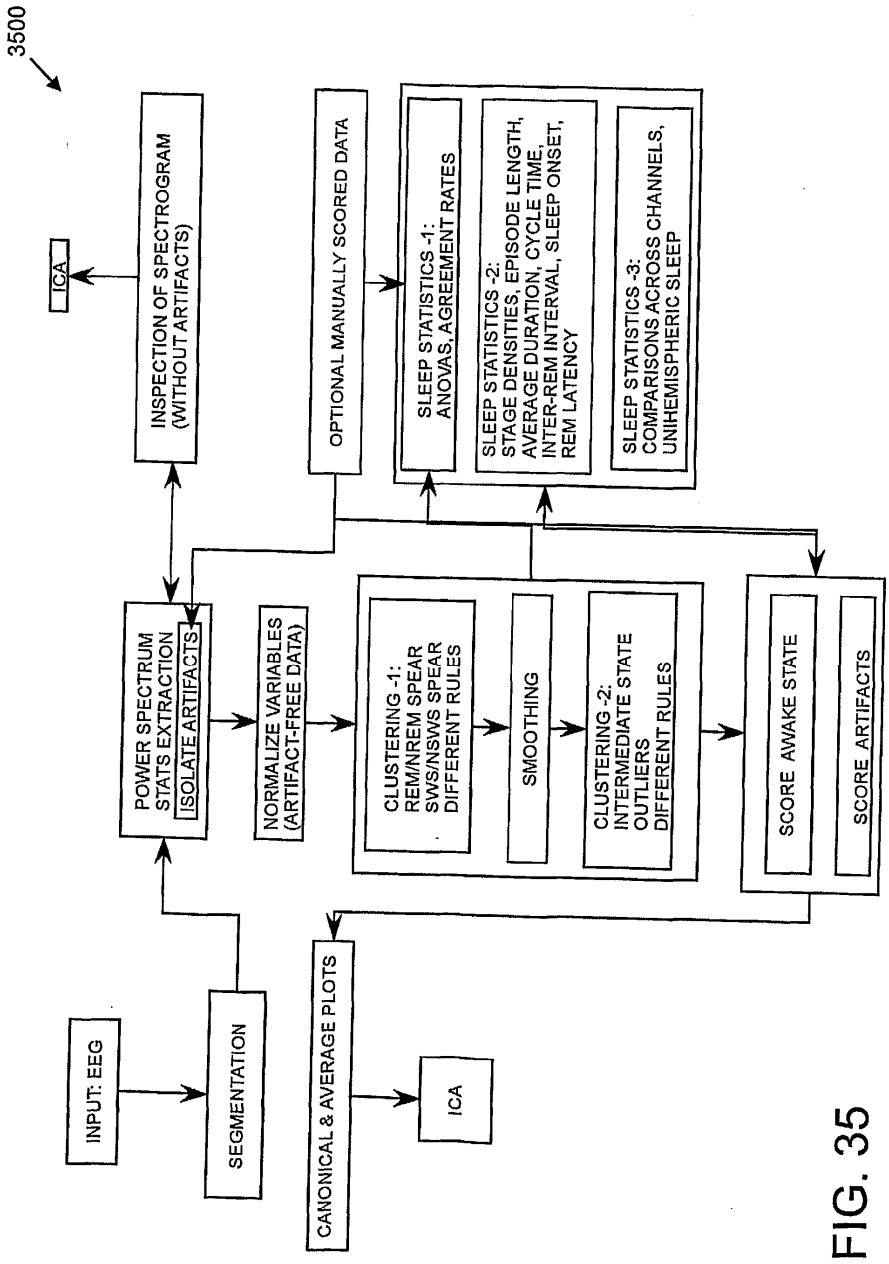
3500
INPUT: EEG
SEGMENTATION
CANONICAL & AVERAGE PLOTS
ICA
POWER SPECTRUM STATS EXTRACTION
ISOLATE ARTIFACTS
NORMALIZE VARIABLES (ARTIFACT-FREE DATA)
CLUSTERING -1: REM/NREM SPEAR SWS/NSWS SPEAR DIFFERENT RULES
SMOOTHING
CLUSTERING -2: INTERMEDIATE STATE OUTLIERS DIFFERENT RULES
SCORE AWAKE STATE
SCORE ARTIFACTS
INSPECTION OF SPECTROGRAM (WITHOUT ARTIFACTS)
ICA
OPTIONAL MANUALLY SCORED DATA
SLEEP STATISTICS -1: ANOVAS, AGREEMENT RATES
SLEEP STATISTICS -2: STAGE DENSITIES, EPISODE LENGTH, AVERAGE DURATION, CYCLE TIME, INTER-REM INTERVAL, SLEEP ONSET, REM LATENCY
SLEEP STATISTICS -3: COMPARISONS ACROSS CHANNELS, UNIHEMISPHERIC SLEEP

FIG. 35

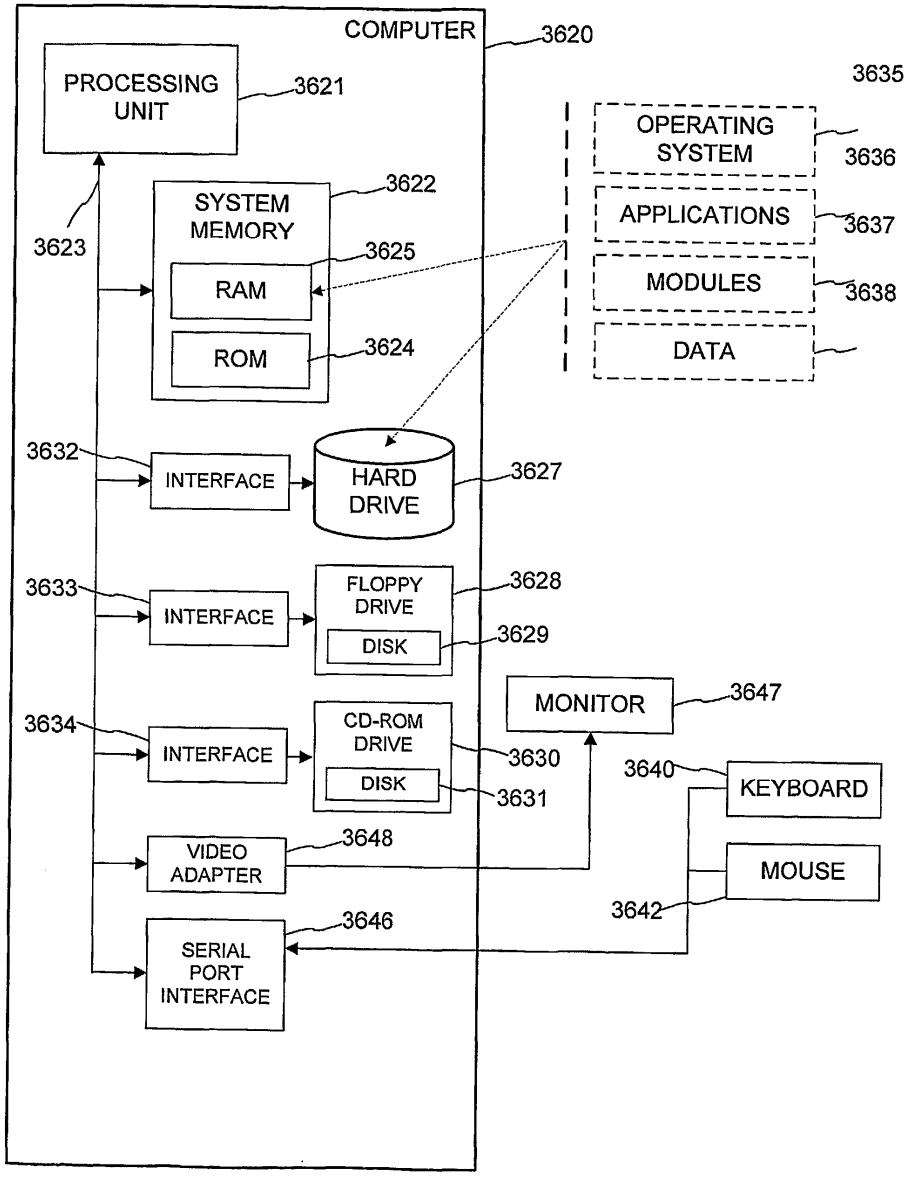
COMPUTER
3620
PROCESSING UNIT
3621
3635
OPERATING SYSTEM
3636
APPLICATIONS
3637
MODULES
3638
DATA
SYSTEM MEMORY
3622
3623
3625
RAM
ROM
3624
3632
INTERFACE
HARD DRIVE
3627
3633
INTERFACE
FLOPPY DRIVE
3628
DISK
3629
3634
INTERFACE
CD-ROM DRIVE
3630
DISK
3631
MONITOR
3647
3640
KEYBOARD
MOUSE
3642
VIDEO ADAPTER
3648
SERIAL PORT INTERFACE
3646

FIG. 36

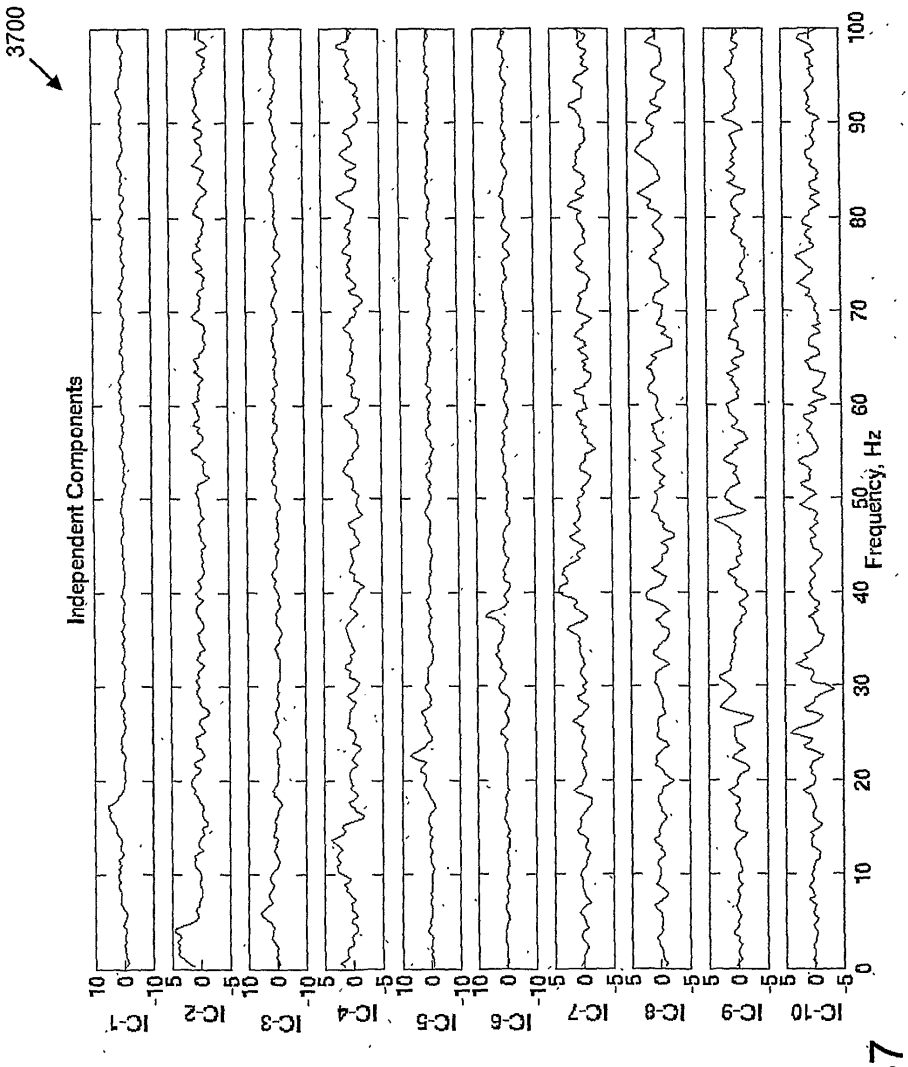
3700
Independent Components
IC-1
IC-2
IC-3
IC-4
IC-5
IC-6
IC-7
IC-8
IC-9
IC-10
Frequency, Hz

FIG. 37

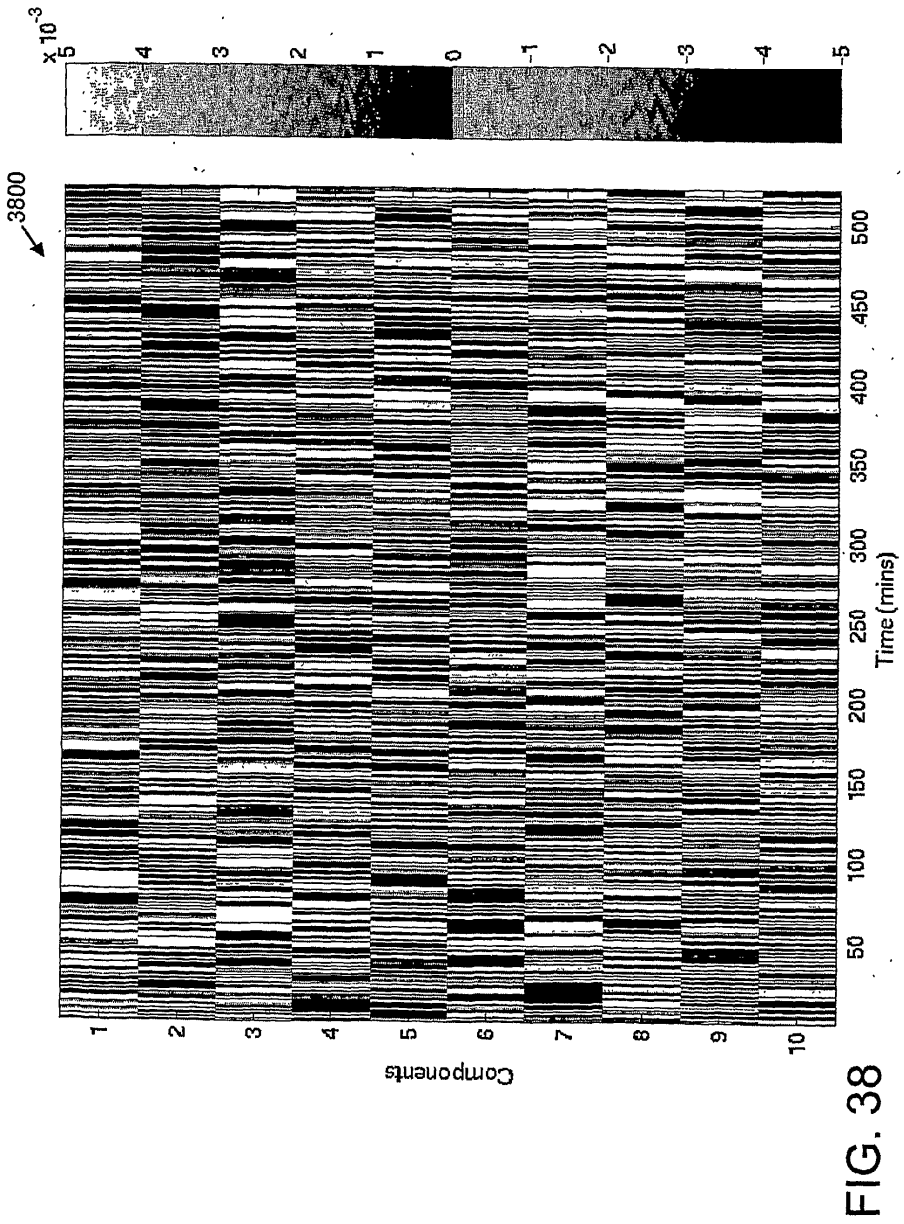
x 10^-3
5
4
3
2
1
0
-1
-2
-3
-4
-5
3800
Components
1
2
3
4
5
6
7
8
9
10
Time (mins)
50
100
150
200
250
300
350
400
450
500

FIG. 38

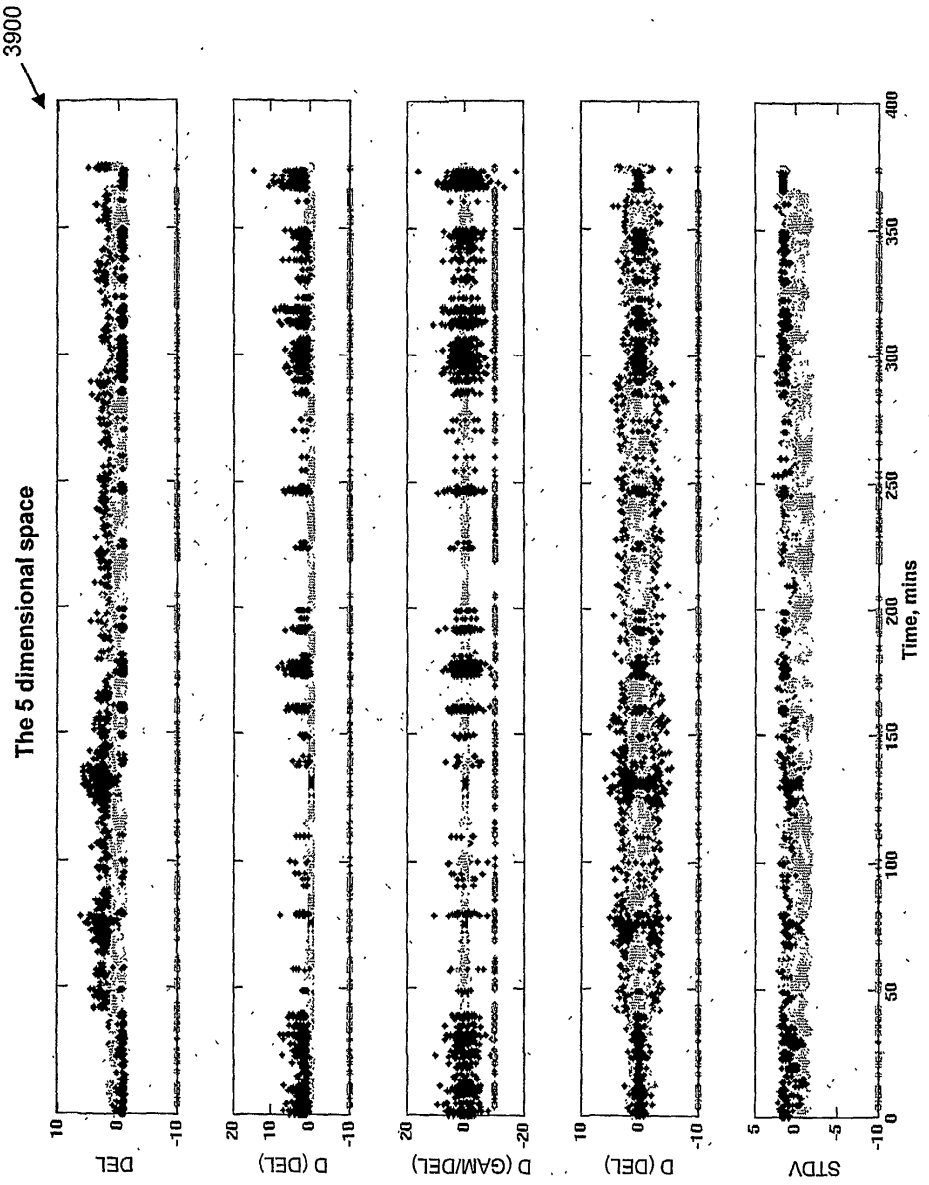
3900
The 5 dimensional space
DEL
D (DEL)
D (GAM/DEL)
D (DEL)
STDV
Time, mins

FIG. 39

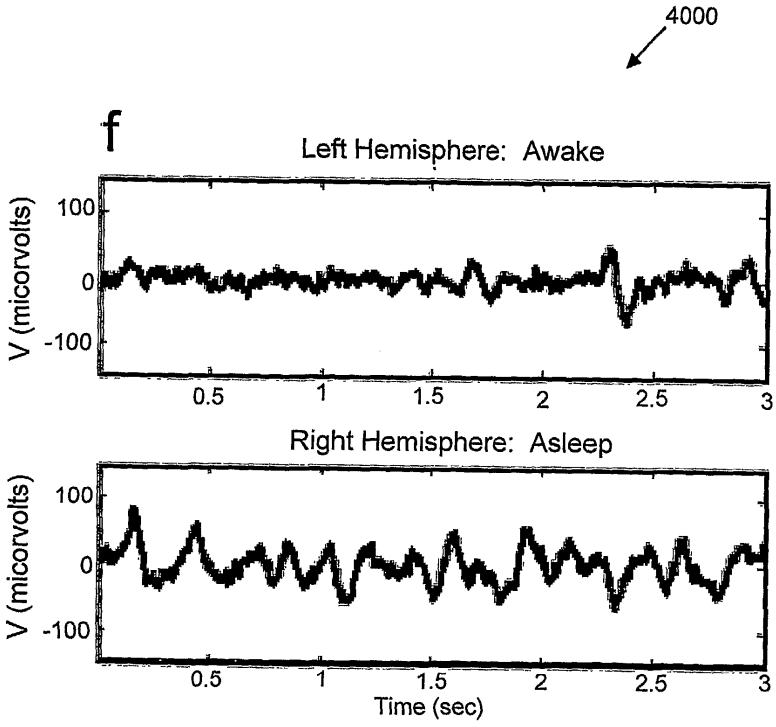
4000
f
Left Hemisphere: Awake
V (micorvolts)
100
0
-100
0.5
1
1.5
2
2.5
3
Right Hemisphere: Asleep
V (micorvolts)
100
0
-100
0.5
1
1.5
2
2.5
3
Time (sec)

FIG. 40

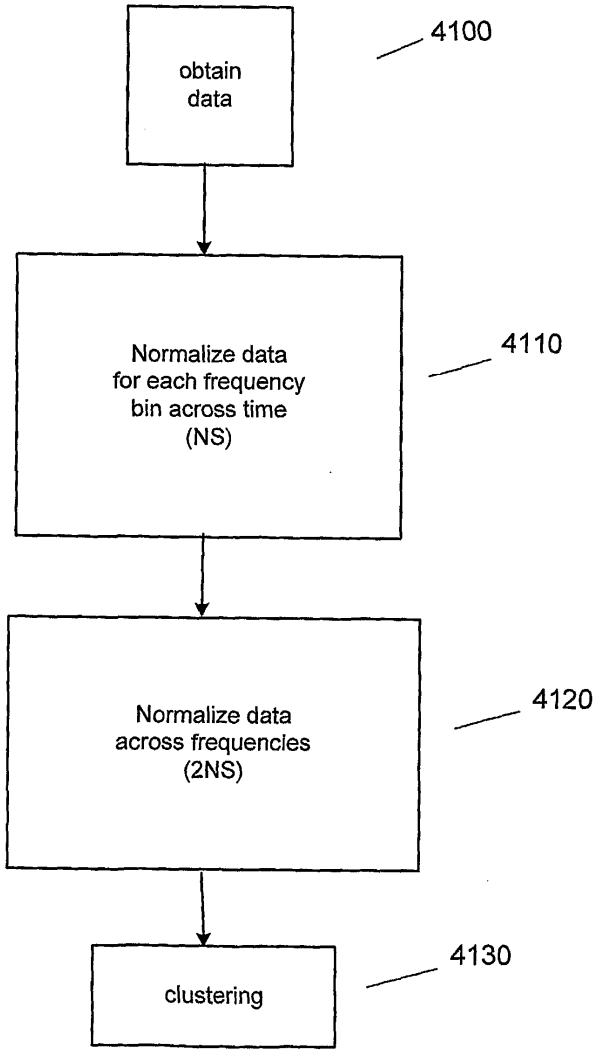
obtain data
4100
Normalize data for each frequency bin across time (NS)
4110
Normalize data across frequencies (2NS)
4120
clustering
4130

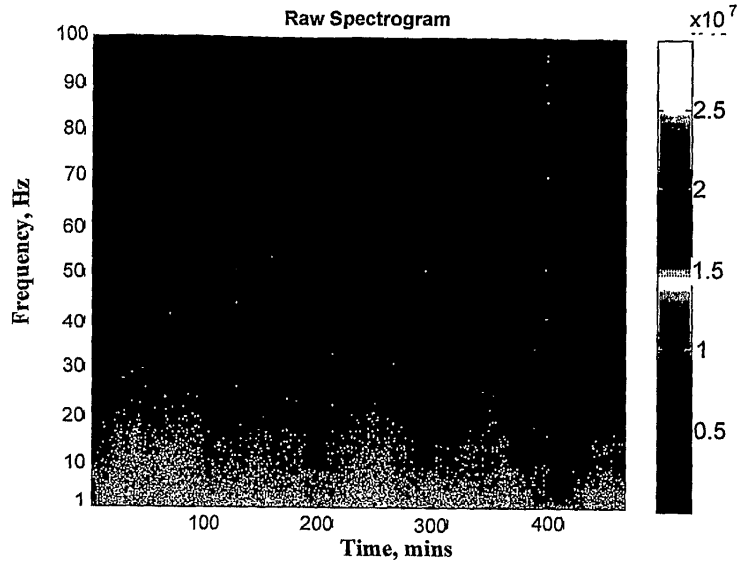

FIG. 42A

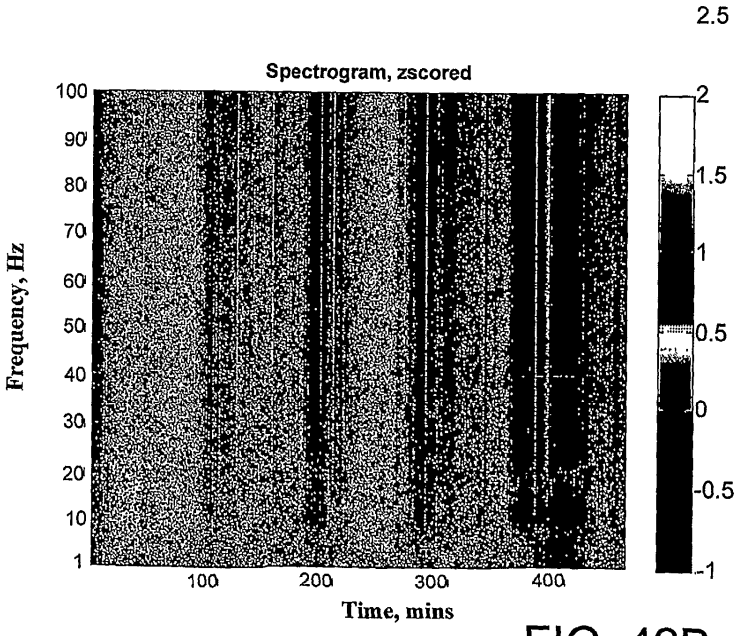

FIG. 42B

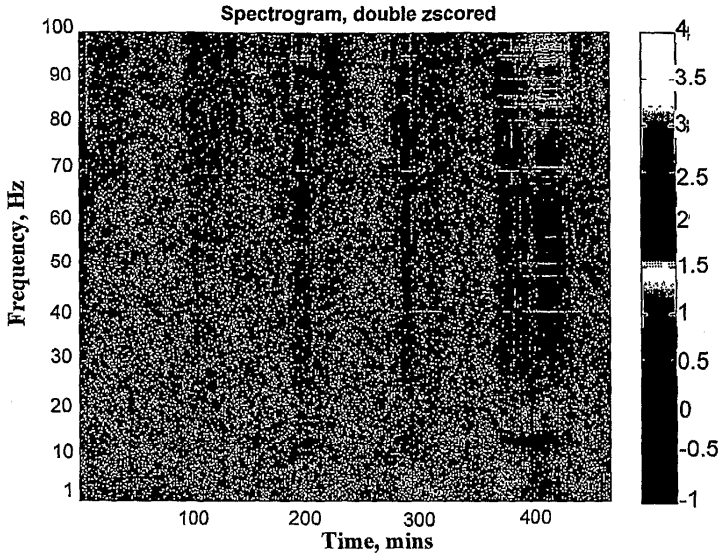

FIG. 42C

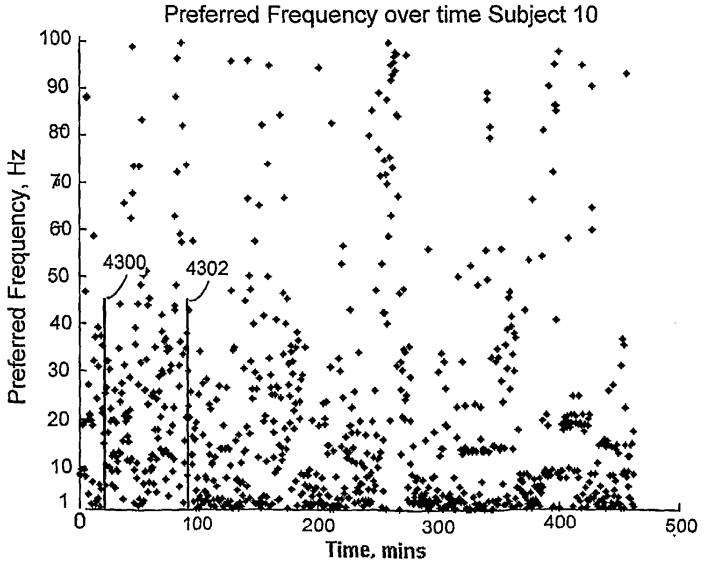

FIG. 43

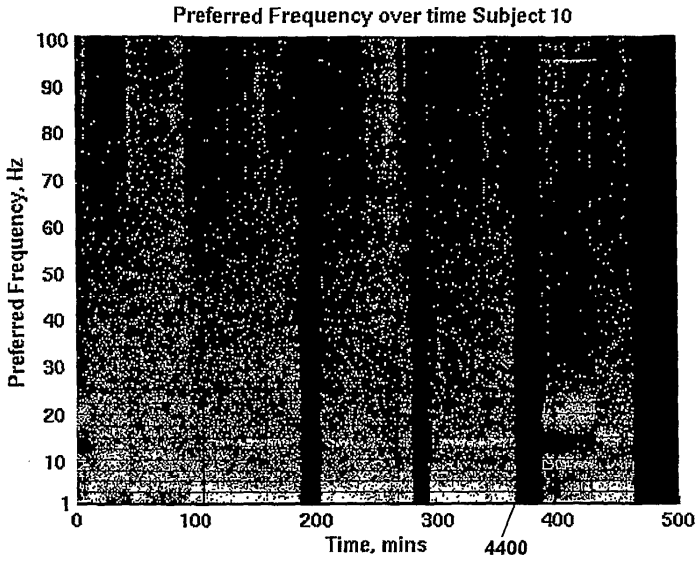
Preferred Frequency over time Subject 10
Preferred Frequency, Hz
100
90
80
70
60
50
40
30
20
10
1
0
100
200
300
400
500
Time, mins
4400

FIG. 44

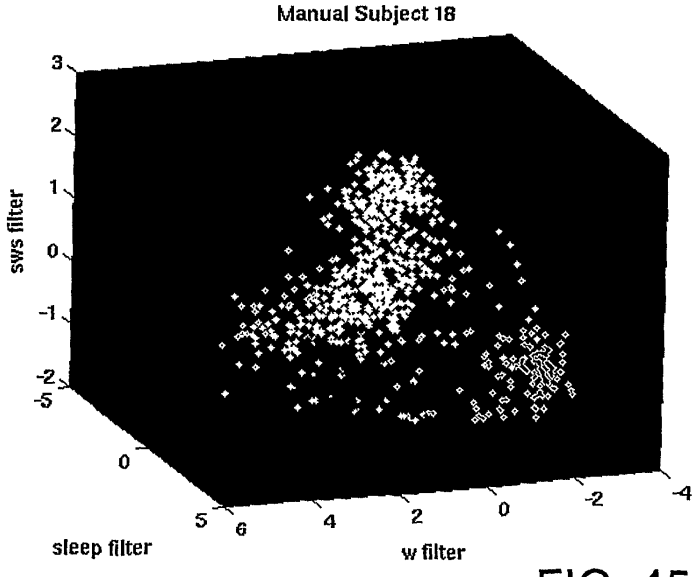
Manual Subject 18
sws filter
3
2
1
0
-1
-2
-5
0
5
6
4
2
0
-2
-4
sleep filter
w filter

FIG. 45

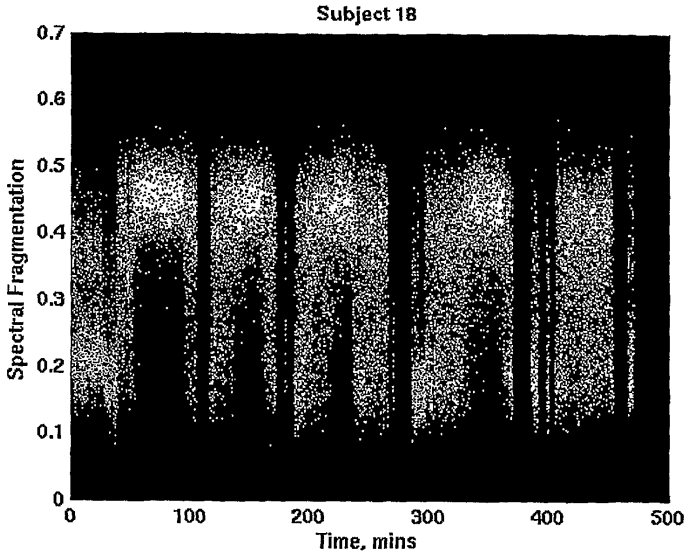
Subject 18
Spectral Fragmentation
0.7
0.6
0.5
0.4
0.3
0.2
0.1
0
0
100
200
300
400
500
Time, mins

FIG. 46